*Progress in*

# PHYSICAL

# ORGANIC

# CHEMISTRY

VOLUME 17

*Progress in*

# PHYSICAL

# ORGANIC

# CHEMISTRY

VOLUME 17

**Editor**

**ROBERT W. TAFT,** *Department of Chemistry*
*University of California, Irvine, California*

*Dedicated to the memory of
Louis P. Hammett*

# Contributors to Volume 17

T. William Bentley
    Department of Chemistry
    University College of Swansea
    Swansea, Wales, United Kingdom

Jean François Gal
    Laboratoire de Chimie Physique Organique
    Université de Nice–Sophia Antipolis
    Nice, France

Ernest Grunwald
    Department of Chemistry
    Brandeis University
    Waltham, Massachusetts

Tadeusz Marek Krygowski
    Department of Chemistry
    University of Warsaw
    Warsaw, Polland

Gareth Llewellyn
    Department of Chemistry
    University College of Swansea
    Swansea, Wales, United Kingdom

Pierre Charles Maria
    Laboratoire de Chimie Physique Organique
    University de Nice–Sophia Antipolis
    Nice, France

John Shorter
    Department of Chemistry
    The University
    Hull, England

R. D. Topsom
    Department of Chemistry
    La Trobe University
    Melbourne, Australia

# Introduction to the Series

Physical organic chemistry is a relatively modern field with deep roots in chemistry. The subject is concerned with investigations of organic chemistry by quantitative and mathematical methods. The wedding of physical and organic chemistry has provided a remarkable source of inspiration for both of these classical areas of chemical endeavor. Further, the potential for new developments resulting from this union appears to be still greater. A closing of ties with all aspects of molecular structure and spectroscopy is clearly anticipated. The field provides the proving ground for the development of basic tools for investigations in the areas of molecular biology and biophysics. The subject has an inherent association with phenomena in the condensed phase and thereby with the theories of this state of matter.

The chief directions of the field are: (a) the effects of structure and environment on reaction rates and equilibria; (b) mechanisms of reactions; and (c) application of statistical and quantum mechanics to organic compounds and reactions. Taken broadly, of course, much of chemistry lies within these confines. The dominant theme that characterizes this field is the emphasis on interpretation and understanding that permits the effective practice of organic chemistry. The field gains its momentum from the application of basic theories and methods of physical chemistry to the broad areas of knowledge of organic reactions and organic structural theory. The nearly inexhaustible diversity of organic structures permits detailed and systematic investigations that have no peer. The reactions of complex natural products have contributed to the development of theories of physical organic chemistry, and, in turn, these theories have ultimately provided great aid in the elucidation of structures of natural products.

Fundamental advances are offered by the knowledge of energy states and their electronic distributions in organic compounds and the relationship of these to reaction mechanisms. The development, for example, of even an empirical and approximate general scheme for the estimation of activation energies would indeed be most notable.

The complexity of even the simplest organic compounds in terms of physical theory well endows the field of physical organic chemistry with the frustrations of approximations. The quantitative correlations employed in this field vary from purely empirical operational formulations to the approach of applying physical principles to a workable model. The most common

procedures have involved the application of approximate theories to approximate models. Critical assessment of the scope and limitations of these approximate applications of theory leads to further development and understanding.

Although he may wish to be a disclaimer, the physical organic chemist attempts to compensate his lack of physical rigor by the vigor of his efforts. There has indeed been recently a great outpouring of work in this field. We believe that a forum for exchange of views and for critical and authoritative reviews of topics is an essential need of this field. It is our hope that the projected periodical series of volumes under this title will help serve this need. The general organization and character of the scholarly presentations of our series will correspond to that of the several prototypes, e.g., *Advances in Enzymology*, *Advances in Chemical Physics*, and *Progress in Inorganic Chemistry*.

We have encouraged the authors to review topics in a style that is not only somewhat more speculative in character but which is also more detailed than presentations normally found in textbooks. Appropriate to this quantitative aspect of organic chemistry, authors have also been encouraged in the citation of numerical data. It is intended that these volumes will find wide use among graduate students as well as practicing organic chemists who are not necessarily expert in the field of these special topics. Aside from these rather obvious considerations, the emphasis in each chapter is the personal ideas of the author. We wish to express our gratitude to the authors for the excellence of their individual presentations.

We greatly welcome comments and suggestions on any aspect of these volumes.

*Robert W. Taft*

# Contents

*Progress in*

# PHYSICAL ORGANIC CHEMISTRY

VOLUME 17

# Hammett Memorial Lecture

BY JOHN SHORTER

*Department of Chemistry*
*The University*
*Hull, England*

CONTENTS

## I.  INTRODUCTION

Louis Plack Hammett was born in Wilmington, Delaware, on 7th April 1894 and died in his ninety-third year at Medford, New Jersey, on 23rd February 1987. Hammett was awarded his bachelor's degree from Harvard University in 1916 and his doctorate from Columbia University, New York City in 1923. He served on the chemistry faculty of Columbia University from 1920 to 1961 (having risen to the status of full professor in 1935) and thereafter he had the title of Mitchill Professor Emeritus of Chemistry at Columbia (1).

Hammett is commonly regarded as one of the founding fathers of physical organic chemistry, particularly in relation to the subject's development in the United States, whose chemical community has contributed so much to the advancement of the subject (2,3). Actually the term "physical organic chemistry" only began to be widely used after Hammett had employed it for the title of the book he published in 1940 (4). By that year the foundations of his own main original contributions to the subject had been well and truly laid. These were, of course, the equation for summarizing the effects of *meta*

**Figure 1**   Professor Louis P. Hammett. (This portrait was taken about 1960. The present author was lent the negative by Professor Hammett for use in connection with reference 75f.)

and *para* substituents on the rate or equilibrium constants for side-chain reactions of benzene derivatives (5) and the study and applications of concentrated solutions of acids, and in particular strong acids, through the acidity function (6). Hammett's preeminent connection with these is indicated by the commonly used terms: the Hammett equation and the Hammett

acidity function, a usage that Hammett himself did not encourage (7). The second edition of his book *Physical Organic Chemistry* was published in 1970 and it contains much evidence of the way in which the first edition and his own original contributions had influenced the development of the subject in the intervening 30 years (8). Hammett retained his interest in physical organic chemistry throughout his quarter century of retirement; indeed, he was 76 years of age when the second edition of *Physical Organic Chemistry* was published.

## II. HAMMETT AS A PHYSICAL CHEMIST

In the last edition of *American Men and Women of Science* (1) to include an entry for him, Hammett described his research area as "Physical organic chemistry; reaction rates and mechanisms," and it is in some such terms that most chemists would expect Hammett to describe his research interests. This description, however, rather obscures the fact that in background, experience, and outlook Hammett was very different from most physical organic chemists, particularly those of the United States. These tend to regard themselves as primarily organic chemists, who use physicochemical techniques to attack problems of structure, mechanism, and reactivity. Hammett regarded himself as a *physical* chemist, who found his research outlet in studying organic compounds and their reactions. In 1961 he was presented with the highest award of the American Chemical Society, the Priestley Medal, and in his acceptance address he stated his position in this way (9): "I have always considered myself a physical chemist, but I find large areas in what is called organic chemistry which interest me very much, and contrariwise large areas in physical chemistry on which I have not thought I could afford to spend time and energy." We can only really begin to understand Hammett as a chemist if we look carefully at the early stages of his career.

## III. HAMMETT'S ORIGINS AS A CHEMIST

The examination of the early stages of Hammett's career is made easier by the fortunate circumstance that when he received the James Flack Norris Award in Physical Organic Chemistry in 1966, he was in a reflective mood and gave an address entitled "Physical Organic Chemistry in Retrospect," which was subsequently published in the *Journal of Chemical Education* (10).

Hammett began this address by pointing out that when he started chemical research half a century earlier, physical organic chemistry as such, let alone the title, scarcely existed. Organic chemistry and physical chemistry

were largely in separate compartments. Organic chemistry was dominated by the drive to synthesize new compounds and to investigate natural products. According to Hammett, physical chemistry appeared mainly to be concerned with such problems as the existence (or otherwise) of unimolecular gas reactions and the behavior of electrolyte solutions which were so dilute that they could be described aptly as slightly polluted water!! In terms of this dichotomy, Hammett characterized as "anomalous" the way in which his own research experience developed from 1916 and through the 1920s. He claimed that what happened was due to a series of accidents.

At Harvard Hammett was greatly impressed by the lectures of E. P. Kohler (1865-1938), who had interests both in synthetic organic chemistry and theoretical organic chemistry, such as it was at that time. Hammett's slightly senior contemporary at Harvard, J. B. Conant (1893-1978), who was later President of Harvard, was similarly impressed and went on to do a substantial part of his Ph.D. under Kohler's supervision (3). Hammett, however, followed in the footsteps of many young American chemists of that era and went to Europe, in fact, to Switzerland, then a haven of relative calm in the midst of the Great War that was raging over much of the Continent. He spent 1916–1917 with H. Staudinger (1881–1965) in the Chemisches Institut of the Eidgenössische Technische Hochschule (E.T.H.) at Zürich, participating in Staudinger's massive work on the preparations and properties of aliphatic diazo compounds and thereby contributing to Parts 21 and 22 of *Über aliphatische Diazoverbindungen* as his first published work (11).

By the time Hammett returned home the United States had entered the war, and he became involved in analytical control work on organic materials and in research on cellulose acetate solutions in connection with aircraft fabric. For about a year and a half after the war he was engaged in development research on dyes and pharmaceuticals for a chemical company in New Jersey, but he then heard through a friend of an opening as instructor in the Chemistry Department of Columbia University, for which he applied successfully. Thus a chance meeting with a friend resulted in employment for the next 40 years!!

In his early years at Columbia, Hammett was particularly influenced by several senior colleagues. There was J. M. Nelson (1876–1965), who had participated in the attempts to work out an electronic theory of valency that had preceded the work of G. N. Lewis (1875-1946) and W. Kossel (1888–1956). Nelson was interested in making various physicochemical measurements on organic systems. There was also James Kendall (1889–1978), a physical chemist who pursued studies of a wide variety of condensed systems, including both electrolyte and nonelectrolyte systems. Hammett, however, chose to pursue his doctoral studies under the analytical chemist Hal T. Beans (1883–1960) in examining the factors that affect the reliability of the hydrogen

electrode (12). The discharge of hydrogen ions at platinum and other metals (13,14), and related matters such as catalytic properties (15) and overvoltage (16), continued to interest Hammett for a number of years; the publication of several papers with various collaborators extended well into the 1930s (17,18).

## IV. HAMMETT'S FIRST BOOK

As an instructor working in analytical chemistry, Hammett became involved in teaching qualitative inorganic analysis and apparently did this for many years (19,20). This work generated his first book, published in 1929 and entitled *Solutions of Electrolytes*, with the subtitle *With Particular Application to Qualitative Analysis* (21). The book was a slim octavo volume in the McGraw-Hill International Chemical Series and appears to have had some success, for it went through a second edition in 1936. The copy I have examined is of the third impression of the second edition. In his preface to the first edition Hammett wrote:

> This book is based upon the belief that a course in qualitative analysis is an ideal method of presenting and of illustrating by copious examples the general principles relating to the behavior of solutions of electrolytes; and that this part of physical chemistry is an indispensable part of the preparation for advanced work in chemistry and for the study of medicine and engineering. It is an attempt to make the fullest use of qualitative analysis as a means of teaching chemistry. The book is not an attempt to teach an immediately useful practical art.

And so Part I, entitled "Principles," and amounting to about three-quarters of the book, expounds the fundamentals of valency, electrolysis, ionization in solution, acids and bases, chemical equilibrium, solubility products, weak electrolytes, the ionization of water, salt hydrolysis, formation of complexes in solution, oxidation–reduction reactions, and oxidation potentials. The rest of the book, Part II, "Experiments," details the course of laboratory instruction to accompany the lectures, including a list of reagents and apparatus required and suggested demonstrations to be carried out by the lecturer during the lectures. Any student pursuing the course conscientiously would certainly have learned a great deal of fundamental inorganic and physical chemistry.

It should also be mentioned that Hammett's participation in analytical chemistry included a research collaboration with his colleague George H. Walden (1894–1973) in the early 1930s. This led to the introduction of the *ortho*-phenanthroline–ferrous ion complex as a high potential indicator for oxidimetric titrations (22–27), particularly with dichromate and ceric ion

solutions, which had previously required the somewhat inconvenient use of an external indicator (28).


## V.  THE ACIDITY FUNCTION

In his Norris Award Address (10) Hammett mentions that in the early 1920s he was profoundly influenced by reading the papers of A. R. Hantzsch (1857–1935), A. Werner (1866–1919), G. N. Lewis, and J. N. Brønsted (1869–1947). The influence of Werner, Lewis, and Brønsted is clearly shown in Hammett's general interest in electrochemistry and particularly in his presentation of the subject matter in his *Solutions of Electrolytes* (21). The influence of Hantzsch was also in connection with electrochemistry. This led to Hammett carrying out a great deal of research and to one of his major contributions to physical organic chemistry: the acidity function.

Hantzsch was one of the most distinguished German organic chemists of the late nineteenth and early twentieth centuries (29). He and his assistants worked on an extraordinary variety of topics, and he was often involved in controversies. Much of his work had a distinctly physical organic flavor, which was unusual at the time it was done, and the results often led Hantzsch to challenge the cherished beliefs of physical chemists. The part of Hantzsch's work that appealed to Hammett was his investigations of acids and bases in nonaqueous solutions, particularly solutions in anhydrous sulfuric acid (30). These studies led Hantzsch to recognize the chemical as opposed to physical role of the solvent in acid–base equilibria in solution. In the light of the then recent advances in the theory of acids and bases through the work of Brønsted (31), Hammett saw the examination of the behavior of organic compounds in solution in highly acidic media as a promising field of research. Maybe it appealed especially to Hammett as an attempt to make sense of the physical chemistry of solutions that were rather different from the usual "slightly polluted water"!

At all events, Hammett's first contribution in this area was published in 1928 (32). In this he proposed a generalized theory of acidity, which was given mathematical expression, and considered both the effect of the basicity and of the dielectric constant of the solvent. He showed that the predictions of the treatment were in agreement with the available evidence on acidity in nonaqueous solutions, including the work of Hantzsch. In his Norris Award address (10) Hammett recalled that he received an appreciative letter from Hantzsch, who was greatly pleased with the quantitative treatment his ideas had been given. Hantzsch asked for a supply of reprints to send to some of the physical chemists who had tended to pay little attention to his own work in this area!! This paper (32) was really Hammett's first paper in physical organic chemistry, and at about the time it appeared he started two graduate students,

Dietz and Deyrup, on experimental work on acid–base systems, which led to the publication of several further papers in physical organic chemistry in the early 1930s.

Dietz's work was on acid–base titrations in the very strongly acid solvent, formic acid (33). There were various interesting findings, but the work of the other student Deyrup has proved to be of more lasting significance, for it was in the first paper of Hammett and Deyrup, published in 1932, that the term "acidity function" was introduced (6). Hammett had recognized that the tendency of a solution to transfer hydrogen ion to a neutral organic molecule would be a particularly valuable, albeit empirical, measure of the acidity of the solution. And so he came to define the acidity function $H_0$ in terms of the equilibrium between a suitable indicator B and its protonated form $BH^+$ in a given solution. Thus:

$$B + H^+ \rightleftharpoons BH^+$$

$$H_0 = pK_{BH^+} - \log\left(\frac{C_{BH^+}}{C_B}\right)$$

where $C_{BH^+}/C_B$ is the directly observable concentration ratio of the indicator in its two differently colored forms and $K_{BH^+}$ is the thermodynamic ionization constant of $BH^+$ in terms of molar concentrations, referred to *ideal dilute solution in water*. Hammett and Deyrup (6) developed a series of indicators whereby $H_0$ could be measured for any solution in the range from dilute aqueous sulfuric acid to 100% sulfuric acid by the so-called step method. They also studied mixtures of perchloric acid and water from 0 to 70% acid. At that time the only instrumentation available was a simple visual colorimeter, and this greatly restricted the choice of indicators, which were mainly nitroanilines. Actually this turned out to be a fortunate circumstance in that it led to a fairly simple pattern of results (10). A wider choice of indicators might well have led to such bewildering results that serious doubts might have been cast on the validity of this approach to acidity and on the worthwhileness of the entire enterprise.

The first paper of Hammett and Deyrup (6) envisages two possible types of application of the indicator method: "One is the determination of the strengths of bases and of acids too weak and too strong, respectively, to permit measurements in aqueous solutions.... The other is in the interpretation of reaction velocity data." The authors then gave a survey for the latter topic, based on available data for acid-catalyzed reactions in sulfuric acid–water mixtures. It was suggested that

An exact parallelism between the reaction velocity and the acidity can only be expected if the velocity is proportional to the concentration of the ion formed by

the addition of one hydrogen ion to one molecule of the neutral substrate, if the
ratio of the concentration of this ion to the total concentration of substrate is
small, and if there is no further ionization by addition of another hydrogen ion. If
these conditions are fulfilled the equation

$$H_0 + \log k = \text{constant}$$

where $k$ is the velocity constant, should hold.


They found just three cases in which the equation held: the decomposition
of malic acid, the cyclization of *ortho*-benzoylbenzoic acid to anthraquinone
by loss of $H_2O$, and the Beckmann transformation of acetophenone oxime.
Several other reactions (all decompositions of carboxylic acids) did not
conform to the equation.

The second paper of Hammett and Deyrup, also published in 1932,
addresses the question of studying very weak bases and very strong acids in
solution in formic acid (34). In such solutions sulfuric acid was found to be a
strong monobasic acid; benzenesulfonic acid, a nearly but not quite strong
acid; and sodium formate and aniline, strong bases. The behavior of
acetanilide and propionitrile as weak bases was also studied. A third paper of
Hammett and Deyrup (35), published in 1933, was devoted to freezing-point
measurements of electrolytes in sulfuric acid, a type of study that had been
pioneered by Hantzsch (29,30). The results of such measurements were
expressed as the van't Hoff $i$ factor. Even at moderately large ionic strengths
the values of $i$ for some inorganic salts were very close to whole numbers,
corresponding to 100% dissociation, for example, for

$$KHSO_4 \rightleftharpoons K^+ + HSO_4^-$$
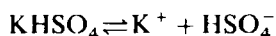
$i \approx 2$. Various organic compounds tested gave no evidence of any behavior as
electrolytes in sulfuric acid (e.g, 1,3,5-trinitrobenzene and picric acid), while
organic bases, including many of the indicators used in Deyrup's work, gave
results corresponding to the equilibrium:

$$B + H_2SO_4 \rightleftharpoons BH^+ + HSO_4^-$$
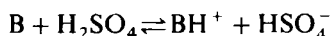
lying well over to the right-hand side, that is, $i \approx 2$. Triphenylcarbinol,
previously studied by Hantzsch (29,30), gave $i \approx 4$, corresponding to

$$Ph_3COH + 2H_2SO_4 \rightleftharpoons Ph_3C^+ + H_3O^+ + 2HSO_4^-$$
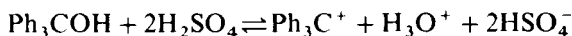
lying well over to the right-hand side (36).

   Hammett pursued research in this general field throughout the 1930s with some seven further collaborators, leading to 17 further papers (37–53). At an early stage he sought to publicize the merits of studies involving strongly acidic solutions through talks given in American Chemical Society (ACS) symposia, whose proceedings were subsequently published in *Chemical Reviews*. At a Symposium on Electrolytes given in the Division of Physical and Inorganic Chemistry at the 85th ACS National Meeting in Washington, D.C. in March 1933, Hammett talked on "The Quantitative Study of Very Weak Bases" (39). At a Symposium on Indicators given in the same division at the 88th ACS National Meeting in Cleveland, Ohio, in September 1934, Hammett talked on "Reaction Rates and Indicator Acidities" (45). The titles of these two talks of course refer to the two main areas of applications of indicator-based acidity functions as envisaged in the first paper of Hammett and Deyrup (6). The study
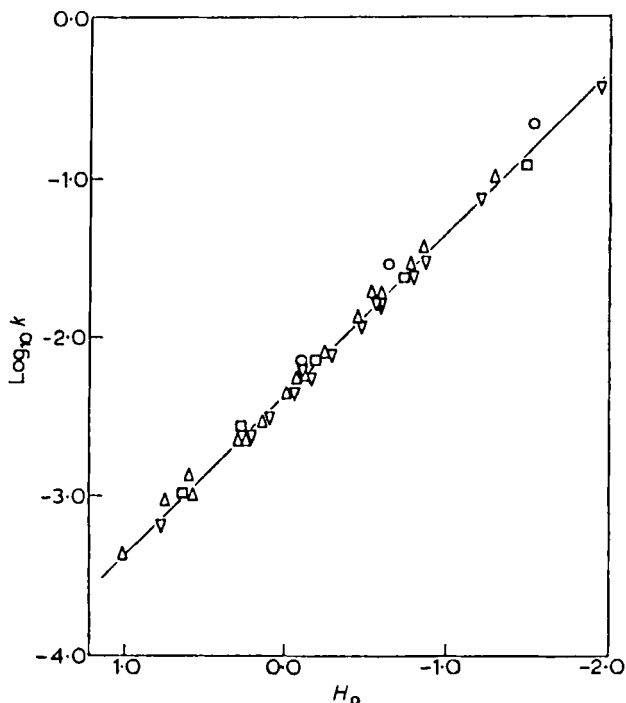


**Figure 2**   Correlation between rate constant and $H_0$ for the hydrolysis of sucrose, 25°C. The catalysing acids were as follows: ○ $HClO_4$; □ $H_2SO_4$; ▽ $HNO_3$; △ HCl. The line drawn is of unit slope. [Diagram as redrawn for C. H. Rochester, *Acidity Functions*, Academic Press, London, 1970; from L. P. Hammett and M. A. Paul, *J. Am. Chem. Soc.*, 56, 830 (1934) and L. P. Hammett, *Chem. Rev.*, 16, 67 (1935). Reproduced by kind permission of Academic Press Inc. (London) Ltd.]
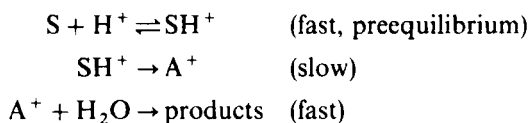
of very weak bases was pursued in work with R. P. Chapman on the solubilities of some organic oxygen compounds in sulfuric acid–water mixtures (37,38), and in particular in work with Dingwall and Flexser on the measurement of the strengths of very weak bases (43,44,48,49). This latter work, published from 1934 onward, saw the extension of colorimetry to the ultraviolet with a crude form of spectrophotometer, thereby increasing very greatly the range of compounds that could be studied. At around the same time, with his collaborator M. A. Paul, Hammett was refining the acidity function scale (40) and pursuing the relationship between the rates of some acid-catalyzed reactions and the acidity function $H_0$ (41). As we shall see shortly in connection with the Hammett equation, Hammett himself was now embarking on kinetic studies, and some of these involved strongly acidic media. Thus Hammett and Paul measured the rate of bromination of *meta*-nitroacetophenone in mixtures of sulfuric acid and acetic acid (46). Perhaps
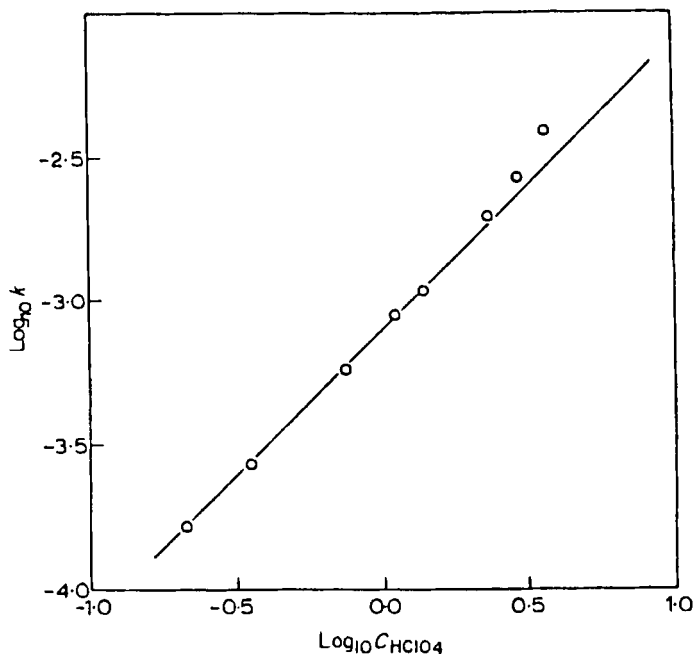


**Figure 3** Correlation between rate constant and acid concentration for the iodination of acetophenone in aqueous $HClO_4$ at 25°C. The line drawn is of unit slope. [Diagram as redrawn for C. H. Rochester, *Acidity Functions*, Academic Press, London, 1970; from L. Zucker and L. P. Hammett, *J. Am. Chem. Soc.*, *61*, 2791 (1939). Reproduced by kind permission of Academic Press Inc. (London) Ltd.]

best known, however, is the series of papers on various aspects of the acid-catalyzed halogenation of acetophenone and a number of its derivatives, published by Zucker and Hammett in 1939 (50–52). These papers led to the ideas that have become known as the "Zucker–Hammett hypothesis." Briefly, it was found that the rates of some acid-catalyzed reactions, such as the hydrolysis of sucrose, conformed to the acidity function (see Fig. 2), while others, such as the iodination of acetophenone, conformed to the *concentration* of strong acid in the medium (see Fig. 3). It was suggested that this indicated a distinction in mechanism. In the modern terminology due to Ingold this would be the difference between the $A_{AC}1$ and the $A_{AC}2$ mechanisms for the hydrolysis of an organic substrate in acidic solution (54,55).

### $A_{AC}1$ Mechanism

$$S + H^+ \rightleftharpoons SH^+ \qquad \text{(fast, preequilibrium)}$$
$$SH^+ \rightarrow A^+ \qquad \text{(slow)}$$
$$A^+ + H_2O \rightarrow \text{products} \qquad \text{(fast)}$$

### $A_{AC}2$ Mechanism

$$S + H^+ \rightleftharpoons SH^+ \qquad \text{(fast, preequilibrium)}$$
$$SH^+ + H_2O \rightarrow \text{products} \qquad \text{(slow)}$$
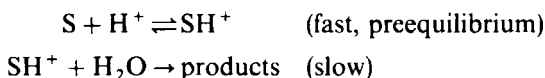
Like many good initial simple generalizations, the Zucker–Hammett criteria were fairly soon recognized to have their limitations, but the development of alternatives continued for many years. Only in the 1960s was there much success, notably in the work of Bunnett and Olsen (56).

Hammett's original contributions to acidity functions and similar ended largely with the work of Zucker and Hammett, apart from a brief excursion into the acidity of solutions of sulfuric acid in nitromethane, in work with L. C. Smith published in 1945 (57) and with H. van Looy published in 1959 (58); the latter paper was Hammett's last publication of experimental work. Hammett himself took no part in the proliferation of acidity functions, which has resulted in the definition of over 400 different types (59)!! It had probably been Hammett's hope that $H_0$ would be applicable to the behavior of a wide range of substrates in highly acidic media. However, in the first edition of *Physical Organic Chemistry* in 1940 (4), he did define the function $H_-$ for the tendency to transfer a proton to a base with a single negative charge and he recognized that, for a given acidic medium, $H_0$ and $H_-$ might have very different values (60).

## VI. STRUCTURE–REACTIVITY RELATIONSHIPS

It has already been mentioned that Hammett was much influenced by reading the papers of Brønsted. These included the paper of Brønsted and Pedersen (61) in 1924 on the decomposition of nitramide catalyzed by general bases, in which it was shown that for a series of bases the values of the logarithm of the rate constant plotted against the values of the logarithm of the ionization constant of the conjugate acid of the catalyst gave a straight line of negative slope. This was the first example of the type of relationship that was generalized by Brønsted to include acid catalysis in 1926 (62). Hammett thus became familiar with the Brønsted equation, and we may remind ourselves of the forms this equation takes by means of Hammett's presentation of it in a *Chemical Reviews* article, which I shall mention again shortly (63).

Hammett represented a general acid-catalyzed reaction as

$$HA + S \rightarrow products + HA$$

where HA is the catalyst and S is the substrate. The Brønsted equation may then be written as

$$k = GK^x \qquad \text{or} \qquad \log k = x \log K + \log G$$

where $k$ is the rate constant of the reaction when catalyzed by an acid whose ionization constant is $K$, and $G$ and $x$ are constants characteristic of the reaction.

Hammett became interested in the possibility of finding analogous relationships for other types of reaction. The initial stage of this interest was his starting of experimental studies on rates of reaction in solution early in the 1930s. By that time Hammett was well aware of what he described in his Norris Award address (10) as the "renaissance of solution kinetics" as a means of studying organic reaction mechanisms and of investigating the relationship between the structure and the reactivity of organic compounds. Studies of reaction mechanisms by kinetic techniques had begun around the turn of the century with the work of G. Bredig (1868–1944), J. F. Norris (1871–1940), A. Lapworth (1872–1941), K. J. P. Orton (1872–1930), and others, but this had not had any great impact on the majority of chemists or on the general nature of organic chemistry. In the late 1920s and early 1930s the field of kinetics and mechanism suddenly began to flourish through the work of C. K. Ingold (1893–1970), E. D. Hughes (1906–1963), C. N. Hinshelwood (1897–1967), R. P. Bell (b. 1907), E. A. Moelwyn–Hughes (1905–1978), J. B. Conant (1893–1978), P. D. Bartlett (b. 1907), and others (64).

Hammett's first kinetics paper, with H. L. Pfluger and published in 1933,

was a study of the reactions of methyl esters with trimethylamine in methanol as solvent (65):

$$RCO_2CH_3 + N(CH_3)_3 \rightarrow RCO_2^- + N(CH_3)_4^+$$
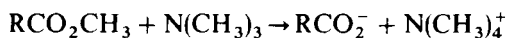
For a variety of groups R they found a logarithmic relation between the rate constants and the ionization constants of the corresponding carboxylic acids in water (see Fig. 4). There was no analogous relationship for the rate constants of the alkaline hydrolysis of the same esters. Hammett and Pfluger attributed this difference to the absence of steric hindrance by R in the amine reaction, involving attack of the trimethylamine on the ester methyl carbon, compared with the ester hydrolysis, which is subject to steric hindrance from R because the $OH^-$ reagent attacks the carbon of the ester carbonyl group.

As the 1930s advanced, Hammett became increasingly aware that there was already a great deal of data scattered throughout the literature that conformed to logarithmic relationships analogous to the Brønsted equation. He drew attention to this situation in a talk given in the Symposium on Kinetics of Reaction held in the Division of Physical and Inorganic Chemistry
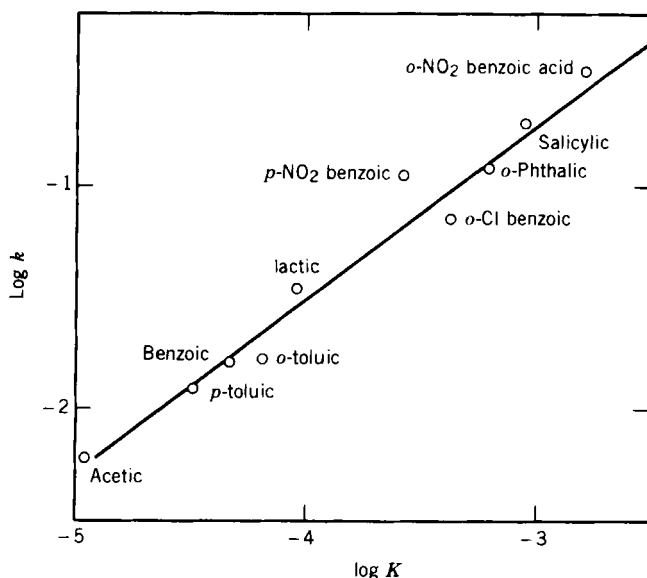


**Figure 4** Correlation between values of log $k$ for the reactions of trimethylamine with methyl esters of carboxylic acids in methanol at 100°C and values of log $K$ for the ionization of the carboxylic acids in water, extrapolated to 100°C. (Reproduced from reference 63 by kind permission of the American Chemical Society.)

at the 89th National Meeting of the ACS in New York City in April 1935 and
later published in *Chemical Reviews* (63). The morning session, arranged by
H. S. Taylor (1890–1974) of Princeton, was devoted to gas-phase reactions
and to the then very new activated complex theory of reaction rates, while the
afternoon session, arranged by Hammett, emphasized reactions in solution.
Hammett's paper contains plots of log $k$ for a variety of reactions against log $K$
for the ionization of carboxylic acids corresponding to the substrates, with an
emphasis on the side-chain reactions of *meta-* and *para*-substituted benzene
derivatives. He also pointed out some analogous relationships for oxidation–
reduction reactions, in which the oxidation–reduction potential played the
role corresponding to log $K$.

The opening sentences of Hammett's article in *Chemical Reviews* (63) are
worth quoting, for they indicate the rather ambiguous environment in which
linear free-energy relationships, as they soon came to be called, were born.

> The idea that there is some sort of relationship between the rate of a reaction and
> the equilibrium constant is one of the most persistently held and at the same time
> most emphatically denied concepts in chemical theory. Many organic chemists
> accept the idea without question and use it, frequently with considerable success,
> but practically every treatise on physical chemistry points out that such a
> relationship has no theoretical basis and that it is in fact contradicted in many
> familiar cases. The contradiction is, however, more apparent than real. It is true
> that there is no universal and unique relation between the rate and equilibrium of
> a reaction; it is equally true that there frequently is a relation between the rates
> and the equilibrium constants of a group of closely related reactions. It is the
> purpose of this paper to review the known examples of this kind of relationship,
> to point out the quantitative form which it assumes, and to state certain
> limitations to its application.

Subsequent to Hammett's talk at the ACS meeting and to his finalization
of the paper for submission to *Chemical Reviews*, Hammett became aware of
the work of G. N. Burkhardt (b. 1900) at the University of Manchester in
England (3). Burkhardt had been a pupil of Arthur Lapworth, and in the mid-
1930s he was actively pursuing structure–reactivity relationships through
kinetic studies. Burkhardt and his collaborators had found, independently of
Hammett, the widespread occurrence of logarithmic relationships involving
rate or equilibrium constants for the side-chain reactions of *meta-* and *para*-
substituted benzene derivatives (66). One of their papers contains about ten
examples of plots based on their own work and on other people's work in
which values of log $k$ (or log $K$) for a certain side-chain reaction of a series of
benzene derivatives are plotted against values of log $K$ for the ionization of the
corresponding substituted benzoic acids as a convenient standard of com-
parison (67). Burkhardt's contribution has been rather overlaid by Hammett's,

although Hammett in his later publications was always very careful to give Burkhardt due credit and to acknowledge his own indebtedness to Burkhardt's work (68). Undoubtedly the reason why Hammett rather than Burkhardt is commonly remembered in this connection is because Hammett went on to develop the delightfully simple summarizing relation that we know as the "Hammett equation."

Hammett was probably working on this in the latter part of 1935 and through much of 1936, for his paper on "The Effect of Structure upon the Reactions of Organic Compounds. Benzene Derivatives" was received by the American Chemical Society on November 7, 1936 and was published in the January 1937 issue of the *Journal of the American Chemical Society* (5,69). Here I need do no more than refer briefly to Hammett's putting forward of the equation:

$$\log k = \log k^\circ + \rho\sigma \quad \text{for rates}$$

or

$$\log K = \log K^\circ + \rho\sigma \quad \text{for equilibria}$$

to summarize the effects of *meta-* and *para*-substituents on the rate constants $k$ or the equilibrium constants $K$ of side-chain reactions of benzene derivatives. The symbol $k^\circ$ or $K^\circ$ denotes the statistical quantity (intercept term) approximating to $k$ or $K$ for the "parent" or "unsubstituted" compound. The *substituent constant* $\sigma$ measures the polar (electronic) effect of replacing H by a given substituent (in the *meta* or *para* position) and is, in principle, independent of the nature of the reaction. The *reaction constant* $\rho$ depends on the nature of the reaction (including conditions such as solvent and temperature) and measures the susceptibility of the reaction to polar effects. With $\rho$ defined as 1.000 for the ionization of substituted benzoic acids in water at 25°C, Hammett was able to tabulate about 15 $\sigma$ values and to double this number by including secondary values derived from correlations of various reaction series by means of the primary $\sigma$ values. Hammett found in the literature some 38 reaction series on which to test the equation, which he considered to be validated to within reasonable limits as indicated by median deviation. Figure 5 shows the first ever published Hammett plots of log $k$ or log $K$ versus $\sigma$ (5).

I think that in later life Hammett was rather surprised by what his eight-page paper in the *Journal of the American Chemical Society* for January 1937 had started. He himself made little contribution to refining and extending the Hammett equation. Later, in September 1937, he introduced the $\rho\sigma$ equation personally to Europe in a paper presented in the Faraday Society Discussion on Reaction Kinetics at Manchester. This paper, subsequently published in the *Transactions*, seems to be the first in which the term "linear free-energy relationships" was extensively used; indeed, its title was "Linear Free Energy
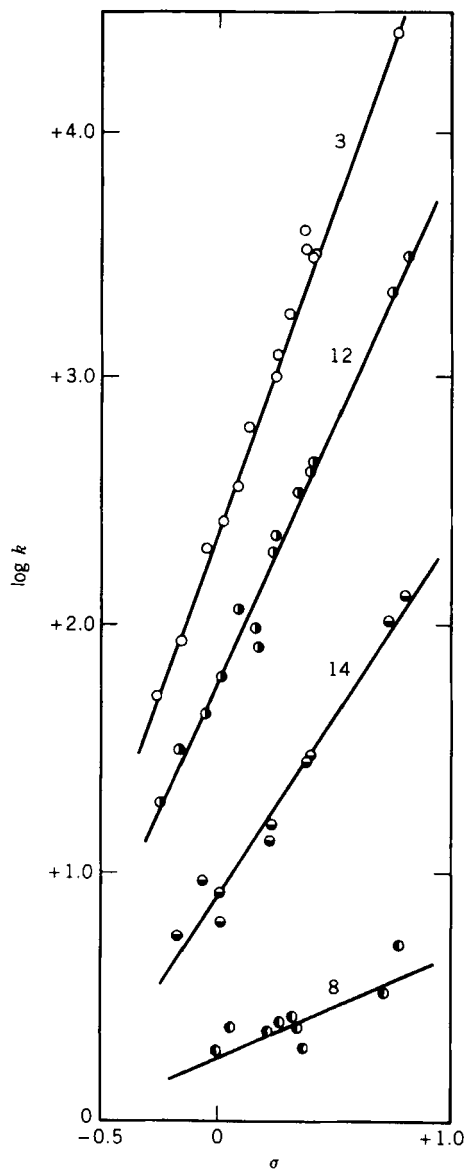
**Figure 5** The first published Hammett plots of log $k$ or log $K$ versus $\sigma$ for various reactions, reproduced from reference 5 by kind permission of the American Chemical Society. The numbered lines correspond to the following reactions: 3 — ionization of substituted anilinium ions in water at $25^\circ$C; 8 — bromination of substituted acetophenones in acetic acid–water–sodium acetate at $25^\circ$C; 12 – Ionization of substituted phenylboric acids in $25\%$ ethanol at $25^\circ$C; 14 — solvolysis of substituted benzoyl chlorides in methanol at $25^\circ$C. The position of the scale of ordinates is arbitrary.

16

Relationships in Rate and Equilibrium Phenomena" (70). It does not seem to have been received with enormous enthusiasm. The $\rho\sigma$ relation did, of course, feature a year or two later in Hammett's book *Physical Organic Chemistry* as part of Chapter VII: "The Effect of Structure on Reactivity" (4,71). I have the feeling that interest in the Hammett equation was slow to develop among the chemical community until H. H. Jaffé gave it extensive exposure in his "Re-examination of the Hammett Equation" published in *Chemical Reviews* in 1953, in which the application of the Hammett equation to about 400 reaction series was presented (72). At around the same time Robert W. Taft, who had done postdoctoral work with Hammett in the late 1940s, began to publish work on the systems for which no simple Hammett-type treatment had been found to apply, notably most of the reactions of aliphatic systems and of *ortho*-substituted benzene derivatives (73). Taft's successful work in this area became well known after it was featured in the book *Steric Effects in Organic Chemistry* edited by M. S. Newman in 1956 (74). Thus the 1950s saw the real flowering of what Hammett had started in structure–reactivity relationships: the refine-ment and extension of the Hammett equation (75); the proliferation of different types of sigma value [notably $\sigma^+$ (76) and $\sigma^-$] (75); the dissection into $\sigma_I$ and $\sigma_R$ (77); the separation of polar, steric, and resonance effects (to use Taft's own phrase) through $\sigma^*$ and $E_s$ (73, 74, 78); the treatments proposed by Wepster (79) and by Yukawa and Tsuno (80); the dual substituent–parameter equation (81); the application of Hammett-type treatments to spectroscopic data [notably NMR] (82); and so on. But in all of this Hammett was content to be an observer, duly recording what went on up to about 1970 in the second edition of his *Physical Organic Chemistry* (8), with some *caveats* (83). We should recall, however, Hammett's recognition in 1937 (5) that the *para*-nitro group required on occasion an exalted $\sigma$ value (now designated $\sigma^-$), thereby indicating one of the directions in which the $\rho\sigma$ equation would be further developed (84).

Although Hammett made no attempt to follow up the $\rho\sigma$ relation through experimental work of his own (85), he did continue kinetic studies of various kinds in the 1930s. These were mainly on substitution reactions, and they continued through the period of World War II to the later 1940s, leading to 12 papers (86–97). The topics investigated were the reaction of benzyl chloride with mercuric salts (86); the Walden inversion in the solvolysis of $\alpha$-phenylethyl chloride (87); water catalysis in the alcoholysis of benzhydryl chloride (88, 89); the reactions of benzyl chloride with water, hydroxide ion, and acetate ion (90); various reactions of ethyl and other $p$-toluenesulfonates (92, 95); reactions of $t$-butyl and benzyl nitrate with water and hydroxide ion (93); and reactions of alkyl bromides with thiosulfate ion (96, 97). There were also some studies of reactions of the carbonyl group (91, 94). All this work, with various collaborators, was designed and carried out very carefully.

## VII. *PHYSICAL ORGANIC CHEMISTRY*, 1940

There is no doubt that Hammett's book *Physical Organic Chemistry*, published in 1940, made him much better known in the worldwide chemical community than had been the case hitherto. The influence of the book grew slowly, probably because at the time the book was published some of the world was already at war and most of the rest of the world became so involved shortly afterward. It was reviewed for the *Journal of the American Chemical Society* by Paul Bartlett, who regarded it highly (98). We will reproduce some passages from the review.

> Courses in physical organic chemistry are now offered in an increasing number of chemistry departments. Of the very few books in the field, this one is the first which can be unqualifiedly recommended as a text for a course dealing with the mechanisms of organic reactions. As a physical chemist whose researches on rates, equilibria, and mechanisms of reactions in solutions have been of basic importance to theoretical organic chemistry, Professor Hammett is uniquely qualified to write this book.

> The book as a whole is characterized by the maturity and discrimination with which it is assembled. The viewpoint is systematic rather than historical. Little attention is given to discarded ideas, however widely believed or recently upset.

> The author writes like a physical chemist in that the discussions are quantitative and are developed algebraically whenever this contributes to sharpness of definition. He writes like an organic chemist in that no general statement is found very far from its supporting evidence.

The presentation of the subject matter of the book does, in fact, contrast in various ways with the forms adopted in other physical organic books of the time, notably those by Waters (first published in 1935) (99), Watson (first published in 1937) (100), and Branch and Calvin (published in 1941) (101). The high quality of Hammett's book is confirmed by its endurance as a source cited by the authors of papers. In the Five-Year Volumes (1965–1969) of *Science Citation Index*, Hammett's book secures about 600 citations, that is, an average of about 120 a year; this was for a book that was already a quarter of a century old. In 1987, 17 years after the second edition appeared, the first edition still secured 22 citations, compared with 40 citations for the second edition (including its various translations into foreign languages).

## VIII. HAMMETT AFTER 1940

During World War II, like many senior scientists of the time, Hammett was engaged in war work, particularly in the development of explosives and

**Figure 6**    Professor Louis P. Hammett. (The original print is in the archives of the National Academy of Sciences in Washington, D.C. and is dated June 1944. The portrait was taken by W. O. Breckon Studios, Pittsburgh, Pennsylvania.)

rocket propellants. At the end of the war Hammett was 51 years of age and could hopefully look forward to about 15 years of academic work before retirement. As far as experimental research was concerned, he appears to have looked around for some topics that would be largely fresh and thus stimulating to him but within the general field of solution kinetics. One topic was a revival of a slight interest of some years earlier: the acid-catalyzed hydration of olefines, on which he had published a paper with G. R. Lucas in 1942 (102). Among those involved in the later study of olefin hydration was

R. W. Taft, then doing postdoctoral work with Hammett. Taft's name appears on all four papers on olefine hydration, along with J. B. Levy and D. Aaron (103–106). A second topic pursued by Hammett in the later 1940s and 1950s was the hydrolysis of esters catalyzed by cation exchange resins (107–113). The main series of the papers, published between 1953 and 1958, was under the general title of "Specific Effects in Acid-Catalysis by Ion Exchange Resins" (108–111,113). A third area of research was essentially concerned with developing techniques for studying faster reactions than could be dealt with by the kinetic procedures of the times. Thus Hammett worked with several collaborators on the stirred flow reactor (114–118), studying various reactions, including the alkaline bromination of acetone (114) and the alkaline hydrolysis of methyl and ethyl formate (117) and of diethyl succinate (118). The work with the stirred-flow reactor well reveals Hammett's interest in carrying out elegant experimental studies, a feature characteristic of so much of his work.

## IX. THE TEXTBOOK OF PHYSICAL CHEMISTRY

In 1952 Hammett's long experience of teaching physical chemistry came to fruition with the publication of his book *Introduction to Physical Chemistry* (119). This was another contribution to McGraw-Hill's International Chemical Series, of which Hammett had been Consulting Editor since 1940. The book was designed for a one-year course and was rather narrower in its scope than most textbooks of physical chemistry. Thus its emphasis was primarily on thermodynamics, chemical equilibrium, gases and kinetic theory, the phase rule, dilute solutions, electrochemistry, and homogeneous chemical kinetics. There was no treatment of atomic and molecular structure, spectroscopy of any type, or the solid state; and there was only very brief treatment of surface chemistry. Mathematical difficulties were not avoided, and there was generous provision of numerical problems for the student to work. The book was doubtless very sound but does not seem to have achieved the success which came to certain other American textbooks of physical chemistry, which had their origins around the 1950s and have been through several editions, so that they are still greatly used (120).

## X. HAMMETT THE ELDER STATESMAN

In 1954 Hammett passed his sixtieth birthday and in the 1950s and early 1960s began to accumulate the responsibilities and rewards that come to those who are recognized as elder statesmen in their particular disciplines. In March 1954 he addressed the General Meeting at the 125th National Meeting of the

American Chemical Society in Kansas City on "Rights and Responsibilities in the Search for Knowledge" (121). From about 1954 to 1960 Hammett was a member of the important Committee on Professional Training of the American Chemical Society and was its chairman during the latter part of his membership thereof. He received the Nichols award of the American Chemical Society in 1957, the James Flack Norris Award twice (in 1960 and 1966), the Priestley Medal (9, 122) and also the Willard Gibbs Medal in 1961, the Lewis Medal in 1967, the Chandler Medal and a National Medal of Science in 1968, and the Barnard Medal in 1975. At various times he acquired emeritus status in not only his own Columbia University but also in the American Chemical Society and the National Academy of Science; he also became an Honorary Fellow of the Royal Society of Chemistry.

## XI. HAMMETT IN "RETIREMENT"

Hammett retired in 1961, one year in advance of the compulsory retirement regulation of Columbia University, and he and his wife went to live year-round in what had previously been their summer home in Newton, New Jersey. It was "retirement" only in the sense of withdrawing from full-time paid employment, for in the 1960s Hammett continued to keep well in touch with developments in physical organic chemistry and began to revise his 1940 book for its second edition, which finally appeared in 1970 (8). In his preface to the second edition Hammett indicated that it grew out of lectures and seminars presented when he was a guest at various universities and institutions. In the outcome, the second edition was really an "edition" in name only; it is effectively an entirely new book. He himself points out the contrasts with the situation 30 years earlier. The book is still concerned with reaction rates, equilibria, and mechanisms (as its subtitle indicates), but in order to keep the size of the book within reasonable bounds, some topics in the first edition had to be dropped entirely from the second, notably free-radical reactions and molecular orbital theory, which were given 27 pages and 5 pages, respectively, in the first edition. By the 1960s these topics had become the subjects of books of about 600 pages (123) and 460 pages (124), respectively!! Furthermore, even within the subjects dealt with, Hammett's emphasis is on principles and illustration by carefully selected examples, rather than on an encyclopedic treatment.

My own personal contacts with Hammett were regrettably few. In 1969, arising from the Second Conference on Linear Free Energy Relationships (LFER) held at Irvine, California, the previous year, I wrote an article on LFER for *Chemistry in Britain* (125). I sent Hammett a copy, congratulating him at the same time on attaining three-quarters of a century. I received a very

gracious and encouraging reply, which I still treasure. My feelings were perhaps rather akin to those of Hammett himself when he received an encouraging letter from Hantzsch 40 years earlier (10)!! Around 1970 Hammett very kindly agreed to write a foreword to *Advances in Linear Free Energy Relationships*, edited by N. B. Chapman and myself, which was the first international research monograph on LFER, ultimately appearing in 1972 (126). This foreword seems to have aroused quite a lot of interest, for I have heard it quoted in lectures and have seen references to it in the literature (127). I like very much the sentence: "To my mind a particularly happy aspect of the existence of linear free energy relationships has been the proof it supplies that one need not suppose that the behavior of nature is hopelessly complicated merely because one cannot find a theoretical reason for supposing it to be otherwise." I also like his mildly disapproving quotation of certain (unnamed) authors who claim that "there are at least five different processes by which substituents can affect a distant reaction center."

In July 1975 Marek Krygowski (128) and I were both staying with Marvin (129) and Barbara Charton in Brooklyn Heights, Brooklyn, N. Y. By that time the Hammetts had moved to a Quaker Retirement Community in Medford, New Jersey. One day Marvin Charton, Marek Krygowski, and I journeyed



**Figure 7**   Professor and Mrs. Hammett at home in Medford, New Jersey, July 1975, reproduced by courtesy of Professor Marvin Charton.

out to Medford by bus, about a two-hour ride from Manhattan. We spent a delightful day with the Hammetts. Professor Hammett was then in his eighty-second year and still showed a keen interest in physical organic chemistry. The photograph of Professor and Mrs. Hammett in Fig. 7, taken by Marvin Charton, records the occasion. This was the only time I met Professor Hammett.

In September 1983 a Symposium on the History of Physical Organic Chemistry was arranged in Hammett's honor by the Divisions of the History of Chemistry and of Organic Chemistry of the American Chemical Society as part of the 186th National Meeting in Washington, D.C. This was a few months before Hammett's ninetieth birthday. At that time his health was not too good and he was, unfortunately, not able to attend in person, but tapes and transcriptions of the lectures were sent to him.

My final contact with him was in 1986, about a year before he died. A lecture on "The Hammett Equation and All That after Fifty Years," which I had given several times in the Federal Republic of Germany and elsewhere, had been translated into German for the magazine *Chemie in unserer Zeit* (75f). Hammett had kindly given me permission to use in this article the portrait shown in Fig. 1 of this chapter. I sent Hammett a copy of the article and received an appreciative reply. He wrote:

> I take pleasure from reading your lecture in the *Chemie in unserer Zeit* which recently reached me. It was another pleasant reminder that there are still enthusiasts for a branch of chemistry which I had some hand in starting; it also reminded me that I can still read scientific German and supplied me with an excellent group picture of friends and supporters.

The group picture referred to was that of speakers and organisers for the Second Conference on Correlation Analysis in Organic Chemistry at the University of Hull in 1982.

It has been a great privilege to give this Hammett Memorial Lecture as the opening Plenary Lecture in a Symposium named in Hammett's honor. Our presence here in Poznań for the Fourth Conference on Correlation Analysis in Organic Chemistry, coming as we do from about 15 countries worldwide, is a great tribute to his continuing influence. Evidently we have inherited the enthusiasm that Hammett had for our part of physical organic chemistry. I can think of no better way of concluding this lecture than by quoting the words with which Hammett closed his Norris Award address some 22 years ago (10), since they express an attitude to our subject and a confidence in its future which I hope we can still share. Hammett said: "So, for many years to come, I am sure physical organic chemistry will continue to be fun, as it has been all the time I have been a chemist" (130).

# REFERENCES AND NOTES

1. *American Men and Women of Science*, 15th ed., Vol. 3, Bowker, New York, 1982, p. 449.

2. D. S. Tarbell and A. T. Tarbell, *The History of Organic Chemistry in the United States, 1875–1955*, Folio Publishers, Nashville, Tenn., 1986, 434 pp.

3. M. D. Saltzmann, "The Development of Physical Organic Chemistry in the United States and the United Kingdom, 1919–1939. Parallels and Contrasts," *J. Chem. Educ.*, **63**, 588 (1986).

4. L. P. Hammett, *Physical Organic Chemistry*, McGraw-Hill, New York, 1940, 404 pp.

5. L. P. Hammett, *J. Am. Chem. Soc.*, **59**, 96 (1937).

6. L. P. Hammett and A. J. Deyrup, *J. Am. Chem. Soc.*, **54**, 2721 (1932).

7. See reference 8, p. 355.

8. L. P. Hammett, *Physical Organic Chemistry*, 2nd ed., McGraw-Hill, New York, 1970, 420 pp.

9. L. P. Hammett, *Chem. Eng. News*, **39** (15), 94 (1961). Biographical material is appended on p. 98, and this has occasionally been used for the present article to supplement references 1 and 10.

10. L. P. Hammett, *J. Chem. Educ.*, **43**, 464 (1966).

11. (a) H. Staudinger and L. Hammet (*sic*), *Helv. Chim. Acta*, 4, 217 (1921); (b) H. Staudinger, L. Hammet (*sic*), and J. Siegvart, *Helv. Chim. Acta*, 4, 228 (1921).

12. H. T. Beans and L. P. Hammett, *J. Am. Chem. Soc.*, 47, 1215 (1925).

13. L. P. Hammett, *J. Am. Chem. Soc.*, 46, 7 (1924).

14. L. P. Hammett and A. E. Lorch, *J. Am. Chem. Soc.*, 54, 2128 (1932).

15. L. P. Hammett and A. E. Lorch, *J. Am. Chem. Soc.*, 55, 70 (1933).

16. L. P. Hammett, *Trans. Faraday Soc.*, 29, 770 (1933).

17. R. Rosenthal, A. E. Lorch, and L. P. Hammett, *J. Am. Chem. Soc.*, 59, 1795 (1937).

18. R. E. Plump and L. P. Hammett, *Trans. Electrochem. Soc.*, 73, 523 (1938).

19. L. P. Hammett and C. T. Sottery, *J. Am. Chem. Soc.*, 47, 142 (1925).

20. L. P. Hammett, *J. Chem. Educ.*, 17, 131 (1940).

21. L. P. Hammett, *Solutions of Electrolytes*, McGraw-Hill, New York, 1929; 2nd ed., 1936, 242 pp.

22. G. H. Walden, L. P. Hammett, and R. P. Chapman, *J. Am. Chem. Soc.*, 53, 3908 (1931).

23. G. H. Walden, L. P. Hammett, and R. P. Chapman, *J. Am. Chem. Soc.*, 55, 2649 (1933).

24. G. H. Walden, L. P. Hammett, and S. M. Edmonds, *J. Am. Chem. Soc.*, 56, 57, 350 (1934).

25. L. P. Hammett, G. H. Walden, and S. M. Edmonds, *J. Am. Chem. Soc.*, 56, 1092 (1934).

26. G. H. Walden, L. P. Hammett, and A. Gaines, *J. Chem. Phys.*, 3, 364 (1935).

27. A. Gaines, L. P. Hammett, and G. H. Walden, *J. Am. Chem. Soc.*, 58, 1668 (1936).

28. Hammett's association with Beans and Walden had one curious outcome: U. S. Patent 2029012, in the names of H. T. Beans, G. H. Walden, and L. P. Hammett, January 28, 1936, for Phonograph Records. According to *Chem. Abstr.*, 30, 1905 (1936), "A record material is prepared by heating a mixture of resorcinol, alcohol, and *p*-nitroaniline at 70° to form a solution, adding 40% formaldehyde, and further heating at about 70° until the precipitate formed is dissolved and a viscous liquid is formed, adding alcohol, cooling the solution to 30°, and adding Turkey red oil." (Beans had previously taken out other patents for new materials for sound recording.)

29. See "The Hantzsch Memorial Lecture" by T. S. Moore, *J. Chem. Soc.*, 1051 (1936).

30. Hantzsch's cryoscopic work in sulfuric acid has been reviewed by G. Scorrano and W. Walter, *J. Chem. Educ.*, 56, 728 (1979). These authors are concerned to point out that extensive work of the same kind was done by Hantzsch's Italian contemporary G. Oddo (1865–1954). There was, in fact, considerable rivalry between the two men. Oddo's work, published mainly in *Gazzetta Chimica Italiana*, does not seem to have had the same impact on Hammett as that of Hantzsch, at least to Hammett's recollection in later life (10).

31. J. N. Brønsted, *Rec. Trav. Chim. Pays-Bas*, 42, 718 (1923). Hammett admits (10) that he did not know, until later, of the contemporary contribution to acid-base theory by T. M. Lowry, *J. Soc. Chem. Ind. (London)*, 42, 43 (1923). [This reference may also be written as *Chem. Ind. Rev.*, 1, 43 (1923).]

32. L. P. Hammett, *J. Am. Chem. Soc.*, 50, 2666 (1928).

33. L. P. Hammett and N. Dietz, *J. Am. Chem. Soc.*, 52, 4795 (1930).

34. L. P. Hammett and A. J. Deyrup, *J. Am. Chem. Soc.*, 54, 4239 (1932).

35. L. P. Hammett and A. J. Deyrup, *J. Am. Chem. Soc.*, 55, 1900 (1933).

36. According to Scorrano and Walter (30), Oddo, rather than Hantzsch, should be given the credit for cryoscopic demonstration of the formation of the triphenylmethyl carbenium ion.

37. R. P. Chapman and L. P. Hammett, *Ind. Eng. Chem., Anal. Ed.*, 5, 346 (1933).

38. L. P. Hammett and R. P. Chapman, *J. Am. Chem. Soc.*, 56, 1282 (1934).

39. L. P. Hammett, *Chem. Rev.*, 13, 61 (1933).

40. L. P. Hammett and M. A. Paul, *J. Am. Chem. Soc.*, 56, 827 (1934).

41. L. P. Hammett and M. A. Paul, *J. Am. Chem. Soc.*, 56, 830 (1934).

42. L. P. Hammett and F. A. Lowenheim, *J. Am. Chem. Soc.*, 56, 2620 (1934).

43. L. P. Hammett, A. Dingwall, and L. A. Flexser, *J. Am. Chem. Soc.*, 56, 2010 (1934).

44. L. A. Flexser, L. P. Hammett, and A. Dingwall, *J. Am. Chem. Soc.*, 57, 2103 (1935).

45. L. P. Hammett, *Chem. Rev.*, 16, 67 (1935).

46. M. A. Paul and L. P. Hammett, *J. Am. Chem. Soc.*, 58, 2182 (1936).

47. H. P. Treffers and L. P. Hammett, *J. Am. Chem. Soc.*, 59, 1708 (1937).

48. L. A. Flexser and L. P. Hammett, *J. Am. Chem. Soc.*, 60, 885 (1938).

49. L. A. Flexer and L. P. Hammett, *J. Am. Chem. Soc.*, 60, 3097 (1938). (This is a brief correction to reference 44).

50. L. Zucker and L. P. Hammett, *J. Am. Chem. Soc.*, 61, 2779 (1939).

51. L. Zucker and L. P. Hammett, *J. Am. Chem. Soc.*, 61, 2785 (1939).

52. L. Zucker and L. P. Hammett, *J. Am. Chem. Soc.*, 61, 2791 (1939).

53. L. P. Hammett, *J. Chem. Phys.*, 8, 644 (1940).

54. C. K. Ingold, *Structure and Mechanism in Organic Chemistry*, 2nd ed., Bell, London, 1969, Chap. XV.

55. C. H. Rochester, *Acidity Functions*, Academic Press, London, 1970, Chap. 4.

56. J. F. Bunnett and F. P. Olsen, *Can. J. Chem.*, 44, 1899, 1917 (1966).

57. L. C. Smith and L. P. Hammett, *J. Am. Chem. Soc.*, 67, 23 (1945).

58. H. Van Looy and L. P. Hammett, *J. Am. Chem. Soc.*, 81, 3872 (1959).

59. R. A. Cox and K. Yates, *Can. J. Chem.*, 61, 2225 (1983).

60. Reference 4, pp. 269–270.

61. J. N. Brønsted and K. Pedersen, *Z. Physik. Chem.*, 108, 185 (1924).

62. J. N. Brønsted, *Om Syre- og Base-katalyse,* University of Copenhagen, 1926; English translation, *Chem. Rev.,* 5, 231 (1928).

63. L. P. Hammett, *Chem. Rev.,* 17, 125 (1935).

64. While summarizing what Hammett wrote in reference 10, pp. 465–467, I have ventured to include certain additional names, particularly of chemists in the United Kingdom. This is to make clear that the British contributions to solution kinetics were not limited to Lapworth in the earlier period and Ingold in the later period, as these are the names that Hammett makes prominent. To follow Hammett exactly here might encourage a misleading impression, which Hammett can hardly have intended to give. In particular, Orton deserves mention, not only for his own contributions but also because of the later distinction of several of his pupils at the University College of North Wales, Bangor, including E. D. Hughes, the long-time collaborator of Ingold. (Hughes is mentioned in passing by Hammett.) Further, the contribution of chemists at the University of Oxford should certainly not be ignored. Bell is mentioned in passing by Hammett (reference 10, p. 464), but not Hinshelwood, whose main interest in the 1920s was gas kinetics, but who developed in the 1930s a strong interest in solution kinetics, initially in association with Moelwyn-Hughes, cf. Hammett's remark (reference 10, p. 466) that "Chemists working on kinetics in solution and those working on kinetics in the gas-phase have tended to be intolerant of each other and communication has been decidedly limited". For further details on these matters, see reference 3; also J. Shorter, *CHEMTECH* (4), 252 (1985). (The title of this article, "The British School of Physical Organic Chemistry," is misleading, as it has been changed without the author's permission from "The Contributions of British Physical Chemists to Physical Organic Chemistry.")

65. L. P. Hammett and H. L. Pfluger, *J. Am. Chem. Soc.,* 55, 4079 (1933).

66. G. N. Burkhardt, *Nature, 136,* 684 (1975).

67. G. N. Burkhardt, W. G. K. Ford, and E. Singleton, *J. Chem. Soc.,* 17 (1936).

68. See reference 4, p. 186; reference 8, p. 351 and reference 10, p. 467.

69. The form of words chosen by Hammett for the title of the paper in reference 5 rather suggests that he may have envisaged the producing of at least one further paper on other "derivatives". At all events, no paper that was explicitly or implicitly Part 2 ever appeared. [Hammett had previously used the first sentence of the title of reference 5 in L. P. Hammett, *J. Chem. Phys.,* 4, 613 (1936), a short note dealing with influences of temperature and solvent.] One might, perhaps, see Hammett's continuing influence in the work of his postdoctoral assistant R. W. Taft (73, 74). However, in a personal communication to the present author (October 1988), Professor Taft wrote as follows: "You are right, I think, in believing that Louis had no interest himself in extending his equation. He always encouraged me in my attempts to do so, however. He offered critical comments about concerns that he had. When I first arrived at Columbia I was very anxious to talk with him about the Ingold relationship and the results I had at hand to use it to define $\sigma^*$ values, particularly for alkyl substituents. He was highly skeptical."

70. L. P. Hammett, *Trans. Faraday Soc., 34,* 156 (1938).

71. Some developments had occurred, as between the presentations in reference 5 and 4. Further experimental studies had appeared, and the number of reaction series to which the $\rho\sigma$ relation could be applied had been increased from 38 to 51. The number of $\sigma$ values tabulated had been increased from 31 to 44.

72. H. H. Jaffé, *Chem. Rev., 53,* 191 (1953).

73. R. W. Taft, *J. Am. Chem. Soc., 74,* 2729, 3120 (1952); 75, 4231, 4534, 4538 (1953).

74. R. W. Taft, in M. S. Newman, Ed., *Steric Effects in Organic Chemistry*, Wiley, New York, 1956, Chap. 13.

75. The history of the refinement and extension of the Hammett equation, beginning in the 1950s, may be followed through several review articles and books, for example: (a) O. Exner, "The Hammett Equation—the Present Position," in N. B. Chapman and J. Shorter, Eds., *Advances in Linear Free Energy Relationships*, Plenum, London, 1972, Chap. 1; (b) J. Shorter, "Multiparameter Extensions of the Hammett Equation," in N. B. Chapman and J. Shorter, Eds., *Correlation Analysis in Chemistry: Recent Advances*, Plenum, New York, 1978, Chap. 4; (c) M. Charton, "Applications of Linear Free Energy Relationships to Polycyclic Arenes and to Heterocyclic Compounds," in N. B. Chapman and J. Shorter, Eds., *Correlation Analysis in Chemistry: Recent Advances*, Plenum, New York, 1978, Chap. 5; (d) C. D. Johnson, *The Hammett Equation*, University Press, Cambridge, 1973; (e) J. Shorter, "The Hammett Equation and Its Extensions," in *Correlation Analysis of Organic Reactivity, with Particular Reference to Multiple Regression*, Research Studies Press, Wiley, Chichester, U.K., 1982, Chap. 3; (f) J. Shorter, "Die Hammett-Gleichung – und was daraus in fünfzig Jahren wurde," *Chem. in uns. Zeit, 19*, 197 (1985).

76. (a) H. C. Brown and Y. Okamoto, *J. Am. Chem. Soc., 79*, 1913 (1957); *80*, 4979 (1958); (b) L. M. Stock and H. C. Brown, *Adv. Phys. Org. Chem., 1*, 35 (1963).

77. R. W. Taft and I. C. Lewis, *J. Am. Chem. Soc., 80*, 2436 (1958); *81*, 5343 (1959).

78. This topic has been reviewed several times by the present author: (a) J. Shorter, *Quart. Rev. Chem. Soc., 24*, 433 (1970); (b) J. Shorter, in reference 75a, Chap. 2; (c) J. Shorter, in reference 75e, Chap. 4.

79. H. van Bekkum, P. E. Verkade, and B. M. Wepster, *Rec. Trav. Chim. Pays-Bas, 78*, 815 (1959).

80. (a) Y. Yukawa and Y. Tsuno, *Bull. Chem. Soc. Jpn., 32*, 971 (1959); (b) Y. Yukawa, Y. Tsuno, and M. Sawada, *Bull. Chem. Soc. Jpn., 39*, 2274 (1966).

81. (a) S. Ehrenson, *Progr. Phys. Org. Chem., 2*, 195 (1964); (b) S. Ehrenson, R. T. C. Brownlee, and R. W. Taft, *Progr. Phys. Org. Chem., 10*, 1 (1973).

82. For appropriate reviews, see: (a) D. F. Ewing, in reference 75b, Chap. 8 (survey for chemical shifts of $^1$H, $^{13}$C, and $^{19}$F); (b) A. R. Katritzky and R. D. Topsom, in reference 75a, Chap. 3. (Review for infrared and ultraviolet spectroscopy, both frequencies and intensities.)

83. For example, see reference 8, p. 365. "It does not always seem to be recognized that effective evidence for the Yukawa-Tsuno hypothesis is obtainable only from correlations which include more than one strong through-resonating substituent and for which the value of $r$ is neither close to unity nor close to zero."

84. Rather curiously Hammett did not give in either reference 5 or 4 (Chap. VII) any explanation of the need for an exalted $\sigma$ value for $p$-$NO_2$ in treating the reactions of anilines and phenols. The appropriate explanation is given in reference 8, pp. 357–358.

85. The only published example of Hammett using his own experimental results in connection with the $\rho\sigma$ equation was his use of data from L. A. Wooten and L. P. Hammett, *J. Am. Chem. Soc., 57*, 2289 (1935) on the relative strengths of benzoic acids in *n*-butyl alcohol (5). The $\rho$ value was considerably enhanced, relative to the value in water, in the less polar solvent. A kinetic study of the ammonolysis of phenylacetic esters in methanol solution by R. L. Betts and L. P. Hammett, *J. Am. Chem. Soc., 59*, 1568 (1937) did not involve sufficient *meta*- or *para*-substituents for the application of the $\rho\sigma$ relation to be worthwhile.

86. I. Roberts and L. P. Hammett, *J. Am. Chem. Soc., 59*, 1063 (1937).

87. J. Steigman and L. P. Hammett, *J. Am. Chem. Soc.*, 59, 2536 (1937).

88. N. T. Farinacci and L. P. Hammett, *J. Am. Chem. Soc.*, 59, 2542 (1937).

89. N. T. Farinacci and L. P. Hammett, *J. Am. Chem. Soc.*, 60, 3097 (1938). (This paper makes a correction to reference 88.)

90. G. W. Beste and L. P. Hammett, *J. Am. Chem. Soc.*, 62, 2481 (1940).

91. F. P. Price and L. P. Hammett, *J. Am. Chem. Soc.*, 63, 2387 (1941).

92. H. R. McCleary and L. P. Hammett, *J. Am. Chem. Soc.*, 63, 2254 (1941).

93. G. R. Lucas and L. P. Hammett, *J. Am. Chem. Soc.*, 64, 1928 (1942).

94. J. D. Gettler and L. P. Hammett, *J. Am. Chem. Soc.*, 65, 1824 (1943).

95. F. C. Foster and L. P. Hammett, *J. Am. Chem. Soc.*, 68, 1736 (1946).

96. T. I. Crowell and L. P. Hammett, *J. Am. Chem. Soc.*, 70, 3444 (1948).

97. P. M. Dunbar and L. P. Hammett, *J. Am. Chem. Soc.*, 72, 109 (1950).

98. P. D. Bartlett, *J. Am. Chem. Soc.*, 62, 1882 (1940).

99. W. A. Waters, *Physical Aspects of Organic Chemistry*, Routledge, London, 1935, 501 pp.

100. H. B. Watson, *Modern Theories of Organic Chemistry*, Clarendon Press, Oxford, 1937, 218 pp.

101. G. E. K. Branch and M. Calvin, *The Theory of Organic Chemistry*, Prentice-Hall, Englewood Cliffs, N.J., 1941, 523 pp.

102. G. R. Lucas and L. P. Hammett, *J. Am. Chem. Soc.*, 64, 1938 (1942).

103. J. B. Levy, R. W. Taft, D. Aaron, and L. P. Hammett, *J. Am. Chem. Soc.*, 73, 3792 (1951).

104. R. W. Taft, J. B. Levy, D. Aaron, and L. P. Hammett, *J. Am. Chem. Soc.*, 74, 4735 (1952).

105. J. B. Levy, R. W. Taft, and L. P. Hammett, *J. Am. Chem. Soc.*, 75, 1253 (1953).

106. J. B. Levy, R. W. Taft, D. Aaron, and L. P. Hammett, *J. Am. Chem. Soc.*, 75, 3955 (1953).

107. V. C. Haskell and L. P. Hammett, *J. Am. Chem. Soc.*, 71, 1284 (1949).

108. S. A. Bernhard and L. P. Hammett, *J. Am. Chem. Soc.*, 75, 1798 (1953).

109. S. A. Bernhard and L. P. Hammett, *J. Am. Chem. Soc.*, 75, 5834 (1953).

110. S. A. Bernhard, E. Garfield, and L. P. Hammett, *J. Am. Chem. Soc.*, 76, 991 (1954).

111. P. Riesz and L. P. Hammett, *J. Am. Chem. Soc.*, 76, 992 (1954).

112. H. Samelson and L. P. Hammett, *J. Am. Chem. Soc.*, 78, 524 (1956).

113. C. H. Chen and L. P. Hammett, *J. Am. Chem. Soc.*, 80, 1329 (1958).

114. H. H. Young and L. P. Hammett, *J. Am. Chem. Soc.*, 72, 280 (1950).

115. J. Saldick and L. P. Hammett, *J. Am. Chem. Soc.*, 72, 283 (1950).

116. M. J. Rand and L. P. Hammett, *J. Am. Chem. Soc.*, 72, 287 (1950).

117. H. M. Humphreys and L. P. Hammett, *J. Am. Chem. Soc.*, 78, 521 (1956).

118. R. L. Burnett and L. P. Hammett, *J. Am. Chem. Soc.*, 80, 2415 (1958).

119. L. P. Hammett, *Introduction to Physical Chemistry*, McGraw-Hill, New York, 1952, 420 pp.

120. For example, W. J. Moore, *Physical Chemistry*, Prentice-Hall, New York, 1950 ran through five editions to 1972 and now has a new lease of life as *Basic Physical Chemistry*, 1983.

121. L. P. Hammett, *Chem. Eng. News*, 32, 1462 (1954).

122. Hammett's Priestley Medal Address was entitled "Choice and Chance in Scientific Communication."

123. C. Walling, *Free Radicals in Solution*, Wiley, New York, 1957, 631 pp.

124. M. J. S. Dewar, *The Molecular Orbital Theory of Organic Chemistry*, McGraw-Hill, New York, 1969, 484 pp.

125. J. Shorter, *Chem. Brit.*, *5*, 269 (1969).

126. Individual chapters of this are cited as references 75a, 78b, and 82b.

127. For example, S. Wold and M. Sjöström, *Acta Chem. Scand. B*, *40*, 270 (1986).

128. Professor of Chemistry, University of Warsaw, Poland.

129. Professor of Chemistry, Pratt Institute, Brooklyn, N.Y.

130. By a happy coincidence, just before the conference (July 1988) there appeared a further book in which the Hammett equation and related topics are prominent: O. Exner, *Correlation Analysis of Chemical Data*, Plenum, New York, and SNTL Prague, 1988, 275 pp.

# Thermodynamics of Molecular Species

BY Ernest Grunwald

*Department of Chemistry*
*Brandeis University*
*Waltham, Massachusetts*

## CONTENTS

## I. INTRODUCTION

In contrast to traditional thermodynamics, which confines itself to macroscopic observations, chemical thermodynamics includes molecular theory, building a bridge between macroscopic observations, and events taking place on the molecular level. The difference between the two sciences begins with the specification of composition. In traditional thermodynamics the independent variables are the components, defined as an irreducible set of substances needed to specify the composition. In chemical thermodynamics the composition is specified by the molecular species in as much detail as those species are known. As a minimum, one chooses the components of traditional thermodynamics to be *formal* components, that is, to be pure substances whose chemical or empirical formulas are known. The resulting composition is the *formal* composition. However, while specification of the formal composition is necessary to an understanding of reactivity on the molecular level, it may not be sufficient, because new molecular species appear if the

formal molecules associate, dissociate, or react. For example, when the formal component NaCl is dissolved in dimethylsulfoxide, the molecular species are NaCl ion pairs, solvated sodium ions, and solvated chloride ions. The mole numbers $n_A, n_B, \ldots$ (letter subscripts) of the molecular species are related to the formula-weight numbers $n_1, n_2, \ldots$ (number subscripts) of the formal components according to the laws of stoichiometry.

In this chapter we deal with the relationships between the thermodynamic properties of formal components and those of molecular species. The nomenclature used to describe the two kinds of property is confusingly similar, yet in fact there is a marked difference between them. Properties of formal components are defined for homogeneous phases at full equilibrium, while those of molecular species are defined for homogeneous phases that may depart from chemical equilibrium. Experimental thermodynamic properties (as listed in standard tables) are properties of formal components, while chemical equilibria, rate processes, and reaction mechanisms are described by properties of molecular species. The transformations between the two kinds of property employ constraints of stoichiometry and of chemical equilibrium.

## II.  REACTIVITY AND GIBBS FREE ENERGY

It is convenient to begin with the Gibbs free energy $G$ because of the close connection between this function and rate and equilibrium constants. At constant $T$ and $P$ (temperature and pressure), the equilibrium constant $K$ is related to the standard free-energy change $\Delta G^\circ$ by Equation 1 (1). The rate constant $k$, according to transition state theory (2), is related to the standard free energy of activation $\Delta G^\#$ by Equation 2.

$$\ln K = \frac{-\Delta G^\circ}{RT} \tag{1}$$

$$\ln k = \ln\left(\frac{k_B T}{h}\right) - \frac{\Delta G^\ddagger}{RT} \tag{2}$$

The free-energy changes in these equations are those of molecular species.

In a rate process, or approach to chemical equilibrium, as described by the transition state theory, the molecular energy distributions for all species are relaxed to a uniform temperature $T(2)$. Because such relaxation takes time. Equation 2 does not apply to chemical reactions with very short half-times. In liquid solutions this is rarely a limitation, however, because relaxation to a uniform temperature is known to be quite fast (3). A rough estimate based on

realistic relaxation rates shows that Equation 2 applies to reactions with half-times as short as $10^{-8}$ s.

## III.  PARTIAL MOLAR FREE ENERGY

As stated above, the macroscopic measurements of thermodynamics yield partial molar free energies for formal components, while the reactivity relationships require partial molar free energies for molecular species. The properties of an isotropic phase at constant $T$ and $P$ are defined when the mass and composition of the phase are specified. If the phase is at chemical equilibrium, one may specify either the mole numbers of the molecular species or the formula-weight numbers of the formal components. If the phase is not at chemical equilibrium, however, one must specify the mole numbers. The formula-weight numbers are not suitable because they do not indicate just *how* the formal components deviate from equilibrium.

For definiteness, let us consider a specific example: a liquid system consisting of the components "triethylamine" and "chloroform." Thermodynamic measurements over the full range of composition show (4) that on the molecular level one must consider three species: triethylamine monomer (A), chloroform monomer (B), and triethylamine·chloroform hydrogen-bonded complex (C), according to (3).

$$(C_2H_5)_3N + CHCl_3 = (C_2H_5)_3N \cdot HCCl_3$$
$$A \quad + \quad B \quad = \quad C$$
$$(3)$$
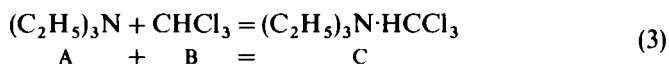
When chemical equilibrium exists, the free energy $G$ at constant $T$ and $P$ may be expressed as a function of the formula-weight numbers $n_1$ of triethylamine and $n_2$ of chloroform. Moreover, $G$ satisfies the mathematical conditions of Euler's theorem for a homogeneous function of the first degree (1) and thus may be expressed by Equation 4.

$$G = n_1 \left( \frac{\partial G}{\partial n_1} \right)_{n_2} + n_2 \left( \frac{\partial G}{\partial n_2} \right)_{n_1} = n_1 G_1 + n_2 G_2 \qquad (4)$$

$$G_1 = \left( \frac{\partial G}{\partial n_1} \right)_{n_2} \qquad G_2 = \left( \frac{\partial G}{\partial n_2} \right)_{n_1} \qquad (5)$$

The partial derivatives denoted by $G_1$ and $G_2$ in Equation 5 are the partial molar free energies.

Because $G$ is a function of $n_1$ and $n_2$, its differential is expressed in terms of $G_1$ and $G_2$ by Equation 6. Differentiation of Equation 4 and introduction of

Equation 6 then yields the Gibbs–Duhem equation (Equation 7) (1):

$$dG = G_1\, dn_1 + G_2\, dn_2 \tag{6}$$

$$n_1 dG_1 + n_2 dG_2 = 0 \tag{7}$$

Because the variables in Equations 4–7 are the formula-weight numbers $n_1$ and $n_2$, $G_1$ and $G_2$ are the partial molar free energies of the *formal components*. To express $G$ in terms of molecular species, one expresses it as a function the mole numbers $n_A$, $n_B$, and $n_C$. As before, the liquid mixture is isotropic and at constant $T$ and $P$. The development starting with Euler's theorem now takes the form

$$G = n_A G_A + n_B G_B + n_C G_C \tag{8}$$

$$G_A = \left(\frac{\partial G}{\partial n_A}\right)_{n_B, n_C} \qquad G_B = \left(\frac{\partial G}{\partial n_B}\right)_{n_A, n_C} \qquad G_C = \left(\frac{\partial G}{\partial n_C}\right)_{n_A, n_B} \tag{9}$$

$$n_A\, dG_A + n_B\, dG_B + n_C\, dG_C = 0 \tag{10}$$

The mathematical conditions for Euler's theorem are satisfied by any phase whose intensive properties are uniform throughout. Existence of chemical equilibrium is not required. This explains why Equation 8 shows three independent variables whereas Equation 4, which applies only at chemical equilibrium, shows only two. It also explains the peculiar definition of partial molar free energies in Equation 9. Physically it is not possible to vary $n_A$ at constant $n_B, n_C$ unless the solution is allowed to depart from chemical equilibrium.

To relate the partial molar free energies of the formal components to those of the molar species, one begins with Equation 8, introduces constraints of stoichiometry (Equation 11), and minimizes the free energy at chemical equilibrium by solving Equation 12. The result, when combined with Equation 10, yields Equation 13 and permits elimination of $n_C$ from Equation 11 to yield Equation 14. Equation 13 will be used in the next Section to derive an expression for the equilibrium constant.

$$G = (n_1 - n_C)G_A + (n_2 - n_C)G_B + n_C G_C \tag{11}$$

At chemical equilibrium:

$$\left(\frac{\partial G}{\partial n_C}\right)_{n_1, n_2} = 0 \tag{12}$$

$$G_C - G_A - G_B = \Delta G = 0 \tag{13}$$

$$G = n_1 G_A + n_2 G_B \tag{14}$$

To obtain the desired relationship between partial molar free energies of formal components and those of molecular species, we note that Equations 4 and 14 express $G$ as a function of the same independent variables: $n_1$ and $n_2$. The coefficients of $n_1$ and $n_2$ must therefore be equal. On introducing Equation 13, one obtains a further relationship for the complex C. The results are

$$G_A = G_1; \qquad G_B = G_2; \qquad G_C = G_1 + G_2 \tag{15}$$

It is convenient to summarize the results of the present development in the form of two general theorems:

**Theorem A:** In a solution at equilibrium, the partial molar free energy of a component with a given chemical or empirical formula is identical to that of the molecular species with the same formula.

**Theorem B:** For any chemical reaction at equilibrium, $\Delta G = 0$.


## IV.   STANDARD PARTIAL MOLAR FREE ENERGY

The partial molar free energies considered in the preceding section are functions of the concentrations, while the common measures of reactivity— equilibrium and rate constants—express normalized reactivities at unit concentrations. To relate the equilibrium and rate constants to partial molar free energies one therefore needs a set of normalized partial molar free energies at unit concentrations. Members of this normalized set are called *standard* partial molar free energies. Because the standard partial molar free energies are used to account for normalized reactivities, they need be defined only for molecular species, not for formal components, and this will be done in the present section. Unfortunately, the term "standard partial molar free energy" is also used to describe standard *formal* free energies, that is, partial molar free energies of formal components normalized to unit *formal* concentrations. Standard formal free energies will be defined and considered in Section VII.

To describe the normalization procedure, it is convenient to begin with molecular species in the gas phase and then consider their transfer into a liquid solution. The partial pressure $p_J$ of a gaseous species $J$ is defined by $p_J = N_J P$, where $N_J$ is the mole fraction and $P$ the total pressure. To the ideal-gas

approximation the partial molar free energy is then

$$G_J(g) = G_J^\circ(g) + RT \ln p_J \tag{16}$$

The pressure-independent term, $G_J^\circ(g)$, is the standard free energy of the gaseous species — in this case, the partial molar free energy normalized to unit partial pressure.

   To derive the partial molar free energy of the same species $J$ in a liquid solvent medium M, one combines Equation 16 with the free energy of solvation, $J(g) \rightarrow J(M)$. We shall specify that $J$ is a dilute solute so that the concentration $c_J$ is related to $p_J$ by Henry's law (Equation 17). The Henry's law constant $H_J(M)$ is a parameter depending on the solute, the solvent medium, and the temperature.

$$\frac{c_J}{p_J} = H_J(M) \tag{17}$$

At equilibrium $G_J(g) = G_J(M)$. Substituting in Equation 16 and applying Equation 17 one arrives at

$$G_J(M) = G_J^\circ(g) - RT \ln H_J(M) + RT \ln c_J \tag{18}$$

By definition, the standard partial molar free energy $G_J^\circ(M)$ is the value of $G_J(M)$ normalized to unit concentration. Accordingly, $G_J^\circ(M)$ is expressed by Equation 19 and $G_J(M)$ by Equation 20:

$$G_J^\circ(M) = G_J^\circ(g) - RT \ln H_J(M) \tag{19}$$

$$G_J(M) = G_J^\circ(M) + RT \ln c_J. \tag{20}$$

   Equation 19 represents $G_J^\circ(M)$ as a sum consisting of an intrinsic term and a solvation term. Equation 20 may be regarded as more general than Equation 18 from which it was derived, because it applies to any solute whose concentration is "dilute," even if a real Henry's law constant can not be measured. In practice this means that (20) applies to any normal uncharged solute up to concentrations of the order of 0.1 molar. Equation 20 also applies to ionic solutes, although only well below 0.1 molar and not in the presence of extremely positive or negative electrical potentials.

   In addition to depending on the solvent medium, $G_J^\circ$ also depends on the choice of concentration units. The latter dependence is trivial, without new physical content. In contrast to $G_J$, which is a function of state, $G_J^\circ$ is not a

function of state, because in dilute solution $G_j^\circ = G_j - RT \ln c_j$ and thus depends on the units chosen for $c_j$. Let the given concentration $c_j$ in the medium M be expressed in two different units, such that the value of $c_j$ is either $x$ or $y$, and let $y = \eta x$. The units may be conventional concentration units such as mole fraction or molarity, or operational units such as an optical absorbance or a biochemical activity. Then $G_j^\circ(y) + RT \ln y = G_j^\circ(x) + RT \ln x$, both being equal to $G_j$ for the given state. The resulting dependence on concentration units is

$$y = \eta x; \qquad G_j^\circ(y) = G_j^\circ(x) - RT \ln \eta \qquad (21)$$

For mole fraction, molality, and molarity in dilute solutions, the particular relationships are Equations 22 and 23, where $M_{solvent}$ denotes the solvent's molecular weight and $\theta$ the density.

$$G_j^\circ(\text{molality scale}) = G_j^\circ(\text{mole fraction scale}) - RT \ln\left(\frac{1000}{M_{solvent}}\right) \quad (22)$$

$$G_j^\circ(\text{moles/liter scale}) = G_j^\circ(\text{mole fraction scale}) - RT \ln\left(\frac{1000\theta}{M_{solvent}}\right) \quad (23)$$

The solvent medium M may be a pure liquid (such as pure benzene) or a nominal solvent consisting of two or more components in a constant ratio. Examples of a mixed nominal solvent are a liquid consisting of 80 wt% acetone–20 wt% methanol, or a 3 $M$ solution of NaCl is water. Indeed, any liquid in which the solvation of an added species conforms to Henry's law is a nominal solvent in this context.

To illustrate the relationship between standard partial molar free energies and equilibrium constants, we shall return to Equation 3, which is of the form A + B = C. The molecular species A, B, and C are now dilute solutes in a constant solvent medium M. Partial molar free energies will conform to Equation 20. Beginning with Equation 13, one then obtains

$$G_C^\circ - G_A^\circ - G_B^\circ + RT \ln\left(\frac{c_C}{c_A c_B}\right) = 0 \qquad (24)$$

For the chosen reaction, the last term on the left is $RT \ln K$. Thus Equation 24 is equivalent to the familiar Equation 1.

$$\Delta G^\circ = - RT \ln K \qquad (1)$$

## V.  SUBSPECIES

To do justice to the rich detail of chemical reactivity, the analysis of formal components into molecular species must go beyond the stoichiometric formula. Molecular ensembles with a given stoichiometric formula always consist of subensembles of molecules distinguishable by their interatomic geometry, quantum properties, and reactivity. For example, these subensembles or *subspecies* of the overall molecular species might be structural isomers, conformational isomers, discrete electronic states, or states differing in nuclear spin. Indeed, the complete set of conceivable subspecies is unlimited, because even the populations of individual energy levels show distinctive reactivities in molecular beam experiments (5).

Although the subspecies may differ greatly in their structural and quantum properties, it can be shown that at equilibrium, all subspecies of a given molecular species have exactly the same partial molar free energy, which, in turn, is equal to the partial molar free energy of the overall molecular species. To illustrate the proof of this theorem we shall use a rather simple example, a dilute solution of butadiene (B) in liquid cyclohexane (A). The overall species "butadiene" will be analyzed into two subspecies Equation (25), distinguishable by a *cis* or *trans* geometry about the central bond (6).



$$CH_2\!=\!\!CH\!-\!\!CH\!=\!\!CH_2 \qquad\qquad\qquad\qquad\qquad\qquad\qquad (25)$$
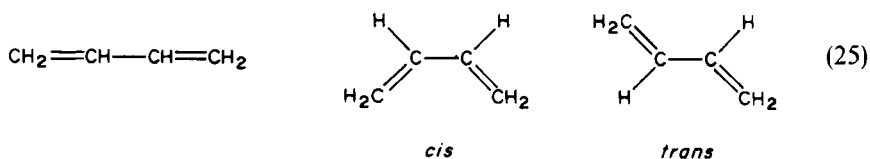
The solvent, cyclohexane, will not be analyzed into subspecies. The free energy of the solution then is expressed by Equation 26 in terms of overall molecular species and by Equation 27 in terms of subspecies.

$$G = n_A G_A + n_B G_B \qquad\qquad\qquad\qquad\qquad\qquad (26)$$

$$G = n_A G_A + n_{cis} G_{cis} + n_{trans} G_{trans}; \qquad n_{cis} + n_{trans} = n_B \qquad (27)$$

It will be convenient to express $n_{cis}$ in terms of $n_B$ and the fraction $\alpha = n_{cis}/n_B$ of *cis*-butadiene in the overall butadiene. Equation 27 then transforms to

$$G = n_A G_A + n_B(\alpha G_{cis} + [1 - \alpha] G_{trans}) \qquad\qquad (28)$$

In Equation 28, the fraction $\alpha$ need not be that for the subspecies at equilibrium. As equilibrium is reached at constant $T, P, n_A,$ and $n_B$, $G$ goes to a

minimum and $\partial G/\partial \alpha$ goes to zero. Moreover, the Gibbs–Duhem equation takes the form $n_A dG_A + n_B(\alpha dG_{cis} + [1 - \alpha]dG_{trans}) = 0$. Thus solving Equation 28 for subspecies equilibrium, we obtain

$$G_{cis} = G_{trans} \tag{29}$$

$$G = n_A G_A + n_B G_{cis} \tag{30}$$

Equations 26 and 30 are alternative expressions for the free energy at subspecies equilibrium, in terms of the same independent variables $n_A$ and $n_B$. On equating the coefficients we obtain the trivial result, $G_A = G_A$, and the significant result

$$G_B = G_{cis} \tag{31}$$

The conclusions derived from Equations 29 and 31 may be stated in the form of a general theorem.

**Theorem C:** When subspecies of a molecular species exist in equilibrium, their partial molar free energies are all equal. The common value of the partial molar free energies of the subspecies is equal to the partial molar free energy of the overall molecular species.

While the partial molar free energies of the subspecies at equilibrium are all equal, the standard partial molar free energies are characteristically different and reflect the inherent differences in stability. To illustrate the proof of this, we shall continue with the example. Equations 32–34 express the partial molar free energies of the respective species as functions of their concentrations in dilute solutions:

$$G_B = G_B^\circ + RT \ln c_B, \quad \text{at } cis\text{–}trans \text{ equilibrium} \tag{32}$$

$$\begin{aligned} G_{cis} &= G_{cis}^\circ + RT \ln (\alpha c_B) \\ &= G_{cis}^\circ + RT \ln \alpha + RT \ln c_B \end{aligned} \tag{33}$$

$$G_{trans} = G_{trans}^\circ + RT \ln (1 - \alpha) + RT \ln c_B \tag{34}$$

At equilibrium, $\alpha = \alpha_{eq}$ and $G_B = G_{cis} = G_{trans}$. The desired relationships among the standard partial molar free energies are therefore expressed as

$$G_B^\circ = G_{cis}^\circ + RT \ln \alpha_{eq} = G_{trans}^\circ + RT \ln (1 - \alpha_{eq}) \tag{35}$$

The implications of Equation 35 may be stated in the form of a general theorem.

**Theorem D:** The standard partial molar free energy of a molecular species B is related to that of its $i$th subspecies B($i$) as follows $G^\circ_{B(i)} = G^\circ_B - RT \ln \alpha(i)$, where $\alpha(i)$ is the mole fraction of B($i$) in B at equilibrium. Because $0 \leqslant \alpha(i) < 1$ for all $i$, the standard partial molar free energy of the overall species is always less than that of any of its subspecies. Unstable subspecies, with small $\alpha(i)$, have relatively high standard partial molar free energies.

There is a useful alternative form of Theorem D. Multiply Equation 33 by $\alpha$ and Equation 34 by $(1 - \alpha)$, and add. The result is

$$G^\circ_B = \alpha G^\circ_{cis} + (1 - \alpha)G^\circ_{trans} + RT(\alpha \ln \alpha + [1 - \alpha] \ln [1 - \alpha]) \qquad (36)$$

According to Equation 36, $G^\circ_B$ is a sum consisting of the mole-fraction average of $G^\circ_{cis}$ and $G^\circ_{trans}$, and an inherently negative term proportional to the entropy of mixing of the subspecies:

$$\Delta S_{mixing} = -R(\alpha \ln \alpha + [1 - \alpha] \ln [1 - \alpha]) \qquad (37)$$

Equation 36 can be generalized to apply to any species B with an arbitrary number of subspecies B($i$) whose respective equilibrium mole fractions are denoted by $\alpha(i)$, $\sum \alpha(i) = 1$. The result is Equation 38, where the summations extend over all subspecies. The analysis of B into subspecies may be as fine-grained as desired:

$$G^\circ_B = \sum \alpha(i) G_B(i)^\circ + RT \sum \alpha(i) \ln \alpha(i) \qquad (38)$$

## VI. EQUILIBRIUM PERTURBATION OF THE SOLVENT

The equilibrium among the subspecies of a molecular species varies with the liquid medium. The introduction of a solute into a dilute solution changes the medium and thus, in principle, shifts the subspecies equilibrium of the solvent. If the solute is introduced slowly so that the shift occurs at equilibrium, the process is called an *equilibrium perturbation* of the solvent. At constant $T$ and $P$, the free energy of the solution, which changes during an equilibrium perturbation, is constrained to remain at a minimum. The imposition of this constraint has an important consequence. While other thermodynamic properties of the solute somehow, more or less, reflect the equilibrium perturbation of the solvent, the partial molar free energy of the

solute is *insensitive to this perturbation* and thus is phenomenologically simpler. The insensitivity extends to the *standard* partial molar free energy of the solute and, as a consequence, to rate and equilibrium constants measured in dilute solution (7).

To illustrate the proof of this theorem we shall consider dilute solutions at constant $T$ and $P$ in the liquid solvent, 1, 2-dichloroethane (A), which consists of a nonpolar *trans-* and a polar *gauche*-subspecies, as shown



$CICH_2CH_2CI$                                                            (39)

      (A)                *trans*                     *gauche*
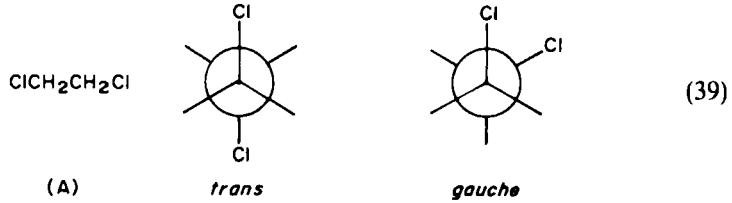
Addition of a highly polar solute (B) such as propylene carbonate raises the dielectric constant, thereby causing an increase in the amount of polar *gauche* at equilibrium (8). Let $n_1$ denote the formula weights of solvent, $n_2$ those of solute, and $\alpha$ the mole fraction of *trans*-isomer, ($\alpha = [trans]/[trans + \text{gauche}]$). At this point the solvent subspecies need not be at equilibrium, and $\alpha$ is a variable. Thus, at constant $T$ and $P$, the free energy of the solution at constant $n_1$ is a function of $n_2$ and $\alpha$, as

$$(dG)_{n_1} = \left(\frac{\partial G}{\partial n_2}\right)_{\alpha, n_1} dn_2 + \left(\frac{\partial G}{\partial \alpha}\right)_{n_2, n_1} d\alpha \tag{40}$$

In an equilibrium perturbation, $\alpha$ adjusts itself as the solute is introduced so that the free energy of the solution remains at a minimum. Thus at any stage during the equilibrium perturbation, $(\partial G/\partial \alpha)_{n_1, n_2} = 0$. To be able to specify this constraint, one introduces a new variable, $y = (\partial G/\partial \alpha)_{n_1, n_2}$. By virtue of its definition, $y$ is zero when $\alpha$ is at equilibrium and departs monotonically from zero as $\alpha$ moves away from equilibrium. Indeed, $-y = -\partial G/\partial \alpha$ expresses the affinity of $\alpha$ to increase spontaneously.

The mathematical transformation of $G(n_2, \alpha)$ into $G(n_2, y)$ is accomplished in Equation 41. At equilibrium $y = 0$ and Equation 41 reduces to Equation 42:

$$\left(\frac{\partial G}{\partial n_2}\right)_{y, n_1} = \left(\frac{\partial G}{\partial n_2}\right)_{\alpha, n_1} + y\left(\frac{\partial \alpha}{\partial n_2}\right)_{y, n_1} \tag{41}$$

                           isodelphic         lyodelphic

$$G_2 = \left(\frac{\partial G}{\partial n_2}\right)_{y=0, n_1} = \left(\frac{\partial G}{\partial n_2}\right)_{\alpha_{eq}, n_1} \tag{42}$$

Let us examine the physical significance of these equations. In Equation 41, where the constraint $y = 0$ has not yet been imposed, $(\partial G/\partial n_2)_y$, at constant $n_1$ is a sum consisting of an *isodelphic* and a *lyodelphic* term. The isodelphic term, $(\partial G/\partial N_2)_\alpha$, expresses the partial molar change in free energy when the solute is introduced so that $\alpha$ does not shift. The lyodelphic term expresses the effect of the shift in $\alpha$: $(\partial \alpha/\partial n_2)_y$ expresses the shift in $\alpha$ per mole of solute, and $y( = \partial G/\partial \alpha)$ expresses the response of $G$ to a shift in $\alpha$.

Equation 42 imposes the equilibrium constraint that $y = 0$. Hence $(\partial G/\partial n_2)_{y=0}$ may be identified with the partial molar free energy $G_2$, and the lyodelphic term becomes zero. In other words, the partial molar free energy of the solute is not affected by the equilibrium perturbation of the solvent. This conclusion is of general validity and does not depend on the specific example chosen (7).

To extend this conclusion to the standard partial molar free energy, we write $G_2^\circ = G_2 - RT \ln c_2$. Since $G_2$ is isodelphic, $G_2^\circ$ will likewise be isodelphic if $c_2$ is insensitive to a shift in $\alpha$ (at constant $n_1, n_2$). This is, in fact, the case—exactly so if $c_2$ is the mole fraction or the molal concentration, and practically so in dilute solution if $c_2$ is the molar concentration.

## VII.   ENTHALPY AND ENTROPY

Partial molar enthalpies and entropies are used for predicting the effect of temperature on reactivity. The key equations are Equations 43 and 44 (1, 2):

$$\ln K = \frac{\Delta S^\circ}{R} - \frac{\Delta H^\circ}{RT} \tag{43a}$$

$$d\ln K/dT = \frac{\Delta H^\circ}{RT^2} \tag{43b}$$

$$\ln k = \ln\left(\frac{k_B T}{h}\right) + \frac{\Delta S^\ddagger}{R} - \frac{\Delta H^\ddagger}{RT} \tag{44a}$$

$$\frac{d\ln k}{dT} = \frac{\Delta H^\ddagger + RT}{RT^2} \tag{44b}$$

Equation 44 is based on transition-state theory.

The $\Delta S$ and $\Delta H$ functions in Equations 43 and 44 are those for molecular species, while the macroscopic measurements of thermodynamics operate on formal components. This section will consider the relationships between formal and molar enthalpies and entropies.

We shall assume that the chemical system of variable temperature is a closed system, that is, the set $\{n\}$ of formula-weight numbers of all components remains constant. Moreover, the system consists of a single phase, and at any given temperature, chemical equilibrium is approached at constant pressure. Under such conditions, the criterion for chemical equilibrium is that the Gibbs free energy $G$ be at a minimum. To apply this criterion mathematically, it is convenient to let $G$ be the primary variable. The enthalpy $H$ and entropy $S$ then are related to $G$ according to

$$G = H - TS \tag{45}$$

$$S = -\left(\frac{\partial G}{\partial T}\right)_{P,\{n\}} \tag{46}$$

$$H = G - T\left(\frac{\partial G}{\partial T}\right)_{P,\{n\}} \tag{47}$$

The partial molar free energy, enthalpy, and entropy of the $i$th component are obtained by taking partial derivatives with respect to the formula-weight number $n_i$, as in Equation 48, where $T, P$, and all other formula-weight numbers are understood to be constant. Relationships between $G_i, H_i$, and $S_i$ are obtained by partial differentiation of (Equations 45–47) with respect to $n_i$:

$$G_i = \frac{\partial G}{\partial n_i}; \qquad H_i = \frac{\partial H}{\partial n_i}; \qquad S_i = \frac{\partial S}{\partial n_i} \tag{48}$$

$$G_i = H_i - TS_i \tag{49}$$

$$S_i = -\left(\frac{\partial G_i}{\partial T}\right)_P \tag{50}$$

$$H_i = G_i - T\left(\frac{\partial G_i}{\partial T}\right)_P \tag{51}$$

In order to derive the standard partial molar enthalpies and entropies of the molecular species from the preceding partial molar properties of the formal components, it is useful to introduce some intermediary variables, which will be called standard *formal* free energies, enthalpies, and entropies and will be denoted by $G_i^*, H_i^*$, and $S_i^*$, respectively. (The superscript * will be used for standard *formal* properties, while the superscript ° is used for standard partial *molar* properties.) In dilute solutions $G_i^*$ is defined in Equation 52, where $c_i$

denotes the formal (rather than the molar) concentration. By application of Equations 50 and 51, the corresponding expressions for the entropy and enthalpy are 53 and 54:

Dilute solutions:

$$G_i = G_i^* + RT \ln c_i \tag{52}$$

$$S_i = -\left(\frac{\partial G_i^*}{\partial T}\right)_P - R \ln c_i - RT\left(\frac{\partial \ln c_i}{\partial T}\right)_{P,\{n\}} \tag{53}$$

$$H_i = G_i^* - T\left(\frac{\partial G_i^*}{\partial T}\right)_P - RT^2\left(\frac{\partial \ln c_i}{\partial T}\right)_{P,\{n\}} \tag{54}$$

The partial derivative $(\partial \ln c_i/\partial T)_{P,\{n\}}$ appears in these equations because the formal concentration $c_i$ varies with the temperature when the concentration units are temperature-dependent. Among the common units, formula-weight fractions and formalities (formula weights of solute per kilogram of solvent) are independent of $T$, while volume concentrations vary with $T$. However, the actual values of $[\partial \ln c_i/\partial T]_{P,\{n\}}$, when not zero, are small and nearly independent of $c_i$. The corresponding terms therefore become part of the standard formal entropies and enthalpies, as follows.

Dilute solutions:

$$S_i = S_i^* - R \ln c_i \tag{55}$$

$$S_i^* = -\left(\frac{\partial G_i^*}{\partial T}\right)_P - RT\left(\frac{\partial \ln c_i}{\partial T}\right)_{P,\{n\}} \tag{56}$$

$$H_i = H_i^* \tag{57}$$

$$H_i^* = G_i^* - T\left(\frac{\partial G_i^*}{\partial T}\right)_P - RT^2\left(\frac{\partial \ln c_i}{\partial T}\right)_{P,\{n\}} \tag{58}$$

where $S_i^*$ depends on both the concentration units (through the term $R \ln c_i$) and their temperature derivative and $H_i^*$ depends only on the temperature derivative of the concentration units.

The preceding equations apply to the formal components. To obtain the relationships for molecular species, let us return to the example of Equation 3 and consider a *dilute solution* of chloroform (component 2) in triethylamine (component 1). The molecular species are triethylamine monomer (A), chloroform monomer (B), and triethylamine–chloroform hydrogen-

bonded complex (C) (4). According to Equation 15, $G_A = G_1, G_B = G_2$, and $G_C = G_1 + G_2$. In dilute solutions, focusing on the solute, $G_B = G_B^\circ + RT \ln c_B$, and $G_2 = G_2^* + RT \ln c_2$. Let $\alpha_2$ denote the fraction of chloroform monomer in the overall chloroform component: $\alpha_2 = c_B/c_2$. Then $G_2^*$ and $G_2^\circ$ are related according to

$$G_2^* = G_B^\circ + RT \ln \alpha_2 \tag{59}$$

Partial differentiation with respect to $T$ yields the corresponding relationships for the standard entropy and enthalpy:

$$\left(\frac{\partial G_2^*}{\partial T}\right)_P = \left(\frac{\partial G_B^\circ}{\partial T}\right)_P + R \ln \alpha_2 + RT\left(\frac{\partial \ln \alpha_2}{\partial T}\right)_{P,\{n\}} \tag{60}$$

$$S_2^* = S_B^\circ - R \ln \alpha_2 - RT\left(\frac{\partial \ln \alpha_2}{\partial T}\right)_{P,\{n\}} \tag{61}$$

$$H_2^* = H_B^\circ - RT^2\left(\frac{\partial \ln \alpha_2}{\partial T}\right)_{P,\{n\}} \tag{62}$$

The preceding results may be stated in the form of a general theorem.

**Theorem E:** Let Formula $i$ denote the chemical formula adopted for the $i$th component, and let $S(i)$ denote the molecular species whose real formula is Formula $i$. Let $\alpha_i = c_{S(i)}/c_i$ denote the fraction of $S(i)$ in the overall $i$th component at equilibrium. The relationships between standard formal and standard partial molar properties then are as follows:

$$G_i^* = G_{S(i)}^\circ + RT \ln \alpha_i$$

$$\left(\frac{\partial G_i^*}{\partial T}\right)_P = \left(\frac{\partial G_{S(i)}^\circ}{\partial T}\right)_P + R \ln \alpha_i + RT\left(\frac{\partial \ln \alpha_i}{\partial T}\right)_{P,\{n\}}$$

$$S_i^* = S_{S(i)}^\circ - R \ln \alpha_i - RT\left(\frac{\partial \ln \alpha_i}{\partial T}\right)_{P,\{n\}}$$

$$H_i^* = H_{S(i)}^\circ - RT^2\left(\frac{\partial \ln \alpha_i}{\partial T}\right)_{P,\{n\}}$$

The fraction $\alpha_i$ is in the range $1 \geqslant \alpha_i > 0$. If the component enters the solution with negligible reaction, $\alpha_i$ may be as high as unity. If the component

reacts to form new species, $\alpha_i$ may become stoichiometrically insignificant. In that case, $\alpha_i$ does not go strictly to zero, however, because the final state is a state of chemical equilibrium rather than of complete reaction. $(\partial \ln \alpha_i / \partial T)_{P,\{n\}}$ may be positive, zero, or negative.

### A.  Equilibrium Perturbation by Solute-Induced Medium Effects

As described earlier (Equation 41), the medium effect inherent in the addition of a solute may shift an existing equilibrium even though the solute itself is unreactive. The shifting equilibrium may, in turn, affect the thermodynamic properties of the unreactive solute. This kind of an equilibrium perturbation has no effect on the partial molar free energy of the unreactive solute, as was illustrated in the example leading to Equation 42. The same perturbation may, however, affect the partial molar enthalpy and entropy.

To make the present development more general, let the variable $\alpha$ express the degree of progress in any reaction in which the $i$th component is not a reagent. The reaction might be an ordinary chemical reaction or an interconversion of subspecies of the solvent. The degree of progress might be measured by the amount of product, expressed as a fraction $\alpha$ of the theoretical amount for complete reaction. The independent variables are $n_i$, $\alpha$, and the temperature $T$. The pressure $P$ and the formula-weight numbers of the other components remain constant. To treat equilibrium perturbations and to specify that $\partial G / \partial \alpha = 0$, one needs the secondary independent variables $n_i$, $T$, and $\partial G / \partial \alpha$. As before, $\partial G / \partial \alpha$ will be denoted by $y$.

Let $X$ denote any function of $T$, $n_i$, and $\alpha$. Transformation of variables to $T$, $n_i$ and $y$ then yields

$$\left(\frac{\partial X}{\partial n_i}\right)_{T,y} = \left(\frac{\partial X}{\partial n_i}\right)_{T,\alpha} + \left(\frac{\partial X}{\partial \alpha}\right)_{T,n_i}\left(\frac{\partial \alpha}{\partial n_i}\right)_{T,y} \tag{63}$$

$$\left(\frac{\partial X}{\partial T}\right)_{n_i,y} = \left(\frac{\partial X}{\partial T}\right)_{n_i,\alpha} + \left(\frac{\partial X}{\partial \alpha}\right)_{T,n_i}\left(\frac{\partial \alpha}{\partial T}\right)_{n_i,y} \tag{64}$$

When $X$ is the free energy $G$, Equation 63 takes the form of Equation 65, which is a generalization of Equation 41:

$$\left(\frac{\partial G}{\partial n_i}\right)_{T,y} = \left(\frac{\partial G}{\partial n_i}\right)_{T,\alpha} + \left(\frac{\partial G}{\partial \alpha}\right)_{T,n_i}\left(\frac{\partial \alpha}{\partial n_i}\right)_{T,y} \tag{65}$$

In taking the derivative of Equation 65 with respect to $T$ at constant $y$, one uses Equation 64 to express the partial derivatives with respect to $T$ of

$(\partial G/\partial n_i)_{T,\alpha}$ and of $(\partial G/\partial \alpha)_{T,n_i}$. The result is

$$
\left(\frac{\partial^2 G}{\partial n_i \partial T}\right)_y = \left(\frac{\partial^2 G}{\partial n_i \partial T}\right)_\alpha + \left(\frac{\partial^2 G}{\partial n_i \partial \alpha}\right)_T \left(\frac{\partial \alpha}{\partial T}\right)_{y,n_i} + \left(\frac{\partial^2 G}{\partial T \partial \alpha}\right)_{n_i} \left(\frac{\partial \alpha}{\partial n_i}\right)_{y,T}
$$
$$
+ \left(\frac{\partial^2 G}{\partial \alpha^2}\right)_{n_i,T} \left(\frac{\partial \alpha}{\partial T}\right)_{y,n_i} \left(\frac{\partial \alpha}{\partial n_i}\right)_{y,T} + \left(\frac{\partial G}{\partial \alpha}\right)_{T,ni} \left(\frac{\partial^2 \alpha}{\partial n_i \partial T}\right)_y \qquad (66)
$$

Equation 66 can be simplified by noting that, at constant $T$

$$
\left(\frac{\partial^2 G}{\partial n_i \partial \alpha}\right) = \left(\frac{\partial y}{\partial n_i}\right)_\alpha = -\left(\frac{\partial \alpha}{\partial n_i}\right)_y \left(\frac{\partial y}{\partial \alpha}\right)_{n_i} = -\left(\frac{\partial^2 G}{\partial \alpha^2}\right)_{n_i} \left(\frac{\partial \alpha}{\partial n_i}\right)_y
$$

A similar operation shows that $(\partial^2 G/\partial T \partial \alpha) = -(\partial^2 G/\partial \alpha^2)(\partial \alpha/\partial T)_y$; hence

$$
\left(\frac{\partial^2 G}{\partial n_i \partial T}\right)_y = \left(\frac{\partial^2 G}{\partial n_i \partial T}\right)_\alpha - \left(\frac{\partial^2 G}{\partial \alpha^2}\right)_{n_i,T} \left(\frac{\partial \alpha}{\partial T}\right)_{n_i,y} \left(\frac{\partial \alpha}{\partial n_i}\right)_{T,y}
$$
$$
+ \left(\frac{\partial G}{\partial \alpha}\right)_{T,n_i} \left(\frac{\partial^2 G}{\partial n_i \partial T}\right)_y \qquad (67)
$$

For equilibrium perturbations, $(\partial G/\partial \alpha)_{eq} = y_{eq} = 0$; hence Equation 68. According to Equations 50 and 51, the partial molar entropy and enthalpy are expressed by Equations 69 and 70:

$$
\left(\frac{\partial^2 G}{\partial n_i \partial T}\right)_{eq} = \left(\frac{\partial^2 G}{\partial n_i \partial T}\right)_\alpha - \left(\frac{\partial^2 G}{\partial \alpha^2}\right)_{n_i,T} \left(\frac{\partial \alpha}{\partial T}\right)_{n_i,eq} \left(\frac{\partial \alpha}{\partial n_i}\right)_{T,eq} \qquad (68)
$$

$$
S_i = (S_i)_\alpha + \left(\frac{\partial^2 G}{\partial \alpha^2}\right) \left(\frac{\partial \alpha}{\partial T}\right)_{n_i,eq} \left(\frac{\partial \alpha}{\partial n_i}\right)_{T,eq} \qquad (69)
$$

$$
H_i = (H_i)_\alpha + T\left(\frac{\partial^2 G}{\partial \alpha^2}\right) \left(\frac{\partial \alpha}{\partial T}\right)_{n_i,eq} \left(\frac{\partial \alpha}{\partial n_i}\right)_{T,eq} \qquad (70)
$$

where $S_i$ and $H_i$ represent the partial molar entropy and enthalpy the $i$th component under conditions of chemical equilibrium at constant $T$ and $P$; $(S_i)_\alpha$ represents $-(\partial^2 G/\partial n_i \partial T)_\alpha$, the partial molar entropy of the $i$th component, added at constant $T$ and $P$ under nonequilibrium conditions such that there is no shift in $\alpha$; and $(H_i)_\alpha$ represents the partial molar enthalpy under the same nonequilibrium conditions.

By hypothesis, the $i$th component is not a reagent in the given system; that is, at equilibrium $c_{S(i)}/c_i = 1$ and, according to Theorem E, the standard formal and standard partial molar properties are equal. Moreover, $c_i$ is virtually unchanged by a change in $\alpha$. As a result, the relationships obtained for $G_i$ and $(G_i)_\alpha$, $S_i$ and $(S_i)_\alpha$, and $H_i$ and $(H_i)_\alpha$ imply the following relationships for the standard properties:

$$G_i^* = G_i^\circ = (G_i^\circ)_\alpha \tag{71}$$

$$H_i^* = H_i^\circ = (H_i^\circ)_\alpha + T\left(\frac{\partial^2 G}{\partial \alpha^2}\right)\left(\frac{\partial \alpha}{\partial T}\right)_{n_i,\text{eq}}\left(\frac{\partial \alpha}{\partial n_i}\right)_{T,\text{eq}} \tag{72}$$

$$S_i^* = S_i^\circ = (S_i^\circ)_\alpha + \left(\frac{\partial^2 G}{\partial \alpha^2}\right)\left(\frac{\partial \alpha}{\partial T}\right)_{n_i,\text{eq}}\left(\frac{\partial \alpha}{\partial n_i}\right)_{T,\text{eq}} \tag{73}$$

|          isodelphic          |          lyodelphic          |

As shown in Equations 71–73, in the case of $G_i^\circ$ the lyodelphic contribution is zero. In the case of $H_i^\circ$ and $S_i^\circ$, on the other hand, the lyodelphic contribution need not vanish. At equilibrium, $\partial^2 G/\partial \alpha^2$ is a positive number. The value $\partial \alpha/\partial T$ varies widely, depending on the endo- or exothermocity of the reaction. It is close to zero for reactions that are close to thermoneutral and exactly zero for identity reactions. The solute-induced medium effect contained in $\partial \alpha/\partial n_i$ similarly varies widely. It tends to be large when the product molecules, in the perturbed equilibrium, differ from the reagent molecules in respect to properties that are sensitive to the microscopic environment, such as charge, polar character, size, or shape.

## B.  Subspecies

*Subspecies* have been defined as distinguishable isomers or fractional populations of a given molecular species, often with distinctive reactivities. The present analysis requires that the subspecies of a given molecular species be in equilibrium. Different molecular species, on the other hand, need not be in chemical equilibrium. For the $J$th species, $G_J^\circ$ for the overall species is related to $G_{J(i)}^\circ$ for its $i$th subspecies according to Equation 74 (see Theorem D), where $\alpha(i)$ is the mole fraction of $J(i)$ in $J$ when the subspecies are at equilibrium. Since $H = G - T(\partial G/\partial T)_P$, $H_{J(i)}^\circ$ is as given in Equation 75:

$$G_{J(i)}^\circ = G_J^\circ - RT \ln \alpha(i) \tag{74}$$

$$H_{J(i)}^\circ = H_J^\circ + RT^2\left[\frac{\partial \ln \alpha(i)}{\partial T}\right]_{P,\{n\}} \tag{75}$$

Equation 75 can be transformed into a more transparent form. Multiply both sides by $\alpha(i)$, add up for all subspecies, and introduce the constraint that $\sum\alpha(i) = 1$. The result is Equation 76, which states that the standard enthalpy of a molecular species is simply the mole-fraction average of the standard enthalpies of its subspecies at equilibrium:

$$H_J^\circ = \sum\alpha(i)H_{J(i)}^\circ \tag{76}$$

The preceding derivation was carried out under conditions of constant $T$ and $P$. Had it been carried out at constant $T$ and $V$, the result would have been

$$E_J^\circ = \sum\alpha(i)E_{J(i)}^\circ \tag{77}$$

It is instructive to compare Equation 77 with a corresponding equation of statistical thermodynamics. The subspecies used in Equation 77 may be as fine-grained as desired, so one may let the $i$th subspecies be the population of an individual energy level. In that case, $E_{J(i)}^\circ = N_0\varepsilon_{J(i)}$, where $N_0$ is Avogadro's number and $\varepsilon_{J(i)}$ is the energy of the $i$th level. Substitution in Equation 77 then leads to $E_J^\circ = N_0\sum\alpha(i)\varepsilon_{J(i)}$. The latter is the expression for the molar energy used in statistical thermodynamics. The two approaches are therefore consistent with each other. Indeed, one may say that analysis into subspecies consisting of distinctive groups of energy levels is an innocent substitute when the detailed information required for analysis into individual energy levels is lacking.

## VIII.  SOLVATION COMPLEXES

The thermodynamics of solvation complexes resembles that of complexes in general and follows Theorems A and B. Let component 1 be the solvent and 2 be the solute. Let M be the formula of the solvent molecules and B that of the unsolvated solute molecules. The solvated solute is a mixture of species of the type B·$h$M ($h = 0, 1, 2, \ldots$), which are in equilibrium with M and B according to Equation 78. The partial molar free energies are related by Equation 79:

$$B + h\text{M} = \text{B·}h\text{M} \tag{78}$$

$$G_{\text{B·}h\text{M}} = G_\text{B} + hG_\text{M} = G_2 + hG_1 \tag{79}$$

Let $\beta_h = c_{\text{B·}h\text{M}}/c_2$, the fraction of $B\cdot h$M in the total solute. The standard partial

molar free energy of $B \cdot h\text{M}$ then is expressed by

$$G_{\text{B} \cdot h\text{M}} = G^\circ_{\text{B} \cdot h\text{M}} + RT \ln \beta_h + RT \ln c_2 \tag{80}$$

On introducing Equation 79, letting $G_1 = G^\circ_1$ and $G_2 = G^*_2 + RT \ln c_2$ in dilute solution, one obtains Equation 81, where $G^\circ_1$ is the standard free energy of the solvent and $G^*_2$ is the standard formal free energy of the solute:

$$G^\circ_{\text{B} \cdot h\text{M}} = G^*_2 + hG^\circ_1 - RT \ln \beta_h \tag{81}$$

To obtain an alternative expression for $G^*_2$, multiply (81) by $\beta_h$ and add up for all $h$:

$$G^*_2 = \left( \sum \beta_h G^\circ_{\text{B} \cdot h\text{M}} \right) - G^\circ_1 \left( \sum h\beta_h \right) + RT \left( \sum \beta_h \ln \beta_h \right) \tag{82}$$

The summations in Equation 82 extend from $h = 0$ to $h = \infty$; $\sum \beta_h G^\circ_{\text{B} \cdot h\text{M}}$ and $\sum h\beta_h$ represent the ensemble averages $\langle G^\circ_{\text{B} \cdot h\text{M}} \rangle$ and $\langle h \rangle$, respectively, and $-R(\sum \beta_h \ln \beta_h)$ is the entropy of mixing of B and its solvates at equilibrium.

To derive expressions for the formal standard enthalpy $H^*_2$ we introduce $H^*_2 = G^*_2 - T(\partial G^*_2 / \partial T)_{P,\{n\}}$ and write similar expressions for $H^\circ_1$ and $H^\circ_{\text{B} \cdot h\text{M}}$. Then $\sum \beta_h = 1$ and $\partial \sum \beta_h / \partial T = 0$. Operation on Equation 82 then yields (83).

$$H^\circ_{\text{B} \cdot h\text{M}} = H^*_2 + hH^\circ_1 + RT^2 \left( \frac{\partial \ln \beta_h}{\partial T} \right) \tag{83}$$

Multiplying by $\beta_h$ and adding up for all solvates ($h = 0$ to $h = \infty$) yields

$$H^*_2 = \left( \sum \beta_h H^\circ_{\text{B} \cdot h\text{M}} \right) - H^\circ_1 \left( \sum h\beta_h \right) \tag{84}$$

where $\sum \beta_h H^\circ_{\text{B} \cdot h\text{M}}$ and $\sum h\beta_h$ represent the ensemble averages $\langle H^\circ_{\text{B} \cdot h\text{M}} \rangle$ and $\langle h \rangle$, respectively.

## IX.  SECOND-ORDER EQUILIBRIUM PERTURBATIONS

In ordinary equilibrium perturbations the addition of a component produces a medium effect that causes shifts in subspecies equilibria in the solution. For instance, the addition of a solute might shift the equilibrium ratios of solvent subspecies. The shifted equilibria produce medium effects of their own, which, in turn, cause further shifts or equilibrium perturbations of *second order*. The ordinary and second-order perturbations tend to be cooperative, and the second-order shifts can be significant. For instance, the

addition of a polar solute favors the formation of polar subspecies in the *solvent*. This, in turn, favors the formation of polar subspecies in the *solute*, rendering the solute even more polar and enhancing its polar medium effect of the solvent subspecies. A full treatment of this effect must be left to those who can cope with the mathematical complexities (9, 10).

The treatment is simplest when there are two stoichiometrically indepen-dent equilibrium ratios. This case has been treated elsewhere (7), and a brief presentation here will fix the ideas. For definiteness, the solvent (component (1) consists of two subspecies in ratio $\alpha/(1-\alpha)$, and the solute (component 2) consists of two subspecies, which may be two different solvates, in the ratio $\beta/(1-\beta)$. At constant $T$ and $P$ the free energy $G = G(n_1, n_2, \alpha, \beta)$. Let $y_1 = (\partial G/\partial \alpha)_{(n),\beta}$, $y_2 = (\partial G/\partial \beta)_{(n),\alpha}$ and transform variables, letting $G = G(n_1, n_2, y_1, y_2)$. In an equilibrium perturbation the interacting $\alpha$ and $\beta$ shift so that $(y_1)_{eq} = (y_2)_{eq} = 0$. A general relationship involving $\partial G/\partial n_2$ at constant $n_1$ then is Equation 85, and the special relationship for $G_2$ in an equilibrium transformation is Equation 86:

$$\left(\frac{\partial G}{\partial n_2}\right)_{y_1, y_2} = \left(\frac{\partial G}{\partial n_2}\right)_{\alpha, \beta} + y_1 \left(\frac{\partial \alpha}{\partial n_2}\right)_{y_1, y_2} + y_2 \left(\frac{\partial \beta}{\partial n_2}\right)_{y_1, y_2} \quad (85)$$

<div align="center">isodelphic          lyodelphic</div>

$$G_2 = \left(\frac{\partial G}{\partial n_2}\right)_{eq} = \left(\frac{\partial G}{\partial n_2}\right)_{\alpha_{eq}, \beta_{eq}} \quad (86)$$

Again $G_2$ is purely isodelphic.

The corresponding expression for the partial molar enthalpy $H_2$, on the other hand, contains explicit terms depending on shifts in both $\alpha$ and $\beta$. On letting $H_2 = G_2 - T(\partial G_2/\partial T)_{(n),P}$, and after some manipulation beginning with Equation 85 (7), one obtains Equation 87 for an equilibrium perturbation. In Equation 87, $P$ and $n_1$ are taken to be constant. The subscript "eq" denotes that the independent variables are $T, n_2, y_1, y_2$ and that $y_1$ and $y_2$ are zero. The subscript "iso" denotes that the independent variables are $T, n_2, \alpha, \beta$ and that $\alpha$ and $\beta$ have their equilibrium values.

$$\left(\frac{H_2}{T}\right)_{eq} = \left(\frac{H_2}{T}\right)_{iso} + \left(\frac{\partial^2 G}{\partial \alpha^2}\right)_{iso} \left(\frac{\partial \alpha}{\partial n_2}\right)_{eq} \left(\frac{\partial \alpha}{\partial T}\right)_{eq}$$

$$+ \left(\frac{\partial^2 G}{\partial \beta^2}\right)_{iso} \left(\frac{\partial \beta}{\partial n_2}\right)_{eq} \left(\frac{\partial \beta}{\partial T}\right)_{eq} + \left(\frac{\partial^2 G}{\partial \alpha \partial \beta}\right)_{iso} \left(\frac{\partial \alpha}{\partial n_2}\right)_{eq} \left(\frac{\partial \beta}{\partial T}\right)_{eq}$$

$$+ \left(\frac{\partial^2 G}{\partial \alpha \partial \beta}\right)_{iso} \left(\frac{\partial \beta}{\partial n_2}\right)_{eq} \left(\frac{\partial \alpha}{\partial T}\right)_{eq} \quad (87)$$

At equilibrium, $\partial^2 G/\partial \alpha^2$ and $\partial^2 G/\partial \beta^2$ are positive; $\partial^2 G/\partial \alpha \partial \beta$ may be either positive, negative, or zero. The value is zero when changes in one (either $\alpha$ or $\beta$) have no effect on the other. The magnitude of $\partial^2 G/\partial \alpha \partial \beta$ obeys the inequality $(\partial^2 G/\partial \alpha \partial \beta)^2 < (\partial^2 G/\partial \alpha^2)(\partial^2 G/\partial \beta^2)$ (11).

## X. CONCLUDING REMARKS

The functions treated in this chapter—free energy, enthalpy, and entropy of molecular species, subspecies, and solvates—are key functions in thermodynamic treatments of reactivity. The concentrations and, indeed, the molecular formulas of such species may be different from those of the formal components. When such differences exist, the thermodynamic properties of the formal components deviate from those of the molecular species with the same chemical formulas and, if the effect is neglected, structure–reactivity correlations will tend to be "noisy." Some of these phenomena, such as the peculiar reactivities of mixtures of conformational isomers in rapid equilibrium, or of component molecules existing in equilibrium with new species, are well known (12). Equilibrium perturbations of the solvent by added solutes are less familiar, perhaps because they produce no effects in structure–free-energy correlations. They do produce effects in structure/enthalpy–entropy correlations, however, and are quite noticeable in hydrogen-bonding solvents, especially in water and in aqueous mixtures (13).

## REFERENCES AND NOTES

1. G. N. Lewis, M. Randall, K. S. Pitzer, and L. Brewer, *Thermodynamics*, McGraw-Hill, New York, 1961; (a) Chaps. 15, 20; (b) p. 210, Equations 17–32 and 17–34; p. 260, Equations 20–19.

2. J. W. Moore, and R. G. Pearson, *Kinetics and Mechanism*, Wiley-Interscience, New York, 1981, Chap. 5.

3. Relaxation times in liquids are approximately 10 ps for vibrational modes, and even shorter for translational and rotational modes. See W. Kaiser and A. Laubereau, "Laser-induced Molecular Processes," *Springer Ser. Chem. Phys.*, 6, 313 (1979).

4. L. G. Hepler, *Thermochimica Acta*, 100, 171 (1986).

5. H. Reisler and C. Wittig, *Ann. Rev. Phys. Chem.*, 37, 307 (1986).

6. P. W. Mui and E. Grunwald, *J. Am. Chem. Soc.*, 104, 6582 (1982).

7. E. Grunwald, *J. Am. Chem. Soc.*, 106, 5414 (1984).

8. K. Kuratani, *Rep. Inst. Sci. Technol., Univ. Tokyo*, 6, 221 (1952); *Chem. Abstr.*, 47, 1493i (1953).

9. I. Prigogine and R. Defaye, *Chemical Thermodynamics*, translated by D. H. Everett, Longmans, London, 1954.

10. M. J. Blandamer and J. Burgess, *J. Chem. Soc. Faraday Trans. 1:* (a) 81, 1495 (1985); (b) 80, 2881 (1984).

11. G. E. F. Sherwood and A. E. Taylor, *Calculus*, Prentice-Hall, New York, 1943, p. 357.
12. J. I. Seeman, *Chem. Rev.*, *83*, 83 (1983).
13. H. S. Frank, *J. Chem. Phys.*, *13*, 493 (1945); H. S. Frank and M. W. Evans, *J. Chem. Phys.*, *13*, 507 (1945); S. Winstein and A. H. Fainberg, *J. Am. Chem. Soc.* 79, 5937 (1957); M. J. Blandamer, J. Burgess, R. E. and Robertson and J. M. W. Scott, *Progr. Phys. Org. Chem.*, *15*, 149 (1985); E. Grunwald, *J. Am. Chem. Soc.*, *108*, 5726 (1986).

# Reaction Coordinates and Structure–Energy Relationships

BY ERNEST GRUNWALD

*Department of Chemistry*
*Brandeis University*
*Waltham, Massachusetts*

## CONTENTS

## I.  INTRODUCTION

Chemical reactivity depends on energy relationships along the reaction coordinate. While some features of reaction coordinates are specific for particular reactions, others are nonspecific and can be classified into broad categories. In this chapter we shall focus on the nonspecific features and examine the implied structure–reactivity relationships.

A reaction coordinate is defined as the path of lowest configurational

energy leading from reagents to products. This lowest configurational energy
is a classical potential energy whenever the reaction coordinate is, or may
be treated as, an intrinsic property of the given reaction, being identical in
all molecular reaction events. When the reaction takes place in a fluid solution,
molecular configurational diversity in the *surroundings* will cause the configu-
rational energy of the *reacting system* to vary. However, the various fluid
surroundings are in rapid exchange, and fluctuations in interaction energies
tend to average out. Indeed, in the *continuum model* of fluids, exchange
averaging is regarded as fully effective and the reaction coordinate becomes
an intrinsic, though temperature-dependent, function of the reaction. Thus,
at this point in our discussion, we shall treat the configurational energy $\Phi$
as a potential energy.

## II.  PROJECTION OF REACTION COORDINATES

    To define the configuration of a molecular system one needs to specify
bond distances and angles, or (more commonly) normal coordinates. For an
$N$-atomic system with a nonlinear structure along the reaction coordinate,
there are $3N - 6$ such coordinates. The reaction coordinate, which is the path
of lowest configurational energy from reagents to products, winds its way
through this high-dimensional space. High-dimensional space is hard to
pictorialize, and since we are interested in pictorial representations, it becomes
necessary to simplify and map out relationships in suitable projection.
Mathematically the simplest projection is a direct linear projection: One
straightens out the reaction coordinate, which is a curve in the original high-
dimensional space, and plots energy as a function of displacement along the
resulting straight line.
    To illustrate this practice, consider an unusually simple case, the
triatomic displacement $X + Y - Z \rightarrow X - Y + Z$. Figure 1 shows a typical
potential energy contour diagram (1). The angle $X \cdots Y \cdots Z$ is fixed at 180°, so
there remain only two configuration variables, the $X \cdots Y$ distance $r_1$ and the
$Y \cdots Z$ distance $r_2$. Reagents and products are located at the ends of the
orthogonal energy valleys, which are connected by a mountain pass whose
peak represents the transition state. Figure 2 represents a view of the surface
from the reagents' valley (2). For simplicity, the bend in the reaction coordinate
has been straightened out.
    Figure 3a is a linear projection of potential energy reaction coordinate,
based on Fig. 1. The abscissa $s$ is the distance from the transition state,
measured with a flexible ruler along the curved reaction coordinate in Fig. 1.
The ordinate is the corresponding potential energy $\Phi$. The transition state is
projected at $s = 0$. In this projection, as in any projection, some information is
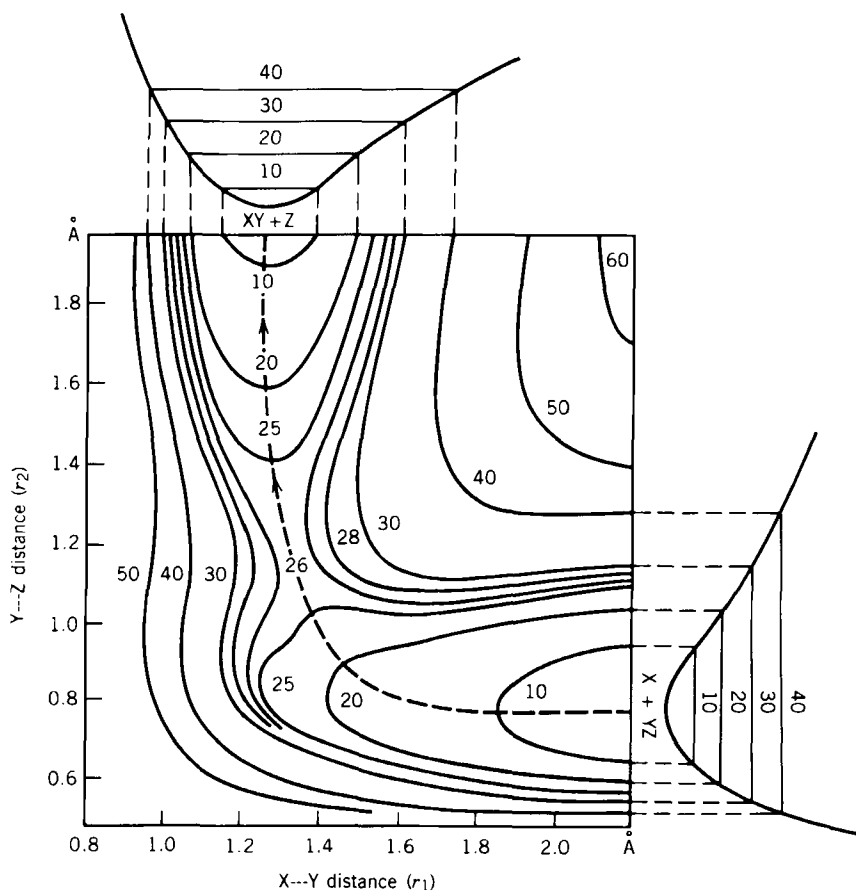
**Figure 1** A typical potential-energy contour diagram for a three-atom reaction. Energy contours are in kcal mole $^{-1}$. The angle X..Y..Z is a constant at 180°. The dashed line is the reaction coordinate. The potential functions at the ends of the valleys are for bond stretching in isolated Y — Z and X — Y molecules. From S. Glasstone, K. J. Laidler, and H. Eyring, *The Theory of Rate Processes*, McGraw-Hill, New York, 1941, p. 96.

lost. In particular, since the abscissa is unbounded (with reagents and products at $s = \pm \infty$), one cannot tell whether the transition state is "early" or "late," that is, whether it occurs before or after the sharp bend in the original reaction coordinate. (Figure 1 shows the transition state to be "late.")

Figure 3b is a quadratic projection (3, 4) of potential energy–reaction coordinate, based on Fig. 1. The abscissa $x$ is the projection of the original reaction coordinate, scaled so that the potential energy $\Phi$ becomes an inverted
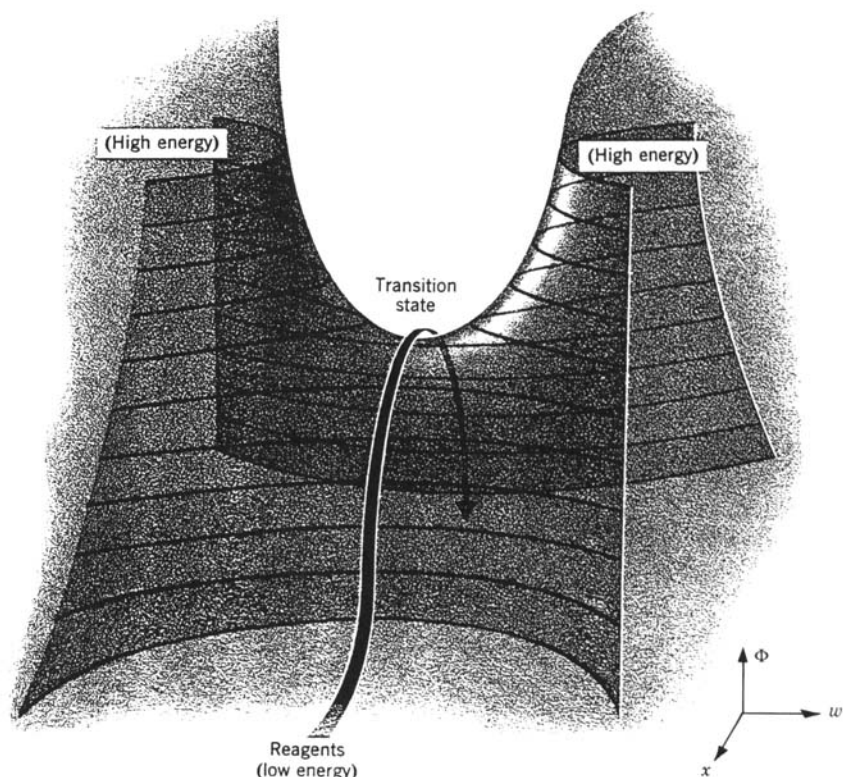
**Figure 2**   View of the potential surface for $X + Y - Z \rightarrow X - Y + Z$ from the reagents' valley. For simplicity, the bend in the reaction coordinate shown in Fig. 1 has been straightened out. The reaction coordinate is plotted along $x$, the $X \leftarrow Y \rightarrow Z$ symmetric stretch along $w$, and potential energy along $\Phi$. From J. E. Leffler and E. Grunwald, *Rates and Equilibria of Organic Reactions*, Wiley, New York, 1963, p. 62.

parabola: $\Phi = a + bx + cx^2$. The $x$-axis is normalized so that the reagents are at $x = 0$ and the products at $x = 1$. Thus, for the reagents $\Phi = a$, and for the products $\Phi = a + b + c$. The transition-state coordinates, that is, the coordinates of the parabolic maximum, are denoted by $(x^\ddagger, \Phi^\ddagger)$. By solving for $d\Phi/dx = 0$, one finds that $x^\ddagger = -b/2c$ and $\Phi^\ddagger = a - b^2/4c$. Accordingly, if $\Phi$ is known for reagents, products, and transition state, the parameters $a$, $b$, and $c$ can be calculated. Note, however, that numerical values of the potential energy are not absolute but are defined with respect to an arbitrary point of zero potential energy. As a result, the $a$ parameter, that is, the intercept of the parabola on the $\Phi$-axis, has no absolute significance. On the other hand, the $b$
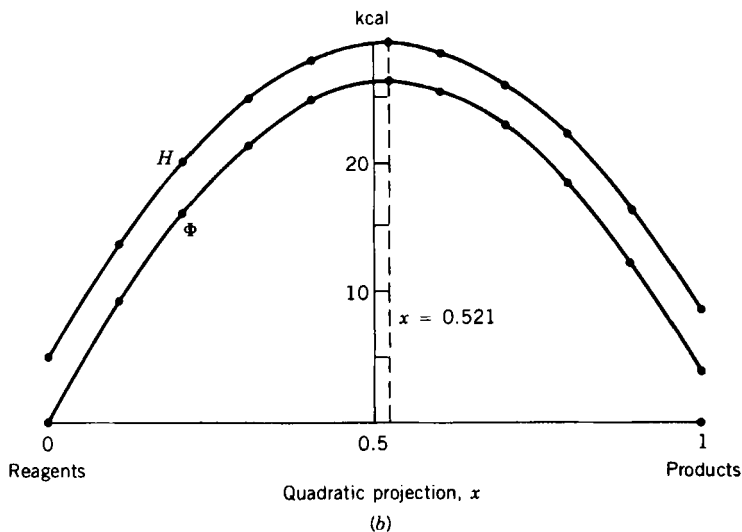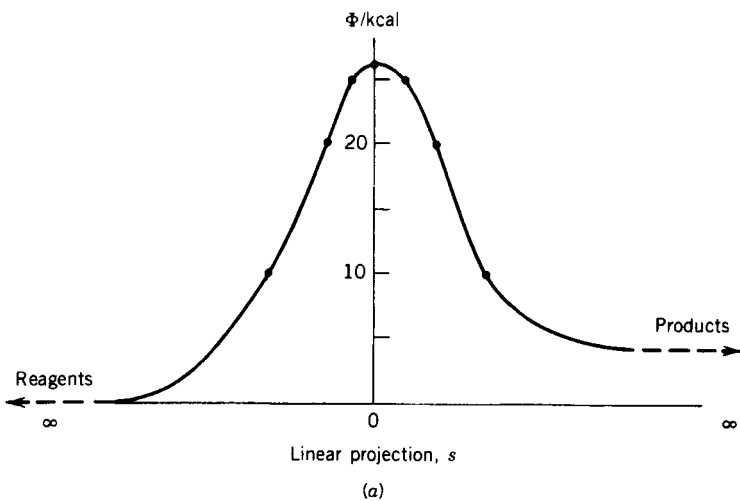
**Figure 3** Projections of data in Fig. 1: (a) linear projection; (b) quadratic projection (filled circles, $\Phi$; half-filled circles, H). The inverted parabola that fits the enthalpy $H$ is calculated from $\Phi$ using plausible values for the zero-point energies and kinetic energies of the monatomic and diatomic reagents and products, and of the transition state.

and $c$ parameters, which define the shape of the parabola, are independent of the zero point and thus absolute. These parameters are derived conveniently from the following potential-energy changes: $\Delta\Phi^\circ = (\Phi$ for products $- \Phi$ for reagents$) = b + c$, and $\Delta\Phi^\ddagger = (\Phi^\ddagger - \Phi$ for reagents$) = - b^2/4c$.

Quadratic projections such as Fig. 3$b$ are useful because the abscissa $x$ simulates the bond order of the newly forming bond. Note, for instance, that the long tails in the linear projection of Fig. 3$a$, which represent states in which the reagents or products are far apart, now collapse into two short segments in which the simulated bond order is either close to zero or close to unity. Note also that the region around the transition state, where small changes in bond distance produce relatively large changes in bond order, is now much broader. Indeed, the resemblance to a plot of bond order is so good that some experts call the quadratic plot a bond-order plot, without qualification.

Note that in Fig. 3$b$, the simulated bond order $x^\ddagger$ at the transition state is greater than 0.5, suggesting that the transition state is "late," in agreement with the original Fig. 1.


## III.  INTERPOLATION BETWEEN THERMODYNAMIC ENERGY POINTS

Experimental structure–energy relationships involve changes in thermodynamic energies rather than of potential energies. Appropriate energy functions are $E$, $H$, $F$, and $G$. These are separate functions, but for the present it will be convenient to denote them collectively as "thermodynamic energy" $E$.

The change of variable from potential energy to thermodynamic energy has a profound effect on mathematical continuity. The potential energy is a microscopic variable; $\Phi$ is defined for any configuration of the set of interacting atoms and thus varies continuously along the reaction coordinate. The thermodynamic energy $E$ for a reaction mixture, on the other hand, can be reduced to molecular properties only in limited detail, by dissection into partial molar energies assignable to chemical species or subspecies (5). In statistical terms, although a chemical species is an ensemble of molecules with a range of properties, all molecules of a species must have *the same* equilibrium configuration. Thus, along a reaction coordinate, one can define only as many chemical species as there are equilibrium configurations.

The term "equilibrium configuration" in this context refers to configurations of mechanical equilibrium, based on zero slopes for the potential energy. On typical plots of potential energy–reaction coordinate (such as Figs. 1 and 3) there are three such configurations: the reagents and products, which are in stable or metastable equilibrium; and the transition state, which is

in unstable equilibrium.* Thus, although the reaction coordinate is continuous, the thermodynamic energy along it is discontinuous.

In the study of structure–energy relationships one often finds that relationships involving $\Phi$ and $E$ are closely similar. We have seen that the continuous plots of $\Phi$ versus reaction coordinate give useful information. One would therefore like to modify the discrete plots of $E$ versus reaction coordinate so that they simulate the continuous behavior of the potential energy. Physically this means that one must use *standard* partial molar energies, since the potential energy of a molecular configuration is independent of the concentration. Mathematically it means that one must fit the discrete energy points to an appropriate continuous function of the reaction coordinate. However, since one has only three energy points to work with, the fitting function cannot have more than three adjustable parameters.

Consider the limitations thus imposed. Let $x$ denote the reaction coordinate. The highest algebraic function $E(x)$ involving no more than three parameters is a parabola, $E(x) = a + bx + cx^2$. To let this parabola simulate the normalized inverted parabola obtained for $\Phi(x)$ in quadratic projection (e.g., Fig. 3b), one lets $x = 0$ for the reagents and $x = 1$ for the products and places $x^{\ddagger}$ for the transition state at the parabolic maximum between reagents and products. The calculation of $a$, $b$, and $c$ then is analogous to that described for $\Phi(x)$ in Section II: $a$ defines the intercept and depends on the arbitrary choice of the energy-zero; $b$ and $c$ define the shape. It is convenient to calculate $b$ and $c$ using the standard energy of reaction $[\Delta E^{\circ} = E^{\circ}(\text{products}) - E^{\circ}(\text{reagents}) = b + c]$ and the standard energy of activation $[\Delta E^{\ddagger} = E^{\ddagger} - E^{\circ}(\text{reagents}) = -b^2/4c]$. These $\Delta E$ quantities are independent of the energy-zero and are measurable.

A simulated quadratic projection of $E(x)$ is shown as a dashed curve in Fig. 3b. In this case the collective symbol $E$ denotes the enthalpy function $H$, and the potential surface is that shown in Fig. 1. The calculation of $H$ from $\Phi$ assumes typical values for the kinetic and zero-point energies of monatomic and diatomic species. There is a close qualitative resemblance between the real quadratic projection of $\Phi(x)$ for this reaction and the simulated quadratic projection of $E(x)$. In particular, the maxima are practically equal. Note, however, that values of $E(x)$ interpolated between the energy points for the reagents, products, and transition state have no thermodynamic significance.

It is convenient to rewrite the equation for the inverted parabola $E(x)$ so that the number of fitting parameters is reduced. This is done in Equation 1.

$$E = -4\gamma(x - \tfrac{1}{2})^2 + \Delta E^{\circ}(x - \tfrac{1}{2}) \tag{1}$$

---

*Potential wells, dips, or bumps, on the reaction coordinate will be considered in Section X.

The energy-zero is shifted to $x = \frac{1}{2}$, $\gamma$ is a parameter— for an inverted parabola $\gamma > 0$, and the standard energy change $\Delta E^\circ$ is introduced directly in place of a second parameter. To simplify the notation, $E^\circ$(reagents) will become $E_r^\circ$, and $E^\circ$ (products) becomes $E_p^\circ$. By letting $dE/dx = 0$, one finds that $x^\ddagger$ at the maximum (which represents the transition state) is given by Equation 2. Energies $E_r^\circ$ and $E_p^\circ$ are given by Equation 3, and the activation energy $\Delta E^\ddagger = E^\ddagger - E_r^\circ$ is given by Equation 4:

$$x^\ddagger = \frac{1}{2} + \frac{\Delta E^\circ}{8\gamma} \tag{2}$$

$$E_r^\circ = E(0) = -\gamma - \frac{\Delta E^\circ}{2}$$

$$E_p^\circ = E(1) = -\gamma + \frac{\Delta E^\circ}{2} \tag{3}$$

$$\Delta E^\ddagger = E(x^\ddagger) - E_r^\circ = \gamma + \frac{\Delta E^\circ}{2} + \frac{(\Delta E^\circ)^2}{16\gamma} \tag{4}$$

Equations 2–4 represent the essence of rate–equilibrium relationships due to R. A. Marcus (6), who also introduced the name *intrinsic barrier* for $\gamma$. The latter name follows from Equation 4, because when $\Delta E^\circ = 0$ (e.g. as in an identity reaction), $\Delta E^\ddagger = \gamma$. Further consideration of Equations 2–4 will be postponed to Section V.

Continuous functions other than inverted parabolas are sometimes useful for fitting the thermodynamic energy points along the reaction coordinate. Such functions must not contain more parameters than there are thermodynamic energy points—normally three. One of the fitting parameters does the trivial job of fixing the energy-zero; the other two are calculated from available values of $\Delta E^\circ$ and $\Delta E^\ddagger$.

A convenient procedure for generating alternative functions is due to J. L. Kurz (4). Briefly, one begins with Equation 1 and transforms the variable plotted along the abscissa. Let $w$ denote any continuous reaction coordinate in the range $w_r$ to $w_p$ (from reagents to products). Let $x$ (the variable in Equation 1) be a continuous, single-valued function $x(w)$ that satisfies the conditions that $x(w_r) = 0$ and $x(w_p) = 1$. Substitution of $x(w)$ in Equation 1 then generates an alternative function $E(w)$ that fits the same thermodynamic energy points.

Some examples in which $\gamma = 20$ kcal and $\Delta E^\circ = -10$ kcal are shown in Fig. 4. The appropriate inverted parabola $(x = w)$ then is shown in Fig. 4a. In Fig. 4b, $x = \exp(w)/[\exp(w) + 1]$; $w_r = -\infty$ and $w_p = +\infty$. The resulting plot, known as an *Eckart barrier* (7), resembles a direct projection, such as that
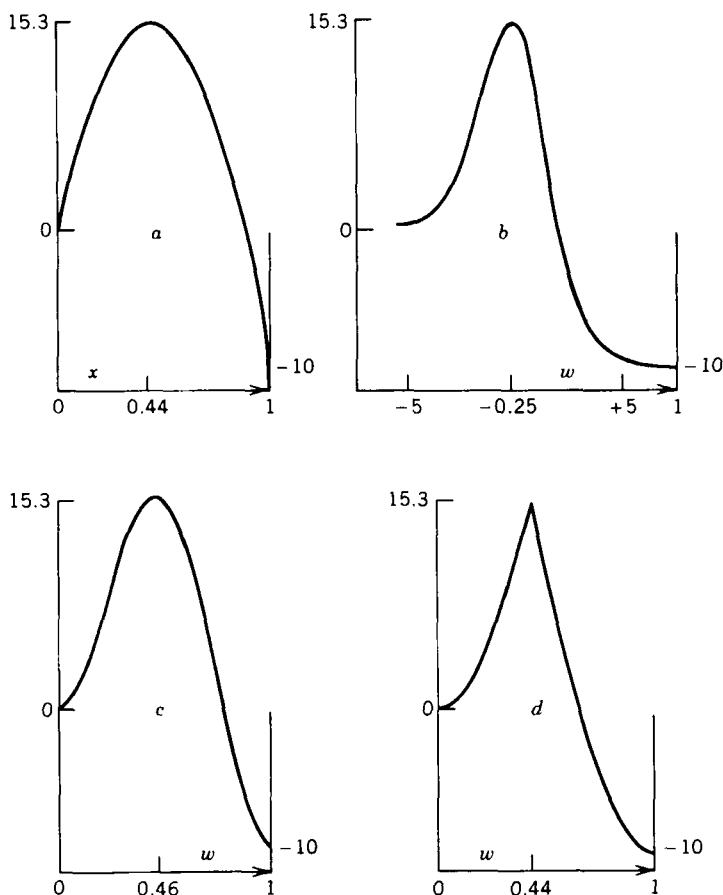
**Figure 4** Some of the many continuous functions that fit a given set of thermodynamic energy values (in this example, $\gamma = 20$ kcal, $\Delta E = -10$ kcal): (a) Inverted parabola; (b) Eckart barrier; (c) sinusoidal barrier; (d) spline function consisting of two upright back-to-back parabolas with equal curvatures, knotted at the transition state. Note that the abscissa for the transition state depends on the function used.

shown in Fig. 3a. The equation for the Eckardt barrier is given in Equation 5; $w$ ranges from $-\infty$ to $+\infty$. Assuming that $\Delta E°$ has been measured, the intrinsic barrier $\gamma$ is the sole fitting parameter.

$$E(w) = \frac{-\gamma[\exp(w) - 1]^2}{[\exp(w) + 1]^2} + \frac{\Delta E°}{2} \frac{[\exp(w) - 1]}{[\exp(w) + 1]} \tag{5}$$

In Fig. 4c, $x = \sin^2(\pi w/2)$ and $0 \leqslant w \leqslant 1$. This figure is more peaked than

the inverted parabola, and a barrier of this shape is often used to represent conformational changes (8).

In Fig. 4d, $E(w)$ is a spline function consisting of two upright parabolas knotted at the transition state (6). The two parabolas have the same absolute curvature $8\gamma$, which is also the curvature of the original inverted parabola of Fig. 4a. Another useful function, not generated by the procedure of Kurz (4), is the Agmon–Levine function (9), $E(x) = x \Delta E^\circ - (\gamma/\ln 2)(x \ln x + [1 - x] \ln [1 - x])$.

The four plots in Fig. 4 differ greatly in appearance, but there is no basic problem with that; all plots fit the given thermodynamic energy points, and all involve a permissible number of parameters. The continuous curves interpolated between the thermodynamic energy points are not real; they simulate the likely appearance of different projections of the reaction coordinate from possibly different potential surfaces.

## IV.  REACTION SERIES AND REACTION ARRAYS

The reaction zone in a one-step reaction consists of all zones in the reagents, products, and the transition state in which changes in formal bond orders take place, that is, in which bonds are made, broken, replaced, reordered, or rearranged. The part structures outside the reaction zone remain formally intact. They are not inert, however; they interact with the reaction zone by physical and electronic mechanisms. Introduction of a substituent outside the reaction zone modifies this interaction and produces a "substituent effect."

A reaction series is a series of reactions with a variable substituent at a particular site outside the reaction zone. Examples are the attack of *meta*- or *para*-substituted phenoxide ions on methyl iodide (Equation 6), and the addition of substituted ethanols to formaldehyde catalyzed by a series of acetate bases (Equation 7):

$$(p, m)\text{-}XC_6H_4O^- + CH_3I \rightarrow (p, m)\text{-}XC_6H_4OCH_3 + I^- \tag{6}$$

$$YCH_2CO_2^- + HO + H_2C-O \rightarrow YCH_2CO_2H + O-CH_2O^- \tag{7}$$
$$\qquad\qquad\quad |\qquad\qquad\qquad\qquad\qquad\qquad |$$
$$\qquad\quad CH_2CH_2Z \qquad\qquad\qquad\qquad CH_2CH_2Z$$
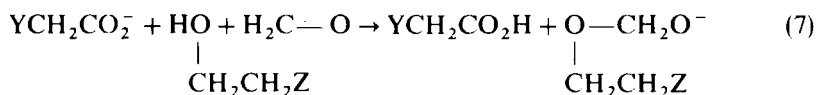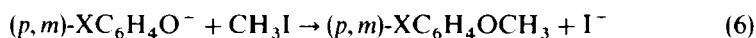
where X, Y, and Z denote variable substituents. The range of possible substituents is wide. The only constraint is that the substituent may not participate directly in the reaction, because that would transform it into part of the reaction zone.

When there are two or more independent sites of substitution, the series of reactions forms a reaction array. For example, Equation 7 indicates two substituent sites: Y in the carboxylate catalyst and Z in the alcohol. Suppose that a given study includes four Y substituents and four Z substituents. This will define the following reaction array:

$$Y_1Z_1 \quad Y_1Z_2 \quad Y_1Z_3 \quad Y_1Z_4$$

$$Y_2Z_1 \quad Y_2Z_2 \quad Y_2Z_3 \quad Y_2Z_4$$

$$Y_3Z_1 \quad Y_3Z_2 \quad Y_3Z_3 \quad Y_3Z_4$$

$$Y_4Z_1 \quad Y_4Z_2 \quad Y_4Z_3 \quad Y_4Z_4$$
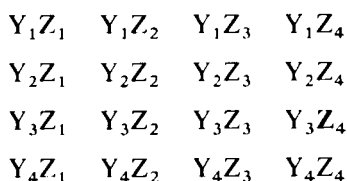
Note that each row and each column in the array is a separate reaction series.

When there are more than two sites of substitution, the reaction array becomes three- or higher-dimensional. Considering that the independent substituents $(X, Y, Z, \ldots)$ can vary widely, the study of substituent effects evidently includes a large body of chemistry.

## A.  Substituent Effects as Perturbations of the Reaction Zone

When the substituent is sufficiently remote from the reaction zone, its effect may be treated as a physical perturbation, which simplifies the mathematics because perturbations by definition are relatively small. To define the "remoteness from the reaction zone" at which such treatment becomes logical, we shall consider a broader problem, the representation of energy quantities (such as $E_r^\circ$ and $E_p^\circ$) as additive–constitutive functions of molecular structure. Such functions can be developed to any desired degree of accuracy. For example, in the scheme described by Benson and Buss (10), the energy of a molecular species in first approximation is a sum of bond-energy terms that are characteristic of the bonded pairs of atoms. In second approximation, the bond-energy term for a pair of bonded atoms depends also on the nature of the neighbor atoms to the bonded atoms. In third approximation, a bond-energy term depends on both the nature of the neighbor atoms and the next-neighbor atoms, and so on. As a corollary, in first approximation $\Delta E^\circ$ for a reaction depends only on the bond changes in the reaction zone. The effects of alterations of structure *outside* the reaction zone are defined in this approximation to be small and may therefore be treated as perturbations. In second approximation, $\Delta E^\circ$ depends on both the bond changes in the reaction zone and the nature of atoms directly bonded to the reaction zone. In this case, structural changes more than one atom removed

from the reaction zone may be treated as perturbations, and so on. Within the framework of this chapter, substituent effects are small enough to be treated as perturbations if the structural change is more than one atom removed from the reaction zone and if the substituent neither encroaches on nor becomes part of the reaction zone.

When substituent effects in a reaction series are treated as perturbations of the reaction zone, there is a characteristic perturbation at every point along the reaction coordinate whose magnitude varies with progress along the reaction coordinate. Our intuition for devising a realistic model for this relationship is perhaps most keenly honed if the projected reaction coordinate simulates a changing bond order in the reaction zone. Quadratic projections such as Equation 1 are therefore especially useful. In the next section we shall explore a model of *linear* perturbations within the framework of quadratic projections.

## V.  LINEAR PERTURBATIONS

The model of linear perturbations by substituents leads to the Marcus equations (6), which will now be derived. Let the subscripts R and 0 denote properties in the presence and absence of the substituent, respectively. Let the reference reaction be that without a substituent, and let the operator $\delta_R$ denote the effect of a substituent. For example, $\delta_R \Delta E°$ denotes $\Delta E_R° - \Delta E_0°$. The perturbation energy $\delta_R E(x)$ then is defined in 8a and is modeled as a linear function of $x$ in Equation 8b. After rewriting Equation 1 with 0 subscripts to indicate the reference reaction, addition of the perturbation energy yields Equation 8c, which can be simplified to Equation 8d:

$$\delta_R E(x) = E_R(x) - E_0(x) \tag{8a}$$

$$\delta_R E(x) = \delta_R \Delta E°(x - \tfrac{1}{2}) \tag{8b}$$

$$E_0(x) + \delta_R E(x) = -4\gamma_0(x - \tfrac{1}{2})^2 + (\Delta E_0° + \delta_R \Delta E°)(x - \tfrac{1}{2}) \tag{8c}$$

$$E_R(x) = -4\gamma_0(x - \tfrac{1}{2})^2 + \Delta E_R°(x - \tfrac{1}{2}) \tag{8d}$$

Equation 8d is formally identical to Equation 1 but differs physically because R is a variable substituent. Thus $\delta_R \Delta E°$ is a variable. The parameter $\gamma$ is not perturbed in Equation 8b and thus remains constant at $\gamma_0$ for the reference reaction.

Equations 9a, b are formally identical to Equations 2 and 4 and are

derived analogously:

$$x_R^{\ddagger} = \frac{1}{2} + \frac{\Delta E_R^{\circ}}{8\gamma_0} \tag{9a}$$

$$\Delta E_R^{\ddagger} = \gamma_0 + \frac{\Delta E_R^{\circ}}{2} + \frac{(\Delta E_R^{\circ})^2}{16\gamma_0} \tag{9b}$$

Moreover, because R is variable, the derivative (Equation 9c) exists. Note that it equals $x_R^{\ddagger}$.

$$\frac{d\,\Delta E_R^{\ddagger}}{d\,\Delta E_R^{\circ}} = \frac{1}{2} + \frac{\Delta E_R^{\circ}}{8\gamma_0} = x_R^{\ddagger} \tag{9c}$$

Equations 9 are the Marcus equations. They are noteworthy because they make clear predictions that enjoy considerable practical success. Equation 9b predicts that in a reaction series, the chemical–kinetic property $\Delta E_R^{\ddagger}$ varies monotonically with the equilibrium property $\Delta E_R^{\circ}$, with uniform curvature. If the collective symbol $E$ is identified with the free energy $G$, this prediction often agrees with experiment, especially for reactions with relatively simple molecular mechanics such as proton (11–13), hydride (14), and methyl (15, 16) transfer. [In liquid solutions, rate–equilibrium relationships involving the enthalpy $H$ tend to show more scatter (2).] According to Equations 9a, c, the slope of the rate–equilibrium relationship (Equation 9b) simulates the fractional conversion of bond order in the reaction zone at the transition state. This prediction agrees with the inductively derived Leffler postulate (17), which often serves as a starting point for the characterization of proton transfer mechanisms. Moreover, Equation 9a predicts that as $\Delta E^{\circ}$ decreases (in the algebraic sense), $x^{\ddagger}$ decreases, that is, the transition state moves along the reaction coordinate toward the reagents. Conversely, as $\Delta E^{\circ}$ increases, the transition state moves toward the products. These predictions agree with the inductively derived Hammond postulate (18) concerning the positions of transition states along reaction coordinates. In contrast to the Hammond postulate, however, Equation 9a imposes a constraint whose significance is controversial: The magnitude of $\Delta E^{\circ}$ cannot exceed $4\gamma$ unless $x^{\ddagger}$ may vary outside its normal range of 0–1.

Because of the simplicity of the model on which Marcus theory is based, one may predict that its use will have limitations. The most obvious deviation from the model is that the perturbations in fact are *not* linear (in the sense of Equation 8b), perhaps because the substituents interact by more than one physical mechanism, or because they interact differently with different parts of

the reaction zone. These complications will be examined in subsequent sections.

## VI.  QUADRATIC PERTURBATIONS

There is long-standing opinion that energy perturbations by substituents are intrinsically nonlinear in their dependence on the changing bond order in the reaction zone. To cite a historic example, the electronic theory of the English school predicts extra inductive and resonance effects for the transition state (19). The theory notes that the transition state is at an energy maximum, and that bonds in the reaction zone are relatively weak. Electron distributions in the reaction zone therefore are extrapolarizable and, because of the raising of energy levels, some electrons become extrasusceptible to resonance interaction with appropriate substituents.

It is convenient to represent a nonlinear perturbation energy as a power series in $(x - \frac{1}{2})$:

Nonlinear perturbation:

$$\delta_R E(x) = \delta_R k \left( x - \frac{1}{2} \right) - 4\delta_R a \left( x - \frac{1}{2} \right)^2 + 4\delta_R b \left( x - \frac{1}{2} \right)^3 - \cdots$$

$$\delta_R E(0) = \frac{-\delta_R k}{2} - \delta_R a - \frac{\delta_R b}{2} - \cdots$$

$$\delta_R E(1) = \frac{+\delta_R k}{2} - \delta_R a + \frac{\delta_R b}{2} - \cdots$$

Truncation of the series at the quadratic term identifies $\delta_R k$ with $\delta_R[E(1) - E(0)]$ and yields Equation 10a. Substitution in Equation 8a and application of Equation 1 to the reference reaction yields Equations 10b and 10c:

Quadratic perturbation:

$$\delta_R k = \delta_R \Delta E^\circ \tag{10a}$$

$$\delta_R E(x) = \delta_R \Delta E^\circ (x - \tfrac{1}{2}) - 4\delta_R a (x - \tfrac{1}{2})^2 \tag{10b}$$

$$E_R(x) = -4(\gamma_0 + \delta_R a)(x - \tfrac{1}{2})^2 + \Delta E_R^\circ (x - \tfrac{1}{2}) \tag{10c}$$

The intrinsic barrier $\gamma_0$ for the reference reaction remains constant throughout the reaction series, but $\delta_R a$ is a variable. One may therefore define a variable intrinsic barrier $\gamma_R$ according to Equation 11a so that Equation 10b becomes

formally identical to Equation 8d. A rate–equilibrium relationship (Equation 11b) may then be written by analogy to Equation 9b:

$$\gamma_R = \gamma_0 + \delta_R a \qquad (11a)$$

$$\Delta E_R^{\ddagger} = \gamma_R + \frac{\Delta E_R^{\circ}}{2} + \frac{(\Delta E_R^{\circ})^2}{16\gamma_R} \qquad (11b)$$

If $\gamma_R$ is a smooth function of $\Delta E_R^{\circ}$, Equation 11b expresses a smooth rate equilibrium relationship. A simple example  a linear function  will be considered below. At this point we shall assume that the relationship is not smooth, so that a plot of $\delta_R a$ versus $\Delta E_R^{\circ}$ shows significant scatter.

From a practical point of view, the sort of scatter one is likely to find may well be tolerable. Typical values of $\gamma_0$ are $> 10$ kcal/mole, while typical scatter magnitudes may well be below 1 kcal/mole. If so, Equation 11b in practice simplifies to Equation 9b, except that the fit is relatively poor. However, the $\gamma$ parameter now no longer represents $\gamma_0$ for the reference reaction, but an appropriate average of $\gamma_R$ for all substituents in the series. Perhaps more important, because the scatter is not statistically random, the slopes of the fitted function deviate by indeterminate amounts from Equation 9c and are therefore unreliable in expressing $x^{\ddagger}$ at the transition state. When Equation 11b in the simplified form of Equation 9b is applied to a family of reaction series in which the substituents interact with the reaction zones by identical physical mechanisms, the scatter patterns will be similar.

## A.   When the Quadratic Coefficients are Linear in $\Delta E^{\circ}$

A key feature of Marcus's theory (Equations 8 and 9) is that the slope $d \Delta E^{\ddagger}/d \Delta E^{\circ}$ of the rate–equilibrium plot is equal to $x^{\ddagger}$, the progress variable that simulates the bond order at the transition state. Since rate–equilibrium relationships are used for the characterization of transition states, the reliability of this approach is of interest.

There are two experimental signs that Equations 8 and 9 are not always reliable. First, reactions whose rate constants can be measured conveniently at ordinary temperatures rarely have very large or very small values for $\Delta E^{\circ}$. As a result, one expects from Equation 9c that the slopes $d \Delta E^{\ddagger}/d \Delta E^{\circ}$ will mostly be near 0.5  say, between 0.4 and 0.6. While many experimental slopes do fall in this range, slopes outside the range are not uncommon; and while the slopes almost always lie between the theoretical limits of 0 and 1, examples are known in which these limits are exceeded.

Second, Equations 8 and 9 predict that the plots of $\Delta E^{\ddagger}$ versus $\Delta E^{\circ}$ are gently curved. In a short reaction series such curvature might be obscured
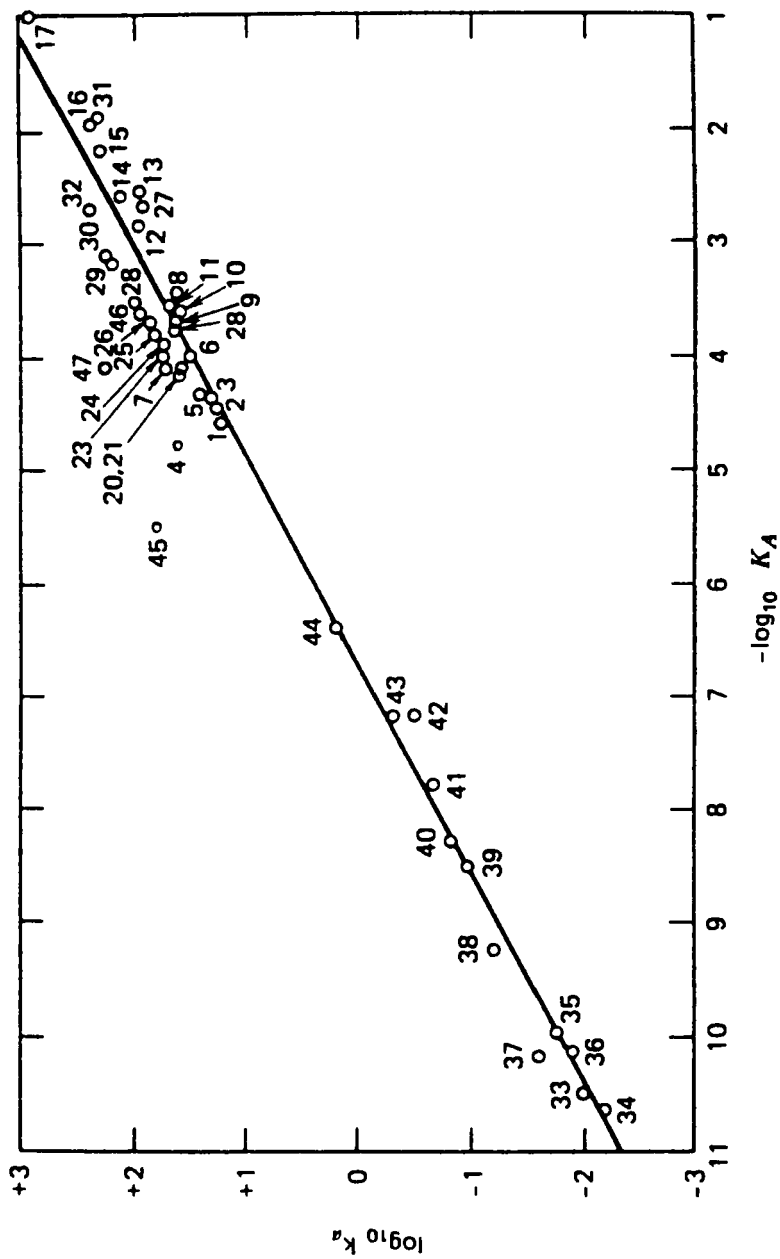
**Figure 5** A classic example of a long and straight rate–equilibrium relationship. Data for the acid-catalyzed dehydration of acetaldehyde hydrate in water from R. P. Bell and W. C. E. Higginson. *Proc. Roy. Soc. (London) A, 197*, 141 (1979). Points 1–32, carboxylic acid catalysts; points 33–47, phenol catalysts. Data points have been corrected by statistical factors when there are equivalent catalytic groups in the acid or its conjugate base.

by experimental error, but in a long series, with a wide range of $\Delta E°$, the curvature should be evident. In fact, there are well-documented cases in which curved plots are expected but the real plots are straight lines. A historic example is shown in Fig. 5 (20). The data are correlated by a straight line with slope 0.54, without statistical evidence for curvature, even though $\Delta E°$ varies by more than 13 kcal/mole.

These facts suggest that the model of *linear* perturbation of a *single* progress variable ($x$ in Equation 8) is not generally valid. There are two approaches for generalizing the model. In one approach, whose discussion begins in the next section, the single progress variable $x$ is replaced by two or more progress variables. In the other approach, described here, the linear perturbations are replaced by smooth quadratic perturbations. We shall find that this approach can overcome the limitations of Equations 8 and 9, but that the slopes $d\Delta E^{\ddagger}/d\Delta E°$ then no longer measure $x^{\ddagger}$ at the transition state.

The basic treatment is that of Equations 10 and 11. A linear relationship between $\gamma_R$ and $\Delta E_R°$ will be assumed. Accordingly, let $\gamma_R = \gamma - \zeta \Delta E_R°$ and $\gamma_0 = \gamma - \zeta \Delta E_0°$, where $\gamma$ and $\zeta$ are intrinsic parameters for the reaction series. The quadratic perturbation energy then is given by Equation 12a, and energy along the reaction coordinate is given by Equation 12b:

$$\delta_R E(x) = 4\zeta \delta_R \Delta E°(x - \tfrac{1}{2})^2 + \delta_R \Delta E°(x - \tfrac{1}{2}) \tag{12a}$$

$$E_R(x) = -4(\gamma - \zeta \Delta E_R°)(x - \tfrac{1}{2})^2 + \Delta E_R°(x - \tfrac{1}{2}) \tag{12b}$$

The coordinate $x^{\ddagger}$ at the transition state, and the rate–equilibrium relationship, are

$$\frac{\partial E_R}{\partial x} = 0; \qquad x^{\ddagger} = \frac{1}{2} - \left(8\zeta - 8\left[\frac{\gamma}{\Delta E_R°}\right]\right)^{-1} \tag{12c}$$

$$\Delta E_R^{\ddagger} = \gamma + \Delta E_R°\left(\frac{1}{2} - \zeta + \Delta E_R° \cdot (16[\gamma - \zeta \Delta E_R°])^{-1}\right) \tag{12d}$$

The slope of the rate–equilibrium relationship is given by Equation 12e. Note that it differs from $x^{\ddagger}$:

$$\frac{d\Delta E_R^{\ddagger}}{d\Delta E_R°} = \frac{1}{2} + \frac{\Delta E_R°}{8\gamma_R} - \zeta\left(1 - \left(\frac{\Delta E_R°}{[4\gamma_R]}\right)^2\right)$$

$$= x^{\ddagger} - \zeta\left(1 - \left(\frac{\Delta E_R°}{[4\gamma_R]}\right)^2\right) \tag{12e}$$

In Equation 12e the term $(\Delta E_R^{\ddagger}/[4\gamma_R])^2$ is almost always negligible compared to unity. Hence Equation 12e in practice reduces to

$$\frac{d\,\Delta E_R^{\ddagger}}{d\,\Delta E_R^{\circ}} \simeq x^{\ddagger} - \zeta \qquad\qquad (12f)$$

In theory there are no constraints on the sign and magnitude of $\zeta$. However, since real slopes rarely exceed the normalized limits of 0 and 1, the magnitude of $\zeta$, given the present model, would rarely exceed $\frac{1}{2}$.

In Equation 12d, the rate-equilibrium relationship is written in a convenient form for assessing the magnitude of the predicted curvature. Curvature enters through the term $\Delta E_R^{\circ} \cdot (16[\gamma - \zeta\,\Delta E_R^{\circ}])^{-1}$ in the coefficient of $\Delta E_R^{\circ}$. This term is relatively small, and its curvature-producing effect is moderated by the appearance of $\Delta E_R^{\circ}$ in both the numerator and the denominator. Thus one can envisage many realistic combinations of $\gamma$, $\zeta$, and a wide-ranging $\Delta E_R^{\circ}$, for which the predicted curvature would be experimentally undetectable.

## VII.  BIMOLECULAR SUBSTITUTION

In this section the basic feature of the Marcus theory (6)    linear perturbation of quadratic projections of the reaction coordinate—will be retained, but reaction progress will be specified by two progress variables. This expansion of the original model is broad enough to embrace that old warhorse of mechanistic theory, the bimolecular substitution reaction.

The essence of bimolecular substitution is symbolized by the equation

$$Y + S - X \rightarrow Y - S + X$$

where S denotes a subtrate radical, X a leaving group, and Y an entering group. In the transition state, the reaction zone $Y \cdots S \cdots X$ is bound by three-center bonds in which Y, S, and X each contribute one atomic orbital. The three resulting three-center molecular orbitals may be classified (in order of increasing energy) as bonding, nonbonding, and antibonding (21). In nucleophilic substitution these orbitals accommodate four electrons; in free-radical substitution they accommodate three; and in electrophilic substitution they accommodate two. In each case the bonding orbital is filled, and, since the next-higher orbital is nonbonding, the formal three-center bond order is 1. The real bond order in the transition state, in contrast to the formal one, varies somewhat with the nature of Y, S, and X and, in a given reaction, is perturbed by substituents.
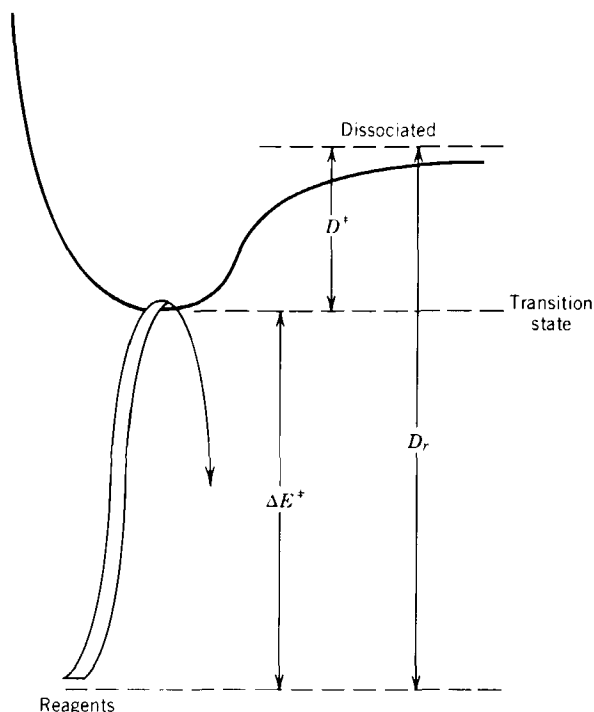
**Figure 6**   Modes of motion on the energy surface for a bimolecular substitution. Front to back, reaction coordinate. Left to right, dissociation mode.

A simplified potential-energy surface for bimolecular substitution is shown in Fig. 6. This surface resembles that in Fig. 2 but focuses on the coherent or "symmetric" stretching mode $[Y \leftarrow S \rightarrow X]$ at the transition state, which is shown as a potential well that is normal to the reaction coordinate. (The reaction coordinate is synonymous with the antisymmetric stretching mode $[Y \rightarrow S \rightarrow X]$ at the transition state.) In the compression phase of the symmetric mode, the energy increases without limit; there are no configurations of zero slope and thus no chemical species with compressed bonds.

In the stretching phase of the symmetric mode, the three-center bond dissociates. There are two types of dissociation, either to radicals or to ions. However, depending on the nature of the substitution, one is likely to focus only on one type. In radical substitution one concentrates on dissociation to radicals. In nucleophilic or electrophilic substitution one considers dissociation to ions. When dealing with perturbations of electric charges in the reaction zone as a result of electron supply or removal by substituents, one is likely to focus on ionic dissociation.

The potential well for the symmetric stretch has the typical shape for a dissociation process and is expressed in first approximation by a Morse curve (22):

$$\Phi = a + D(1 - e^{-\beta[r - r^*]})^2 = a + D(1 - w)^2 \tag{13a}$$

$$w = e^{-\beta[r - r^*]} \tag{13b}$$

where the constant term $a$ defines the zero of energy, $D$ is the dissociation energy, $r$ is the bond distance, and $r^*$ denotes $r$ at the potential minimum. The parameter $\beta$ is adjusted so that $w$ (defined in Equation 13b) simulates bond order during the stretching phase of the bond. In particular, $w = 1$ at the potential minimum and 0 in the dissociation limit, as $r$ approaches infinity. In the compression phase of the bond, bond order has no generally accepted definition, and $w$ merely denotes the quadratic progress variable.

In bimolecular substitution, the configuration at the potential minimum of the dissociating mode is identical with that of the transition state (see Fig. 6). Thus, in the notation of Equation 13, $r^* = r^{\ddagger}$. However, Equation 13 is not flexible enough to simulate substituent effects because at the potential minimum, $w$ is fixed at unity, whereas in theory, the tightness of the $Y \cdots S \cdots X$ bond at the transition state is perturbed by substituents (15, 19). In particular, electron removal from the reaction zone in S tightens the bond (shortens $r^{\ddagger}$ and raises the effective bond order $w^{\ddagger}$) by introducing positive charge between X and Y, and thereby reducing the repulsive forces in bond compression. Electron supply to the reaction zone loosens the bond (lengthens $r^{\ddagger}$ and lowers $w^{\ddagger}$) by reducing the ionic dissociation energy in processes leading to $S^+$.

To permit $w$ at the potential minimum to be a variable, the quadratic form of Equation 13a is generalized by adding a linear term. Furthermore, to permit comparison with thermodynamic data, potential energy $\Phi$ is replaced by thermodynamic energy $E$. The result is

$$E = a + \mu(1 - w)^2 + f(1 - w) \tag{14a}$$

$$\left(\frac{dE}{dw}\right)_{w^{\ddagger}} = 0; \qquad w^{\ddagger} = \frac{1 + f}{2\mu} \tag{14b}$$

Equation 14 is formally similar to Equation 1. The *intrinsic dissociation energy* $\mu$ (which is comparable to the *intrinsic barrier* $\gamma$) is a parameter characteristic of the reaction; $\mu$ is a positive number, used to describe an upright parabola. The slope $f$ of the linear term (comparable to $\Delta E°$ in Equation 1) has the dimensions of energy and varies with the substituent.

The coordinate $w^{\ddagger}$ expresses the tightness, or effective bond order, in the dissociation mode at the transition state. The slope $f$ is positive or negative depending on whether $w^{\ddagger}$ is greater or less than unity. As $f$ goes to zero, $w^{\ddagger}$ approaches unity and $\mu$ approaches the dissociation energy $D$. We shall find that $f = 2[\sqrt{(\mu D)} - \mu] \simeq [D - \mu]$.

Because the transition state now must satisfy two mathematical requirements — a maximum along the reaction coordinate and a minimum for dissociation — description of reaction progress now requires two coordinates. These coordinates may be chosen to be convenient for the problem. A convenient set $(x, w)$ for bimolecular substitution is shown in Fig. 7. The $x$ coordinate represents the direct reagents-to-products mode (r/p mode) with $w$ fixed at unity. The $w$ coordinate represents the dissociation mode. The reaction coordinate $z$ is a function of $x$ and $w$ and is normalized so that $(x, w)$ equals $(0, 1)$ for the reagents and $(1, 1)$ for the products. At the transition state, both coordinates $(x^{\ddagger}, w^{\ddagger})$ are variables depending on the reaction and the substituent.

It will be shown in Section VIII that the reaction mode $z$ and the dissociation mode $w$ are normal modes at the transition state. As a corollary, the reaction coordinate $z$ at the transition state is parallel to the $x$-axis and normal to the $w$-axis, and the modewise energies along $x$ and $w$ are simply additive. Thus $E(x, w)$ for the unsubstituted reference reaction is expressed
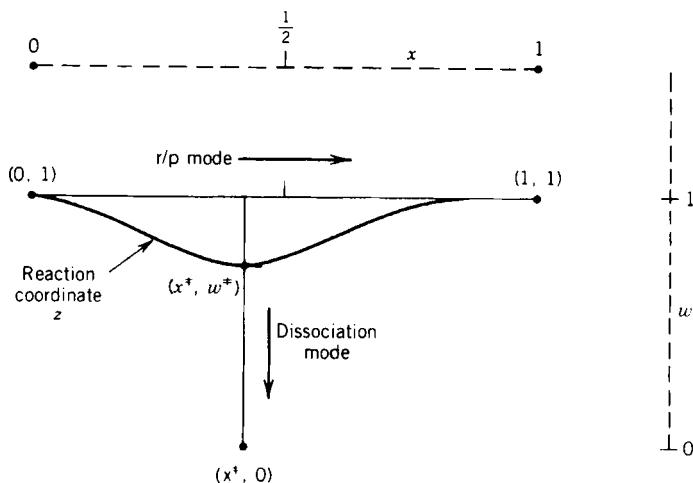


**Figure 7** Normalized $x, w$-axes, reaction coordinate, and coordinates of species in bimolecular substitution. Values of $x^{\ddagger}$ and $w^{\ddagger}$ at the transition state depend on the reaction. The figure shows a reaction in which the transition state is "early" $(x^{\ddagger} < \frac{1}{2})$ and relatively "loose" $(w^{\ddagger} < 1)$.

in Equation 15a as a sum of Equations 8c and 14a:

$$E_0(x, w) = a - 4\gamma_0(x - \tfrac{1}{2})^2 + \Delta E_0^\circ(x - \tfrac{1}{2}) + \mu_0(1 - w)^2 + f_0(1 - w) \quad (15a)$$

Substituent effects are modeled as linear perturbations in Equation 15b:

$$\delta_R E(x, w) = \delta_R \Delta E^\circ(x - \tfrac{1}{2}) + \Delta_R f(1 - w) \tag{15b}$$

Addition yields the energy surface (Equation 16), which represents $E(x, w)$ in the presence of a substituent. Note that $\gamma$ and $\mu$ are not perturbed. Transition-state coordinates for this energy surface are derived in Equation 17:

$$E_R(x, w) = a - 4\gamma_0\left(x - \frac{1}{2}\right)^2 + \Delta E_R^\circ\left(x - \frac{1}{2}\right)$$
$$+ \mu_0(1 - w)^2 + f_R(1 - w) \tag{16}$$

$$\frac{\partial E}{\partial x} = 0; \qquad x_R^\ddagger = \frac{1}{2} + \frac{\Delta E_R^\circ}{8\gamma_0} \tag{17a}$$

$$\frac{\partial E}{\partial w} = 0; \qquad w_R^\ddagger = 1 + \frac{f_R}{2\mu_0} \tag{17b}$$

Coordinates for configurations of mechanical equilibrium and energies of the corresponding chemical species are summarized in Table 1.

### A. Dissociation Mode

Before deriving a structure energy relationship for $\Delta E^\ddagger$, it helps to see how the present model treats dissociation. By applying the energy expressions in Table 1, one obtains Equations 18 (these energy quantities are also depicted in

TABLE 1
Chemical Species in the Two-Mode $(x, w)$ Representation

| Species | Coordinates $(x, w)$ | $E_R(x, w) - a$ |
|---|---|---|
| Reagents | $(0, 1)$ | $E_r = -\gamma_0 - \Delta E_R^\circ/2$ |
| Products | $(1, 1)$ | $E_p = -\gamma_0 + \Delta E_R^\circ/2$ |
| Transition state | $(x^\ddagger, w^\ddagger)$ | $E^\ddagger = (\Delta E_R^\circ)^2/16\gamma_0 - f_R^2/4\mu_0$ |
| Dissociated state | $(x^\ddagger, 0)$ | $E_d = (\Delta E_R^\circ)^2/16\gamma_0 + \mu_0 + f_R$ |

Fig. 6):

$$D_R^{\ddagger} = E_{d,R} - E_R^{\ddagger} = \mu_O + f_R + \frac{f_R^2}{4\mu_O} \qquad (18a)$$

$$D_{r,R} = E_{d,R} - E_{r,R} = \gamma_O + \frac{\Delta E_R^{\circ}}{2} + \frac{(\Delta E_R^{\circ})^2}{16\gamma_O} + \mu_O + f_R \qquad (18b)$$

$$D_{p,R} = E_{d,R} - E_{p,R} = D_{r,R} - \Delta E_R^{\circ} \qquad (18c)$$

$$D_R^{\ddagger} = D_{r,R} - \Delta E_R^{\ddagger} \qquad (18d)$$

The dissociation energy $D_R^{\ddagger}$ of the transition state cannot be measured directly, but can be obtained indirectly by use of Equation 18d by measuring the dissociation energy $D_{r,R}$ of the reagents and the activation energy $\Delta E_R^{\ddagger}$ for reaction.

The intrinsic dissociation energy $\mu_O$ is a constant for the reaction series. This parameter is adjusted to fit $D_R^{\ddagger}$, using Equation 18a or 18b. The fitting procedure is complicated, however, because $f_R$ is a function of $\mu_O$ (see Equation 20, below).

The simulated bond-order $w_R^{\ddagger}$ of the Y..S..X bond in the transition state is derived from $D_R^{\ddagger}$ and $\mu_O$. Elimination of $f_R$ between Equations 17b and 18a yields

$$w_R^{\ddagger} = \left(\frac{D_R^{\ddagger}}{\mu_O}\right)^{1/2} \qquad (19)$$

The linear perturbation slope $f_R$, which enters the model in Equations 14–16, has the dimensions of energy. Elimination of $w_R^{\ddagger}$ between Equations 17b and 19 yields

$$f_R = 2[\sqrt{(\mu_O D_R^{\ddagger})} - \mu_O] \qquad (20)$$

Although Equation 20 is exact, it is sometimes convenient to use approximate expressions without the square root. Such expressions will now be derived. For simplicity of notation, R and O subscripts will be dropped. Rearrangement of 18a gives Equation 21a, which is in a convenient form for solution by successive approximations when $|f_R/4\mu_O| \ll 1$. Let $n$ denote the order of an approximation, and let $f_0 = 0$ be the zeroth approximation. Successive

approximations then are generated by Equation 21b:

$$f = \frac{D^{\ddagger} - \mu}{1 + f/4\mu} \tag{21a}$$

$$f_n = \frac{D^{\ddagger} - \mu}{1 + f_{n-1}/4\mu} \tag{21b}$$

Results for the first three approximations are as follows:

| $n$ | $f$ |
|---|---|
| 1 | $(D^{\ddagger} - \mu)$ |
| 2 | $(D^{\ddagger} - \mu) \times 4\mu/(3\mu + D^{\ddagger})$ |
| 3 | $(D^{\ddagger} - \mu) \times (3\mu + D^{\ddagger})/(2\mu + 2D^{\ddagger})$ |

Exact result: Equation 20

## B. Structure–Energy Relationship

Equation 22 follows directly from energy expressions given in Table 1 for the reagents and transition state.

$$\Delta E_{R}^{\ddagger} = \gamma_O + \frac{\Delta E_{R}^{\circ}}{2} + \frac{(\Delta E_{R}^{\circ})^2}{16\gamma_O} - \frac{f_{R}^{2}}{4\mu_O} \tag{22}$$

The activation energy $\Delta E_{R}^{\ddagger}$ now depends on two energy variables, $\Delta E_{R}^{\circ}$ and $f_{R}$, but in different ways. The variation with $\Delta E_{R}^{\circ}$ is nearly linear, being dominated by the term $\Delta E_{R}^{\circ}/2$, while the variation with $f_{R}$ is purely quadratic. The term $- f_{R}^{2}/4\mu_O$ is negative for any nonzero value of $f_{R}$, regardless of sign. Since a value of $f_{R} = 0$ corresponds to a transition state of unit tightness ($w_{R}^{\ddagger} = 1$), any perturbation of the transition state away from unit tightness, in either direction, should decrease $\Delta E^{\ddagger}$, other things being equal. As a corollary, given a reaction series in which $f_{R}$ passes through zero while $\Delta E^{0}$ remains constant or nearly constant, the rate constant is expected to pass through a minimum at or near the point where $f_{R} = 0$.

In fact, the reaction of a series of $p$-substituted benzyl bromides with a series of thiophenoxide ions in methanol fits this pattern:

$$p\text{-RC}_6\text{H}_4\text{S}^- + p\text{-XC}_6\text{H}_4\text{CH}_2\text{Br} \rightarrow p\text{-XC}_6\text{H}_4\text{CH}_2\text{SC}_6\text{H}_4\text{R(p)} + \text{Br}^- \tag{23}$$
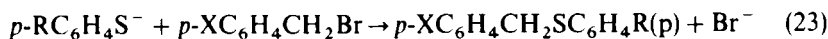
By allowing $p$-X to vary, from electron-removing $p$-NO$_2$ to electron-supplying
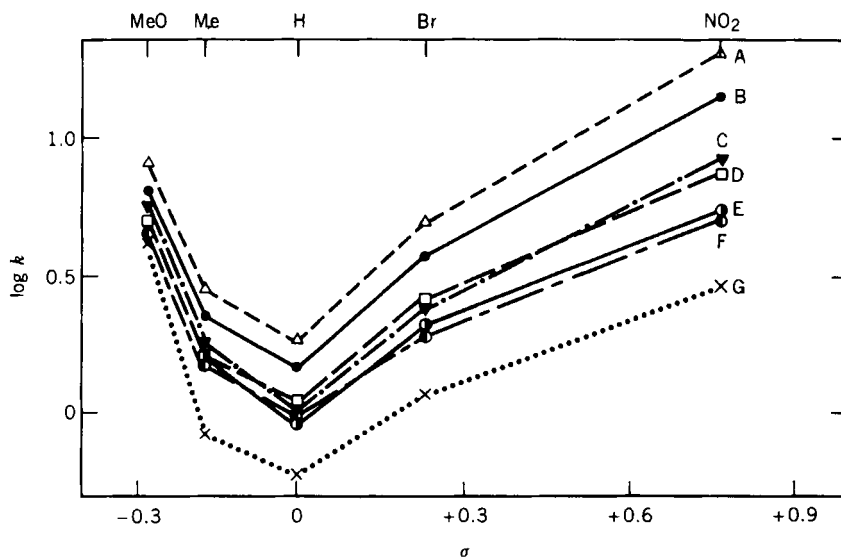
**Figure 8**  Substituent effects in the reaction of thiophenoxide ions ($p$-RC$_6$H$_4$S$^-$) with benzyl bromides ($p$-XC$_6$H$_4$CH$_2$Br) in methanol at 20°C. Benzyl bromides are arranged left to right in order of increasing electron removal by X, as measured by Hammett's $\sigma$. Substituents in thiophenoxide: (A) R = MeO; (B) R = Me; (C) R = F; (D) R = H; (E) R = Br; (F) R = Cl; (G) R = COCH$_3$. From R. F. Hudson and G. Klopman, *J. Chem. Soc., 1962*, 1062.

$p$-OCH$_3$, one perturbs the net charge at the CH$_2$ center and changes the tightness of the transition state. Although $\Delta E^0$ is nearly constant in this series, the rate constants clearly pass through a minimum, as demonstrated by the data of Hudson and Klopman[23] in Fig. 8. Data are lacking for the calculation of $f_R$, so we cannot test whether $f_R$ passes through zero at the kinetic minimum, but within the framework of Equation 22 that is a reasonable inference.

## VIII.  TWO REACTION EVENTS

Reactions in which bonds are made, broken, replaced, reordered, or rearranged at more than one site in the reaction zone, by that very fact, involve more than one reaction event. The reaction sites may be different atoms, or they may be different affinity points on one atom. The reaction events and the sites at which they take place are characteristic of, and define, the reaction mechanism. Thus the mechanism of bimolecular substitution treated in the

preceding section is characterized by bond breaking at one face of a carbon atom and bond making at the opposite face.

The progress of a reaction event during a reaction can be expressed by a progress variable such as a bond order, interatomic distance, or developing electric charge. In principle, there are as many progress variables as there are reaction events, but in the study of reaction series one often finds that the progress variables are not all independent. Operationally, two progress variables are independent if, and only if, the functional relationship between them changes as different members of the reaction series are examined. If the functional relationship is always the same, one variable is sufficient to specify the progress of *both* reaction events.

The number of independent progress variables is found by trial and error. For example, one independent variable ($x$ in Equation 8) is sufficient if the relationship between $\Delta E_R^{\ddagger}$ and $\Delta E_R^{\circ}$ for a reaction series conforms to the Marcus equation (Equation 9b).

In this section we shall analyze reactions with two reaction events—call them A and B, and their corresponding progress variables $u$ and $v$, which, at this point, need not be independent. Logically, with two reaction events there are three possible reaction mechanisms: two stepwise mechanisms, (A followed by B) and (B followed by A), and a concerted mechanism, $\{A + B\}$.

For example, in the termolecular reaction (Equation 24), the two reaction events are proton addition to water oxygen and proton removal from water oxygen:

$$Me_3N-H^+ + OH + OPh^- \rightarrow Me_3N + HO + HOPh \atop \phantom{Me_3N-H^+ +}\big| \phantom{+ OH + OPh^- \rightarrow Me_3N + }\big| \tag{24}$$
$$\phantom{Me_3N-H^+ +}H \phantom{+ OH + OPh^- \rightarrow Me_3N + }H$$
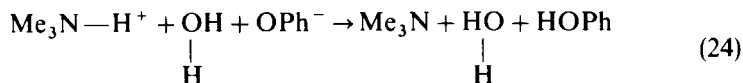
The stepwise mechanisms then are (A) proton removal from HOH followed by proton transfer to $OH^-$ and (B) proton transfer to HOH followed by proton removal from $HOH_2^+$. In the concerted mechanism both protons are transferred in a single step.

(A)   $Me_3N\cdots H^+ + OH + OPh^- \rightarrow Me_3NH^+ + O^- + HOPh \rightarrow products$
$$\phantom{(A)   Me_3N\cdots H^+ +}\big| \phantom{+ OH + OPh^- \rightarrow Me_3NH^+ +}\big|$$
$$\phantom{(A)   Me_3N\cdots H^+ +}H \phantom{+ OH + OPh^- \rightarrow Me_3NH^+ +}H$$

(B)   $Me_3N\cdots H^+ + OH + OPh^- \rightarrow Me_3N + HOH^+ + OPh^- \rightarrow products$
$$\phantom{(B)   Me_3N\cdots H^+ +}\big| \phantom{+ OH + OPh^- \rightarrow Me_3N + HO}\big|$$
$$\phantom{(B)   Me_3N\cdots H^+ +}H \phantom{+ OH + OPh^- \rightarrow Me_3N + HO}H$$
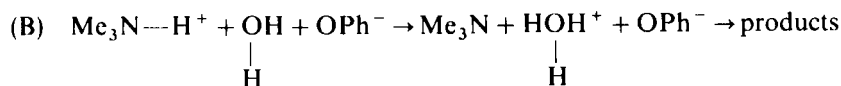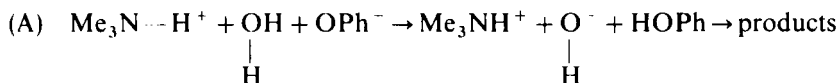
It is convenient to display the three mechanisms on a single diagram. One such diagram is the More O'Ferrall–Jencks diagram shown in Fig. 9(24,25).
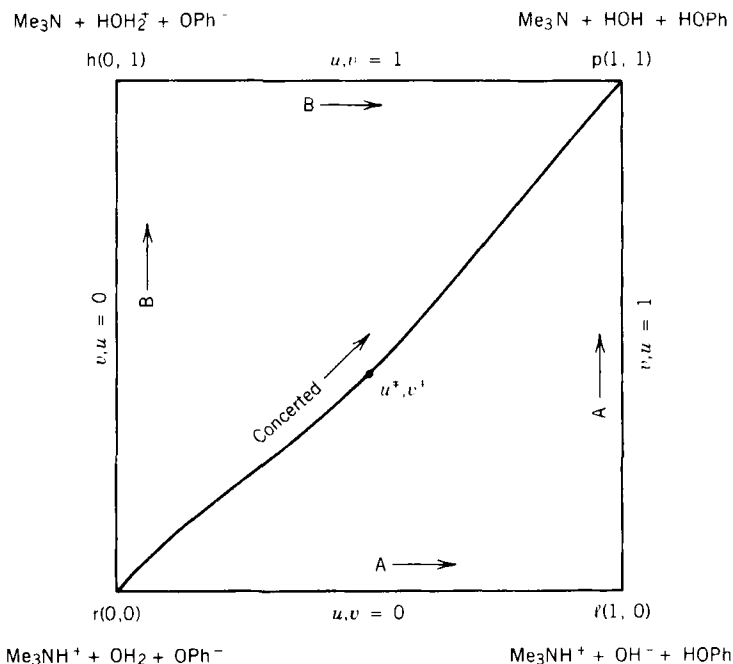
**Figure 9** More O'Ferrall–Jencks diagram for reaction events, progress variables, and reaction coordinate in a concerted two-proton transfer reaction involving an acid, a base, and a solvent water molecule. See Equation 24 and the reactions labeled A and B.

The overall diagram is a square. The axes represent the progress variables $u$ and $v$, which are normalized to vary from 0 to 1. Reagents (r) and products (p) are at the diagonal corners $(0,0)$ and $(1,1)$, respectively. The stepwise intermediates (l and h) are at the other diagonal corners. The stepwise mechanisms touch the corners: $r \rightarrow l \rightarrow p$; and $r \rightarrow h \rightarrow p$. The concerted process moves across the middle. However, as will be shown in the next section, the concerted reaction coordinate need not follow the $(r \rightarrow p)$ diagonal, and the concerted transition state $(u^{\ddagger}, v^{\ddagger})$ need not lie at the midpoint of the diagram.

Energy may be indicated on such a plot by contour lines. Two hypothetical and, perhaps, typical diagrams are shown in Fig. 10. In Fig. 10a the path of lowest energy maximum moves across the middle, showing that in this case a concerted process is the principal reaction mechanism. In Fig. 10b the path of lowest energy maximum is the stepwise process $r \rightarrow l \rightarrow p$.

In problems involving the coupling of the reaction events, the normalized progress variables $x$ and $y$ shown in Fig. 11 are more useful (26). The $x, y$ coordinates are obtained from the $u, v$ coordinates by 45° rotation, translation
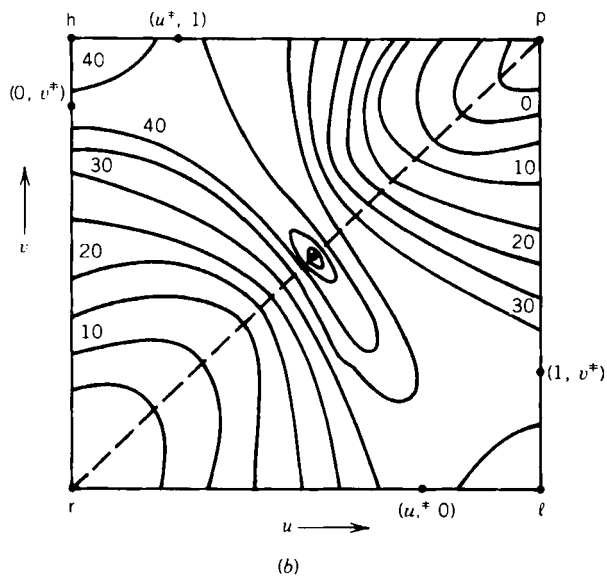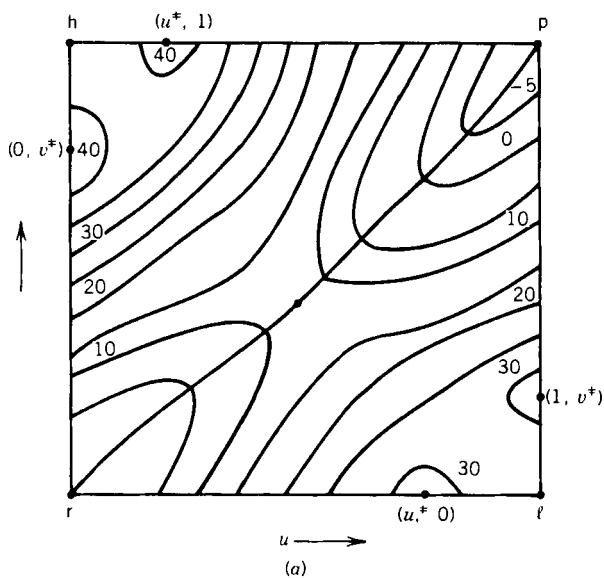
**Figure 10** Possible energy contours on a More O'Ferrall–Jencks diagram: (a) the preferred reaction mechanism is concerted; (b) the preferred reaction mechanism is stepwise via intermediate *ℓ*.

(0, 1)

($\frac{1}{2}$, 1)

h

v

y

x

(0, 0)    r    p

(0, $\frac{1}{2}$)

(x*, y*)

(1, $\frac{1}{2}$)

u

ℓ

($\frac{1}{2}$, 0)

(1, 0)
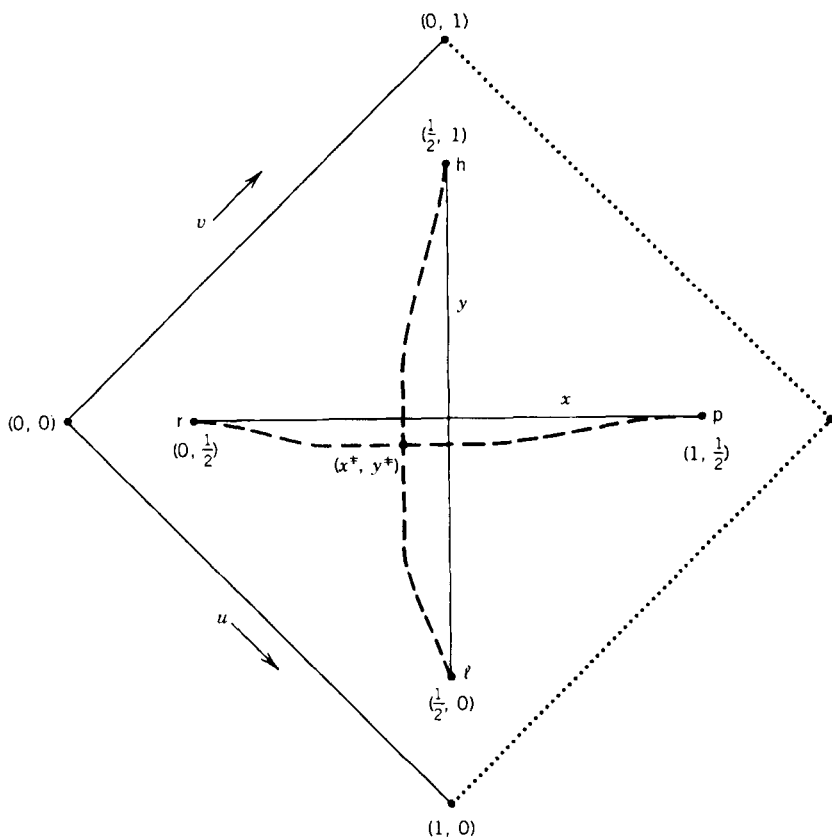
**Figure 11** Mean progress made $x$ and disparity mode $y$ for a concerted reaction involving two coupled reaction events. The progress variables for the individual reaction events are $u$ and $v$.

of the origin, and renormalization. They closely resemble the $x, w$ coordinates used in Fig. 7. The $x$-axis runs from reagents to products. The perpendicular $y$-axis connects the intermediates. The $x, y$-axes intersect at the midpoint $(\frac{1}{2}, \frac{1}{2})$ of the diagram.

The algebraic transformation from normalized $u, v$-axes (Fig. 9) to normalized $x, y$-axes (Fig. 11) is expressed as

$$x = \frac{v + u}{2} \tag{25a}$$

$$y = \frac{v - u}{2} + \frac{1}{2} \tag{25b}$$

In the $u, v$ plane, the reagents are at $0, 0$, the products at $1, 1$, and the two intermediates at $0, 1$ and $1, 0$, respectively. In the $x, y$ plane, the reagents are at $0, \frac{1}{2}$, the products at $1, \frac{1}{2}$, and the two intermediates at $\frac{1}{2}, 0$ and $\frac{1}{2}, 1$, respectively. According to Equation 25a, $x$ measures the mean progress of the two reaction events and will be called the *mean progress mode*. According to Equation 25b, $y$ measures the disparity of progress of the two reaction events, scaled so that zero disparity is expressed by $y = \frac{1}{2}$. Motion along $y$ will be called the *disparity mode*. The macroscopic reaction leading from reagents to products will be called the *main reaction*. The real or hypothetical transformation leading from one intermediate ($f$) to the other (h) will be called the *disparity reaction*.

The dashed lines in Fig. 11 represent possible reaction coordinates in a concerted mechanism. As in Fig. 7 for bimolecular substitution, these reaction coordinates need not coincide with the coordinate axes. Particulars will be derived in the next section.

## A.  Coupling of Two Reaction Coordinates

We shall now show that the two reaction coordinates in a concerted mechanism — the dashed lines in Fig. 11 — are normal modes and thus intersect at right angles at the concerted transition state. The argument makes use of two theorems: (1) for any reaction, motion along the reaction coordinate is a normal mode of motion at the transition state (27) — this normal mode will be called the *reaction mode* here; (2) and when two originally uncoupled normal modes are coupled, both coupled modes are normal modes.

The argument proceeds as follows. When the two reaction events are *not* coupled, they are ordinary chemical reactions such as the proton transfers in reactions A and B on p. 80, or displacement or addition reactions. Each uncoupled reaction coordinate therefore passes through a mechanically unstable transition state at which the respective reaction mode is a normal mode. Because of the mechanical instability, motion in such reaction modes is nonperiodic and consists of two dynamically distinct species: forward motion (f) toward completion of the reaction event and reverse motion (r) toward the initial state.

For the reaction to be concerted, the reaction modes for the two reaction events must be coupled. This is both necessary and sufficient. Other modes of motion may be coupled as well, but such coupling is not relevant to the concertedness of the reaction mechanism.

Let us consider the coupling of two reaction modes. Prior to coupling each reaction mode has two species of motion: $f_1$ and $r_1$ for the first event, and $f_2$ and $r_2$ for the second event. Coupling thus produces four species of coupled motions: $f_1 f_2$, $r_1 r_2$, $f_1 r_2$, and $r_1 f_2$. The notation $f_1 f_2$ means that the transition state moves forward in concerted motion of both reaction events to yield the final products. Similarly, $r_1 r_2$ means that the transition state

moves in concerted reverse motion to yield the original reagents. Thus $f_1r_2$ and $r_1f_2$ means that the transition state—the *same* transition state as for $f_1f_2$ and $r_1r_2$—moves in concerted hybrid motion, one event forward and the other in reverse. Inspection of Fig. 11 then shows that in $f_1r_2$, $u$ increases and $v$ decreases, that is, the reacting system moves from the concerted transition state towards the stepwise intermediate $\ell$. Similarly, in $r_1f_2$ the reacting system moves from the concerted transition state toward the stepwise intermediate h. The species $f_1f_2$ and $r_1r_2$ together form a "symmetric" reaction mode in which the coupled motions are coherent. The species $f_1r_2$ and $r_1f_2$ together form an "antisymmetric" reaction mode in which the coupled motions are 180° out of phase. In view of theorem 2, both coupled modes are normal modes for the concerted transition state. Hence in Fig. 11, the reaction coordinates for $r \to p$ and for $\ell \to h$ intersect at right angles.

The nature of the motions in the coupled normal modes is determined by the mechanical stability (or instability) of the normal modes prior to coupling, and by the strength of the coupling. If both modes prior to coupling are mechanically stable, the resulting coupled modes are either both stable or, if the coupling is strong, one is stable and one is unstable. In the present case, where both normal modes prior to coupling are mechanically *un*stable, the resulting coupled modes are either both *un*stable or, if the coupling is strong, one is unstable and the other is stable. Strong coupling then leads to a concerted reaction mechanism and an energy-contour diagram such as Fig. 10a. Weak coupling leads to a stepwise reaction mechanism and an energy-contour diagram such as Fig. 10b.

## IX. MATHEMATICAL MODEL FOR TWO REACTION EVENTS

In this section we shall derive and test rate–equilibrium relationships for reactions with two reaction events. The $x, y$ coordinates and other notations defined in Fig. 11 will be used. As before, the subscripts O and R denote properties of the unsubstituted reference reagent and of a substituted reagent, respectively; $\Delta E^\circ$ denotes the energy change $E_p^\circ - E_r^\circ$ for the main reaction; and $\Delta E'$ denotes the energy change $E_h^\circ - E_l^\circ$ for the disparity reaction. In the vicinity of the transition state, motions along $x$ and $y$, which are parallel to motions along the reaction coordinates, are normal modes. These modes will be modeled as normal modes over the entire energy surface, so that their modewise energies are simply additive. Adopting a representation of quadratic projections with linear perturbations by substituents, and applying Equation 8d with appropriate modification of symbols, addition of two modewise energies yields a paraboloidal energy surface according to

$$E(x, y) = a - 4\gamma_O(x - \tfrac{1}{2})^2 + \Delta E_R^\circ(x - \tfrac{1}{2}) + 4\mu_O(y - \tfrac{1}{2})^2 + \Delta E_R'(y - \tfrac{1}{2}) \quad (26)$$

The first term on the right in this equation fixes the zero point for energy. The next two terms represent the mean progress mode, and the final two terms represent the disparity mode. As in Equation 8d, $\gamma_0$ is the intrinsic barrier for the mean progress mode; $\mu_0$ is the corresponding intrinsic parameter for the disparity mode. The equation is written so that $\mu_0$ is positive when the reaction mechanism is concerted, that is, when the coupling of the reaction modes is strong and the disparity mode is mechanically stable. Therefore, $\mu_0$ will be called the *intrinsic energy well*. Figure 12 shows two paraboloids of the type in Equation 26—for concerted reaction, with $\mu_0$ positive, on the left; and for stepwise reaction, with $\mu_0$ negative, on the right.

On the basis of Equation 26, the $x, y$ coordinates and energy at the transition state are derived in Equation 27. The corresponding rate-equilibrium relationship is Equation 28:

$$\frac{\partial E}{\partial x} = 0; \qquad x^{\ddagger} = \frac{1}{2} + \frac{\Delta E_R^{\circ}}{8\gamma_0} \tag{27a}$$

$$\frac{\partial E}{\partial y} = 0; \qquad y^{\ddagger} = \frac{1}{2} - \frac{\Delta E_R'}{8\mu_0} \tag{27b}$$

$$E^{\ddagger} = E(x^{\ddagger}, y^{\ddagger}) = a + \frac{(\Delta E_R^{\circ})^2}{16\gamma_0} - \frac{(\Delta E_R')^2}{16\mu_0} \tag{27c}$$

$$\Delta E_R^{\ddagger} = \gamma_0 + \frac{\Delta E_R^{\circ}}{2} + \frac{(\Delta E_R^{\circ})^2}{16\gamma_0} - \frac{(\Delta E_R')^2}{16\mu_0} \tag{28}$$

The present development is conceptually similar to that for bimolecular
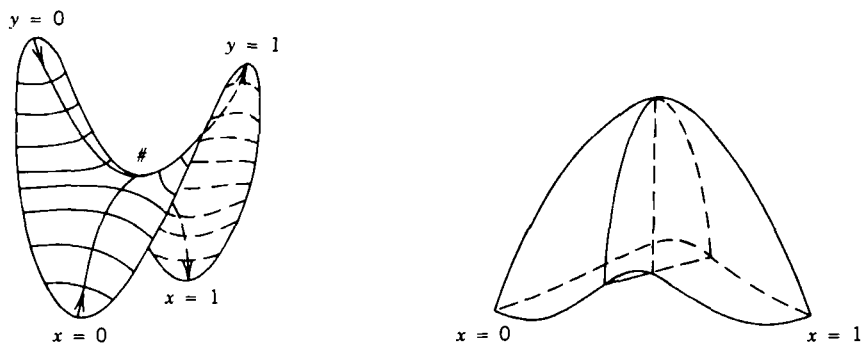


**Figure 12** Paraboloids typical of Equation 26. Left, for concerted reaction, $\mu_0 > 0$. The transition state according to Equation 27 is a saddle point. Right, for stepwise reaction, $\mu_0 < 0$. The transition state according to Equation 27 is a high point in energy.

substitution, but for practical applications there is an important difference. In Fig. 11, which embodies the gist of the present development, both sides of the disparity mode terminate in a chemical species. As a result, $\Delta E_R'$ equals $(E_h - E_l)$ and expresses the energy change in a chemical transformation. Energy changes such as $\Delta E_R'$ can be determined experimentally by appropriate thermodynamic cycles, or they can be calculated quantum-mechanically or predicted by structure–energy relationships. By contrast, the dissociation mode in bimolecular substitution (Fig. 7) terminates in a chemical species on only one side. The variable $f_R$ in Equation 22 (which is formally analogous to $\Delta E_R'$ in Equation 28) thus is physically complex, depending both on a measurable variable $(D_R^{\ddagger})$ and a model parameter $(\mu_O)$.

When applied to a reaction series with a concerted mechanism, Equation 28 permits rate minima because the final term, when $\mu_O$ is positive,
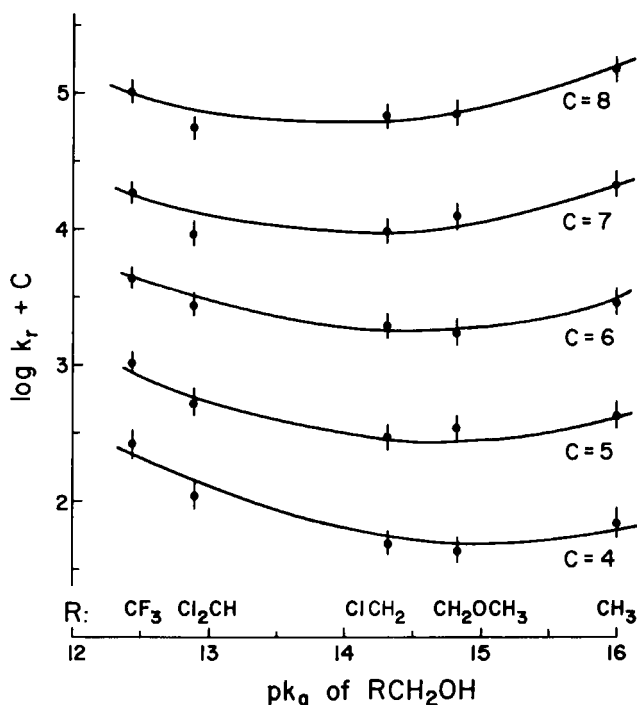


**Figure 13** Logarithmic plot of experimental rate constants versus $pK_a$ of alcohol for base-catalyzed dissociation of a series of hemiacetals of formaldehyde. The base catalysts are a series of carboxylate ions $R'CH_2COO^-$ [$R'$ = (top to bottom) CN, Cl, $CH_3O$, $ClCH_2$, H]. From L. H. Funderburk, L. Aldwin and W. P. Jencks, *J. Am. Chem. Soc.*, *100*, 5444 (1978).

passes through a maximum of zero when $\Delta E'$ is zero. Thus, if $\Delta E'$ and $\Delta E°$ vary monotonically, the activation energy $\Delta E^{\ddagger}$ will pass through a maximum (and the rate constant through a minimum) at a point in the reaction series where $\Delta E'$ is equal to, or close to, zero. The locus of this point can be predicted from Equation 28 and compared with experiment.

As an example we shall describe rate–equilibrium relationships in the base-catalyzed dissociation (Equation 29) of a series of hemiacetals of formaldehyde in water:

$$B^- + RCH_2OCH_2OH \rightarrow HOCH_2R + H_2C{=}O + B^- \qquad (29)$$

Data for this reaction, due to Funderburk et al. (28), are shown in Fig. 13. The substituent R is a variable substituent in the alcohol part of the substrate. The catalysts $B^-$ are a series of carboxylate bases, $R'CH_2COO^-$. For each catalyst, the rate constants pass through a minimum.

The reaction mechanism favored by Funderburk et al. is

$$RCH_2OCH_2OH + B^- = RCH_2OCH_2O^- + BH \qquad (Fast) \quad (30a)$$

$$BH + RCH_2OCH_2O^- \rightarrow B^- + HOCH_2R + H_2C{=}O \quad (Slow) \quad (30b)$$

The rate-determining step (Equation 30b) for this mechanism involves two reaction events: proton transfer from BH to the alcohol oxygen atom $(f_1)$ and rupture of the hemiacetal O—C bond $(f_2)$. The disparity reaction (in the direction $r_1f_2$) for this step is therefore

$$B^- + RCH_2OH^+{\cdot}CH_2O^- \rightarrow BH + RCH_2O^- + H_2C{=}O \qquad (30c)$$
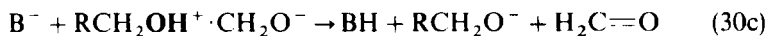
In the author's test (29) of Equation 28, the symbolic energy function $E$ was replaced by the Gibbs free energy $G$. Although the zwitterion species in Equation 30c is unusual, $\Delta G'_R$ for Equation 30c can be estimated by thermodynamic cycles that make use of experimental data and linear free-energy predictions. Figure 14 shows a series of plots — one for each base catalyst — of $\Delta G'$ versus $pK_a$ of the alcohol. These plots are straight lines and permit expressing the rate minima of Fig. 13 as functions of $\Delta G'$ rather than of $pK_a$. The nearly horizontal band in Fig. 14 is the locus of the experimental rate minima. The bandwidth indicates the uncertainity in that locus due to possible systematic error in the estimation of $\Delta G'$. The rate minima predicted by Equation 28 are shown in the same figure as open circles. The vertical error bars reflect the possible systematic error of $\Delta G'$. It is clear that the experimental rate minima are well predicted.
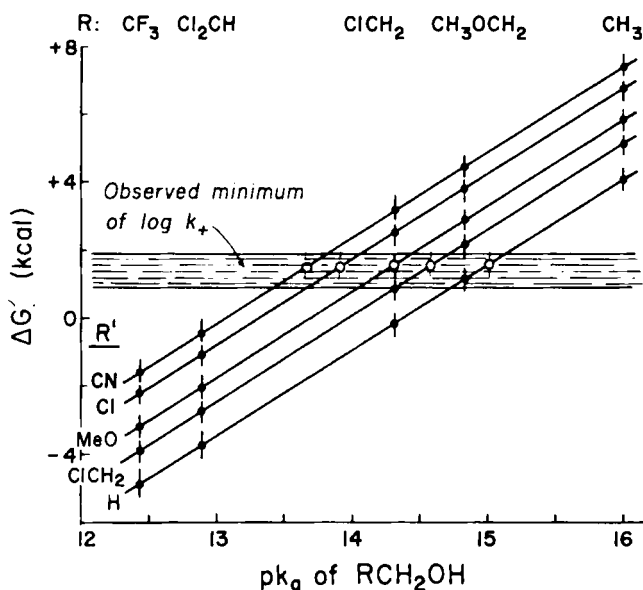
**Figure 14** Plot of $\Delta G'$ for the disparity reaction (Equation 30c) versus $pK_a$ of the alcohol. The base catalysts are a series of carboxylate ions $R'CH_2COO^-$. The nearly horizontal band is the locus of the experimental rate minima seen in Fig. 13. The width of the band represents uncertainty in that locus due to possible systematic error in $\Delta G'$. The predicted rate minima are plotted as open circles with appropriate error bars.

Equation 28 fits not only the rate minima but also the rate constants, with a standard deviation of 0.14 in log $k$, which is compatible with the error of the data. Values for the intrinsic parameters are as follows $\gamma_0 = 12.1 \pm 0.1$ kcal, $\mu_0 = 3.0 \pm 0.6$ kcal. Using these parameters and appropriate values of $\Delta G^0$ and $\Delta G'$, transition-state coordinates $x^{\ddagger}, y^{\ddagger}$ (Equation 27) were calculated and are plotted in Figure 15. While the mean progress variable $x^{\ddagger}$ varies only slightly, the disparity variable $y^{\ddagger}$ varies greatly. Thus, according to this model, the progress variables for the individual reaction events, $u^{\ddagger} = x^{\ddagger} - y^{\ddagger} + \frac{1}{2}$ and $v^{\ddagger} = x^{\ddagger} + y^{\ddagger} - \frac{1}{2}$, also vary greatly with the substituents. In terms of Equation 28, the high variability of $y^{\ddagger}$ stems from the smallness of the disparity parameter $\mu_0$.

Equally important, the fit of Equation 28 is sensitive to reaction mechanism. In particular, Funderburk et al. (28) eliminated the alternate mechanism (Equations 31) on the grounds that for some substituents, reaction in the rate-determining step (Equation 31a) would have to be faster than
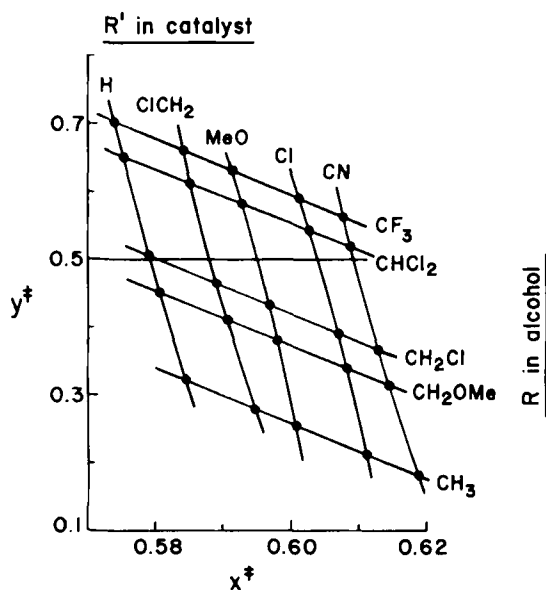
**Figure 15**  Transition-state coordinates predicted for the rate-determining step 30b on the basis of Equations 27 and 28 ($\gamma_0 = 12.1 \pm 0.1$ kcal mole$^{-1}$; $\mu_0 = 3.0 \pm 0.6$ kcal mole$^{-1}$).

diffusion-controlled:

$$RCH_2OCH_2OH + B^- \rightarrow BH + H_2C{=\!=}O + RCH_2O^- \qquad \text{(Slow) (31a)}$$

$$BH + RCH_2O^- = B^- + RCH_2OH \qquad \text{(Fast) (31b)}$$
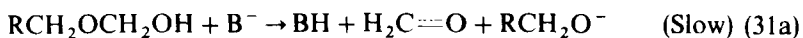
It is therefore significant that this mechanism is also eliminated by Equation 28. The rate-determining step (Equation 31a) involves two reaction events, rupture of the hemiacetal $O{-\!-}C$ bond ($f_1$) and proton transfer from the hemiacetal OH group to $B^-$ ($f_2$). The disparity reaction, in the direction $r_1f_2$, is

$$RCH_2O^- + H_2C{=}OH^+ + B^- \rightarrow RCH_2OCH_2O^- + HB \qquad (31c)$$
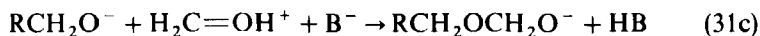
Comparison of Equation 31 with Equation 30 shows that the rate-determining step and the disparity reactions are different. Hence two entirely different sets of free-energy quantities are needed in Equation 28. In fact, when free energies appropriate to Equation 31 are used, the fit of Equation 28 is poor. The standard error of fit in log $k$ is 0.81, which is several times greater than the error of the data.

In conclusion, if and when the mathematical model described in this section applies, it becomes a powerful tool for probing concerted reactions. Because the fit of the model is sensitive to reaction mechanism, a good fit can reinforce evidence for, or even define, a particular mechanism. When the fit is good, progress of the reaction events at the transition state can be evaluated in terms of variables that simulate bond orders, and sensitivity to substituents can be noted.

## A. Simplified Treatments

A full application of the mathematical model for two reaction events requires data for reaction arrays, such as those plotted in Fig. 13. Such data represent a great deal of experimental work, and one may wish to use a shortcut. While rigorous shortcuts may not exist, shortcuts employing plausible model approximations may be tolerable. The following example describes an approach that is sometimes used.

Consider a reaction $r \rightarrow p$ of the type depicted in Equation 32, which involves two reaction events:

$$Y + S_1S_2 \!-\! X \rightarrow Y \!-\! S_1S_2 + X \qquad (32)$$
$$\phantom{Y + S_1S_2 \!-\! X \rightarrow}_{r} \phantom{Y \!-\! S_1S_2 + X}_{p}$$
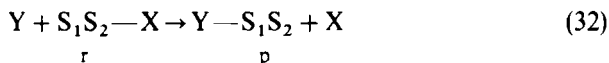
Let $u$ be the progress variable for forming the $Y \!-\! S_1$ bond, and $v$ be that for breaking the $S_2 \!-\! X$ bond. The disparity reaction $l \rightarrow h$, in the direction $u_1 v_0 \rightarrow u_0 v_1$, then is

$$Y \!-\! S_1 S_2 \!-\! X \rightarrow Y + S_1 S_2 + X \qquad (33)$$
$$\phantom{Y \!-\! S_1 S_2 \!-\! X}_{l} \phantom{\rightarrow Y + S_1 S_2 + X}_{h}$$
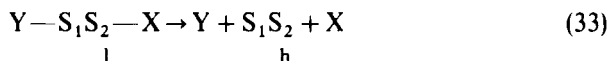
Reactions of this type have the property that if X is kept constant, $\Delta E_{r \rightarrow h}$ is constant. By allowing Y to vary at constant X, one generates a simple reaction series. It may then be possible to measure the activation energy $\Delta E^{\ddagger}$ for the main reaction $r \rightarrow p$, and $\Delta E_{r \rightarrow l}$ (or $\Delta E_{r \rightarrow l}$ + a constant) for the reaction event $r \rightarrow l$. In this notation, $\Delta E^0 = \Delta E_{r \rightarrow l} - \Delta E_{p \rightarrow l}$, and $\Delta E' = \Delta E_{r \rightarrow h} - \Delta E_{r - l}$. Substituting in Equation 28 and applying Equation 27 one can then derive the slope of the plot of $\Delta E^{\ddagger}_{r \rightarrow p}$ versus $\Delta E_{r \rightarrow l}$ for constant X:

$$\frac{\partial \Delta E^{\ddagger}}{\partial \Delta E_{r \rightarrow l}} = x^{\ddagger} - y^{\ddagger} + \frac{1}{2} - x^{\ddagger} \frac{\partial \Delta E_{p \rightarrow l}}{\partial \Delta E_{r \rightarrow l}} \qquad (34)$$

$$= u^{\ddagger} - x^{\ddagger} \frac{\partial \Delta E_{p \rightarrow l}}{\partial \Delta E_{r \rightarrow l}}; \qquad \Delta E_{r \rightarrow h} \text{ is constant}$$

The final term in this equation is often small because $-\Delta E_{p \to 1}$ is the dissociation energy of the $S_2$—X bond according to Y—$S_1S_2$—X → Y—$S_1S_2$ + X, and X is constant. Although the $S_2$—X bond energy in principle depends on Y, the variable Y group is attached at a different site, $S_1$, and may not have much effect. When this argument is valid, the final term in Equation 34 may be neglected. In that case the slope of the plot of $\Delta E_{r \to p}^{\ddagger}$ versus $\Delta E_{r \to 1}$ (or vs. $\Delta E_{r \to 1}$ + a constant), at constant X, approximates the progress variable $u^{\ddagger}$ for forming the Y—$S_1$ bond—even if the reaction mechanism is concerted.

### B.   Maximum Disparity

By definition, both progress variables $u$ and $v$ are zero for the reagents and unity for the products. The disparity between $u$ and $v$ thus is zero in these states. As a reacting system moves along the reaction coordinate from reagents to products, the magnitude (absolute value) of the disparity between $u$ and $v$ increases from zero at the reagents, passes through a maximum, and then decreases to zero at the products. It can be shown that the maximum occurs at the transition state.

The proof is due to Jencks and Jencks (30), who considered a general quadratic energy surface. It is convenient at this point to return to $x, y$ coordinates. Let $y_z$ denote the $y$-coordinate of the reaction coordinate $z$. In this notation, the reaction coordinate is defined when $y_z$ is known as a function of $x$. The derivative $dy_z/dx$ is the slope of the reaction coordinate with respect to the $x$-axis. When $dy_z/dx = 0$, $y_z$ (and the disparity between $u$ and $v$) passes through an extremum, and the reaction coordinate runs parallel to the $x$-axis. On the general quadratic surface analyzed by Jencks and Jencks (30), $dy_z/dx$ need not be zero at the saddle point. However, when the condition is introduced that the reaction modes for the main reaction and the disparity reaction are normal modes, the saddle point becomes equivalent to the transition state for concerted reaction and $dy_z/dx$ becomes identically zero.

The coordinate geometry at the transition state in concerted reactions thus may be summarized as follows. The reaction coordinate for the main reaction runs parallel to $x$. The reaction coordinate for the disparity reaction runs parallel to $y$ and normal to $x$. The disparity between the progress variables $u$ and $v$ for the two reaction events is at an extremum at the transition state.

## X.   MORE ABOUT THE DISPARITY MODE

If the terms "bond breaking" and "bond forming" are broadly defined, then, in a concerted reaction with two reaction events, one "bond" breaks while the

other "bond" forms. In the same terminology, one endpoint of the disparity mode represents a state of dissociation in which both "bonds" are broken, while the other endpoint represents a state of association in which both "bonds" are intact. At both endpoints the states are configurations of mechanical equilibrium. However, while the dissociated state may be either unstable (as in Fig. 6) or metastable, the associated state, barring an improbable coincidence, is metastable.



(a)



(b)
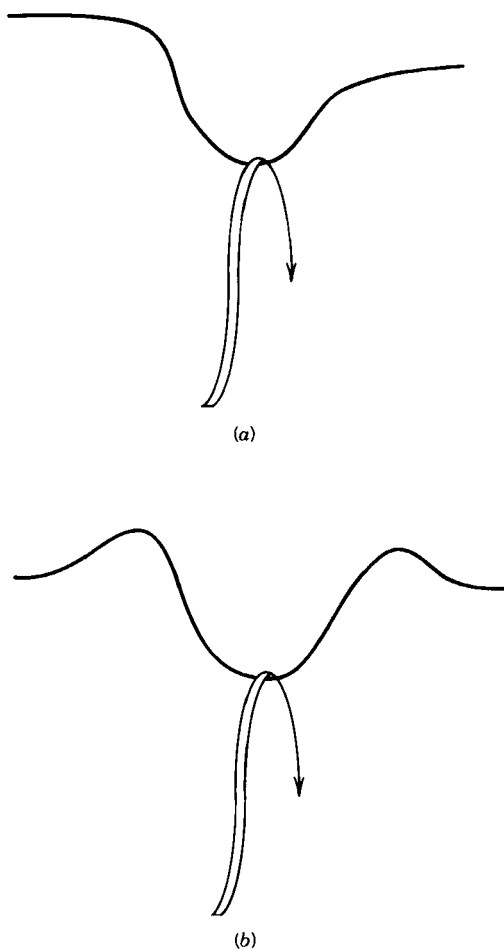
Figure 16   (a) Direct projection consistent with Equation 26. Both endpoints of the disparity mode are mechanically unstable. (b) A similar direct projection in which the disparity endpoints are metastable.

The mathematical model expressed by Equation 26, in which $x$ and $y$ are normalized to vary between 0 and 1, does not fully fit these notions. At first sight the endpoints of the disparity mode do not seem to be states of mechanical equilibrium because the slopes $\partial E/\partial y$ are not zero. However, when one recalls that the slopes of equilibrium states are zero only in linear projection, while $E(x, y)$ is modeled in quadratic projection, this problem dissolves. The real problem is that both endpoints are modeled as energy maxima whereas the associated state almost certainly occupies a metastable energy minimum. This flaw of the model is illustrated qualitatively in *linear* projection in Fig. 16. A formal remedy will be suggested later in this section.

The same semantic device that describes one endpoint of the disparity mode as a dissociated state also integrates the concepts of disparity mode and dissociation mode. A dissociation mode now becomes a special kind of disparity mode in which the associated-state endpoint is missing. The presence or absence of an associated state on the disparity mode is a specific property of the energy surface for the reaction. Indeed, as the energy surface varies in a reaction series, an associated-state endpoint may appear. The factors involved will now be illustrated in terms of resonance among valence-bond structures for the transition state.

## A.   Bimolecular Nucleophilic Substitution Revisited

Valence-bond structures are theoretical models of how a given set of atomic orbitals and electrons can interact to produce a bound molecule with a specified topological structure. In the present example of nucleophilic substitution $(Y + S—X \rightarrow Y—S + X)$ we shall consider two valence-bond structures for the transition state $(Y \cdots S \cdots X)$. These valence-bond structures will be based on four atomic orbitals — one orbital each from X and Y and two unequal orbitals from S—that are bound by four electrons. In the first model, the atomic orbitals from X and Y interact with the lower of the orbitals from S to form a three-center bond. The higher of the orbitals from S remains uninvolved. In the second model, all four atomic orbitals interact to form one two-center $Y \cdots S$ bond and one two-center $S \cdots X$ bond.

Figure 17 shows possible schematic relationships between the dissociation modes for the two valence-bond structures. The abscissa $r$ represents the coordinate for the "symmetric" or coherent $Y \leftarrow S \rightarrow X$ stretch. The valence-bond transition states for nucleophilic substitution are at the potential minima. When the valence-bond minimum with the higher energy has the greater $r$ coordinate, the resonance hybrid resulting from the two valence-bond curves is a dissociation mode (Fig. 17a). However, when the $r$ coordinate is shorter at the higher valence-bond minimum, the resonance hybrid is either a dissociation mode (Fig. 17b) or a disparity mode (Fig. 17c), depending on the
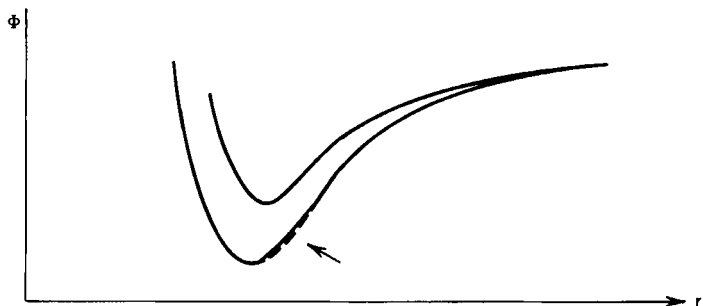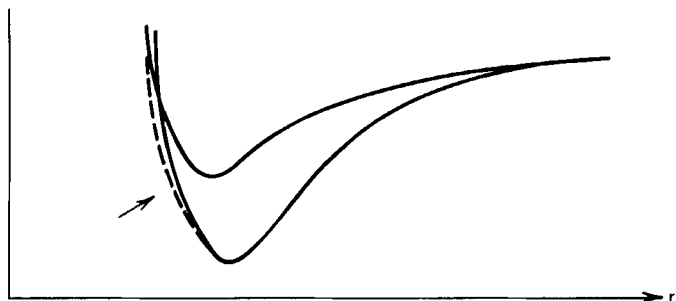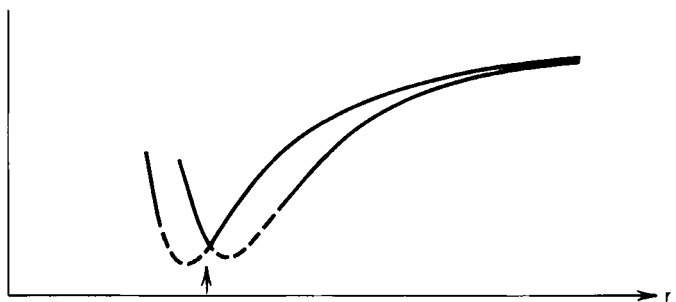
**Figure 17** Examples of model dissociation modes for two valence-bond structures. The model curve for the resonance hybrid (dashes when distinguishable from lower curve) is a dissociation mode in examples *a* and *b* and a disparity mode in example *c*.

specific circumstances. The real substituent change that causes the changeover may be relatively minor. However, because the changeover is a qualitative phenomenon, when it happens there is a distinctive change in the structure–energy relationships.

## B.  Quadratic Projection Outside the Normal Range

As stated above, if $y$ varies only within its normal range of zero to one, Equation 26 cannot reproduce the disparity mode when the endpoint species are metastable, as in Fig. 16b. However, this flaw can be remedied, in a formal way, if $y$ is allowed to exceed its normal range near the endpoints. The following example illustrates this approach.

Introduce a disparity variable $w'$, different from $y$, which varies continuously in the range from zero to one. Let $y$ be a function of $w'$ and specify a relationship $y(w')$ such that, as $w'$ increases from zero to one, $y$ first becomes negative, then reverses itself and increases continuously above one, then reverses itself again, and decreases finally to one. One of the many functions meeting these requirements is given in Equation 35, where the multiplying factor $T[\ldots]$ denotes the truth value, zero or one, of the relationship stated in brackets:

$$y = -0.05\sin^2(10\pi w')\cdot T[w' \leqslant 0.1] + \sin^2\left(\frac{5\pi w'}{8} - \frac{\pi}{16}\right)\cdot T[0.1 < w' \leqslant 0.9]$$

$$+ [1 + 0.05\sin^2(10\pi - 10\pi w')]\cdot T[0.9 < w']; \qquad 0 \leqslant w' \leqslant 1 \qquad (35)$$

A plot of $E$ versus $w'$ at $x = \frac{1}{2}$ is given in Fig. 18. This plot is still based on the model expressed by Equation 26, and the projection of the energy is still basically quadratic. However, $y$ is now an unnormalized parameter driven by a normalized, real disparity variable $w'$.

When one or both endpoints of the disparity mode represent metastable intermediates (e.g., as in Fig. 18), the central energy well still represents unit change in $y$ but, as shown in Fig. 18, represents less than unit change in the real disparity variable $w'$. In other words, the real disparity scale $w'$ is compressed relative to the $y$ scale. As a result, the mathematical model expressed by Equations 26 and 27, which characterizes the transition state in units of $y$, overestimates the true variation in disparity at the transition state in a reaction series.

The device of allowing $y$ to vary outside its normal range was introduced in a purely formal way. There are, however, indications that real progress variables in quadratic projections do sometimes vary outside their normal range. As mentioned in Section V, this controversial issue arises particularly in
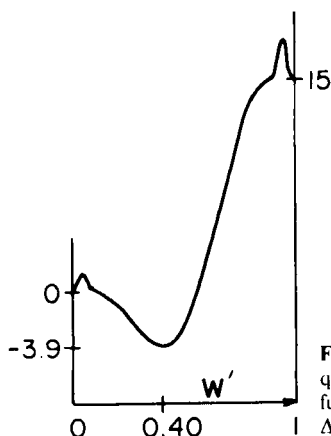
**Figure 18** Energy in the disparity mode, based on quadratic projection for $E(y)$ and the transformation function $y(w')$ given in Equation 35 ($\mu_o = 10\,\text{kcal mole}^{-1}$; $\Delta E' = 15\,\text{kcal mole}^{-1}$).

connection with Marcus theory. (6) The relevant Equations 9, in which $x$ is the progress variable, are repeated below. Elimination of $\Delta E^\circ$ then yields Equation 36:

$$x^{\ddagger} = \frac{1}{2} + \frac{\Delta E^{\circ}}{8\gamma_{0}} \tag{9a}$$

$$\Delta E^{\ddagger} = \gamma_{0} + \frac{\Delta E^{\circ}}{2} + \frac{(\Delta E^{\circ})^{2}}{16\gamma_{0}} \tag{9b}$$

$$\Delta E^{\ddagger} = 4\gamma_{0}(x^{\ddagger})^{2} \tag{36}$$

Equation 9a predicts that $x^{\ddagger}$ at the transition state becomes negative (and thus varies outside the normal range) when $\Delta E^{\circ}/8\gamma_{0} < -\frac{1}{2}$. Moreover, as $\Delta E^{\circ}/8\gamma_{0}$ decreases below $-\frac{1}{2}$, the activation energy $\Delta E^{\ddagger}$ is expected to increase according to Equation 36, and the rate constant accordingly is expected to decrease. This striking prediction that in highly exothermic reactions the rate constant decreases with increasing exothermicity—violates familiar, well-established concepts. In particular, one normally expects that, as $\Delta E^\circ$ in a reaction series becomes more negative, the activation energy $\Delta E^{\ddagger}$ decreases as well, reaching a lower limit that is either zero or equal to the activation energy for diffusion of the reagents. Contrary to Equation 36, these concepts do not provide for $\Delta E^{\ddagger}$ to increase as $\Delta E^\circ$ drops below a critical threshold.

As a matter of fact, Fig. 19 shows free-energy data for the intramolecular electron transfer symbolized by the equation $A—Sp—B^{-} \rightarrow A^{-}—Sp—B$, in dilute solution in 2-methyltetrahydrofuran (31). Sp is the rigid hydrocarbon spacer shown under the curved arrow in the figure, B is 4-biphenylyl, and
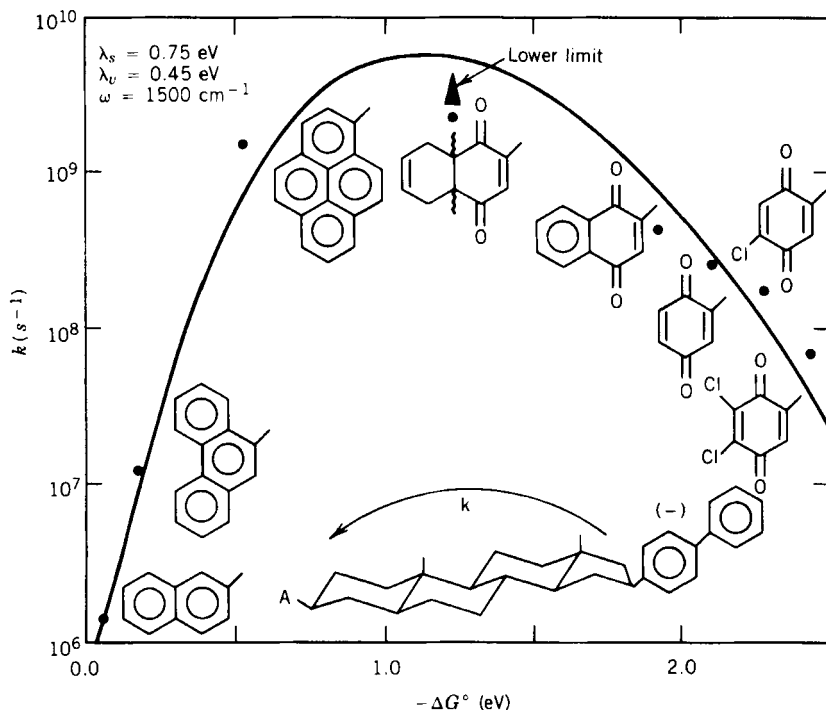
**Figure 19**   Rate-equilibrium plot based on data for intramolecular electron transfer from biphenylyl to a variable acceptor group A across the rigid hydrocarbon spacer shown in the figure. From J. R. Miller, L. T. Calcaterra, and G. L. Closs, *J. Am. Chem. Soc.*, *106*, 3047 (1984), with permission.

A is a variable electron acceptor. The Gibbs free energy $\Delta G^{\ddagger}$ is represented by the rate constant for electron transfer, plotted on a logarithmic scale. The acceptor group A is changed so that $\Delta G^{\circ}$ varies between 0 and $-2.4\,\text{eV}$. The rate constant goes through a well-established maximum when $\Delta G^{\circ} \simeq -1.2\,\text{eV}$. The solid curve, which is based on Equations 9 and 36, fits acceptably well, showing that the data are reproduced by Marcus theory. On the other hand, electron transfer is physically complicated, and this interpretation may not be unique. The free-energy barrier includes terms for solvent reorganization prior to electron tunneling and for electronic effects on internal vibrational modes.

## XI.   THREE REACTION EVENTS

Given the variety and specificity of chemical reactions, there are certain to be reactions that involve more than two reaction events. Potential surfaces

and reaction coordinates for such reactions can be analyzed using the same concepts as before, except that the model equations now are longer. As before, the reaction events may occur in discrete steps or be concerted. When the events are concerted, the eventwise reaction modes interact to produce an equal number of coupled reaction modes, which become normal modes at the concerted transition state.

This section will consider processes with three reaction events. An example is the general acid-catalyzed dissociation of formaldehyde hemiacetals, which, in contrast to the base-catalyzed reaction described in Section IX, appears to involve three reaction events. The mechanism favored by the author (32) is shown in Equations 37. The first step (Equation 37a) is a fast prior equilibrium. The rate-determining step (Equation 37b) involves three concerted reaction events: the proton transfers $u$ and $w$ and the breaking $v$ of the central O—C bond:

$$H_2O + R'CH_2COOH = H_2OH^+ + R'CH_2COO^- \qquad (37a)$$

$$H_2OH^+ + RCH_2O\text{—}CH_2OH + R'CH_2COO^-$$
$$\uparrow\text{——} \text{—} \uparrow \cdots \uparrow \qquad \uparrow\text{———}\uparrow$$
$$\quad u \qquad\quad v \qquad\qquad w$$
$$\rightarrow H_2O + RCH_2OH + H_2C{=}O + R'CH_2COOH \qquad (37b)$$

With three reaction events the coordinate diagram becomes a normalized cube, as in Fig. 20. The axes $u$, $v$, and $w$ express the progress of the respective reaction events, on a scale from 0 for the unreacted event to 1 for the completed event. Thus the corner labeled $(1,1,1)$ represents the products (all three reaction events are complete), and the corner $(0,0,0)$ represents the reagents. The other corners represent the remaining six permutations of 1 and 0 for three reaction events.

To describe concerted transition states, it is convenient to rotate the $u, v$, and $w$ axes by the following values of the Euler angles (33): $\zeta = \cos^{-1}(1/\sqrt{3})$ $= 54°44'$; $\theta = 45°$; $\phi = 0°$. Renormalization and translation of the origin so that the new axes intersect at $(\frac{1}{2},\frac{1}{2},\frac{1}{2})$ then leads to the following coordinates (32):

$$x = \frac{u + v + w}{3} \qquad (38a)$$

$$y_u = \frac{1}{2} + \frac{[v + w]/2 - u}{2} \qquad (38b)$$

$$s_u = \frac{1}{2} + \frac{[w - u] - [v - u]}{2} = \frac{1}{2} + \frac{w - v}{2} \qquad (38c)$$

PRODUCTS



**Figure 20**   The normalized $u,v,w$ cube.

As before, the $x$-axis runs diagonally from reagents to products and measures mean progress; $y_u - \frac{1}{2}$ measures the disparity, relative to $u$, of the mean progress of $v$ and $w$; and $s_u - \frac{1}{2}$ measures the difference between the disparities of progress, relative to $u$, of $w$ and $v$. The subscript $u$ denotes that $u$ is the pivot relative to which disparities of progress are measured. By appropriate alternate rotations, and other sets of variables, $(x, y_v, s_v)$ and $(x, y_w, s_w)$, can be obtained in which $v$ or $w$ is the pivot (32). Their defining equations are analogous to Equations 38, except that the symbols $u$ and $v$, or $u$ and $w$, have been interchanged. The coordinates for states of physical interest are compared in Table 2.

The reagents, products, and endpoints of the $y_u$ axis represent states at corners of the $u, v, w$ cube (Fig. 20). They represent chemical species, just as the states at the corners of a More O'Ferrall–Jencks diagram (Fig. 9) represent chemical species. The energies of these states thus are physically defined and, in principle, measurable. The endpoints of the $s_u$ axis, on the other hand, are not corner species in $(u, v, w)$; they lie at the corners of a square plane normal to the $u$ axis at $u = \frac{1}{2}$. These states are not in mechanical equilibrium and do not represent chemical species. While their potential energy is physically defined, their thermodynamic energy is not defined and must be estimated

## TABLE 2
### Coordinates for States of Physical Interest

| State | $(x, y_u, s_u)$ | $(u, v, w)$ |
|---|---|---|
| Reagents | $(0, \frac{1}{2}, \frac{1}{2})$ | $(0, 0, 0)$ |
| Products | $(1, \frac{1}{2}, \frac{1}{2})$ | $(1, 1, 1)$ |
| Endpoints of | | |
| $y_u$ axis | $(\frac{1}{2}, 0, \frac{1}{2})$ | $(1, 0, 0)$ |
| | $(\frac{1}{2}, 1, \frac{1}{2})$ | $(0, 1, 1)$ |
| $s_u$ axis | $(\frac{1}{2}, \frac{1}{2}, 0)$ | $(\frac{1}{2}, 1, 0)$ |
| | $(\frac{1}{2}, \frac{1}{2}, 1)$ | $(\frac{1}{2}, 0, 1)$ |

by interpolation between thermodynamic energy points. If one adopts a model of quadratic projection in $(x, y_u, s_u)$, with linear perturbations by substituents, one can show that $\Delta E_s$ for the energy change along $s_u$ may be interpolated according to Equation 39 (32):

$$\Delta E_s \text{ for the process } (\tfrac{1}{2}, \tfrac{1}{2}, 0) \rightarrow (\tfrac{1}{2}, \tfrac{1}{2}, 1) \text{ in } x, y_u, s_u$$

$$= (\tfrac{1}{2})\Delta E^{\circ} \text{ for the process } (0, 1, 0) \rightarrow (1, 0, 1) \text{ in } u, v, w$$

$$+ (\tfrac{1}{2})\Delta E^0 \text{ for the process } (1, 1, 0) \rightarrow (0, 0, 1) \text{ in } u, v, w \qquad (39)$$

The two processes on the right in this equation connect diagonal corners of the $u$, $v$, $w$ cube and thus connect chemical species with thermodynamically defined energies.

Expanding the model and the notation used in Equation 26, let $\Delta E^{\circ}$, $\Delta E'$, and $\Delta E_s$ respectively denote the energy difference per mole between the states at the endpoints of the $x$, $y_u$, and $s_u$ axes; let $\gamma$ denote the intrinsic barrier along $x$; and let $\mu'$ and $\mu_s$ denote the intrinsic energy wells along $y_u$ and $s_u$. (Algebraically, $\gamma$ is positive for a barrier, and $\mu'$ and $\mu_s$ are positive for a well.) The model energy surface then is

$$E_R(x, y_u, s_u) = a - 4\gamma(x - \tfrac{1}{2})^2 + \Delta E_R^{\circ}(x - \tfrac{1}{2}) + 4\mu'(y_u - \tfrac{1}{2})^2$$

$$+ \Delta E'_R(y_u - \tfrac{1}{2}) + 4\mu_s(s_u - \tfrac{1}{2})^2 + \Delta E_{s,R}(s_u - \tfrac{1}{2}) \qquad (40)$$

Using the same methods as in Equations 27 and 28, expressions for the transition state coordinates and for $\Delta E_R^{\ddagger}$ can be derived. The resulting rate equilibrium relationship is

$$\Delta E_R^{\ddagger} = \gamma + \frac{\Delta E_R^{\circ}}{2} + \frac{(\Delta E_R^{\circ})^2}{16\gamma} - \frac{(\Delta E'_R)^2}{16\mu'} - \frac{(\Delta E_{s,R})^2}{16\mu_s} \qquad (41)$$
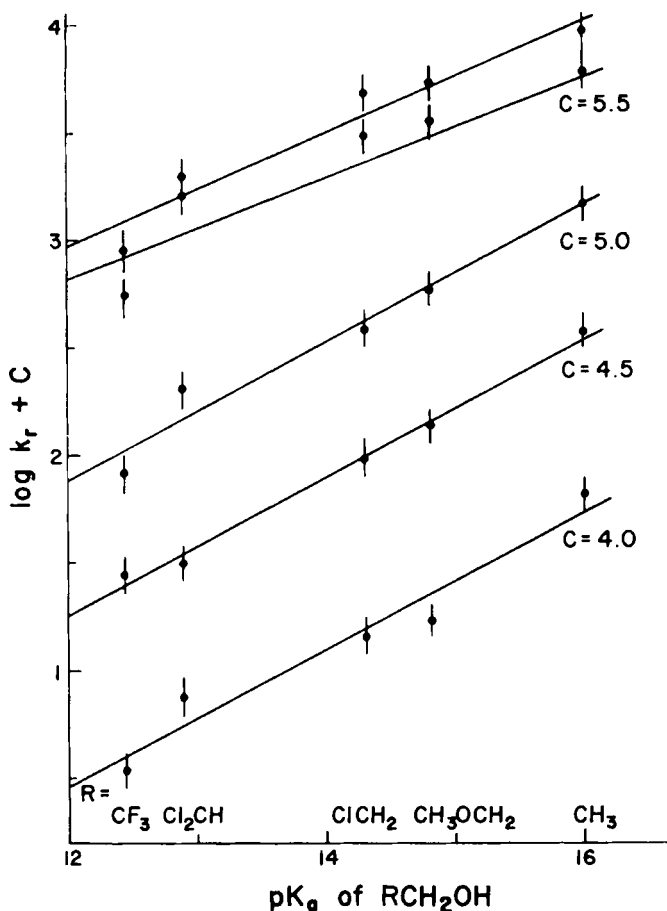
**Figure 21** Logarithmic plot of experimental rate constants versus $pK_a$ of alcohol for acid-catalyzed dissociation of a series of hemiacetals of formaldehyde. The catalysts are a series of carboxylic acids $R'CH_2COOH$ [$R'$ = (top to bottom) CN, Cl, $CH_3O$, $ClCH_2$, H]. From L. H. Funderburk, L. Aldwin, and W. P. Jencks, *J. Am. Chem. Soc.*, *100*, 5444 (1978).

This equation was applied to the acid-catalyzed dissociation of formaldehyde hemiacetals, catalyzed by a series of carboxylic acids (32). The generalized energy $E$ was expressed by the free energy $G$. The rate constants for a $5 \times 5$ reaction array (28) are shown in Fig. 21. The required equilibrium data were based partly on measurement and partly on estimation by linear free-energy relationships. Assuming the mechanism shown in Equation 37, the fit of Equation 41 was good. Per mole of hemiacetal, $\gamma = 18.5 \pm 0.1$ kcal, $\mu' = 25 \pm 7$ kcal, and $\mu_s = 2.8 \pm 0.5$ kcal. The statistical standard error of fit of $\log k$ was 0.11. The corresponding combined error of the kinetic and equilibrium

TABLE 3
Fit of Equation 41 to Data (28) for Acid-Catalyzed Dissociation of Formaldehyde Hemiacetals in
Water at 25°C, Based on the Mechanism of Equation 37

| $R^a$ | $R'^b$ | Pivot | $u^{\ddagger}$ | $v^{\ddagger}$ | $w^{\ddagger}$ |
|---|---|---|---|---|---|
| $CH_3$ | CN | $u$ | .383 | .803 | .343 |
| | | $v$ | .379 | .757 | .392 |
| | | $w$ | .412 | .862 | .254 |
| | | Mean | $.39 \pm .01$ | $.81 \pm .03$ | $.33 \pm .04$ |
| $ClCH_2$ | $CH_3O$ | $u$ | .435 | .779 | .349 |
| | | $v$ | .408 | .734 | .417 |
| | | $w$ | .448 | .795 | .319 |
| | | Mean | $.43 \pm .01$ | $.77 \pm .02$ | $.36 \pm .03$ |
| $CF_3$ | H | $u$ | .493 | .749 | .354 |
| | | $v$ | .440 | .708 | .445 |
| | | $w$ | .448 | .720 | .388 |
| | | Mean | $.47 \pm .02$ | $.73 \pm .01$ | $.40 \pm .03$ |

$^a$In $RCH_2OH$.
$^b$In $R'CH_2COOH$.

data was 0.18. In Equation 41, $u$ is the pivot for expressing disparity of progress. Equally good fits were obtained when analogous equations were used in which $v$ or $w$ was the pivot.

The advantage of having three different pivots is that one can probe the model energy surface (see Equation 41) in different directions. If the real potential surface is well reproduced, the transition-state coordinates $(u^{\ddagger}, v^{\ddagger}, w^{\ddagger})$ are virtually independent of the pivot. A test of this kind for the acid-catalyzed dissociation of formaldehyde hemiacetals is shown in Table 3 (32). Although $u^{\ddagger}, v^{\ddagger}$ and $w^{\ddagger}$ do vary somewhat with the pivot, the overall impression is one of sufficient agreement with the model. As explained in Section X, some model error is to be expected in the likely event that the corner species of the $u, v, w$ cube are mechanically metastable rather than unstable. Table 3 also shows that the transition-state coordinates vary considerably with the substituents.

Equally important, when other reaction mechanisms were considered, the fits were poor (32). Three other mechanisms were tried—two with two reaction events using Equation 26, and one with three reaction events using Equation 41. Thus once again it is clear that this approach distinguishes between reaction mechanisms. Because of the satisfying objectivity of the approach, it is desirable to probe the validity of the results by independent methods.

## XII.  CONCLUDING REMARKS

The methods described in this chapter apply quite generally to rate–equilibrium data for those reaction series whose substituent effects may be

treated as perturbations. First, the reaction coordinate for the reference reaction is projected from high-dimensional potential-energy space onto a low-dimensional space where it becomes a function of one or a small number of progress variables. Second, the substituent effects in the reaction series are treated as linear or, more generally, nonlinear perturbations of the energy along the progress variables.

Models that involve quadratic projections of the reaction coordinates and linear perturbations of the energy along the progress variables are of special interest because of their direct relevance to the characterization of transition states. The rate–equilibrium relationships derived from such models are sensitive to reaction mechanism and, when applied to real data for real reaction series, will fit some mechanisms and discredit others. In cases of good fit, the transition states in the reaction series can be characterized, in terms of the successful model mechanism, by assigning a precise value to each progress variable.

Because of their frequent success, mathematical simplicity, and easy relevance to reaction mechanism, the models that involve quadratic projections of the reaction coordinate and linear perturbations of the energy have dominated most recent discussions. There are cases, however, in which such models fail and in which other projections or other perturbation models need to be explored. This sector of the field is largely unexplored and promises to repay further study.

# REFERENCES

1. S. Glasstone, K. J. Laidler, and H. Eyring, *The Theory of Rate Processes* McGraw-Hill, New York, 1941.
2. J. E. Leffler and E. Grunwald. *Rate and Equilibria of Organic Reactions*, Wiley, New York, 1963.
3. R. P. Bell, *The Tunnel Effect in Chemistry*, Chapman and Hall, London, 1980, Sect. 2.3.
4. J. L. Kurz, *Chem. Phys. Lett.*, 57, 243 (1987).
5. E. Grunwald, *Progr. Phys. Org. Chem.*, 17, 31 (1990).
6. R. A. Marcus, *J. Phys. Chem.*, 72, 891 (1968); *Discus. Faraday Soc.*, 29, 21 (1960).
7. C. Eckart, *Phys. Rev.*, 35, 1303 (1930).
8. D. E. Magnoli and J. R. Murdoch, *J. Am. Chem. Soc.*, 103, 7465 (1981).
9. N. Agmon and R. D. Levine, *Chem. Phys. Lett.*, 52, 197 (1977).
10. S. W. Benson and J. H. Buss, *J. Chem. Phys.*, 29, 546 (1958); S. W. Benson, F. R. Cruickshank, D. M. Golden, G. R. Haugen, H. E. O'Neal. A. S. Rodgers, R. Shaw, and R. Walsh, *Chem. Rev.*, 69, 279 (1969).
11. W. J. Albery, *Faraday Discus. Chem. Soc.*, 74, 245 (1982); *J. Chem Soc., Faraday Trans. 1*, 78, 1579 (1982).
12. A. J. Kresge, *Acc. Chem. Res. 8*, 354 (1975); *Chem. Soc. Rev.*, 2, 475 (1973).

13. M. M. Kreevoy and D. E. Konasewich, *Adv. Chem. Phys.*, *21*, 243 (1971).

14 M. M. Kreevoy and I. S. H. Lee, *J. Am. Chem. Soc.*, *106*, 2550 (1984).

15. W. J. Albery and M. M. Kreevoy, *Adv. Phys. Org. Chem.*, *16*, 87 (1978).

16. E. S. Lewis, S. Kukes, and G. D. Slater, *J. Am. Chem. Soc.*, *102*, 1619 (1980); E. S. Lewis and D. D. Hu *J. Am. Chem. Soc.*, *106*, 3292 (1984).

17. J. E. Leffler, *Science*, *117*, 340 (1953); *J. Chem. Phys*, *23*, 2199 (1955).

18. G. S. Hammond, *J. Am. Chem. Soc.*, *77*, 334 (1955).

19. C. K. Ingold, *Structure and Mechanism in Organic Chemistry*, Cornell University Press, Ithaca,N.Y., 1953.

20. R. P. Bell and W. C. E. Higginson, *Proc. Roy. Soc.* (London) *A*, *197*, 141 (1949).

21. G. C. Pimentel, *J. Chem. Phys.*, *19*, 446 (1951).

22. P. M. Morse, *Phys. Rev.*, *34*, 57 (1929).

23. R. F. Hudson and G. Klopman, *J. Chem. Soc.*, *1962*, 1062.

24. R. A. More O'Ferrall, *J. Chem. Soc. B*, *1970*, 274.

25. W. P. Jencks, *Chem. Rev.*, *72*, 705 (1972); *Chem. Rev.*, *85*, 511 (1985).

26. E. Grunwald, *J. Am. Chem. Soc.*, *107*, 125 (1985).

27. L. Melander and W. H. Saunders, *Reaction Rates of Isotopic Molecules*, Wiley-Interscience, New York, 1980.

28. L. H. Funderburk, L. Aldwin, and W. P. Jencks, *J. Am. Chem. Soc.*, *100*, 5444 (1978).

29. E. Grunwald, *J. Am. Chem. Soc.*, *107*, 4710 (1985).

30. D. A. Jencks and W. P. Jencks, *J. Am. Chem. Soc.*, *99*, 7948 (1977).

31. J. R. Miller, L. T. Calcaterra, and G. L. Closs *J. Am. Chem. Soc.*, *106*, 3047 (1984).

32. E. Grunwald, *J. Am. Chem. Soc.*, *107*, 4715 (1985).

33. See, for example, H. Golstein, *Classical Mechanics*, Addison-Wesley, Reading, Mass., 1950.

# Theoretical Studies of The Effects of Hydration on Organic Equilibria

BY R. D. TOPSOM

*Department of Chemistry*
*La Trobe University*
*Melbourne, Australia*

CONTENTS

## I.  INTRODUCTION

This short review is based on a lecture given by the author at Poznán, Poland in July 1988. The original lecture included quite a bit of introductory material on the theoretical methods employed. This has now been published (1) in the previous volume in this series and is therefore only briefly covered here. On the other hand, the opportunity is taken to include rather more results than were possible in the lecture.

The majority of reactions have been studied in solution, particularly in water rather than in the gas phase. In recent years, however, experimental work involving techniques such as pulsed electron beam mass spectrometry and ion cyclotron resonance has allowed the measurement of equilibria in the gas phase (2, 3). This has given rise to scales of relative acidity and basicity covering a wide range of energy. The existence of these data allows a direct comparison with corresponding values in solution, thus providing inform-

ation on the overall effect of the solvent. Within restricted series of compounds, such as substituted phenols or benzoic acids, it is frequently found that the effects of different substituents in water, for example, are linear, in contrast to those in the gas phase, but of smaller magnitude (2, 4). The reduction in effect is usually in the range of one-third to one-tenth of that in the gas phase. There is also some evidence (4–6) for specific effects on various substituents, but these are usually of less importance than the general effect.

An extension of the gas-phase work has examined the interaction of specific molecules or ions with various numbers of water molecules. Thus, results have been reported of studies on the hydration of substituted ammonium ions (7, 8), pyridines and pyridinium ions (7, 9–11), protonated alcohols (7, 12, 13), phenols (9), and anilines (14). At the same time, theoretical studies have been reported on the hydration of substituted ammonium ions (8, 15), pyridines and pyridinium ions (9, 11), phenols, and phenolates (16).

Rather more limited results were available on the effects of limited numbers of water molecules on equilibria of series of organic molecules. Results included both experimental (9) and theoretical (11) studies of the proton affinities of substituted pyridines, both in the gas phase and with a single molecule of water attached to the pyridinium ions as shown in Equations 1 and 2:
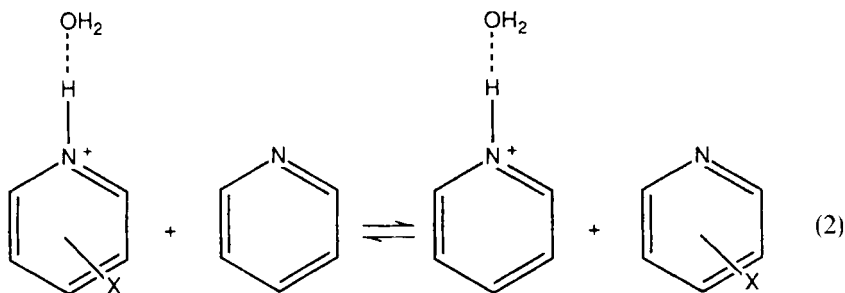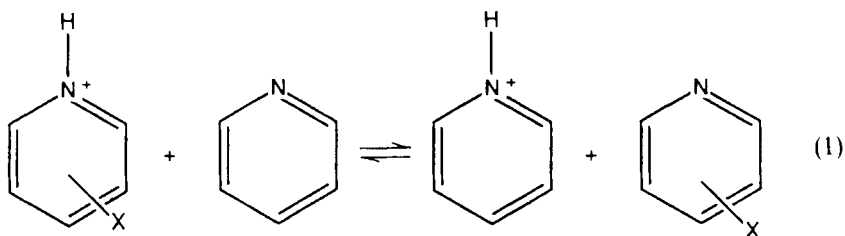


The theoretical and experimental values of the equilibrium energies were in reasonable accord.

A second example (8. 17) was the proton transfer reaction, (Equation 3) of

some substituted amines:

$$RNH_3^+ \cdot xH_2O + CH_3NH_2 \cdot yH_2O \rightleftharpoons CH_3NH_3^+ \cdot xH_2O + RNH_2 \cdot yH_2O \quad (3)$$

The theoretical calculations here for $x = 3, y = 1$ reproduced the aqueous phase results. However, the addition of several molecules of water to the proton-transfer reactions of pyridinium ions (11) and phenols (9, 16) went only part of the way towards results found experimentally in aqueous solution.

The results and discussion below are part of a general study of the effect of water on organic molecules and equilibria.


## II.  THEORETICAL APPROACHES

Ab initio calculations using bases such as STO-3G, 3-21G, 4-31G, and 6-31G* have proved remarkably successful (18) in reproducing ground-state properties of organic molecules. Such calculations also give equilibrium energies usually close to experimental for processes where the number and type of bonds is maintained (so-called isodesmic processes). This includes proton transfer equilibria of the type shown in Equations 1–3. It would be expected that the calculations would progressively give results closer to experimental on going from the minimal basis STO-3G level to the split valence 3-21G or 4-31G bases and then again to the 6-31G* basis containing polarization functions. This, indeed, seems true for many substituents in equilibria involving a series of organic molecules, but we have found (19) in several studies that substituents such as CN, CHO, and $NO_2$, which are electron-withdrawing by resonance, surprisingly seem best treated at the minimal basis level.

Certainly, hydration studies are helped by calculations at the minimal bases in that a larger total number of atoms can be treated. Whatever the basis used, however, it is necessary to study equilibria where it can first be shown that the theoretical calculations fairly closely reproduce the experimental gas-phase data for the nonhydrated process. The examples used below, where this has been done, include the proton affinities of substituted methylamines (20), quinuclidines (21), and pyridines (22) and the acidities of substituted acetic acids (23) and phenols (24).


## III.  HYDRATION AT THE REACTION SITE

The mode of action of water molecules on an equilibrium can be considered as arising in three ways. First, water molecules may be specifically

attached to the reaction site, for example, to the $-NH_3^+$ or $NH_2$ groups in Equation 3. It is known that substituent electronic effects are usually manifest mostly in charged forms rather than in neutral ones, so one might expect hydration effects to be correspondingly more important in, say, $XCH_2NH_3^+$ than in $XCH_2NH_2$. Second, water molecules may be specifically attached to substituents, thus altering their electronic effects. Thirdly, the effect of water could be to exert a general medium effect on the lines of force between the substituent and the reaction site.

The interpretation of aqueous solvent effects in terms of these three possibilities is difficult from purely experimental results but can be investigated using theoretical calculations. This section covers the first possibility, namely, the effect of hydration at reaction sites.

## A.  Acidities of Substituted Acetic Acids

Previous work (23) has shown that calculations at the STO-3G basis level, with geometry optimization, give good agreement with experiment for the acidities of substituted acetic acids:

$$XCH_2CO_2H + CH_3CO_2^- \rightleftharpoons XCH_2CO_2^- + CH_3CO_2H \qquad (4)$$

These results are included in Table 1. We then examined (25) the effect of adding water molecules, to both the neutral acids and the acetate anions. It was found that hydration at the carbonyl oxygen of the acid was not energetically important, compared to hydration at hydration at the $-OH$ group, as in 1:



(1)
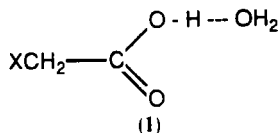
TABLE 1

Acidities of Substituted Acetic Acids ($\Delta G^\circ$ and $\Delta E^\circ$ Values in kcal mole$^{-1}$)

| Substituent | $-\Delta G^\circ_{(gas)}$ | $-\Delta E^\circ_{(gas\ calc)}$ | $-\Delta G^\circ_{(aq)}$ | $-\Delta E^\circ_{(aq\ calc)}$ |
|---|---|---|---|---|
| H | 0.0 | 0.0 | 0.0 | 0.0 |
| Me | 1.2 | 0.73 | −0.08 | −0.44 |
| Et | 2.0 | 1.20 | −0.09 | −0.27 |
| Ph | 6.9 | 8.55 | 0.61 | 3.21 |
| F | 9.6 | 9.16 | 2.96 | 3.37 |
| OMe | 6.0 | 5.61 | 1.62 | 1.37 |
| CF$_3$ | 13.0 | 14.83 | 2.31 | 3.24 |
| CN | 15.3$^a$ | 22.70 | 3.12 | 8.45 |

$^a$Estimated value; see reference 23.

However, the relative differences in energy $\Delta E$

$$XCH_2CO_2H + OH_2 \rightleftharpoons XCH_2CO_2H \cdot OH_2 \qquad (5)$$
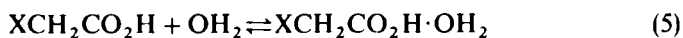
were not great, as $-\Delta E$ values were in the range 8.2–10.2 kcal mole$^{-1}$.

By contrast, the effect of specific bonding of water molecules to the acetates led to greater differences between substituents. It was found that three molecules of water could be incorporated into an inner hydration shell to give preferred structures of the general form **2**:



(2)
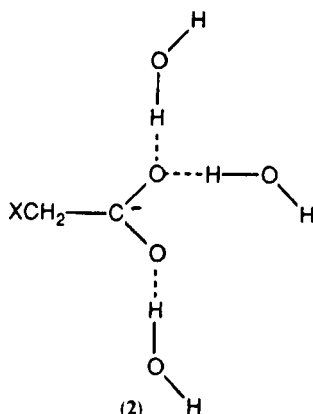
The calculated $-\Delta E$ values for such trihydration of acetates were in the range 51.1–63.6 kcal mole$^{-1}$. In Table 1, we list the calculated values for

$$XCH_2CO_2H(OH_2) + CH_3CO_2^-(H_2O)_3$$

$$\rightleftharpoons XCH_2CO_2^-(H_2O)_3 + CH_3CO_2H(OH_2) \qquad (6)$$
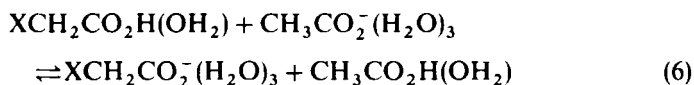
Increasing the number of water molecules hydrated to the acetates to four makes little further relative difference between substituents. It is seen that these are, in most cases, close to the experimental values observed in aqueous solution. The values for X = CN are calculated to be greater than those observed in both the gas phase (difference of 7.4 kcal mole$^{-1}$) and aqueous solution (difference of 5.3 kcal mole$^{-1}$). Overall, however, it seems that nearly all the energetic effect observed on the equilibrium in going from the gas to aqueous solution is accounted for by this specific solvation at the reaction site.

## B.  Acidities of Substituted Methylammonium Ions

As mentioned previously, earlier work (17) had shown that calculations of the presence of three water molecules attached to the charged $NH_3^+$ group and

one water molecule attached to the $NH_2$ group in Equation 3, yielded results close to those observed in aqueous solution. The number of substituents was very limited. We have studied a larger series of results for substituted methylamines. Here, theoretical calculations at the STO-3G basis gave (20) equilibrium energies in reasonable agreement with experiment for

$$XCH_2NH_3^+ + CH_3NH_2 \rightleftharpoons XCH_2NH_2 + CH_3NH_3^+ \tag{7}$$
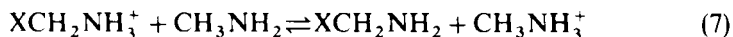
Thus, for 10 substituents, the average deviation from experimental gas-phase values was only 1.2 kcal mole$^{-1}$ at the STO-3G//STO-3G basis.

A study of the neutral amines (26) showed that hydration at the nitrogen was the preferred form leading to a range of energies of 4.4–5.8 kcal mole$^{-1}$ for

$$XCH_2NH_2 + H_2O \rightleftharpoons XCH_2NH_2 \cdot (H_2O) \tag{8}$$

An inner hydration shell of three molecules of water could be arranged around the $-NH_3^+$ cation, with one water hydrogen-bonded to each acidic hydrogen atom. Energies calculated for

$$XCH_2NH_3^+ + 3H_2O \rightleftharpoons XCH_2NH_3^+(3H_2O) \tag{9}$$

were in the range 72.7 84.2 kcal mole$^{-1}$. Thus, once again, most of the differential effect occurs in the charged species rather than in the neutral.

TABLE 2

Acidities of Substituted Methylamines ($\Delta G$ and $\Delta E$ Values in kcal mole$^{-1}$, Calculations at the STO-3G//STO-3G Basis)

| Substituent | $-\Delta G_{(gas)}$ | $-\Delta E_{(gas\ calc)}$ | $-\Delta G_{(aq)}$ | $-\Delta E_{(aq\ calc)}$ |
|---|---|---|---|---|
| H | 0.0 | 0.0 | 0.0 | 0.0 |
| CN | $-16.0$ | $-16.7$ | $-7.3$ | $-8.33$ |
| Me | 2.8 | 4.0 | 0.1, 0.7 | 0.11 |
| $C_2H_3$ | 2.6 | 1.9 | $-1.6$ | $-1.16$ |
| Et | 4.3 | 4.7 | 0.1 | 0.10 |
| $CH_2F$ | $-1.2$ | 2.2 | | $-0.77$ |
| $CHF_2$ | $-5.7$ | $-4.2$ | | $-2.33$ |
| $CF_3$ | $-11.7$ | $-10.2$ | $-6.9, -6.2$ | $-5.35$ |
| $C_2H$ | $-2.4$ | $-2.5$ | | $-2.35$ |
| $CH_2CF_3$ | $-2.4$ | $-3.5$ | | $-3.93$ |
| $CH_2CN$ | $-7.2$ | $-8.6$ | $-4.7$ | $-7.13$ |
| CHO | — | $-6.9$ | $-4.2$ | $-5.72$ |

Table 2 lists the values calculated for

$$XCH_2NH_3^+(3H_2O) + CH_3NH_2(H_2O)$$

$$\rightleftharpoons XCH_2NH_2(H_2O) + CH_3NH_3^+(3H_2O) \tag{10}$$
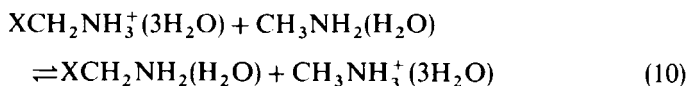
Also listed in Table 2 are calculated and experimental figures for the gas phase.

Although the total number of overall comparisons is restricted by the paucity of experimental data, it is clear that calculations using Equation 10 give values close to those experimentally observed in aqueous solution. Thus, once again, it appears that a limited number of water molecules attached to the reaction site, particularly in the charged species, explain almost all the change in substituent effects in going from the gas phase to aqueous solution.

## C.  Acidities of Substituted Quinuclidinium and Pyridinium Ions

As mentioned earlier, ab initio molecular orbital calculations give (22) results in fair accord with experiment for the relative gas-phase acidities of substituted pyridines (Equation 1). However, calculations (11) with a single water molecule attached to the acidic hydrogen in the ion (Equation 2), or in addition with one bonded to the nitrogen in the neutral pyridines, do not change the relative energies of the substituent effects to anything like the results observed experimentally in aqueous solution. The addition of one or two further molecules of water does not change the results greatly.

We have found a similar situation recently in 4-substituted quinuclidines. Calculations at the STO-3G basis give (21) equilibrium energies for process 11 in good agreement with experimental gas-phase results.



$$\tag{11}$$
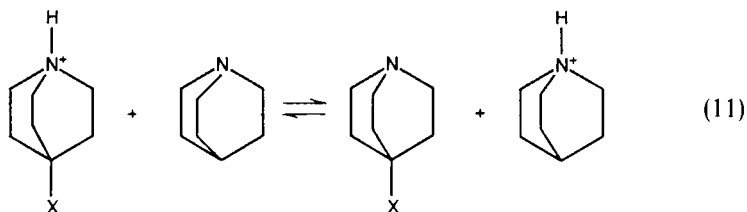
Calculations have also been made with three molecules of water attached to the acidic hydrogen (one in a primary shell, two in a secondary). Comparisons are once again restricted by the limited experimental results available for both the gas phase and aqueous solution, but results are shown in Table 3. It seems that, as with the pyridines, the limited number of water molecules bonded around the reaction site is quite inadequate to explain the

TABLE 3

Acidities of Substituted Quinuclidinium Ions ($\Delta G^\circ$ and $\Delta E^\circ$ Values in kcal mole$^{-1}$, Calculations at the STO-3G Basis)

| Substituent | $-\Delta G^\circ_{(gas)}$ | $-\Delta E^\circ_{(gas\ calc)}$ | $-\Delta G^\circ_{(aq)}$ | $-\Delta E^\circ_{(aq\ calc)}$ |
|---|---|---|---|---|
| H | 0.0 | 0.0 | 0.0 | 0.0 |
| F | 6.7 | 5.37 | 3.51 | 3.72 |
| CN | 12.9 | 10.48 | 4.15 | 7.34 |
| CF$_3$ | 8.1 | 5.74 | 2.34 | 4.11 |
| NO$_2$ | — | 13.96 | 4.75 | 10.44 |

change observed experimentally in going from the gas phase to aqueous solution.

## D.  Acidities of Substituted Phenols

A similar situation has been observed in the case of 3- and 4-substituted phenols. It was shown earlier (24) that calculations at the STO-3G basis for



$$\tag{12}$$
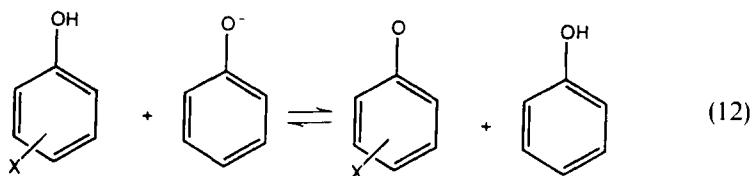
gave results in good accord with experimental gas-phase data for most substituents. Subsequent calculations (96) have been made of this process with three molecules of water arranged around the oxygen in the anions and three bonded to the acidic proton in the neutral phenols. This limited number of water molecules proves inadequate to explain most of the changes observed experimentally in going from the gas phase to aqueous solution. Thus, for the *para*-cyano substituent, the $\Delta G^\circ_{(gas)}$ value is $-16.6$ kcal mole$^{-1}$, while $\Delta G^\circ_{(aq)}$ is $-2.76$ kcal mole$^{-1}$. The corresponding calculated $\Delta E^\circ$ values are $-21.4$ and $-11.2$ kcal mole$^{-1}$. Similarly, for the *para*-trifluoromethyl substituent, the experimental values are $-11.9$(gas) and $-1.81$ kcal mole$^{-1}$, while the calculated values are $-11.5$ and $-6.1$ kcal mole$^{-1}$ respectively.

It thus appears that, with small molecules, the specific hydration at the reaction site by a limited number of water molecules is sufficient to explain most of the effect observed on going from the gas phase to aqueous solution. For larger molecules, however, while hydration at the reaction site is still important, it explains only a percentage of the overall observed effect of the water. We return to this in Section V.

## IV.  HYDRATION AT THE SUBSTITUENT

The hydration of a substituent might be expected to alter the electronic effects—the field, resonance, and electronegativity effects, as well as the polarizability—of that substituent. In substituent parameter terms, these are designated $\sigma_F$, $\sigma_R$, $\sigma_\chi$ and $\sigma_\alpha$, respectively. Since some substituents, such as amino or methoxy, seem likely to form hydrogen bonds of significant energy with water while others, such as methyl and trifluoromethyl, do not, this effect should lead to a lack of proportionality of the electronic effect between substituents as the medium changes. For neutral substituents, however, this effect would appear to be less important energetically than hydration at a charged reaction site. The results below indicate this to be true.

### A.  Modification of Substituent Field Effects by Hydration

Substituent field effects are a very important constituent in the study of the electronic influences of substituents (27). The corresponding $\sigma_F$ parameters are crucial to the analysis and understanding of data relating to series of organic molecules. It is known (1, 3), however, that the relative field effects of some substituents alter from one solvent to another. These effects have been termed (28) substituent solvation-assisted field (SSAF) effects. Scales of $\sigma_F$ values have been published for the gas phase, for nonpolar solvents and for polar solvents, but precise values for most substituents are not available. In particular, it is difficult to obtain accurate $\sigma_F$ values for aqueous solution, since direct measurement from 4-substituted bicyclooctyl carboxylic acids is restricted by low solubility. Thus, values are obtained mainly by the separation of field and resonance effects in series such as *meta-* and *para-* substituted benzoic acids.

We have examined this theoretically by adapting a model system (3) that we earlier used successfully (29) to calculate inherent (i.e., not affected by the medium) $\sigma_F$ values.

$$\Delta q_\alpha$$
$$\text{H-H} \qquad\qquad\qquad \text{H-X}$$
$$\underset{4\text{Å}}{\underline{\qquad\qquad\qquad}}$$

(3)
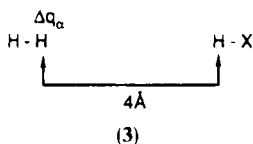
In this system, the field effect of the substituent leads to a polarization of the electrons in the hydrogen molecule. The use of isolated molecules avoids the possibility of other substituent electronic effects. The values of the change in electron population ($\Delta q_\alpha$) at one of the hydrogen atoms were found to be accurately proportional to $\sigma_F$ values for substituent X where such values were

well established. This allowed the derivation of an equation which yielded $\sigma_F$ values for many other substituents.

The new model (30) (4) incorporates water molecules bound around the substituent.

$$\Delta q_\alpha$$

H - H                                    H - X(nH$_2$O)

4Å

(4)
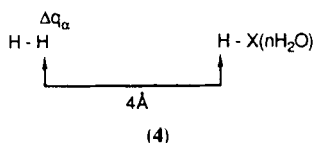
Such hydration will be important only if the HX ($n$H$_2$O) species has an appreciable existence. This suggests that the energy $-\Delta E°$ of

$$HX + H_2O \Rightarrow HX \cdot H_2O \tag{13}$$

should be significant compared to the formation of the water dimer (7.9 kcal mole$^{-1}$ at the 4-31G basis) In practice, for substituents such as H, alkyl, or CF$_3$, the energy is less than 2.5 kcal mole$^{-1}$ at this basis and no specific effect of hydration is anticipated. For substituents NO$_2$, F, CCH, and CN, the range of $-\Delta E°$ values for Equation 13 is 4–5.2 kcal mole$^{-1}$. Such hydration may be important with limited numbers of water molecules in the gas phase, but it is unlikely to be of significance in aqueous solution. However, for NMe$_2$, NH$_2$, OH, OMe, CHO, COMe, and CO$_2$Me, the $\Delta E°$ values are all greater than 6.5 kcal mole$^{-1}$ and the hydration is likely to be significant in determining $\sigma_F$ values.

These conclusions fit in with experimental observations. For example, a comparison (28) of the acidity of substituted phenols has been made between values in the gas phase and in aqueous solution. In the *meta*-substituted derivatives, resonance effects should not be important and here good linearity is found between results in the gas phase and in water, for substitutents such as CF$_3$, NO$_2$, CN, and Me, indicating no specific solvent effects. However, for the substituents CHO, COMe and CO$_2$Me, values deviate in the direction of indicating enhanced field effects in aqueous solution. Similar conclusions (31) can be drawn from solvent effects on the infrared stretching frequencies of the carbonyl group in 4-substituted camphors.

In Table 4 we list some calculated and experimental $\sigma_F$ values for both aqueous solution and the gas phase. The substituents all have calculated (4-31G//4-31G) interaction energies of more than 6.5 kcal mole$^{-1}$ with water. Values are not included for the OH substituent, since hydration is likely at both the oxygen and hydrogen atoms, and these lead to opposite effects on $\sigma_F$ values. Hydration of NH$_2$, however, clearly occurs preferentially at the nitrogen atom.

TABLE 4
Calculated and Experimental $\sigma_F$ Values in the Gas Phase and in Aqueous Solution

| Substituent | $\sigma_F$ (gas) | $\sigma_F$ (gas, calc) | $\sigma_F$ (aq) | $\sigma_F$ (aq, calc) |
|---|---|---|---|---|
| NMe$_2$ | 0.10[a] | 0.14 | 0.17[b], 0.19[c] | 0.24 |
| NH$_2$ | 0.14[a] | 0.15 | 0.17[b], 0.19[c] | 0.25 |
| OMe | 0.25[a] | 0.29 | 0.29[b] | 0.41 |
| CHO | 0.31[a] | 0.22 | 0.34[c] | 0.32 |
| COMe | 0.26[a] | 0.19 | 0.30[b], 0.30[c] | 0.25 |
| CO$_2$Me | 0.24[a] | 0.24 | 0.32[b], 0.31[c] | 0.33 |

[a] Ref. 3.
[b] M. Charton, *Progr. Phys. Org. Chem.*, **13**, 119 (1981).
[c] Ref. 35.

The general agreement between calculation and experiment is excellent; this suggests that the theoretical method can be usefully extended to a greater range of substituents and to other solvents. The results are also in accord with qualitative expectation. Thus, hydration of the lone pair in NMe$_2$, NH$_2$, and OMe should increase the effective C—N or C—O dipole, leading to an increase in $\sigma_F$ as found. Hydration of the oxygen atom in COX substituents should likewise increase the effective dipole and the $\sigma_F$ values.

## B.    Modification of Substituent Resonance Effects by Hydration

A similar approach can be taken to the theoretical investigation of the effect of hydration on substituent resonance effects $\sigma_R$. Such resonance effects measure the $\pi$-electron donation or withdrawal by the substituent when attached directly to a suitable system of $\pi$-orbitals. This occurs notably in substituted benzenes, where substituents such as NH$_2$, OMe, and F can donate $\pi$-electron to the benzene system, while others, such as CN, CHO, and NO$_2$, withdraw it. Indeed, the calculated $\pi$-electron transfer between a substituent and the benzene nucleus in monosubstituted benzenes (**5**) can be

X

(5)
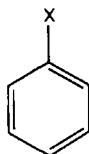
used (32) to derive a scale of resonance values $\sigma_R^\circ$ (appropriate system without special $\pi$-electron demands).

In practice, we have used (33) the simpler system of substituted ethylenes (6) to derive a theoretical scale of $\sigma_R^\circ$ values for many substitutents. These values are generally in excellent agreement with experimental values, for example, those determined directly from infrared intensity measurements on substituted benzenes.



(6)                                    (7)
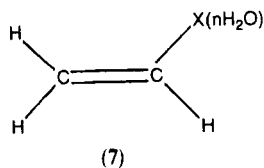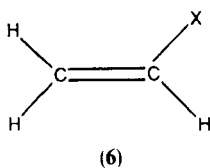
We have modified this sytem to 7 to incorporate the effects of hydration.

As with the field effects, hydration is likely to be important here only for substituents such as $NMe_2$, $NH_2$, OMe, and COX, where the hydrated complex has reasonable stability. Calculations of the $\pi$-electron transfer to or from the vinyl group allow the determination of $\sigma_{R(aq)}^\circ$ values, using the equation previously developed. Values are shown in Table 5. Once again, OH is not considered, since hydration at the oxygen and at the hydrogen atom are both likely, but lead to opposite effects on $\sigma_R^\circ$ values.

The results show a significant dimunition in the $\pi$-electron donation by $NMe_2$ and $NH_2$ and, to a lesser extent, by OMe on hydration. This is as expected, since the lone pair will be less available to conjugate with the $\pi$-electron system of the ethylene. By contrast, hydration at the oxygen atom of the COX group should increase the demand of the carbon on the $\pi$-electron system of the ethylene, leading to an increase in the $\sigma_R$ values. This is observed for COH, to a lesser extent for COMe, and not for COOR. This suggests that the demands of the carbonyl group are met by the directly attached Me and, particularly, the OR group.

TABLE 5
Calculated $\sigma_R^\circ$ Values

| Substituent | $\sigma_{R(inherent)}^\circ$ | $\sigma_{R(aq)}^\circ$ |
|---|---|---|
| $NMe_2$ | $-0.58$ | $-0.45$ |
| $NH_{2(pl)}$ | $-0.52$ | — |
| $NH_{2(tetr)}$ | $-0.32$ | $-0.29$ |
| OMe | $-0.39$ | $-0.35$ |
| CHO | 0.17 | 0.20 |
| COMe | 0.15 | 0.16 |
| $CO_2Me$ | 0.17 | 0.17 |

Experimental observations (35) have suggested rather more significant effects of hydration of COX and even $NO_2$ groups when attached to an electron-rich $\pi$-system such as *para*-substituted phenoxides, or even *para*-substituted anilines. Further theoretical work is under way to examine this.

## V.  SUMMARY

It is clear that specific hydration at the substituent may modify its field and resonance effects for groups such as $NMe_2$, OMe, and COX. The variation in $\sigma_F$ may be up to 50%, somewhat less in $\sigma_R^\circ$. Nevertheless, these are percentages of the effect in water, which is generally much less than the differences in overall effect between the gas phase and aqueous solution. Thus, these SSAF and SSAR effects are of considerably less importance overall than the effect of hydration at a charged reaction center. In the case of small molecules, it appears that these two effects may be sufficient to account for almost the whole of the change observed in going from the gas phase to water. This is apparently not true for larger molecules. The most likely explanation is that in the small molecules studied (substituted methyl amines and acetic acids), the lines of force of the substituent electronic effects are mainly within the molecule. In the larger molecules, where the distance between the reaction site and the substituent is much greater, the bulk solvent obviously exerts more effect. This may involve lines of force or hydration effects on intervening bonds, notably CH, polarized at the charged site. Further theoretical work is under way to clarify these matters.

## REFERENCES

1. R. D. Topsom, *Progr. Phys. Org. Chem.*, **16**, 125 (1987).
2. See, for example, R. W. Taft, *Progr. Phys. Org. Chem.*, **14**, 247 (1983).
3. R. W. Taft and R. D. Topsom, *Progr. Phys. Org. Chem.*, **16**, 1 (1987).
4. R. W. Taft and F. G. Bordwell, *Acc. Chem. Res.*, **21**, 463 (1988).
5. M. Mishima, R. T. McIver, R. W. Taft, F. G. Bordwell, and W. N. Olmstead, *J. Am. Chem. Soc.*, **106**, 2717 (1984).
6. C. Laurence, M. Berthelot, M. Lucon, M. Helbert, D. G. Morris, and J.-F. Gal, *J. Chem. Soc. Perkin II*, 705 (1984).
7. M. Meot-Ner, *J. Am. Chem. Soc.*, **106**, 1257, 1265 (1984).
8. Y. K. Lau and P. Kebarle, *Can. J. Chem.*, **59**, 151 (1981).
9. W. R. Davidson, J. Sunner, and P. Kebarle, *J. Am. Chem. Soc.*, **101**, 1675 (1979).
10. P. Kebarle, W. R. Davidson, J. Sunner, and S. Meza-Hojer, *Pure Appl. Chem.*, **51**, 63 (1979).
11. E. M. Arnett, B. Chawla, L. Bell, M. Taagepera, W. J. Hehre, and R. W. Taft, *J. Am. Chem. Soc.*, **99**, 5729 (1977).

12. K. Hiraoka, H. Takimoto, and K. Morise, *J. Am. Chem. Soc.*, **108**, 5683 (1986).

13. Y. K. Lau, S. Ikuta, and P. Kebarle, *J. Am. Chem. Soc.*, **104**, 1462 (1982).

14. Y. K. Lau, K. Nishizawa, A. Tse, R. S. Brown, and P. Kebarle, *J. Am. Chem. Soc.*, **103**, 6291 (1981).

15. D. A. MacDonaill and D. A. Morton-Blake, *Theor. Chim. Acta*, **65**, 13 (1984).

16. J. Bromilow, R. W. Taft, and R. D. Topsom, unpublished results.

17. M. Taagepera, D. De Frees, W. J. Hehre, and R. W. Taft, *J. Am. Chem. Soc.*, **102**, 424 (1980).

18. See, for example, W. J. Hehre, L. Radom, J. A. Pople, and P. von R. Schleyer, *Ab Initio Molecular Orbital Theory*, Wiley, New York, 1986.

19. S. Marriott, A. Silvestro, and R. D. Topsom, *J. Chem. Soc. Perkin II*, 457 (1988) and references cited therein.

20. A. Silvestro, R. D. Topsom, C. W. Bock, and R. W. Taft, *J. Mol. Struct. (Theochem)*, **184**, 33 (1989).

21. S. Marriott, R. W. Taft, and R. D. Topsom, unpublished results.

22. M. Taagepera, K. D. Summerhays, W. J. Hehre, R. D. Topsom, A. Pross, L. Radom, and R. W. Taft, *J. Org. Chem.*, **46**, 891 (1981); G. L. Butt, R. D. Topsom, and R. W. Taft, *J. Mol. Struct. (Theochem)*, **153**, 141 (1987).

23. J. Cai, R. D. Topsom, A. D. Headley, I. Koppel, M. Mishima, R. W. Taft, and S. J. Veji, *J. Mol. Struct. (Theochem)*, **168**, 141 (1988).

24. A. Pross, L. Radom, and R. W. Taft, *J. Org. Chem.*, **45**, 818 (1980).

25. J. Cai and R. D. Topsom, *J. Mol. Struct. (Theochem)*, **188**, 45 (1989).

26. J. Cai and R. D. Topsom, *J. Mol. Struct. (Theochem)*, in press.

27. See, for example, references 1, 3, 29 and M. Charton, *Progr. Phys. Org. Chem.*, **16**, 287 (1987).

28. M. Fujio, R. T. McIver, Jr., and R. W. Taft, *J. Am. Chem. Soc.*, **103**, 4017 (1981); M. Mishima, R. T. McIver, R. W. Taft, F. G. Bordwell, and W. N. Olmstead, *J. Am. Chem. Soc.*, **106**, 2717 (1984).

29. S. Marriott and R. D. Topsom, *J. Am. Chem. Soc.*, **106**, 7 (1984).

30. J. Cai and R. D. Topsom, *J. Mol. Struct. (Theochem)*, in press.

31. C. Laurence, M. Berthelot, M. Lucon, M. Helbert, D. G. Morris, and J.-F. Gal, *J. Chem. Soc., Perkin II*, 705 (1984).

32. W. J. Hehre, R. D. Topsom, and R. W. Taft, *Progr. Phys. Org. Chem.*, **12**, 159 (1976) and references cited therein.

33. See reference 19 and S. Marriott and R. D. Topsom, *J. Chem. Soc., Perkin II*, 1045 (1985).

34. J. Cai and R. D. Topsom, unpublished results.

35. R. W. Taft and F. G. Bordwell, *Acc. Chem. Res.*, **21**, 463 (1988); T. Yokoyama, I. Hanazome, M. Mishima, M. J. Kamlet, and R. W. Taft, *J. Org. Chem.*, **52**, 163 (1987).

# $Y_X$ Scales of Solvent Ionizing Power

BY T. WILLIAM BENTLEY AND GARETH LLEWELLYN

*Department of Chemistry*
*University College of Swansea*
*Swansea, Wales, United Kingdom*

## CONTENTS

## 1. INTRODUCTION

The $Y_X$ scales of solvent ionizing power are recent adaptions of the Grunwald–Winstein (GW) equation taking account of effects due to specific solvation of the leaving group X. In the original GW equation, rates of solvolyses of *tert*-butyl chloride in any solvent $k$ relative to solvolyses in 80% ethanol–water $k_0$ at 25°C define the solvent ionizing power $Y$ (1):

$$\log\left(\frac{k}{k_0}\right)_{t-\text{BuCl}} = Y \qquad (1)$$

Inclusion of a slope parameter $m$ and an intercept $c$ (usually very small) permits the correlation and prediction of solvolysis rates for any substrate

RX:

$$\log\left(\frac{k}{k_0}\right)_{RX} = mY + c \tag{2}$$

The background to the development of the GW equation (Equation 2) has recently been given by Grunwald (2). Applications of the GW equation were further stimulated by the later determination of additional $Y$ values for many binary mixtures of solvents (3). Although reports of limitations of the GW equation have been appearing since the 1950s, many $Y$ values for aqueous binary mixtures (typical cosolvents are methanol, ethanol, acetone, and dioxan) are still useful for modern correlations of rate data, because these solvent mixtures have similar nucleophilicities (4). Other correlations may be successful fortuitously because changes in solvent ionizing power may be proportional to changes in solvent nucleophilicity (5).

Alternatives to *tert*-butyl chloride as the model compound (Equation 1) have been considered for many years, as described in an earlier review (6). A systematic approach has recently been developed using solvolyses of 1-adamantyl (structure 1) and 2-adamantyl (structure 2) substrates to provide a relatively constant alkyl group, and permitting kinetic studies of a wide range of solvents and leaving groups (7). These results can be incorporated into a modified GW equation (Equation 3).

$$\log\left(\frac{k}{k_0}\right)_{AdX} = Y_X \tag{3}$$



(1)                    (2)
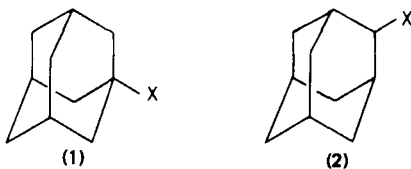
In Equation 3, $k$ is the solvolysis rate in any solvent relative to 80% ethanol–water $(k_0)$ for solvolyses of adamantyl-X substrates, X is the leaving group and $Y_X$ is the scale of solvent ionizing power for the heterolytic process as shown in

$$(R-X)_{solvated} \longrightarrow (R^+)_{solvated} + (X^-)_{solvated} \tag{4}$$
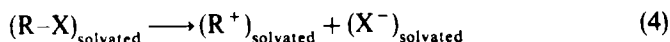
*Hence in Equation 3 explicit consideration is given to effects due to changes in specific solvation of the leaving group.*

Unfortunately, it has not always been possible to obtain all the required

experimental data for adamantyl substrates directly at 25°C. Extrapolations using the Arrhenius equation are frequently required. To avoid the accumulation of extrapolation errors, some $Y_X$ values have not been defined at 25°C. Also for various reasons (e.g., low solubility of adamantyl compounds in highly aqueous media), other reference compounds have also been used.

As rapid progress has been made over the past 5 years, with major contributions from several research groups, a summary of recent progress in the development of $Y_X$ scales is now appropriate. Emphasis will be given to kinetic data—typical products of solvolytic reactions are substitution, elimination, and/or rearrangement, with substitution predominating for solvolyses of adamantyl substrates. Previously unpublished results are also included.

## II.  DEVELOPMENT OF $Y_X$ SCALES OF SOLVENT IONIZING POWER

### A.  The $Y_{OTs}$ Scale of Solvent Ionizing Power

#### 1.  Choice of Model Substrate

One of the most frequently employed leaving groups in organic chemistry is the tosylate group (OTs where Ts = $p$-methylbenzenesulfonyl). Solvolyses of the bridgehead 1-adamantyl tosylate (structure 1, X = OTs) were first reported in 1961 (8). The caged structure prevents rearside attack by nucleophiles and the bridgehead structure greatly inhibits elimination. Solvolyses of 1-adamantyl substrates were considered at that time to be unexpectedly rapid (8, 9), in view of the bridgehead compounds of other ring systems then known. It has since been observed that, in the gas phase, the 1-adamantyl cation is more stable than the more flexible $tert$-butyl cation (10–12). These results cannot be explained solely by enhanced effects of alkyl group polarizability in the gas phase (13), because equilibria between stable ions in solution show $\Delta G \sim 0$ for anion exchange between $tert$-butyl and 1-adamantyl cations (14).

In contrast to the approximately $10^3$-fold greater reactivity of solvolyses of $tert$-butyl substrates than 1-adamantyl substrates in ethanol (8), solvolyses in the very weakly nucleophilic solvent, hexafluoroisopropanol, occur at almost the same rate (15–17). These observations are consistent with the stable ion data discussed above. Hence, in contrast to earlier views (8, 9), it now appears that solvolyses of $tert$-butyl substrates in nucleophilic solvents (e.g., ethanol) are unexpectedly rapid. Nucleophilic solvent assistance in solvolyses of $tert$-butyl substrates can explain these observations (15–17). These results and earlier communications (18, 19) provided further impetus to the development of alternative $Y$ scales of solvent ionizing power, replacing $tert$-butyl

chloride as the model substrate. Relative rates of solvolyses of 1-adamantyl
and other bridgehead systems can be correlated using force field calculations
(20, 21), further supporting the consistency of the interpretation of the kinetic
data.

Although solvolyses of 1-adamantyl tosylate (structure **1**, X = OTs) were
studied by several groups in the 1970s (22  25), it is relatively reactive and was
investigated only in less ionizing solvents having $Y \leqslant 0$ (e.g., acetic acid,
ethanol). Also 1-adamantyl tosylate is extremely sensitive to moisture (23).

The secondary 2-adamantyl system (structure **2**) provides alternative
model substrates for $Y_X$ scales. It was proposed (26) that nucleophilic solvent
participation in solvolyses of 2-adamantyl substrates would be prevented
because the necessary pentacoordinate intermediate or transition state
(structure **3**) would be strongly hindered by the axial hydrogen atoms shown.



(3)
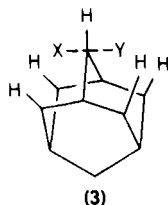
This proposal is now additionally supported by the correlations of solvolysis
rates (see Fig. 1, discussed in more detail later), and by the low reactivity of 2-
adamantyl sulfonates even under vigorous $S_N2$ reaction conditions (27, 28).
The first solvolytic rate data for solvolyses of 2-adamantyl tosylate (structure
**2**, X = OTs) were reported in 1970 (26, 29), and additional studies followed
rapidly (30–33).

After considering various other alternative model compounds (34),
solvolyses of 2-adamantyl tosylate at 25°C were chosen (35) to define a $Y_{OTs}$
scale of solvent ionizing power based on Equation 3 for tosylates and related
compounds. Many useful correlations of typical solvolysis rate data have
been carried out using $Y_{OTs}$ values (see Section IV). However, the need for
additional model compounds became apparent when studies of a wider range
of solvents were attempted. Because of the low solubility of 2-adamantyl
tosylate in highly aqueous media, solvolyses of 2-adamantyl mesylate
(X = $OSO_2CH_3$) were required to obtain the $Y_{OTs}$ value for water (36).

## 2.   An Alternative Model Substrate for Solvolyses in
Highly Aqueous Media

A more convenient substrate for solvolyses in highly aqueous media is 2-
*endo*-norbornyl mesylate (2-NbOMs, structure **4**).
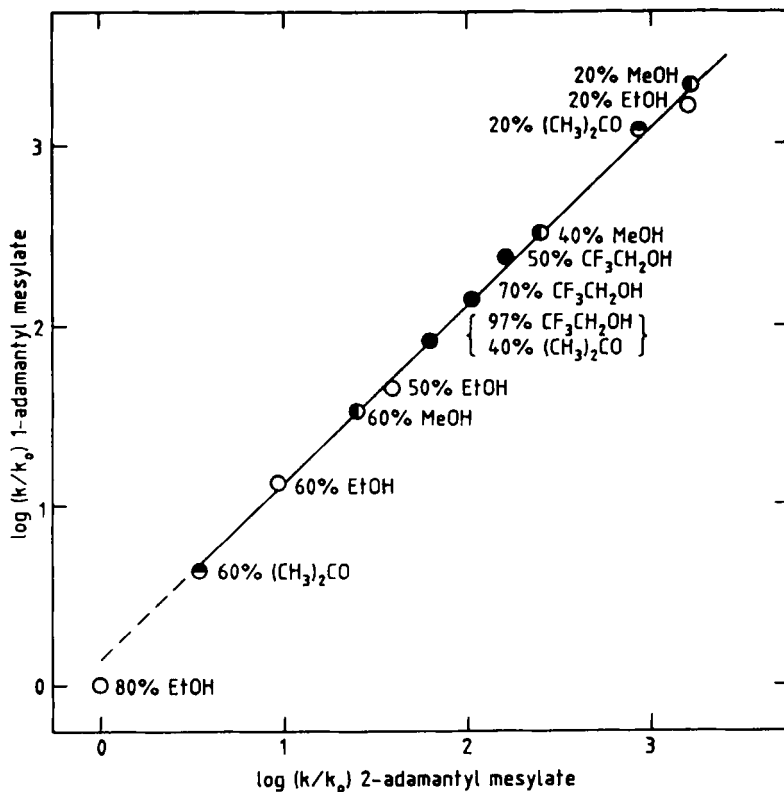
**Figure 1** Correlation (Equation 7) of logarithms of solvolysis rates for 1-adamantyl mesylate versus 2-adamantyl mesylate; kinetic data from references 7 and 41 and Tables 1 and 2. Water is the cosolvent for each of the solvent mixtures; $k_0$ for 2-adamantyl mesylate was calculated assuming a OTs/OMs rate ratio of 1.0 for 80% ethanol–water (41), but the data point was excluded from the least-squares analysis (slope $0.982 \pm 0.016$, intercept $0.144 \pm 0.035$, $r = 0.99$).

This substrate was shown to be only weakly sensitive to nucleophilic solvent assistance (37–39) , although it was later established that $S_N2$ attack by stronger nucleophiles can occur (28). A relationship (Equation 5) was established for 12 solvent mixtures for which kinetic data for both

OMs
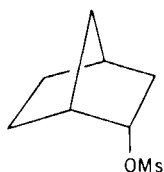
**(4)**

2-adamantyl tosylate and 2-*endo*-norbornyl mesylate could be obtained (40a).

$$Y_{OTs} = 1.41 \log\left(\frac{k}{k_0}\right)_{2-NbOMs} + 0.17 \qquad (5)$$

Then $Y_{OTs}$ values could be calculated from equation (5), with knowledge of only the rate data for solvolyses of 2-*endo*-norbornyl mesylate. The $Y_{OTs}$ value calculated (40b) for pure water was 3.78, significantly less than the previous estimate (36) of 4.1. Possible causes of this discrepancy include small changes in tosylate/mesylate rate ratios (e.g., from 0.5 to 2.1), not accounted for in Equation 5. Tosylate/mesylate rate ratios depend significantly on solvent composition and to a much lesser degree on the nature of the alkyl group (36, 41). Solvolyses of 2-adamantyl *p*-nitrobenzenesulfonate, which has a leaving group somewhat more hydrophilic than that of tosylate, were investigated to define $Y_{OTs}$ values for aqueous acetonitrile (42); a small leaving group effect on these values is expected, and $Y_{OTs}$ for water was found to be a slightly low value of 3.9.

Solvolyses of 2-*endo*-norbornyl mesylate were also studied to obtain $Y_{OTs}$ values for aqueous sulfuric acid mixtures (43). An equation similar to Equation 5 was obtained using only one leaving group (tosylate), and was further refined to allow a small contribution from solvent nucleophilicity:

$$\log\left(\frac{k}{k_0}\right)_{2-NbOTs} = 0.05 N_{OTs} + 0.72 Y_{OTs} \qquad (+0.009) \qquad (6)$$

In this equation, $N_{OTs}$ is the solvent nucleophilicity, obtained from solvolyses of methyl tosylate (35, 44), and 0.05 represents the small sensitivity of solvolyses of 2-*endo*-norbornyl tosylate to solvent nucleophilicity. Rate data for 2-*endo*-norbornyl mesylate were converted to rate data for the tosylate, using appropriate tosylate/mesylate ratios (e.g., based on solvolyses of 2-propyl for which experimental data were available for both tosylates and mesylates). This procedure (Equation 6) gave a $Y_{OTs}$ value for pure water of 4.04, in satisfactory agreement with the value of 4.1 obtained (36) from solvolyses of 2-adamantyl mesylate. Hence, in general, it seems likely that use of Equation 6, in combination with OTs/OMs rate ratios, is a more accurate procedure than Equation 5 for dealing with the problem of low solubility of 2-adamantyl tosylate and mesylate in highly aqueous media.

### 3.   An Alternative Model Substrate for Solvolyses in Less Polar and Aprotic Media

A second disadvantage of 2-adamantyl tosylate is its low reactivity in less polar media. When $Y_{OTs} < 0$ solvolyses become inconveniently slow and

extrapolations of rate data from data at higher temperatures are then required. As $Y_{OTs}$ decreases, uncertainties in these extrapolations increase. Eventually there comes a point where it is better to define an alternative model substrate and to accept the additional uncertainty in overlapping results for the two substrates. Solvolyses of 1-adamantyl mesylate are approximately $10^5$ times faster than solvolyses of 2-adamantyl mesylate or tosylate (7). Hence, long extrapolations from kinetic data at high temperatures ($> 50°C$) are not required, but in some cases small extrapolations from kinetic data at lower temperatures are required.

Also, compared with 1-adamantyl tosylate, more rapid solvolyses of the mesylate can be examined because the mesylate dissolves quickly (7). Using a rapid injection conductimetric technique (45) and temperature extrapolations from 0 to 25°C, the range of accessible experimental data can be extended from

TABLE 1
Rate Constants for Solvolyses of 1-Adamantyl Mesylate (1) (X = OMs)

| | Rate Constants $(k, s^{-1})^a$ | | | | $\Delta H^{\ddagger}$ | $\Delta S^{\ddagger}$ |
|---|---|---|---|---|---|---|
| Solvent | $-10°C$ | $0°C$ | $10°C$ | $25°C$ | kcal mole$^{-1}$ | cal mole$^{-1}$ K$^{-1}$ |
| 40% EtOH | | | 0.136 | 0.63 | 16.6 | −3.9 |
| 80% MeOH | | | | 0.0102 | | |
| 60% MeOH | | 0.00798 | | 0.144 | 18.2 | −1.5 |
| 40% MeOH | 0.0263 | 0.088$^b$ | 0.279 | 1.33$^c$ | 16.9 | −1.2 |
| 20% MeOH | 0.151 | 0.534 | | 8.7$^c$ | 17.5 | 4.5 |
| 90% $(CH_3)_2CO$ | | | | $2.42 \times 10^{-5}$ | | |
| 80% $(CH_3)_2CO$ | | | | $4.63 \times 10^{-4}$ | | |
| 97% $CF_3CH_2OH$ | | | | 0.35$^d$ | 14.7 | −11.4 |
| | | | | 0.37$^e$ | 14.1 | −13.4 |
| | | | | 0.92$^{c,f}$ | 17.6 | 0.4 |
| 97% $(CF_3)_2CHOH$ | 1.65$^g$ | | | 22$^{c,h}$ | (11)$^h$ | (−16)$^h$ |
| $CH_3CO_2H^i$ | | | | $6.2 \times 10^{-4}$ | | |
| $HCO_2H$ | | | 1.2$^j$ | 5.0$^c$ | 15 | −4 |

$^a$Determined conductimetrically at least in duplicate; errors < ± 5%, typically ± 2%; solvent compositions refer to % v/v solvent–water, except for fluorinated alcohols, which are in % w/w.

$^b$Single measurement of rate constant; three other attempts gave less precise data and up to 10% lower values.

$^c$Calculated from rate data at lower temperatures.

$^d$Reference 7, error ±0.2.

$^e$Single measurements of rate constant: °C, $k$, s$^{-1}$; 30.0°C, 0.516; 34.6°C, 0.77; 39.8°C, 1.15; 46.0°C, 1.86 ± 0.14 (triplicate measurement), hence calculated for 70°C, $k$ = 9.3.

$^f$Tosylate data extrapolated from $-10°C$ (reference 47); hence calculated for 70°C, $k$ = 52.4.

$^g$Error ± 0.2; average of five measurements with larger than normal errors (± 10%) because of high amplification of signals.

$^h$Assumed value for $\Delta H^{\ddagger}$; see trend of Table III in reference 7.

$^i$Determined titrimetrically in duplicate.

$^j$Also at 5.5°C, $k$ = (7.6 ± 0.2) × 10$^{-1}$.

$Y_{OTs} \leqslant 0$ to $Y_{OTs} \sim 3$, for example to 20% (v/v) ethanol–water (7). More detailed experimental studies of similarly difficult solvolyses with improved equipment have shown that the experimental technique is reliable (46), and further studies of 1-adamantyl mesylate (Table 1) now extend the earlier work (7).

Because of these improvements in experimental technique, almost the same upper limit of solvent polarity ($Y_{OTs} \sim 3$) is now accessible via 1-adamantyl mesylate as is accessible via 2-adamantyl tosylate. (For this substrate, insurmountable solubility problems in aqueous media remain.) In retrospect it would probably have been advantageous to have chosen 1-adamantyl mesylate as the main model substrate for a $Y_{sulfonate}$ scale of solvent ionizing power. These solvolyses would link better to solvolyses of 2-*endo*-norbornyl mesylate (see above), and the question of $\sigma$-bridging in solvolyses of 2-adamantyl (48, 49) would not be directly relevant. On the other hand, considerably more rate data are available in the literature for tosylates than for mesylates. Also, although 1-adamantyl mesylate is relatively easy to prepare (50), it decomposes on storage even in the freezer. Solutions may be more stable (51)– even 1-adamantyl triflate can be stored in hexane if a small amount of 2, 6-di-*tert*-butyl pyridine is added as a stabilizer (52).

Fortunately, it is possible to overlap $Y_{OTs}$ scales based on solvolyses of 1- and 2-adamantyl sulfonates. The first approach was to convert data for solvolyses of 1-adamantyl mesylate to tosylate data by estimating OTs/OMs rate ratios. A plot (7) of logarithms of rate data for eight calculated rates of solvolyses of 1-adamantyl tosylate and four directly determined rate constants (23) versus $Y_{2-AdOTs}$ gave a slope of $1.08 \pm 0.02 (r = 0.998)$. It has been pointed out that this plot is "mildly curved" (53). For $Y_{OTs} < 0$, solvolyses of 2-adamantyl tosylate are very slow ($k < 10^{-8} \, s^{-1}$) and may be subject to extrapolation errors. Assigning a slope of 1.00 to solvolyses of 1-adamantyl tosylate permits calculation of some revised and some additional $Y_{OTs}$ values (7, 54). However, more recent studies (40b) have indicated a significantly higher slope of 1.15 (1/0.868) based exclusively on tosylate data — ignoring extrapolation errors, we estimate an uncertainty of about 10% in this plot. Fortuitously, exactly the same slope has recently been reported (52) for solvolyses of 1- and 2-adamantyl tresylates ($X = OSO_2CH_2CF_3$) in eight solvents.

To remove the ambiguities associated with OTs/OMs rate ratios in our earlier work (7), we have obtained additional rate data for solvolyses of 2-adamantyl mesylate (Table 2).

To reduce uncertainties due to extrapolation errors in data for 2-adamantyl mesylate, only values corresponding to $Y_{OTs} > 0$ were considered. Data for 12 solvents (Figure 1, p. 125) give

$$\log\left(\frac{k}{k_0}\right)_{1-AdOMs} = 0.982 \log\left(\frac{k}{k_0}\right)_{2-AdOMs} + 0.144 \qquad (r = 0.999) \qquad (7)$$

TABLE 2
Rate Constants for Solvolyses of 2-Adamantyl Mesylate (2) (X = OMs)

| Solvent[a] | Rate Constants $(10^5 k, s^{-1})$[b] | | | | $\Delta H^{\ddagger}$ (kcal mole$^{-1}$) | $\Delta S^{\ddagger}$ cal mole$^{-1}$ K$^{-1}$ |
|---|---|---|---|---|---|---|
| | 75°C | 50°C | 40°C | 25°C | | |
| 97% CF$_3$CH$_2$OH | 42.9 | 3.18 | | 0.154[c] | 22.6 | −9.4 |
| 70% CF$_3$CH$_2$OH | 96.1 | 6.24 | | 0.257[c] | 23.8 | −4.3 |
| 50% CF$_3$CH$_2$OH | 197 | 11.3 | | 0.404[c] | 24.9 | 0.3 |
| 97% (CF$_3$)$_2$CHOH | | | 49 | 10.4[d] | 18.6 | −14.5 |
| HCO$_2$H | | 65[e] | | 2.66[e] | 23.9 | 0.6 |

[a]Solvent compositions for fluorinated alcohols are in % w/w, with water cosolvent.
[b]Determined conductimetrically at least in duplicate; errors < ± 5%, typically ± 2%.
[c]Calculated from rate data at lower temperatures.
[d]Error ± 0.2, literature $k = (1.13 \pm 0.03) \times 10^{-4} s^{-1}$ (reference 45).
[e]Determined titrimetrically.

Within experimental uncertainty, the slope is very close to 1.000. *These results support the application of Equation 3 to the determination of consistent $Y_X$ scales of solvent ionizing power, based on solvolyses of either 1-adamantyl-X or 2-adamantyl-X.* When the two model substrates give different $Y_X$ values, it is difficult to assess quantitatively the possible contributing factors such as experimental errors, extrapolation errors, minor solvation differences or minor mechanistic changes (e.g., $\sigma$-bridging, ion pair return). If the positive intercept in Equation 7 is reliable, the plot (Figure 1) may indeed be part of a shallow curve (53), and this would explain why others (52) have obtained higher slopes when $Y_{OTs}$ values < 0 are included. Some revised judgements of "best" $Y_{OTs}$ values have been made for the compilations given later (Section VI), including the recommendation that 1-adamantyl tosylate be used as the model substrate for $Y_{OTs}$ < 0. Because of the unit slope of Figure 1 and the likelihood of close similarity of OTs/OMs rate ratios for 1- and 2-adamantyl, the $Y_{OTs}$ scale is now very strongly related to solvolyses of 1-adamantyl tosylate. Since solvolyses of 2-adamantyl tosylate occur concurrently with $^{18}$O-scrambling of sulfonyl oxygens (55), it would be interesting to see whether 1-adamantyl tosylate or mesylate behaved similarly.

Our work described above has been directed toward a definition of one "general-purpose" scale of solvent ionizing power for sulfonates termed $Y_{OTs}$. Many other Y scales have also been proposed (Section VI), including (56) a $Y_{OMs}$ scale for mesylates based on our earlier data (7). A $Y_{OMs}$ scale for mesylates can be justified; for instance, mesylate data is easier to obtain in highly aqueous media (see above); mesylate is a leaving group different from tosylate, and relative rates for these two sulfonates are slightly solvent dependent. However, coexistence of $Y_{OTs}$ and $Y_{OMs}$ scales is a precedent likely

to lead to proliferation of similar $Y_X$ scales for only slightly different leaving groups. An alternative approach, using rate ratios for leaving groups (e.g., $k_{OBs}/k_{OTs}$ or $k_{OTs}/k_{OMs}$), has been used for many years to compare data for different sulfonates; rate data for a particular sulfonate can be converted to rate data for a "similar" sulfonate. If, as seems likely from available data (e.g., references 32, 36, 41), these leaving group ratios depend to only a small extent on the alkyl group of the substrate,* only one $Y_X$ scale for "similar" sulfonates would be required.

Solvolytic reactions can also be used to define the ionizing power of aprotic solvents. Data for solvolytic elimination of $p$-toluenesulfonic acid from $p$-methoxyneophyl tosylate (structure 5, Z = OMe) has previously been used for this purpose (57).



**(5)**
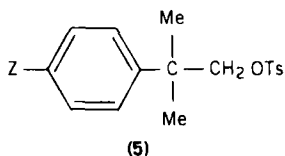
Similarly, an adamantyl scale could be derived from elimination of $N_2O$ from 2-adamantyl azoxytosylate (structure **6**) (58).



**(6)**
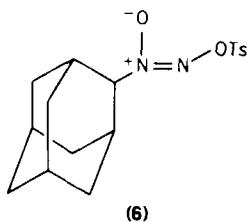
Solvolyses of 1-adamantyl tosylate may also be studied in aprotic solvents such as acetonitrile (59) and amides (60).

## B.  Comparisons of $Y$ and $Y_X$ Scales

The various $Y_X$ scales based on Equation 3 are summarised in Section VI. Because of the high reactivity of 2-adamantyl triflate (structure **2**, X =

*Hammett $\rho$ values for ethanolyses of esters having various sulfonate leaving groups at 70°C for different alkyl groups are as follows: methyl ($\rho = 1.32 \pm 0.05$), ethyl ($\rho = 1.30 \pm 0.07$), 2-propyl ($\rho = 1.55 \pm 0.07$), 2-adamantyl ($\rho = 1.80 \pm 0.05$). Values for 1-adamantyl are virtually the same as for 2-adamantyl (32). For brosylates and tosylates the difference in $\sigma$ values is 0.4, and the calculated OBs/OTs rate ratios vary from 3.3 to 5.2, depending on $\rho$.

(7)
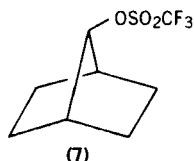
$OSO_2CF_3$) (61), solvolyses of 7-norbornyl triflate (structure 7) provided the first extensive $Y_{OTf}$ data (62). These $Y_{OTf}$ values are substantially lower than corresponding $Y_{OTs}$ values for fluorinated alcohols and carboxylic acid solvents. Although solvolyses of 7-norbornyl and 2-adamantyl substrates are similar in that they are only weakly sensitive to solvent nucleophilicity (63), different $Y_{OTf}$ values have been obtained for the two triflates (62,64,65). Additional kinetic data for solvolyses of 2-adamantyl triflate are shown in Table 3, and data are now available for a wide range of solvents at 25°C. For consistency, we now suggest that $Y_{OTf}$ values should be based on solvolyses of 2-adamantyl triflate (64,65) at 25°C; these $Y_{OTf}$ values are closer to corresponding $Y_{OTs}$ values. The $Y_X$ values derived from solvolyses of other sulfonates, such as pentafluorobenzenesulfonates (66), $OSO_2CH_2CF_3$ (tresylates) (52,67), and $2\text{-}AdOSO_2CH_2CH_2NMe_3^+$ (68) are very similar to $Y_{OTs}$. The anomalous behaviour of triflate may be associated with the weakly basic nature of the leaving group (62). For example, electrophilic assistance by hydrogen bonding may be reduced. It may be significant that $\Delta S^{\ddagger}$ values for 2-adamantyl triflate (Table 3) are more positive than for corresponding tosylates and mesylates (Table 2). Incorporation of an extra $CH_2$ as in tresylates (52, 67),

TABLE 3
Rate Constants for Solvolyses of 2-Adamantyl Triflate (2) (X = $OSO_2CF_3$)

| Solvent[a] | Rate Constants ($k$, $s^{-1}$)[a] | | | | $\Delta H^{\ddagger}$ kcal mole$^{-1}$ | $\Delta S^{\ddagger}$ cal mole$^{-1}$ K$^{-1}$ |
| | −20°C | −10°C | 0°C | 25°C | | |
|---|---|---|---|---|---|---|
| 97% $CF_3CH_2OH$ | | | 0.0081 | 0.16 | 18.8 | 0.7 |
| 97% $CF_3CH_2OH^b$ | | 0.0021 | 0.0079$^c$ | 0.15$^c$ | 18.3 | −0.9 |
| 70% $CF_3CH_2OH$ | | | 0.0186 | 0.45 | 20.1 | 7.3 |
| 50% $CF_3CH_2OH$ | | | 0.030 | 0.94 | 22 | 14 |
| 97% $(CF_3)_2CHOH$ | 0.0268 | 0.107 | 0.345 | 5.5$^{c,d}$ | 17.2 | 2.5 |
| $HCO_2H$ | | | 0.035 | 0.75 | 19.3 | 5.5 |

[a]Determined conductimetrically in duplicate, unless stated otherwise; errors < ± 5%; solvent compositions for fluorinated alcohols are % w/w alcohol–water; the triflate was dissolved in acetonitrile before being injected into the thermostatted solvent.

[b]Reference 65.

[c]Calculated from rate data at other temperatures.

[d]Previous approximate value (reference 65) $k = \sim 8\,s^{-1}$.

or retaining the $CF_3$ group but in trifluoroacetates (17), leads to much better correlations with $Y_{OTs}$.

The $Y_X$ values for X = Cl, Br, and I are similar, but show two consistent effects. Relative to $Y_{Cl}$ slopes of correlations versus other $Y_X$ scales are $Y_{Br}$ (0.96), $Y_I$(0.85), and $Y_{OTs}$ (0.80); these trends are explained by *electrostatic effects* due to charge delocalization on anions of different sizes (69). This first effect on slopes
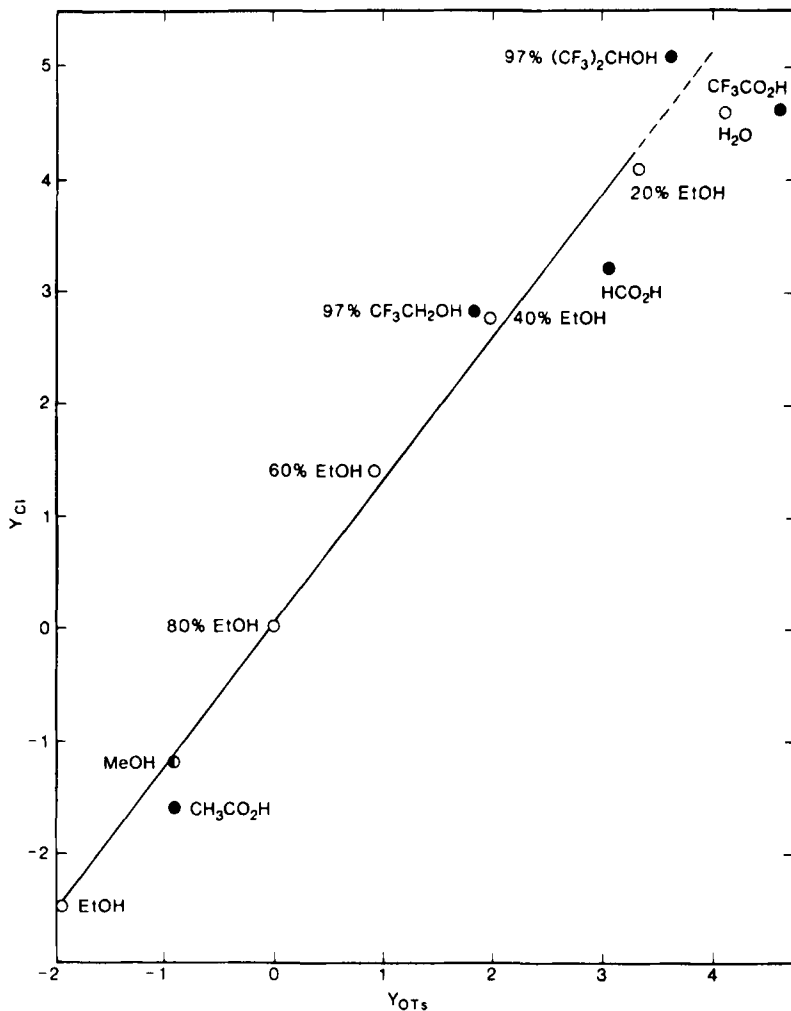


**Figure 2**   Correlation of $Y_{Cl}$ versus $Y_{OTs}$. The correlation line is fitted to the open circles excluding pure water (slope = 1.28 ± 0.04, r = 0.998), data from Tables 5 and 8.

(*m*) is most apparent in solvolyses of picrates (65), a leaving group on which the negative charge can be highly delocalized. Deviations from the main trend lines occur for carboxylic acid solvents, presumably because of *electrophilic assistance*: OTs > Cl > Br > I (69, 70). This second effect is illustrated in the $Y_{Cl}$ versus $Y_{OTs}$ plot (Fig. 2), in which the $Y_{OTs}$ values for $CH_3CO_2H$, $HCO_2H$, and $CF_3CO_2H$ are higher than expected from the data points for ethanol–water mixtures. In contrast, data points for fluorinated alcohols [$CF_3CH_2OH$ and $(CF_3)_2 CHOH$] deviate slightly in the opposite direction. For solvolyses of 1-adamantyl substrates, a $Y_{Cl}$ versus $Y_{OMs}$ plot (not published) shows the same trends.

From calculations of chlorine kinetic isotope effects, strong hydrogen bonding to the incipient chloride ion has been suggested for ethanol–water mixtures (71). A corresponding amount of electrophilic solvent assistance
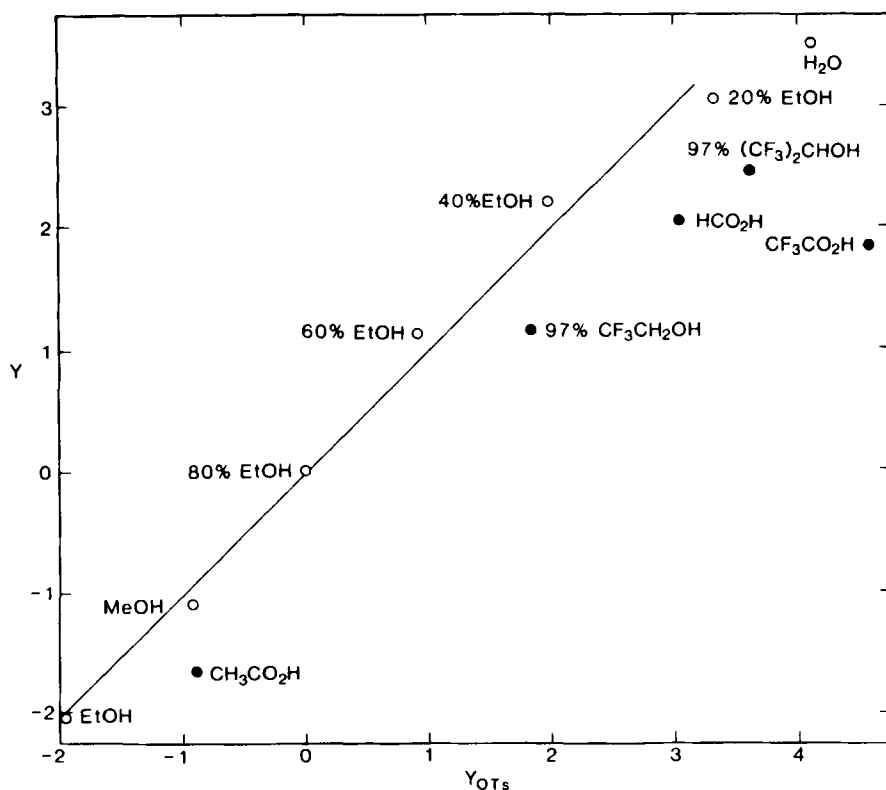


**Figure 3** Correlation of $Y$ versus $Y_{OTs}$. The correlation line is fitted to the open circles excluding pure water (slope $= 1.00 \pm 0.05$, $r = 0.995$); data from Tables 5 and 6.

between initial and transition states is accepted, and $Y_X$ values probably include different amounts of assistance for each solvent; thus, $Y_X$ is a blend of electrostatic and electrophilic solvation effects for which one adjustable parameter $(m)$ is adequate in most cases for quantitative correlations (exceptions include carboxylic acid solvents for all leaving groups and also perhaps fluorinated alcohols for triflate leaving groups). Additional adjustable parameters are being investigated, for example, an $\alpha$ scale of hydrogen bond donation (72), but unfortunately reliable $\alpha$ values are not yet available for the most appropriate solvents (carboxylic acids).

In addition to the two major solvation effects (electrostatic and electrophilic), more specific solvation effects occur in $Y_{OClO_3}$ and $Y_{Pic}$ (54, 65) particularly in high percentage acetone–water mixtures.

The original $Y$ values are compared with $Y_{OTs}$ in Fig. 3; marked deviations for both fluorinated alcohols and carboxylic acids can be explained by nucleophilic solvent assistance in solvolyses of the model substrate tert-butyl chloride (15, 16). An alternative explanation (73) using the solvatochromic method is that, in fluorinated alcohols, solvolyses of tert-butyl chloride have a lower sensitivity to solvent electrophilicity (measured by the hydrogen bond donation parameter $\alpha$) than solvolyses of 1-adamantyl chloride (15) or 2-adamantyl tosylate (Fig. 3). According to this explanation, $Y$ values are a blend of $\pi^*$ (solvent dipolarity) and $\alpha$ (74), but it is not explained why the additional electrophilicity term for fluorinated alcohols is absent in comparisons of $Y_{OTs}$ with $Y_{Cl}$ (Fig. 2) as well as with $Y_{Br}$, $Y_I$, and $Y_{Pic}$ (65). Also, for solvolyses of alkyldimethylsulfonium ions, solvent electrophilicity is relatively unimportant and the effects of the low nucleophilicities of fluorinated alcohols can be observed (16).

Because many aqueous binary mixtures (excluding fluorinated alcohols) have very similar nucleophilicites, the original $Y$ values are closely related to $Y_X$ values, for example $Y \simeq 0.75 \ Y_{Cl}$ (see column 5 of Table 8, later) and $Y \simeq Y_{OTs}$ (e.g., data for the solvent range ethanol–20% ethanol water shown in Fig. 3).

## III.  DEVELOPMENT OF MECHANISTIC CRITERIA

### A.  Correlations of Solvolysis Rates

The simplest useful equation incorporating $Y_X$ values is

$$\log\left(\frac{k}{k_0}\right)_{RX} = mY_X + c \tag{8}$$

This equation can be applied in the same way as for Equation 2, and has the

advantage that explicit consideration is given to effects due to specific solvation of the leaving group X. As most of the recent work has been done with $X = OTs$ or a similar sulfonate, correlations using $Y_{OTs}$ will be described.

Equation 8 will successfully correlate solvolysis rate data under the following three circumstances:

1. Sterically hindered substrates reacting by $S_N1$ (limiting) mechanisms give $m$ values close to 1.00 (Scheme 1);



$m = 1.0$          $m = 1.03$ (ref. 39)          $m = 1.01$ (ref. 75)

$m = 1.07$ (ref. 39)     $m = 1.01$ (ref. 76)     $m = 0.85$ (ref. 78)
                         $m = 1.09$ (ref. 77)
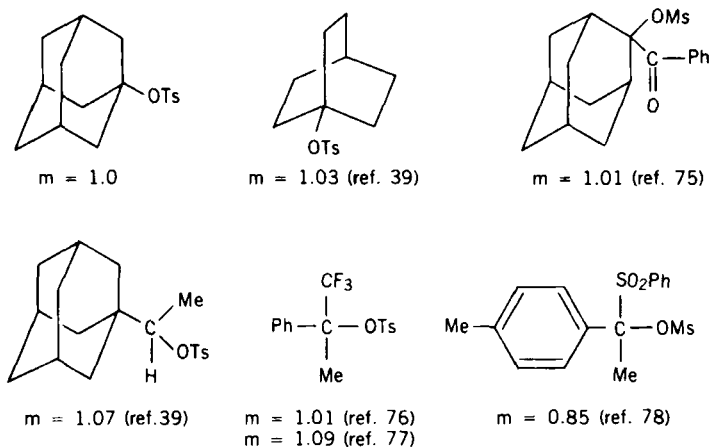
**Scheme 1**

2. Substrates reacting by neighbouring group participation ($k_\Delta$ processes) give $m$ values significantly less than 1.00, probably because of delocalization of positive charge (39, 79).

3. Substrates reacting by nucleophilic solvent assistance ($k_s$ processes) also give $m$ values significantly less than 1.00, probably because of delocalization of positive charge onto the attacking nucleophile (35, 80). These correlations are successful for solvents of similar nucleophilicities (e.g., ethanol–water mixtures give $m_{EW}$ values) (34, 81) and are fortuitous for solvents where changes in $Y$ are proportional to changes in solvent nucleophilicity (5).

A more general equation (9) incorporates terms for the sensitivity

$$\log\left(\frac{k}{k_0}\right)_{ROTs} = lN_{OTs} + mY_{OTs} \tag{9}$$

($l$) of the substrate to nucleophilicity ($N_{OTs}$), defined by

$$N_{OTs} = \log\left(\frac{k}{k_0}\right)_{CH_3OTs} - 0.3\,Y_{OTs} \tag{10}$$

The background to studies of solvent nucleophilicity has recently been reviewed (44), including consideration of alternative $N$ scales (82–84). Briefly, Equation 10 arises from Equation 9 by substituting $l = 1$ and $m = 0.3$ for solvolyses of methyl tosylate (35). The choice of $m = 0.3$ is still being debated (44, 85), and an alternative value of 0.55 has been suggested (85), but it is agreed that consistent correlations can be obtained using $N_{OTs}$ (85). One justification for $m = 0.3$ was the similar nucleophilicities of acetic and formic acids determined in liquid sulfur dioxide — the $N_{PW}$ scale (86). Setting the $N_{OTs}$ values for these two solvents to be equal gives $m = 0.3$ (actually 0.306) from Equation 9, using data for methyl and 2-adamantyl tosylates (i.e., $Y_{OTs}$) in acetic and formic acids (35). Although we have now recommended a revised $Y_{OTs}$ for acetic acid (Section II.A.3), the definition of $N_{OTs}$ using $m = 0.3$ (Equation 10) need not be changed; $m$ would be 0.283 if acetic and formic acids were assumed to have equal nucleophilicities.

Equations 11 and 12 have also proved useful (4, 35, 39) because only one adjustable parameter is required.

$$\log\left(\frac{k}{k_0}\right)_{ROTs} = Q\log\left(\frac{k}{k_0}\right)_{2-AdOTs} + (1-Q)\log\left(\frac{k}{k_0}\right)_{CH_3OTs} \tag{11}$$

$$\log\left(\frac{k}{k_0}\right)_{ROTs} = Q'\log\left(\frac{k}{k_0}\right)_{2-AdOTs} + (1-Q')\log\left(\frac{k}{k_0}\right)_{2-PrOTs} \tag{12}$$

The success of Equations 11 and 12 indicates that $m$ and $l$ (Equation 9) may not be independent. An increase in sensitivity to solvent nucleophilicity ($l$) may *cause* a decrease in sensitivity to solvent ionizing power ($m$) (34, 35), and relationships between $m$, $l$, and $Q$ are as follows:

$$l = \frac{1-m}{0.7} \tag{13}$$

$$l = 1 - Q \tag{14}$$

$$m = 0.3 + 0.7Q \tag{15}$$

Freely adjusted $l$ and $m$ values from Equation 9 often fit Equation 13, even for solvolyses of benzyl tosylate (87), which from an initial study with limited data appeared not to fit Equation 13 (35). Allyl tosylate gives $m = 0.53$ and $l = 0.81$ (85) in approximate agreement with Equation 13.

These detailed studies of relatively simple aliphatic and alicyclic substrates established general trends and helped to define "normal" expected behavior. A disadvantage is that a wide range of solvolytic data is needed for the correlations using Equation 9 (particularly solvents having a diversity of $N$ and $Y$ values); typically data for about 10 solvents can be obtained, but an even wider range would be beneficial.

## B. Mechanistic Information from a Restricted Number of Solvents

Useful information can be obtained from data for a few solvents using Equation 8. As 80% v/v ethanol–water is the standard solvent for correlations, it is desireable to obtain this result experimentally. Additional data in the range 100% ethanol to 40% v/v ethanol–water give $m_{EW}$; the exact value would depend on the range of solvents studied because the plots may be slightly curved. If data in the region of $Y_{OTs} \sim -1$ were conveniently accessible, useful information could be obtained from the rate ratio $k_{90\%\,EtOH}/k_{AcOH}$, which refers to solvents of similar $Y_{OTs}$ and different $N_{OTs}$ values. For 1-adamantyl tosylate, this ratio is 1.38. Significantly higher ratios would be evidence for nucleophilic solvent assistance (88). More exactly, the ratio $[k_{EW}/k_{AcOH}]_{Y(OTs)}$ could be evaluated (34, 81, 88) by interpolating the ethanol–water plot to $Y_{OTs} = -0.9$, the value for acetic acid. Similarly, a ratio $[k_{EW}/k_{HCO_2H}]_{Y(OTs)}$ may be investigated (88), but the relevant ethanol–water composition is $< 30\%$ v/v. Studies of tosylates become difficult in this region. (Mesylates are a more soluble alternative.)

Another useful rate ratio is $k_{40\%\,EtOH}/k_{97\%\,CF_3CH_2OH}$ (89). This ratio is relatively independent of leaving group solvation by electrophilicity effects, as shown by the following data:

2-Adamantyl tosylate, $k_{40\%\,EtOH}/k_{97\%\,CF_3CH_2OH}$     $= 1.38$
1-Adamantyl mesylate, $k_{40\%\,EtOH}/k_{97\%\,CF_3CH_2OH}$     $= 1.76$
1-Adamantyl chloride, $k_{40\%\,EtOH}/k_{97\%\,CF_3CH_2OH}$     $= 0.83$
1-Adamantyl bromide, $k_{40\%\,EtOH}/k_{97\%\,CF_3CH_2OH}$     $= 1.23$
1-Adamantyl trifluoroacetate, $k_{40\%\,EtOH}/k_{97\%\,CF_3CH_2OH}$     $= 1.01$

Few applications of this mechanistic probe have been published to date, but the "Raber–Harris probe" (90, 91) is based on the same principles. In this approach, solvolyses are investigated in three or more compositions of both ethanol–water and trifluoroethanol–water. If Equation 8 correlates all of the data satisfactorily, nucleophilic solvent assistance is judged to be unimportant. When solvent nucleophilicity is significant, separate correlation lines of greatly different slopes are required for each of the two solvent pairs.

Other rate ratios have also been applied to mechanistic interpretations. The rate ratio $k_{97\%(CF_3)_2CHOH/H_2O}/k_{HCO_2H}$ depends strongly on solvent nucleophilicity, varying from 0.017 for $CH_3OTs$ to 3.7 for 2-AdOTs (92), and can be applied when more nucleophilic solvents undergo competing pathways. The rate ratio $k_{80\%EtOH}/k_{97\%CF_3CH_2OH}$ depends on both $m$ and $l$ (Equation 9), but was useful (93) in cases where $m > 0.6$ and $l$ is small. In these cases nucleophilic solvent assistance is difficult to detect, for instance, for solvolyses of 2-*endo*-norbornyl sulfonates (structure 4) and derivatives (37–39). Using similar arguments, relative rates for two tertiary substrates in 80% acetone–water and 97% trifluoroethanol have been quoted (94) as evidence for similar mechanisms.

Mixtures of ethanol–water (EW) and acetic acid–formic acid (AF) have also been investigated for the development of mechanistic criteria (81, 95–97). For this work, solvolyses of neophyl tosylate (structure 5, Z = H) were chosen as the reference substrate. Slopes of correlations $b_{EW}$ and $b_{AF}$ were plotted and the patterns of the two lines were categorized as parallel but not dispersed, parallel but dispersed, diverging as $Y$ increases, or converging as $Y$ increases. However, assignment of results to a particular category could not be done merely by considering slopes and $\pm$ errors. Results for 2-adamantyl tosylate ($b_{EW} = 1.56 \pm 0.04$,  $b_{AF} = 1.35 \pm 0.04$) were considered from statistical evidence to be parallel, whereas results for pinacolyl brosylate ($b_{EW} = 1.38 \pm 0.02$, $b_{AF} = 1.17 \pm 0.03$) were considered to be divergent. Hence, it is not clear how sensitive these criteria are for weak nucleophilic solvent assistance.

Solvolyses of cyclopentyl and cyclohexyl tosylates showed $b_{EW} = b_{AF}$ (within errors) and the lines were dispersed consistent with nucleophilic solvent assistance ($k_s$ processes). Neopentyl solvolyses also showed $b_{EW} = b_{AF}$ but no dispersion, consistent with the accepted views (98, 99) that methyl participation (bridging) occurs in the rate-determining step in an analogous way to the phenyl participation in neophyl (the reference substrate). A distinction was made between bridging and $\sigma$-conjugation (with little motion of the neighboring group), although this may not be clear-cut (98). Diverging lines were explained by the greater "cation solvating power" of water than formic acid, consistent with $\sigma$-conjugation leaving the rearside open to solvation (structure 8) compared with bridging (structure 9).
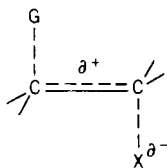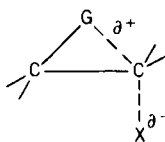


(8)          (9)

However, this explanation requires that these mechanistic criteria are sufficiently finely tuned to distinguish between cation solvating power and weak nucleophilic solvation. In both cases the solvent interacts with the accessible rearside of a carbon atom on which a positive charge is developing. This problem was considered in detail for solvolyses of *tert*-butyl chloride, and it was concluded that solvents such as water, methanol, and ethanol interact nucleophilically in the transition state rather than by dipole–dipole interactions, because the behavior of benzhydryl chloride (rearside accessible) was similar to that of 1-adamantyl chloride (100).

Another factor that could influence the slopes of ethanol–water and acetic acid–formic acid plots is internal ion pair return, usually greater in ethanol or acetic acid than water or formic acid (34). A series of sterically hindered pinacolyl derivatives was examined (101) and for these solvolyses internal ion pair return is probably absent (55). For these substrates divergent patterns were attributed (101) to a rate-limiting ionization mechanism with "cation solvation."

## IV. APPLICATIONS AND LIMITATIONS

Applications of the mechanistic criteria (Section III) include studies of many reactive intermediates in which positive charge is developed on carbon, but there are also studies of nitrenes (102) and substitutions of metal complexes (103). Weakly nucleophilic solvents are usually included in these studies, although investigations of inorganic reaction mechanisms have not yet adopted these solvents. The following examples illustrate the *scope* of recent published work on carbocations. Studies of solvent effects are just one of several pieces of mechanistic evidence used by the various authors to interpret their data, so the original articles should be consulted for discussion of each topic.

Nucleophilic solvent assistance has been observed in the bromination of alkenes (104, 105) and bromination of hexynes has been examined in a range of solvents (106). An m value close to unity has been obtained for bromination of phenol (107). Vinyl cation intermediates have been formed in various solvents by addition (108) and by solvolytic reactions (108, 109).

An extremely active area of recent solvolytic investigations is destabilized secondary and tertiary carbocations, $R_1R_2ZC^+$, where Z is an electron-withdrawing group (110–112); for example, $Z = CN$ (110), $CF_3$ (76, 77, 113–115), COR (61, 75, 116–118), $SO_2CF_3$ (119), P(O) $(OEt)_2$ (92, 120), or P(S) $(OEt)_2$ (121). Doubly deactivated carbocations have also been examined, having two $CF_3$ groups (115) or a $CF_3$ and a CN group (122). Electron demand is then so different from "typical" solvolyses that m and l values (Equation 9)

(10)
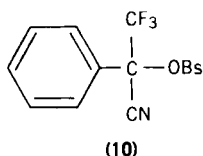
deviate from those predicted in Equation 13; for instance, $m = 0.88$ and $l = 0.49$ for the brosylate (structure **10**) (122). Other applications of Equation 8 include solvolyses of benzhydryl *p*-nitrobenzoates (123) and tosylates derived from substituted α-phenylethanols (124, 125).

Electronic effects of substituents are solvent-dependent and vice versa (126). Not surprisingly, correlations and interpretations of $Y_X$ plots may be complicated by this interplay. A well-established example is protonation of, or hydrogen bonding to, methoxyl groups by carboxylic acids (79); for instance, in aromatic ethers the tendency for electron donation to the benzene ring is significantly reduced. A similar effect has been proposed (127) for aliphatic ethers in fluorinated alcohols. Rates of solvolyses of the two allylic *p*-nitrobenzoates (structures **11** and **12**) are very similar in a range of solvents from 96% ethanol to 40% acetone.



(11)                    (12)
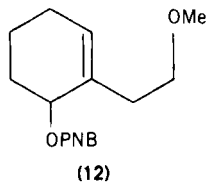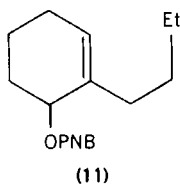
In 97% hexafluoroisopropanol and 97% trifluoroethanol, rates for the ether (structure **12**) are about seven times lower than for the hydrocarbon analog (structure **11**). There are two unexpected features of these results: (1) both fluorinated alcohols deactivate to the same extent, although they differ in acidity by three $pK_a$ units (44); and (2) a plot versus $Y_{OTs}$ is linear for all solvents for the ether (structure **12**) and not, as would be expected, for structure **11**. Although detailed studies of solvolyses of adamantyl *p*-nitrobenzoates have not yet been made, solvolysis of benzhydryl *p*-nitrobenzoate in ethanol–water and trifluoroethanol–water gives $m_{OTs} = 0.82$ at 100°C (123) and solvolysis of 1-adamantyl trifluoroacetate gives $m_{OTs} = 0.94$ at 50°C (17).

Hydrogen-bonding to the OH of mustard chlorohydrin (structure **13**) may account for a major part of the "failure of the Raber–Harris probe" –the incorrect prediction of nucleophilic solvent assistance in solvolyses of structure **13** (128).

$$HO(CH_2)_2S(CH_2)_2Cl$$
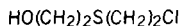
**(13)**

In the absence of the oxygen atom, the deviation $k_{EW}/k_{97\%\,CF_3CH_2OH}$ is small (53), although kinetic data for two groups disagree (53, 129), and the substrates are susceptible to salt formation (130, 131). Differences between SMe and SPh substituents (53) may be caused by greater hydrogen bonding to the more basic $SCH_3$ group. Hydrogen bonding to nitrogen may influence the reactivity of dimethylamino compounds (e.g., structure **14**) (115), which also shows deviations in a Raber–Harris plot versus $Y_{OTs}$ (53).
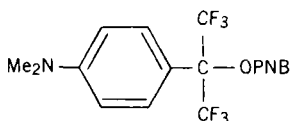


**(14)**

During the initial work on $Y_X$ scales and on the correlations of solvolysis rates, (15, 34, 35, 39), the presence of extra functional groups was deliberately avoided. Subsequent studies of a wider range of compounds show additional solvation effects; for example, $S_N1$ solvolyses of carboxylic acid chlorides do not correlate well with $Y_{Cl}$ (46). The possibility of additional specific solvation effects limits the precision of correlations using $Y_X$ scales. For $k_\Delta$ processes, it is possible that $mY_X$ plots will be curved because the extent of anchimeric assistance may depend on the solvent ionizing power (132). For nucleophilically assisted processes, steric effects on solvent nucleophilicity may be important (44, 133). Ion pair return is another possible cause of complications.

## V.  CONCLUSIONS

Data for a wide range of leaving groups are now available to establish "normal" behavior for expected kinetic effects of protic solvents on the heterolytic step of solvolytic reactions. Normally expected effects of solvent nucleophilicity are also established. The $Y_X$ solvent scales will be useful for the correlation and interpretation of new experimental data and for the identification of "anomalous" results. Investigations of "anomalous" results by independent mechanistic probes should then lead to increased understanding of specific solvation effects and/or mechanistic changes.

The empirical parameters ($Y_X$ and $N$) describe the microscopic events occurring between the initial state and the transition state of solvolytic

reactions. Although their relationship to other empirical parameters is of interest, there is no directly analogous parameter (either empirical or macroscopic). Relationships between $Y$ and $Y_X$ scales for "well-behaved" solvents will be useful for further extending the scope of data available for correlations. For those averse to "proliferation" of empirical scales, we note that $Y_{OTs}$ may be a useful "general-purpose" scale of solvent ionizing power, in cases where data for the most appropriate $Y_X$ scale are not available.

## VI.  COMPILATIONS

A summary of available data is shown in Table 4. Details are given in Tables 5–9. Because some $Y_{OTs}$ values have been changed from previously recommended values, $N_{OTs}$ values have also been revised (Table 5). There are similarities between $Y_{OMs}$ and $Y$ (Table 6) and between $Y_{Cl}$ and $Y/0.75$ (Table 8), particularly for aqueous alcohol mixtures. Values for $Y_X$ are quoted to a maximum of two decimal places—a difference in $Y$ value of 0.01 corresponds to a rate ratio of 1.023. Most of the original $Y$ values were quoted (3) to three decimal places, corresponding to a precision that is difficult to reproduce, particularly in different batches of the "same" solvent. The uncertainties in relatively slow solvolyses are increased by extrapolations from

TABLE 4

Range of Leaving Groups for Currently Available $Y_X$ Scales of Solvent Ionizing Power

| Leaving Group Name, Formula | $Y_X$ scale | Table | Comment |
|---|---|---|---|
| Bromide, Br | $Y_{Br}$ | 8 | |
| Brosylate, $SO_2C_7H_7Br$ | $Y_{OTs}$ | 5 | Using OBs/OTs ratios |
| Chloride, Cl | $Y_{Cl}$ | 8 | |
| Dimethylsulfonium, $^+SMe_2$ | $Y^+$ | 9 | |
| Dinitrophenolate, $OC_6H_3(NO_2)_2$ | —[a] | —[b] | |
| Heptafluorobutyrate, $OCOC_3F_7$ | —[a] | 7 | |
| Iodide, I | $Y_I$ | 8 | |
| Mesylate, $SO_2CH_3$ | $Y_{OTs}$ | 5 | Using OTs/OMs ratios |
| | $Y_{OMs}$ | 6 | |
| Pentafluorobenzenesulfonate | $Y_{PFBS}$ | 6 | |
| Perchlorate, $OClO_3$ | $Y_{OClO_3}$ | 9 | |
| Picrate, $OC_6H_2(NO_2)_3$ | $Y_{Pic}$ | 9 | |
| Tosylate, $SO_2C_7H_8$ | $Y_{OTs}$ | 5 | |
| Tresylate, $SO_2CH_2CF_3$ | $Y_{OTr}$ | 6 | |
| Triflate, $SO_2CF_3$ | $Y_{OTf}$ | 7 | |
| Trifluoroacetate, $OCOCF_3$ | — | 7 | |

[a]A specific code has not been assigned to the scale.

[b]Limited data available (145).

TABLE 5

$Y_{OTs}$ Values of Solvent Ionizing Power Defined from Rate Constants for Solvolyses of 1- or 2-Adamantyl Tosylates at 25°C

| Solvent[a] | Rate Constants ($k$, s$^{-1}$) | | $k_{OTs}/k_{OMs}$[c] | $Y_{OTs}$[d] | $N_{OTs}$[e] |
|---|---|---|---|---|---|
| | 2-Ad($10^5 k$) | 1-Ad($k$)[b] | | | |
| EtOH | | 0.000044 | 1.77[f] | −1.96 | 0.06 |
| 90% EtOH | | 0.000688 | | −0.77 | 0.07 |
| 80% EtOH | 0.0024[g,h] | 0.00403[i] | 0.97[j] | 0.00 | 0.00 |
| 70% EtOH | | | | 0.47[k] | −0.05 |
| 60% EtOH | 0.020[g] | (0.0422)[f] | 0.87[l] | 0.92 | −0.08 |
| 50% EtOH | 0.047[g] | (0.151)[f] | 0.5[l,m] | 1.29 | −0.09 |
| 40% EtOH | 0.225[n] | | | 1.97 | −0.23 |
| 30% EtOH | | | | 2.84[k] | −0.35 |
| 20% EtOH | 5.06[o] | | 1.32[l] | 3.32 | −0.34 |
| 10% EtOH | | | | 3.78[k] | −0.41 |
| $H_2O$ | 31.5[p] | | 2.1[q] | 4.1 | −0.44 |
| MeOH | | 0.00048 | 1.71[j] | −0.92 | −0.04 |
| 90% MeOH | | 0.00361 | 1.72[j] | −0.05 | −0.05 |
| 80% MeOH | | | | 0.47[k] | −0.05 |
| 70% MeOH | | | | 1.02[k] | −0.08 |
| 60% MeOH | 0.008[p] | | 1.35[j] | 1.52 | −0.13 |
| 50% MeOH | | | | 2.00[k] | −0.19 |
| 40% MeOH | 0.64[o] | | 1.03[j] | 2.43 | −0.21 |
| 30% MeOH | | | | 2.97[k] | −0.30 |
| 20% MeOH | 5.9[o] | | 1.48[j] | 3.39 | −0.35 |
| 10% MeOH | | | | 3.78[k] | −0.41 |
| 95% $(CH_3)_2CO$ | | 0.00000448 | | −2.95 | |
| 90% $(CH_3)_2CO$ | | 0.0000416 | 1.81[r] | −1.99 | −0.39 |
| 80% $(CH_3)_2CO$ | | 0.000461 | 0.98[r] | −0.94 | −0.42 |
| 70% $(CH_3)_2CO$ | | | | 0.07[k] | −0.42 |
| 60% $(CH_3)_2CO$ | 0.0111[s] | | 1.26[l] | 0.66 | −0.41 |
| 50% $(CH_3)_2CO$ | | | | 1.26[k] | −0.39 |
| 40% $(CH_3)_2CO$ | 0.17[t] | | 1.13[l] | 1.85 | −0.38 |
| 30% $(CH_3)_2CO$ | | | | 2.50[k] | −0.40 |
| 20% $(CH_3)_2CO$ | 2.7[t] | | 1.31[l] | 3.05 | −0.38 |
| 10% $(CH_3)_2CO$ | | | | 3.58[k] | −0.41 |
| 90% dioxan | | 0.0000157 | | −2.41 | −0.51 |
| 80% dioxan | | 0.000201 | | −1.30 | −0.29 |
| Acetonitrile–water mixtures (% w/w) (42) | | | | | |
| 50% $CH_3CN$ | | | | 1.2 | |
| 35% $CH_3CN$ | | | | 1.8 | |
| 30% $CH_3CN$ | | | | 1.9 | |
| 25% $CH_3CN$ | | | | 2.5 | |
| 20% $CH_3CN$ | | | | 2.7 | |
| 10% $CH_3CN$ | | | | 3.6 | |

TABLE 5 (Continued)

| Solvent[a] | Rate Constants ($k, s^{-1}$) | | $k_{OTs}/k_{OMs}$[c] | $Y_{OTs}$[d] | $N_{OTs}$[e] |
|---|---|---|---|---|---|
| | 2-Ad($10^5 k$) | 1-Ad($k$)[b] | | | |
| i-PrOH | | $5.98 \times 10^{-6}$ | | $-2.83$ | 0.12 |
| t-BuOH | | $7.40 \times 10^{-7}$ | | $-3.74$ | |
| CF$_3$CH$_2$OH–water mixtures (% w/w) | | | | | |
| CF$_3$CH$_2$OH | $0.142^u$ | $(0.578)^f$ | | 1.77 | $-3.07^v$ |
| 97% CF$_3$CH$_2$OH | $0.164^{w,x}$ | | $1.06^y$ | 1.83 | $-2.79$ |
| 85% CF$_3$CH$_2$OH | $0.200^z$ | | | 1.92 | $-2.01$ |
| 70% CF$_3$CH$_2$OH | $0.243^{w,aa}$ | | $0.95^y$ | 2.00 | $-1.20$ |
| 50% CF$_3$CH$_2$OH | $0.335^z$ | | $0.83^y$ | 2.14 | $-0.93$ |
| (CF$_3$)$_2$CHOH | $15.7^{bb}$ | | | 3.82 | |
| 97% (CF$_3$)$_2$CHOH | $9.75^{w,cc}$ | | $0.94^y$ | 3.61 | $-4.27$ |
| 90% HFIP/PDT | $2.16^{dd}$ | | | 2.95 | $-0.64$ |
| CH$_3$CO$_2$H | $(0.00059)^{ee}$ | $0.00053^{ff}$ | $0.85^{gg}$ | $-0.9$ | $-2.28$ |
| 75% AF$^{hh}$ | 0.012 | | | 0.70 | |
| 50% AF$^{hh}$ | 0.10 | | | 1.62 | |
| 25% AF$^{hh}$ | 0.52 | | | 2.34 | |
| HCO$_2$H | $2.65^g$ | | $1.00^y$ | 3.04 | $-2.35$ |
| CF$_3$CO$_2$H | $90^{ii}$ | | $0.44^{jj}$ | 4.57 | $-5.56$ |
| CF$_3$CH$_2$OH–EtOH mixtures (% v/v) | | | | | |
| 80% | $0.0218^{kk}$ | | | 0.98 | $-1.72^{ll}$ |
| 60% | $0.00376^{kk}$ | | | 0.21 | $-1.01^{mm}$ |
| 40% | $0.00084^{kk}$ | | | $-0.44$ | $-0.55^{mm}$ |
| H$_2$SO$_4$ H$_2$O mixtures (% w/w)$^{nn}$ | | | | | |
| 20% | | | 1.8 | 4.39 | $-0.71$ |
| 40% | | | 1.6 | 4.67 | $-1.20$ |
| 60% | | | 1.1 | 5.29 | $-2.02$ |
| Aprotic and other solvents | | | | | |
| CH$_3$CN$^{oo}$ | | $2.51 \times 10^{-6}$ | | $-3.21$ | |
| HCONHCH$_3$$^{pp}$ | | $8.03 \times 10^{-5}$ | | $-1.70$ | |
| CH$_3$CONHCH$_3$$^{pp}$ | | $8.25 \times 10^{-6}$ | | $-2.69$ | |
| HCON(CH$_3$)$_2$$^{pp}$ | | $2.89 \times 10^{-7}$ | | $-4.14$ | |
| CH$_3$CON(CH$_3$)$_2$$^{pp}$ | | $4.15 \times 10^{-8}$ | | $-4.99$ | |

[a] Solvent compositions refer to % v/v water, before mixing, except where stated otherwise.

[b] Reference 23.

[c] Based on adamantyl solvolyses unless stated otherwise.

[d] All values quoted previously have been retained, unless a significant change ( > 0.05) appears to be warranted; newly revised values are underlined; values of rate constants in columns 2 or 3 show the model system chosen.

[e] Calculated from Equation 10; data for solvolyses of methyl tosylate at 50°C from reference 35.

[f] Data from reference 52.

TABLE 5 *(Continued)*

---

[a] Reference 34.

[b] Additional result: $k = 2.3 \times 10^{-8} \, s^{-1}$ (reference 67).

[i] Additional result (interpolated): $k = 4.24 \times 10^{-3} \, s^{-1}$ (reference 134).

[j] Mesylate data from reference 7.

[k] Interpolated from a plot of log $k$ vs. $Y$.

[l] Mesylate data from reference 41.

[m] Anomalously low value in comparison with data for cyclohexyl sulfonates (reference 41).

[n] Reference 81.

[o] Reference 7.

[p] Calculated from rate data for the mesylate, assuming the OTs/OMs rate ratio shown.

[q] Based on kinetic data for 2-propyl sulfonates (reference 36).

[r] Additional rate constants for 1-adamantyl mesylate from Table 1 and reference 52.

[s] Reference 33.

[t] Reference 41.

[u] Average ($\pm 0.02$) of two independent values (references 39, 67).

[v] Reference 135.

[w] Reference 35.

[x] Additional result: $k = 1.02 \times 10^{-6} \, s^{-1}$ (reference 58).

[y] Rate constant for 2-adamantyl mesylate from Table 2.

[z] Reference 37.

[aa] Additional result: $k = 2.3 \times 10^{-6} \, s^{-1}$ (reference 37).

[bb] References 39 and 136.

[cc] Additional values given in Table II of reference 39 and in reference 58.

[dd] Reference 136; PDT is propanedithiol (mole/mole).

[ee] Reference 26.

[ff] Average of four independent measurements (references 8, 22, 24, 25).

[gg] Rate constant for 1-adamantyl mesylate from Table 1; a rate constant for 2-adamantyl mesylate (116) gives OTs/OMs = 0.81.

[hh] Data for acetic acid/formic acid mixtures from reference 81.

[ii] Reference 30.

[jj] Based on kinetic data for 2-propyl sulfonates (116, 137).

[kk] Reference 67.

[ll] Data for methyl tosylate from reference 138.

[mm] Data for methyl tosylate from reference 135.

[nn] Data from reference 43; results for other solvent compositions available; OTs/OMs rate ratios based on 2-propyl.

[oo] Reference 59.

[pp] Reference 60.

TABLE 6

$Y_X$ Values of Solvent Ionizing Power Defined for Solvolyses of Other Sulfonates at 25°C

| Solvent[a] | $Y_{OMs}$[b] | $Y_{PFBS}$[c] | $Y_{OTr}$[d] | $Y$[e] |
|---|---|---|---|---|
| EtOH | −2.22[f] | −1.72 | −1.89 | −2.03 |
| 90% EtOH | −0.82[g] | −0.63 | −0.72 | −0.75 |
| 80% EtOH | 0.00 | 0.00 | 0.00 | 0.00 |
| 70% EtOH | 0.60[g] | 0.43 | 0.49 | 0.60 |
| 60% EtOH | 1.13 | | 0.95 | 1.12 |
| 50% EtOH | 1.65 | | 1.41 | 1.66 |
| 40% EtOH | 2.18 | | | 2.20 |
| 30% EtOH | 2.82[g] | | | 2.72 |
| 20% EtOH | 3.21 | | | 3.05 |
| McOH | −1.17 | −1.02 | −1.11 | −1.09 |
| 90% MeOH | −0.30 | −0.29 | −0.31 | −0.30 |
| 80% MeOH | 0.39 | 0.33 | 0.36 | 0.38 |
| 70% MeOH | 0.98[g] | | 0.91 | 0.96 |
| 60% MeOH | 1.54 | | 1.42 | 1.49 |
| 50% MeOH | 2.05[g] | | 2.14 | 1.97 |
| 40% MeOH | 2.50 | | | 2.39 |
| 30% MeOH | 2.95[g] | | | 2.75 |
| 20% MeOH | 3.32 | | | 3.03 |
| 95% $(CH_3)_2CO$ | | −2.11 | $(−2.18)$[h] | |
| 90% $(CH_3)_2CO$ | −2.26[f,i] | −1.57 | −1.75[f] | −1.86 |
| 80% $(CH_3)_2CO$ | −0.95[f,i] | −0.81 | −0.93 | −0.67 |
| 70% $(CH_3)_2CO$ | −0.10[g] | −0.24 | −0.24 | 0.13 |
| 60% $(CH_3)_2CO$ | 0.66 | 0.30 | 0.40 | 0.80 |
| 50% $(CH_3)_2CO$ | 1.28[g] | | 1.02 | 1.40 |
| 40% $(CH_3)_2CO$ | 1.94 | | | 1.98 |
| 30% $(CH_3)_2CO$ | 2.53[g] | | | 2.48 |
| 20% $(CH_3)_2CO$ | 3.08 | | | 2.91 |
| 95% dioxan | | −2.74 | $(−2.96)$[h] | |
| 90% dioxan | | −2.00 | $(−2.09)$[h] | −2.03 |
| 80% dioxan | | −1.13 | −1.20 | −0.83 |
| 70% dioxan | | −0.46 | −0.46 | 0.01 |
| 60% dioxan | | | 0.25 | 0.72 |
| 50% dioxan | | | 0.95 | 1.36 |
| $CF_3CH_2OH$ | 1.90[f] | 1.11 | 1.71 | 1.15[k] |
| 97% $CF_3CH_2OH$[j] | 1.92 | 1.15 | 1.73 | 1.15[l] |
| 90% $CF_3CH_2OH$[j] | | 1.21 | 1.79 | 1.25[l] |
| 80% $CF_3CH_2OH$[j] | | 1.30 | 1.84 | 1.46[l] |
| 70% $CF_3CH_2OH$[j] | 2.15 | | 1.97 | 1.66[l] |
| 50% $CF_3CH_2OH$[j] | 2.38 | | 2.16 | 2.23[l] |
| 97% $(CF_3)_2CHOH$[j] | 3.72 | | 3.40 | 2.46[m] |
| 90% $(CF_3)_2CHOH$[j] | | | 2.89 | 1.99[m] |
| 80% $(CF_3)_2CHOH$[j] | | | 2.60 | 1.86[m] |

TABLE 6 (*Continued*)

| Solvent[a] | $Y_{OMs}$[b] | $Y_{PFBS}$[c] | $Y_{OTr}$[d] | $Y$[e] |
|---|---|---|---|---|
| $CH_3CO_2H$ | −0.83 | −1.41 | −0.93 | −1.67 |
| $HCO_2H$ | 3.08 | | 3.00[n] | 2.05 |
| $CF_3CH_2OH$–EtOH | | | | |
| 80% | | 0.42 | 0.92 | 0.41[k] |
| 60% | | −0.22 | 0.16 | −0.27[k] |
| 40% | | −0.80 | −0.57 | −0.87[k] |
| 20% | | −1.30 | −1.24 | −1.52[k] |

[a]Solvent compositions refer to % v/v water, before mixing, except where stated otherwise.

[b]Based on solvolyses of 1-adamantyl mesylate; data from reference 7 and Table 1, unless stated otherwise.

[c]Based on solvolyses of 2-adamantyl pentafluorobenzenesulfonate (reference 66).

[d]Based on solvolyses of 2-adamantyl tresylate (reference 67); additional values for 1-adamantyl tresylate are available in reference 52.

[e]Reference 3.

[f]Reference 52.

[g]Interpolated from a plot versus $Y$.

[h]Data at 50°C.

[i]Table 1.

[j]Solvent compositions are % w/w water.

[k]References 135 and 138.

[l]Reference 139.

[m]References 45 and 140.

[n]Reference 52 quotes a value of 2.64.

## TABLE 7
### $Y_x$ Values of Solvent Ionizing Power for Perfluoroalkyl Leaving Groups

| Solvent[a] | $Y_{7,NbOTf}^b$ (25°C) | $Y_{OTf}^c$ | | $\log(k/k_0)_{1\text{-}AdOCOCF_3}^d$ (50°C) | $\log(k/k_0)_{1\text{-}AdOCOC_3F_7}^e$ (50°C) |
|---|---|---|---|---|---|
| | | (25°C) | (−20°C) | | |
| **EtOH** | −1.50 | −1.66[f] | −1.84[g] | | |
| 90% EtOH | 0.00 | 0.00 | −0.65[g] | | |
| 80% EtOH | | | 0.00 | 0.00 | 0.00 |
| 70% EtOH | | | 0.53[g] | | |
| 60% EtOH | 0.88 | | 0.94[g] | | |
| 50% EtOH | | 1.35 | | | |
| 40% EtOH | | 2.13 | | 2.26[h] | |
| 30% EtOH | | 2.9 | | | |
| 20% EtOH | | 3.1 | | | |
| MeOH | | −0.79 | −0.88[g] | | |
| 90% MeOH | | | −0.10[g] | | |
| 80% MeOH | | 0.52 | 0.71[h] | 0.63 | 0.93 |
| 70% MeOH | | | 1.26[g] | | |
| 60% MeOH | | 1.53 | 2.04[g] | 1.50 | 1.62 |
| 50% MeOH | | | | | |
| 40% MeOH | | 2.51 | | 2.59 | 2.59 |
| 30% MeOH | | 2.8 | | | |
| 95% (CH₃)₂CO | | −1.15[i] | −0.79[g] | | |
| 90% (CH₃)₂CO | | −0.64[i] | −0.35[g] | | |
| 80% (CH₃)₂CO | | 0.04 | 0.24[g] | −0.41 | |
| 70% (CH₃)₂CO | | | 0.78[g] | | |
| 60% (CH₃)₂CO | | 1.03 | 1.30[g] | 0.78 | 0.98 |
| 50% (CH₃)₂CO | | | 1.88[g] | | |

| Solvent | | | | | |
|---|---|---|---|---|---|
| 40% (CH₃)₂CO | | 2.00 | | | 1.78 | |
| 30% (CH₃)₂CO | | 2.5 | | | | |
| i-PrOH | | −2.16[f] | | | | |
| t-BuOH | | −2.66[f] | | | | |
| CF₃CH₂OH | 0.40 | | | | | |
| 97% CF₃CH₂OH[j] | | 0.96 | 1.23[a] | 2.25 | |
| 90% CF₃CH₂OH[j] | | | 1.36[a] | | 2.45 |
| 70% CF₃CH₂OH[j] | | 1.42 | 1.61[a] | | |
| 50% CF₃CH₂OH[j] | | 1.74 | | | |
| 97% (CF₃)₂CHOH[j] | 1.65 | 2.51 | | 3.37 | 3.32 |
| CH₃CO₂H | −1.78 | −1.57[f] | | | |
| HCO₂H | 1.49 | 1.64 | | | |
| CF₃CO₂H | 1.76 | | | | |
| CF₃CH₂OH–EtOH mixtures | | | | | |
| 80% | | | 0.26[a] | | |
| 60% | | | −0.31[a] | | |
| 40% | | | −1.02[a] | | |
| 20% | | | −1.48[a] | | |

[a] Solvent compositions refer to % v/v water, before mixing, except where stated otherwise.

[b] Based on solvolyses of 7-norbornyl triflate at 25°C (62).

[c] Based on solvolyses of 2-adamantyl triflate at 25°C; data from reference 65 and Table 3, except where stated otherwise.

[d] Based on solvolyses of 1-adamantyl trifluoroacetate at 50°C (17).

[e] Based on solvolyses of 1-adamantyl heptafluorobutyrate at 50°C (17).

[f] Data from reference 64, using $k_0 = 1.7 \times 10^{-2}$ s⁻¹ (65); we have obtained an independent value of $1.79 \times 10^{-2}$ at 25°C, significantly lower than an extrapolated titrimetric value of $2.13 \times 10^{-2}$ (64).

[g] Values at −20°C (64).

[h] This work.

[i] Reference 61.

[j] Solvent compositions are % w/w.

[k] Revised value quoted in Table 5 of reference 66.

TABLE 8

$Y_x$ Values of Solvent Ionizing Power for Solvolyses of Halides at 25°C

| Solvent[a] | $Y_I^b$ | $Y_{Br}^c$ | $Y_{Cl}^c$ | $Y/0.75^d$ |
|---|---|---|---|---|
| EtOH | −2.2[r] | −2.4[e] | −2.5[e] | −2.71 |
| 90% EtOH | −0.81[e] | −0.84[e] | −0.9[e] | −1.00 |
| 80% EtOH | 0.00 | 0.00 | 0.00 | 0.00 |
| 70% EtOH | 0.71[f] | 0.68[f] | 0.8 | 0.79 |
| 60% EtOH | 1.22[f] | 1.26 | 1.38 | 1.50 |
| 50% EtOH | 1.79 | 1.88 | 2.02 | 2.21 |
| 40% EtOH | 2.46[f] | 2.62 | 2.75 | 2.93 |
| 30% EtOH | 3.17[f] | 3.40 | 3.53 | 3.63 |
| 20% EtOH | 3.68 | 3.92 | 4.09 | 4.07 |
| 10% EtOH | 3.95[f] | 4.17 | 4.40 | 4.42 |
| $H_2O$ | 4.24 | 4.44 | 4.57 | 4.66 |
| MeOH | −0.84 | −1.12[e] | −1.2[e] | −1.45 |
| 90% MeOH | 0.01[f] | −0.14[e] | −0.2[e] | −0.40 |
| 80% MeOH | 0.76 | 0.70[f] | 0.67[e] | 0.51 |
| 70% MeOH | 1.46[f] | 1.42 | 1.46 | 1.28 |
| 60% MeOH | 1.97 | 2.04 | 2.07 | 1.99 |
| 50% MeOH | 2.54[f] | 2.61 | 2.70 | 2.63 |
| 40% MeOH | 3.02 | 3.14 | 3.25 | 3.19 |
| 30% MeOH | 3.43[f] | 3.61 | 3.73 | 3.67 |
| 20% MeOH | 3.77 | 3.94 | 4.10 | 4.03 |
| 10% MeOH | 4.01[f] | 4.17 | 4.39 | 4.37 |
| 80% $(CH_3)_2CO$ | −0.17 | −0.7[e] | −0.8[e] | −0.90 |
| 70% $(CH_3)_2CO$ | 0.58[f] | 0.2[e] | 0.17[e] | 0.17 |
| 60% $(CH_3)_2CO$ | 1.20 | 1.03 | 1.00[e] | 1.06 |
| 50% $(CH_3)_2CO$ | 1.82[f] | 1.74 | 1.73 | 1.86 |
| 40% $(CH_3)_2CO$ | 2.43 | 2.44 | 2.46 | 2.64 |
| 30% $(CH_3)_2CO$ | 2.99[f] | 3.11 | 3.21 | 3.31 |
| 20% $(CH_3)_2CO$ | 3.49 | 3.66 | 3.77 | 3.88 |
| 10% $(CH_3)_2CO$ | 3.79 | 4.05 | 4.28 | 4.31 |
| 5% $(CH_3)_2CO$ | 3.97 | | 4.44 | |
| 80% dioxan | | −0.60[g] | | −1.11 |
| 70% dioxan | | −0.01[g] | | 0.02 |
| 60% dioxan | | 0.82[g] | | 0.95 |
| 80% DMSO | | 0.22[h] | | −0.44[i] |
| 70% DMSO | | 0.82[h] | | 0.67[i] |
| 60% DMSO | | 1.71[h] | | 1.64[i] |
| 50% DMSO | | 2.46[h] | | 2.29[i] |
| $CF_3CH_2OH$ | | 2.53 | | 1.53 |
| 97% $CF_3CH_2OH^j$ | 2.22 | 2.53 | 2.83 | 1.53 |
| 80% $CF_3CH_2OH^j$ | | 2.67[g] | | 1.95 |
| 70% $CF_3CH_2OH^j$ | 2.61 | 2.79 | 2.96 | 2.21 |
| 60% $CF_3CH_2OH^j$ | | 2.91[g] | | 2.53 |
| 50% $CF_3CH_2OH^j$ | 2.87 | 3.04 | 3.16 | 2.97 |
| 97% $(CF_3)_2CHOH^j$ | 3.84 | 4.51 | 5.08 | 3.28 |
| $CH_3CO_2H$ | −2.2 | −2.1 | −1.6 | −2.23 |
| $HCO_2H$ | 1.6 | 2.47 | 3.20 | 2.74 |

TABLE 8 (*Continued*)

| Solvent[a] | $Y_I{}^b$ | $Y_{Br}{}^c$ | $Y_{Cl}{}^c$ | $Y/0.75^d$ |
|---|---|---|---|---|
| CF$_3$CO$_2$H | | | 4.6 | 2.45[k] |
| CF$_3$CH$_2$OH–EtOH mixtures | | | | |
| 80% | | 1.62[l] | | 0.55 |
| 60% | | 0.31[l] | | −0.36 |
| 40% | | −0.57[l] | | −1.16 |
| 20% | | −1.42[l] | | −2.03 |

[a]Solvent compositions refer to % v/v water, before mixing, except where stated otherwise.

[b]Reference 69.

[c]Reference 15.

[d]$Y$ values from Table 6, except where noted otherwise.

[e]Extrapolated from a plot vs. $Y$.

[f]Interpolated value.

[g]Reference 141.

[h]Reference 142.

[i]$Y$ values from footnote $i$ of Table 2 in reference 141.

[j]Solvent compositions are % w/w.

[k]Reference 143.

[l]Rates at 25°C estimated from rate data (135) at 35°C by assuming that the change in $\Delta H^{\ddagger}$ from 20 to 24 kcal mole$^{-1}$ (for trifluoroethanol to ethanol) occurs in 1-kcal-mol$^{-1}$ steps for each 20% change in solvent composition.

## TABLE 9
$Y_X$ Values of Solvent Ionizing Power for Perchlorates, Picrates, and Dimethylsulfonium Ions

| Solvent[a] | $Y_{OClO_3}$[b] (0°C) | $Y_{Pic}$[c] (25°C) | $Y^+$[d] (70.4°C) |
|---|---|---|---|
| EtOH | -1.83 | -1.37[e] | -0.02 |
| 90% EtOH | -0.70 | | |
| 80% EtOH | 0.00 | 0.00 | 0.00 |
| 70% EtOH | 0.53 | | |
| 60% EtOH | 1.22 | | 0.05 |
| 50% EtOH | 1.53[c] | 0.92 | |
| 40% EtOH | 2.32[c] | 1.28 | 0.10 |
| 30% EtOH | 3.07[c] | 1.53 | |
| 20% EtOH | 3.42[c] | 1.98 | 0.20 |
| Water | | | 0.26 |
| MeOH | -0.84 | -0.97[e] | 0.04 |
| 90% MeOH | -0.06 | | |
| 80% MeOH | 0.66[f] | 0.05 | 0.09 |
| 70% MeOH | 1.30 | | |
| 60% MeOH | 1.74[c] | 0.71 | 0.10 |
| 50% MeOH | | | |
| 40% MeOH | 2.73[c] | 1.44 | 0.12 |
| 30% MeOH | 3.06[c] | | |
| 20% MeOH | 3.24[c] | | 0.15 |
| 95% (CH$_3$)$_2$CO | -0.23 | | 0.14 |
| 90% (CH$_3$)$_2$CO | 0.16 | -0.79[g] | 0.14 |
| 80% (CH$_3$)$_2$CO | 0.78[j] | -0.29 | 0.12 |
| 70% (CH$_3$)$_2$CO | 1.31 | 0.06[h] | |
| 60% (CH$_3$)$_2$CO | 1.73[f] | 0.44 | 0.11 |
| 50% (CH$_3$)$_2$CO | 2.17 | | |
| 40% (CH$_3$)$_2$CO | 2.59[c] | 1.15 | 0.13 |
| 30% (CH$_3$)$_2$CO | 3.09[c] | 1.47 | |
| 20% (CH$_3$)$_2$CO | 3.38[c] | 1.82 | 0.18 |
| 10% (CH$_3$)$_2$CO | 3.47[c] | 2.21 | |
| 95% dioxan | | | -0.24 |
| 90% dioxan | (-0.97)[i] | | -0.13 |
| 80% dioxan | (-0.07)[i] | | -0.11 |
| 70% dioxan | 0.72 | | -0.04 |
| 60% dioxan | 1.34 | | 0.00 |
| 50% dioxan | 2.02 | | |
| 40% dioxan | | | 0.01 |
| 20% dioxan | | | 0.08 |
| i-PrOH | -2.44 | | -0.13 |
| t-BuOH | -2.68 | | -0.32 |
| CF$_3$CH$_2$OH | (1.21)[i] | | 0.46 |
| 97% CF$_3$CH$_2$OH[j] | 1.55[c,k] | 1.22 | 0.39 |
| 90% CF$_3$CH$_2$OH[j] | 1.65 | | 0.37 |
| 80% CF$_3$CH$_2$OH[j] | 1.92 | | |
| 70% CF$_3$CH$_2$OH[j] | 2.07[f] | 1.34 | 0.34 |
| 60% CF$_3$CH$_2$OH[j] | 2.13 | | |

TABLE 9 (*Continued*)

| Solvent[a] | $Y_{OClO_3}$[b] (0°C) | $Y_{Pic}$[c] (25°C) | $Y^+$[d] (70.4°C) |
|---|---|---|---|
| 50% $CF_3CH_2OH$[j] | 2.28[f] | 1.43 | 0.29 |
| 97% $(CF_3)_2CHOH$[j] | 3.7[c] | | 0.50 |
| 90% $(CH_3)_2CHOH$[j] | | | 0.49 |
| 70% $(CF_3)_2CHOH$[j] | | | 0.36 |
| 50% $(CF_3)_2CHOH$[j] | | | 0.33 |
| $CH_3CO_2H$ | −1.36 | −0.90 | 0.07 |
| $HCO_2H$ | | | 0.04 |
| $CF_3CH_2OH$−EtOH mixtures | | | |
| 80% | | | 0.33 |
| 60% | | | 0.18 |
| 40% | | | 0.12 |
| 20% | | | 0.06 |

[a] Solvent compositions refer to % v/v water, before mixing, except where stated otherwise.
[b] Reference 54.
[c] Reference 65.
[d] Reference 16.
[e] Reference 144.
[f] Average of two independent values (54, 65).
[g] Reference 145.
[h] Interpolated.
[i] Approximate value.
[j] Solvent compositions are % w/w.
[k] Alternative value: 1.30 (54).

data at higher temperatures and/or from data in more polar solvents, although it is possible to minimise such errors by monitoring some reactions for long periods (over a month). Possible sources of systematic error that may be been underestimated are dissolving the substrate (ultrasonics is very useful) and the hygroscopic nature of alcohols (e.g., trifluoroethanol).

Additional results are available for solvolyses of 1-adamantyl nitrate, for which a good correlation with $Y_{OTs}$ has been established (146). Further work on charged sulfonate leaving groups is also in progress (147); because of their hydrophilicity, such leaving groups are particularly useful for highly aqueous media (68, 148).

For the compilations of data (Tables 5–9), we have excluded solvent mixtures that have not been studied extensively and that give anomalous results in Grunwald–Winstein plots or small responses of rates to changes in solvent composition. Rate maxima over a relatively small range of reactivity have been observed for solvolyses in methanol-acetonitrile mixtures of $t$-butyl halides (149) and of 1-adamantyl halides and tosylate (150)—also for solvolyses of 2-adamantyl perchlorate in methanol-acetone mixtures (151) and for solvolyses of 1-adamantyl picrate (144).

## ACKNOWLEDGEMENTS

## REFERENCES

1. E. Grunwald and S. Winstein, *J. Am. Chem. Soc.*, 70, 846 (1948).

2. E. Grunwald, Current Contents, 43, 18 (1984).

3. A. H. Fainberg and S. Winstein, *J. Am. Chem. Soc.*, 78, 2770 (1956).

4. T. W. Bentley, F. L. Schadt, and P. von R. Schleyer, *J. Am. Chem. Soc.*, 94, 992 (1972).

5. J. Kaspi and Z. Rappoport, *Tetrahedron Lett.*, 2035 (1977).

6. T. W. Bentley and P. von R. Schleyer, *Adv. Phys. Org. Chem.*, 14, 32–40 (1977).

7. T. W. Bentley and G. E. Carter, *J. Org. Chem.*, 48, 579 (1983).

8. P. von R. Schleyer and R. D. Nicholas, *J. Amer. Chem. Soc.*, 83, 2700 (1961).

9. H. Stetter, J. Mayer, M. Schwarz, and K. Wulff, *Chem. Ber.*, 93, 226 (1960).

10. R. H. Staley, R. D. Wieting, and J. L. Beauchamp, *J. Am. Chem. Soc.*, 99, 5964 (1977).

11. R. Houriet and H. Schwarz, *Angew. Chem. Int. Edn. Engl.*, 18, 951 (1979).

12. R. B. Sharma, E. K. Sen Sharma, K. Hiraoka, and P. Kebarle, *J. Am. Chem. Soc.*, *107*, 3747 (1985).

13. J. I. Brauman and L. K. Blair, *J. Am. Chem. Soc.*, *90*, 6561 (1968).

14. D. Mirda, D. Rapp, and G. M. Kramer, *J. Org. Chem.*, *44*, 2619 (1979).

15. T. W. Bentley and G. E. Carter, *J. Am. Chem. Soc.*, *104*, 5741 (1982).

16. D. N. Kevill and S. W. Anderson, *J. Am. Chem. Soc.*, *108*, 1579 (1986).

17. T. W. Bentley and K. Roberts, *J. Chem. Soc. Perkin II*, 1055 (1989).

18. T. W. Bentley, C. T. Bowen, W. Parker, and C. I. F. Watt, *J. Am. Chem. Soc.*, *101*, 2486 (1979).

19. D. N. Kevill, W. A. Kamil, and S. W. Anderson, *Tetrahedron Lett.*, *23*, 4635 (1982).

20. R. C. Bingham and P. von R. Schleyer, *J. Am. Chem. Soc.*, *93*, 3189 (1971).

21. P. Müller and J. Mareda, *Helv. Chim. Acta*, *70*, 1017 (1987).

22. B. R. Ree and J. C. Martin, *J. Am. Chem. Soc.*, *92*, 1660 (1970).

23. D. N. Kevill, K. C. Kolwyck, and F. L. Weitl, *J. Am. Chem. Soc.*, *92*, 7300 (1970).

24. M. L. Sinnott and M. C. Whiting, *J. Chem. Soc. B*, 965 (1971).

25. T. S.-C. C. Huang and E. R. Thornton, *J. Am. Chem. Soc.*, *98*, 1542 (1976).

26. J. L. Fry, C. J. Lancelot, L. K. M. Lam, J. M. Harris, R. C. Bingham, D. J. Raber, R. E. Hall, and P. von R. Schleyer, *J. Am. Chem. Soc.*, *92*, 2538 (1970).

27. K. Banert and W. Kirmse, *J. Am. Chem. Soc.*, *104*, 3766 (1982).

28. K. Banert and A. Kurnianto, *Chem. Ber.*, *119*, 3826 (1986).

29. P. von R. Schleyer, J. L. Fry, L. K. M. Lam, and C. J. Lancelot, *J. Am. Chem. Soc.*, *92*, 2542 (1970).

30. J. M. Harris, R. E. Hall, and P. von R. Schleyer, *J. Am. Chem. Soc.*, *93*, 2551 (1971).

31. V. J. Shiner, Jr. and R. D. Fisher, *J. Am. Chem. Soc.*, *93*, 2553 (1971).

32. D. N. Kevill, K. C. Kolwyck, D. M. Shold, and C.-B. Kim, *J. Am. Chem. Soc.*, *95*, 6022 (1973).

33. D. Lenoir, R. E. Hall, and P. von R. Schleyer, *J. Am. Chem. Soc.*, *96*, 2138 (1974).

34. T. W. Bentley and P. von R. Schleyer, *J. Am. Chem. Soc.*, *98*, 7658 (1976).

35. F. L. Schadt, T. W. Bentley, and P. von R. Schleyer, *J. Am. Chem. Soc.*, *98*, 7667 (1976).

36. T. W. Bentley, and C. T. Bowen, *J. Chem. Soc. Perkin II*, 557 (1978).

37. J. M. Harris, D. L. Mount, and D. J. Raber, *J. Am. Chem. Soc.*, *100*, 3139 (1978).

38. H. C. Brown, M. Ravindranathan, F. J. Chloupek, and I. Rothberg, *J. Am. Chem. Soc.*, *100*, 3143 (1978).

39. T. W. Bentley, C. T. Bowen, D. H. Morten, and P. von R. Schleyer, *103*, 5466 (1981).

40. B. Allard and E. Casadevall (a) *Nouv. J. Chim.*, *7*, 569 (1983); (b) *Nouv. J. Chim.*, *9*, 565 (1985).

41. T. W. Bentley, C. T. Bowen, H. C. Brown, and F. J. Chloupek, *J. Org. Chem.*, *46*, 38 (1981).

42. C. A. Bunton, M. M. Mhala, and J. R. Moffatt, *J. Org. Chem.*, *49*, 3637 (1984).

43. T. W. Bentley, S. Jurczyk, K. Roberts, and D. J. Williams, *J. Chem. Soc. Perkin II*, 293 (1987).

44. T. W. Bentley, *Adv. Chem. Series* No. 215, Chap. 18 (1987).

45. T. W. Bentley, C. T. Bowen, W. Parker, and C. I. F. Watt, *J. Chem. Soc. Perkin II*, 1244 (1980).

46. T. W. Bentley, H. C. Harris, and I. S. Koo, *J. Chem. Soc. Perkin II*, 783 (1988).

47. R. Bielmann, M. Christen, P. Flury, and C. A. Grob, *Helv. Chim. Acta*, *66*, 2154 (1983).

48. H. J. Storesund and M. C. Whiting, *J. Chem. Soc. Perkin II*, 1452 (1975).

49. C. K. Cheung, L. T. Tseng, M.-H. Lin, S. Srivastava, and W. J. Le Noble, *J. Am. Chem. Soc.*, *108*, 1598 (1986).
50. R. K. Crossland and K. L. Servis, *J. Org. Chem.*, *35*, 3195 (1970).
51. X. Creary, *J. Am. Chem. Soc.*, *103*, 2463 (1981).
52. K. Takeuchi, K. Ikai, T. Shibata, and A. Tsugeno, *J. Org. Chem.*, *53*, 2852 (1988).
53. S. P. McManus, M. R. Sedaghat-Herati, R. M. Karaman, N. Neamati-Mazraeh, S. M. Cowell, and J. M. Harris, *J. Org. Chem.*, *54*, 1911 (1989).
54. D. N. Kevill, M. S. Bahari, and S. W. Anderson, *J. Am. Chem. Soc.*, *106*, 2895 (1984).
55. C. Paradisi and J. F. Bunnett, *J. Am. Chem. Soc.*, *107*, 8223 (1985).
56. S. P. McManus, R. M. Karaman, R. Sedaghat-Herati, N. Neamati-Mazraeh, B. A. Hovanes, M. S. Paley, and J. M. Harris, *J. Org. Chem.*, *52*, 2518 (1987).
57. S. G. Smith, A. H. Fainberg, and S. Winstein, *J. Am. Chem. Soc.*, *83*, 618 (1961).
58. H. Maskill, J. T. Thompson, and A. A. Wilson, *J. Chem. Soc. Perkin II*, 1693 (1984).
59. D. N. Kevill and C. B. Kim, *J. Org. Chem.*, *39*, 3085 (1974).
60. S. Saito, K. Doihara, T. Moriwake, and K. Okamoto, *Bull Chem. Soc. Jpn.*, *51*, 1565 (1978).
61. X. Creary, *J. Am. Chem. Soc.*, *98*, 6608 (1976).
62. X. Creary and S. R. McDonald, *J. Org. Chem.*, *50*, 474 (1985).
63. D. E. Sunko, H. Vancik, V. Deljac, and M. Milun, *J. Am. Chem. Soc.*, *105*, 5364 (1983).
64. D. N. Kevill and S. W. Anderson, *J. Org. Chem.*, *50*, 3330 (1985).
65. T. W. Bentley and K. Roberts, *J. Org. Chem.*, *50*, 4821 (1985).
66. D. C. Hawkinson and D. N. Kevill, *J. Org. Chem.*, *53*, 3857 (1988).
67. D. N. Kevill and D. C. Hawkinson, *J. Org. Chem.*, *54*, 154 (1989).
68. D. N. Kevill and R. W. Bahnke, *Tetrahedron*, *44*, 7541 (1988).
69. T. W. Bentley, G. E. Carter, and K. Roberts, *J. Org. Chem.*, *49*, 5183 (1984).
70. S. Winstein, A. H. Fainberg, and E. Grunwald, *J. Am. Chem. Soc.*, *79*, 4146 (1957).
71. D. J. McLennan, A. R. Stein, and B. Dobson, *Can. J. Chem.*, *64*, 1201 (1986).
72. M. J. Kamlet, J. L. M. Abboud, and R. W. Taft, *Progr. Phys. Org. Chem.*, *13*, 485 (1981).
73. J. M. Harris, S. P. McManus, M. R. Sedaghat-Herati, N. Neamati-Mazraeh, M. J. Kamlet, R. M. Doherty, R. W. Taft, and M. H. Abraham, *Adv. Chem. Series* No. 215, Chap. 17 (1987).
74. R. W. Taft and M. J. Kamlet, *J. Chem. Soc. Perkin II*, 1723, 1979.
75. X. Creary, *J. Am. Chem. Soc.*, *106*, 5568 (1984).
76. A. D. Allen, M. P. Jansen, K. M. Koshy, N. N. Mangru, and T. T. Tidwell, *J. Am. Chem. Soc.*, *104*, 207 (1982).
77. K.-T. Liu, M.-Y. Kuo, and C.-F. Shu, *J. Am. Chem. Soc.*, *104*, 211 (1982).
78. X. Creary, M. E. Mehrsheikh-Mohammadi, and M. D. Eggers, *J. Am. Chem. Soc.*, *109*, 2435 (1987).
79. F. L. Schadt, C. J. Lancelot, and P. von R. Schleyer, *J. Am. Chem. Soc.*, *100*, 228 (1978).
80. S. Winstein, E. Grunwald, and H. W. Jones, *J. Am. Chem. Soc.*, *73*, 2700 (1951).
81. D. D. Roberts, *J. Org. Chem.*, 49, 2521 (1984).
82. D. N. Kevill and G. M. L. Lin, *J. Am. Chem. Soc.*, *101*, 3916 (1979).
83. D. N. Kevill, *Adv. Chem. Series*, No. 215, Chap. 19, (1987).
84. D. N. Kevill, and S. W. Anderson, *J. Org. Chem.*, *51*, 5029 (1986).
85. D. N Kevill, and T. J. Rissmann, *J. Org. Chem.*, *50*, 3062 (1985).

86. P. E. Peterson and F. J. Waller, *J. Am. Chem. Soc.*, *94*, 991 (1972).

87. D. N. Kevill, and T. J. Rissmann, *J. Chem. Res.*, 252 (1986).

88. A. Streitwieser, Jr., *Chem. Rev.*, *56*, 635 637 (1956).

89. L. F. R. Cafferata, O. E. Desvard, and J. E. Sicre, *J. Chem. Soc. Perkin II*, 940 (1981).

90. D. J. Raber, W. C. Neal, Jr., M. D. Dukes, J. M. Harris, and D. L. Mount, *J. Am. Chem. Soc.*, *100*, 8137 (1978).

91. J. M. Harris, D. L. Mount, M. R. Smith, W. C. Neal, Jr., M. D. Dukes, and D. J. Raber, *J. Am. Chem. Soc.*, *100*, 8147 (1978).

92. X. Creary and T. L. Underiner, *J. Org. Chem.*, *50*, 2165 (1985).

93. T. W. Bentley, B. Goer, and W. Kirmse, *J. Org. Chem.*, *53*, 3066 (1988).

94. Y. Apeloig and A. Stanger, *J. Am. Chem. Soc.*, *107*, 2807 (1985).

95. D. D. Roberts and R. C. Snyder, Jr., *J. Org. Chem.*, *44*, 2860 (1979).

96. D. D. Roberts and R. C. Snyder, Jr., *J. Org. Chem.*, *45*, 4052 (1980).

97. D. D. Roberts, *J. Org. Chem.*, *47*, 561 (1982).

98. T. Ando, H. Yamataka, H. Morisaki, J. Yamawaki, J. Kuramochi, and Y. Yukawa, *J. Am. Chem. Soc.*, *103*, 430 (1981).

99. V. J. Shiner, Jr., and J. J. Tai, *J. Am. Chem. Soc.*, *103*, 436 (1981).

100. C. A. Bunton, M. M. Mhala, and J. R. Moffatt, *J. Org. Chem.*, *49*, 3639 (1984).

101. D. D. Roberts and E. W. Hall, *J. Org. Chem.*, *53*, 2573 (1988).

102. M. Demeunynck, N. Tohmé, M.-F. Lhomme, J. M. Mellor, and J. Lhomme, *J. Am. Chem. Soc.*, *108*, 3539 (1986).

103. A. C. Dash and J. Pradham, *J. Chem. Soc. Faraday Trans. 1*, *84*, 2387 (1988).

104. M.-F. Ruasse and B.-L. Zhang, *J. Org. Chem.*, *49*, 3207 (1984).

105. M.-F. Ruasse and E. Lefebvre, *J. Org. Chem.*, *49*, 3210 (1984).

106. G. Modena, F. Rivetti, and U. Tonellato, *J. Org. Chem.*, *43*, 1521 (1978).

107. O. S. Tee and J. M. Bennett, *J. Am. Chem. Soc.*, *110*, 269 (1988).

108. K. Yates and G. Mandrapilias, *J. Org. Chem.*, *45*, 3892 (1980).

109. M. Ladika, P. J. Stang, M. D. Schiavelli, and M. R. Hughey, *J. Org. Chem.*, *47*, 4563 (1982); R. H. Summerville, C. A. Senkler, P. von R. Schleyer, T. E. Dueber, and P. J. Stang, *96*, 1100 (1974).

110. P. G. Gassman and T. T. Tidwell, *Acc. Chem. Res.*, *16*, 279 (1983).

111. T. T. Tidwell, *Angew. Chem. Int. Edn. Engl.*, *23*, 20 (1984).

112. X. Creary, *Acc. Chem. Res.*, *18*, 3 (1985).

113. A. D. Allen, C. Ambidge, C. Che, H. Micheal, R. J. Muir, and T. T. Tidwell, *J. Am. Chem. Soc.*, *105*, 2343 (1983).

114. A. D. Allen, R. Girdhar, M. P. Jansen, J. D. Mayo, and T. T. Tidwell, *J. Org. Chem.*, *51*, 1324 (1986).

115. A. D. Allen, V. M. Kanagasabapathy, and T. T. Tidwell, *J. Am. Chem. Soc.*, *108*, 3470 (1986).

116. X. Creary and C. C. Geiger, *J. Am. Chem. Soc.*, *104*, 4151 (1982).

117. X. Creary and C. C. Geiger, *J. Am. Chem. Soc.*, *105*, 7123 (1983).

118. K. Takeuchi, F. Akiyama, K. Ikai, T. Shibata, and M. Kato, *Tetrahedron Lett.*, 873 (1988).

119. X. Creary, *J. Org. Chem.*, *50*, 5080 (1985).

120 X. Creary, C. C. Geiger, and K. Hilton, *J. Am. Chem. Soc.*, *105*, 2851 (1983).

121. X. Creary and M. E. Mehrsheikh-Mohammadi, *J. Org. Chem.*, *51*, 7 (1986).

122. R. Fujiyama, I. Kamimura, M. Yoshida, K. Susuki, S. Kiyooka, A. Murata, M. Goto, M. Fujio, and Y. Tsuno, *Chem. Lett.*, 1043 (1987).

123. D. J. McLennan and P. L. Martin, *J. Chem. Soc. Perkin II*, 1091 (1982).

124. A. D. Allen, J. M. Kwong-Chip, J. Mistry, J. F. Sawyer, and T. T. Tidwell, *J. Org. Chem.*, *52*, 4164 (1987).

125. A. D. Allen, V. M. Kanagasabapathy, and T. T. Tidwell, *J. Am. Chem. Soc.*, *107*, 4513 (1985).

126. R. W. Taft, E. Price, I. R. Fox, I. C. Lewis, K. K. Andersen, and G. T. Davis, *J. Am. Chem. Soc.*, *85*, 3146 (1963).

127. B. Juršić, M. Ladika, and D. E. Sunko, *Tetrahedron*, *42*, 911 (1986).

128. S. P. McManus, N. Neamati-Mazraeh, B. A. Hovanes, M. S. Paley, and J. M. Harris, *J. Am. Chem. Soc. 107*, 3393 (1985).

129. D. E. Sunko, B. Juršić, and M. Ladika, *J. Org. Chem.*, *52*, 2299 (1987).

130. Y.-C. Yang, L. L. Szafraniec, W. T. Beaudry, and J. R. Ward, *J. Org. Chem.*, *52*, 1637 (1987).

131. S. P. McManus, M. R. Sedaghat-Herati, and J. M. Harris, *Tetrahedron Lett.*, *28*, 5299 (1987).

132. J. Laureillard, A. Casadevall, and E. Casadevall, *Helv. Chim. Acta*, *67*, 352 (1984).

133. S. P. McManus, *J. Org. Chem.*, *46*, 635 (1981).

134. C. A. Grob and B. Schaub, *Helv. Chim. Acta*, *65*, 1720 (1982).

135. J. Kaspi and Z. Rappoport, *J. Am. Chem. Soc.*, *102*, 3829 (1980).

136. S. P. McManus and A. Safavy, *J. Org. Chem.*, *51*, 3532 (1986).

137. P. E. Peterson, R. E. Kelley, Jr., R. Belloli, and K. A. Sipp, *J. Am. Chem. Soc.*, *87*, 5169 (1965).

138. D. A. da Roza, L. J. Andrews, and R. M. Keefer, *J. Am. Chem. Soc.*, *95*, 7003 (1973).

139. V. J. Shiner. Jr., W. Dowd, R. D. Fisher, S. R. Hartshorn M. A. Kessick, L. Milakofsky, and M. W. Rapp, *J. Am. Chem. Soc.*, *91*, 4838 (1969).

140. D. E. Sunko and I. Szele, *Tetrahedron Lett.*, 3617 (1972).

141. D. J. Raber, R. C. Bingham, J. M. Harris, J. L. Fry, and P. von R. Schleyer, *J. Am. Chem. Soc.*, *92*, 5977 (1970).

142. J. Delhoste, G. Lamaty, and G. Gomez, *C. R. Acad. Sci.*, *266*, 1468 (1968).

143. P. Haake and P. S. Ossip, *J. Am. Chem. Soc.*, *93*, 6924 (1971).

144. P. R. Luton and M. C. Whiting, *J. Chem. Soc. Perkin II*, 1507 (1979).

145. P. R. Luton and M. C. Whiting, *J. Chem. Soc. Perkin II*, 507 (1979).

146. D. C. Hawkinson, Ph.D. thesis, Northern Illinois University, August 1988.

147. D. N. Kevill, private communication.

148. P. E. Peterson and D. W. Vidrine, *J. Org. Chem.*, *44*, 891 (1979).

149. I. Lee, B. Lee, I. S. Koo, and S. C. Sohn, *Bull. Korean Chem. Soc.*, *4*, 189 (1983).

150. I. Lee, B. Lee, S. C. Sohn, and B. C. Lee, *Bull. Korean Chem. Soc.*, *6*, 19 (1985).

151. D. N. Kevill and M. S. Bahari, *J. Chem. Soc. Chem. Commun.*, 572 (1982).

# Correlation Analysis of Acidity and Basicity: From the Solution to the Gas Phase

BY JEAN-FRANÇOIS GAL AND PIERRE-CHARLES MARIA
*Laboratoire de Chimie Physique Organique*
*Université de Nice–Sophia Antipolis*
*Nice, France*

## CONTENTS

*Dedicated to the memory of Mortimer J. Kamlet*
*for his major contributions to Physical Organic Chemistry*

# I.  INTRODUCTION

The attractive interactions between chemical entities (atoms, molecules, ions) allow their approach to either react and form new compounds, or assemble and constitute a new material.

The tropisms exhibited by these entities may be separated conveniently (but somewhat arbitrarily) into physical interactions modelized by the classical electrostatics, and chemical interactions such as chemical bonds, in particular acid–base interactions.

It is therefore understandable that in an effort to rationalize the chemical reactivity, many studies have been devoted to the search for relationships between structure and acidity or basicity (1).

In fact, L. P. Hammett, in his seminal work on the substituent effects (2), as well as many followers (3), used proton transfer equilibria in hydroxylic solvents such as

$$ArCO_2H \rightleftarrows ArCO_2^- + H^+ \tag{1}$$

$$XCH_2CO_2H \rightleftarrows XCH_2CO_2^- + H^+ \tag{2}$$

$$ArOH \rightleftarrows ArO^- + H^+ \tag{3}$$

$$ArNH_2 + H^+ \rightleftarrows ArNH_3^+ \tag{4}$$
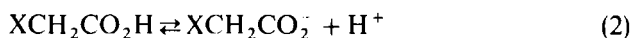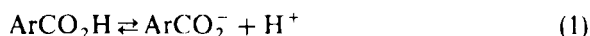
to define substituent constants.

The substituent constants are calculated by using Equation 5, the so-called Hammett equation:

$$\log\left(\frac{K}{K_0}\right) = \rho\sigma \tag{5}$$

In this archetype of substituent effect Gibbs free-energy relationships, the relative Gibbs free energy, $\delta\Delta G° = -RT\ln(K/K_0)$, is the product of two independent variables:

- A reaction constant $\rho$, which depends on the nature of the reaction center and on the structure of the transmitting molecular framework that bears

the substituent and the reacting function, as well as on experimental conditions (medium, temperature, pressure . . .).

- A substituent constant $\sigma$.

If all the experimental variables are taken into account in $\rho$, the substituent constant $\sigma$ depends only on the substituent characteristics, and, in the case of conjugated systems, on its position on the framework transmitting the substituent effect.

Therefore, the substituent constant represents some intrinsic property usually discussed in terms of electronic effects that are likely to represent fundamental potential energy perturbations free from surroundings effects. In an effort to differenciate the effects inherent in the substituent from those due to its surroundings, L. G. Hepler has put forth a model separating internal and environmental contributions to substituent effects on acid ionization in a solvent (4). However, he has shown later that there are difficulties to extend it to the gas phase acidities and basicities (5).

In fact, acidity and basicity measurements in the gase phase, largely proton transfer, provide an approach to separate intrinsic structural effects from solvation effects. Experimental gas-phase data of sufficient precision became available during the 1970s to test this approach (1g, 6).

It was therefore feasible to evaluate the possible extension, beyond the condensed phase, of the range of validity of the Hammett equation and similar extrathermodynamic relationships applied to acidity and basicity. There were, however, a few attempts to apply the Hammett equation to gas-phase reactions not involving intermolecular ion (proton or metal ion) transfer processes. For example, we may cite:

- The unimolecular decomposition of neutral molecules such as the ester pyrolysis (7–9).
- The unimolecular decomposition of ions studied by mass spectrometry (10).
- The Lewis acid–base interaction between neutrals (11).

The scope of these studies is too limited and does not lead to useful generalization concerning the applicability of relationships between structural effects in solution and in the absence of solvent.

On the other hand, the recent accumulation of data related to gas-phase ion transfers, acidities (proton abstraction and anions binding), and basicities (proton and other cations binding) allow fruitful comparisons with the corresponding condensed-phase structural effects.

In this chapter we shall focus on the possible routes of relating acid/base interactions in various media.

Before this analysis, we shall describe briefly the acidity- or basicity-dependent properties for which extended scales are available and present significant mutual overlap. The salient features of the experimental methods will be discussed when relevant.

## II.  ACIDITY–BASICITY SCALES IN SOLUTION

### A.  Proton Transfer in Water and in Dimethyl Sulfoxide

Proton transfer between solute molecules is a very important process because of its fundamental role in synthetic and natural systems, especially in water and in aqueous solutions.

In this regard it is of prime importance to quantitatively characterize the protonation or deprotonation propensity. This demand is fulfilled by the $pK_a$ for practical reasons. A vast body of accurate data is available in the literature (12), and the experimental methods of measurements are well known (13) even for very weak bases (14) and acids (14a).

The $pK_a$ is directly related to the Gibbs free-energy change of the proton exchange between the acidic or basic solute and the amphiprotic solvent. The theory of the electronic effects leads to interpretations in terms of potential energies, the variations of which would be best mirrored by the enthalpy change.

Unfortunately, this thermodynamic quantity is more difficult to obtain and less accurate. As a matter of fact, the literature is poorer in enthalpies of proton exchange (15) than is the corresponding Gibbs free energies. The proportionality between these two thermodynamic quantities has been clearly established in some cases. This proportionality, historically the so-called isokinetic relationship, implies the existence of an enthalpy–entropy relationship (16). It has been shown that there are several limitations to the existence of the above condition.

When both $\Delta H$ and $\Delta G$ values are available, we believe that considering these two quantities may bring complementary informations.

Water may act alternatively as a hydrogen-bond acceptor (HBA) or as a hydrogen-bond donor (HBD). Consequently water strongly solvates cations as well as anions.

Studies in ionizing and dissociating but non-HBD solvents provide additional elements to be used in the analysis of anions solvation. Such is the case for acidities measured in dimethyl sulfoxide (DMSO).

The $pK_a$ values measured in this solvent are absolute (free from ion pairing), which allows for direct comparisons with gas-phase acidities (17). In

addition, the availability of values for heats of ionization in DMSO from Arnett's laboratory (18) affords opportunity to search for a possible entropy effect on going from the solution to the gas phase.

### B.  Complex Formation with Lewis Acids

Many scales of thermodynamic parameters related to the Lewis acid–base reaction leading to a complex formation have been proposed. A detailed account of works published before 1970 is given by Gur'yanova et al. (19).

In 1980 Jensen reviewed the Lewis acid–base concepts and applications and added considerable depth and breadth to the subject (20). The second edition of the Reichardt's book on solvent effects (21) emphasizes the role played by Lewis acid–base interactions on solvation. Most of the thermodynamic parameters are derived from enthalpies measured by calorimetry using solvents of relatively low dipolarity as reaction media.

Drago has used enthalpies of adduct formation in an inert solvent (tetrachloromethane or n-hexane) to derive the $E$ and $C$ parameters (22) for acids and bases. On the basis of these parameters, it is possible to predict the enthalpies of Lewis acid–base reactions, $\Delta H_{AB}$, even for reactions that might be inaccessible experimentally, by using

$$\Delta H_{AB} = E_A E_B + C_A C_B \tag{6}$$

where subscripts A and B refer to acid and base parameters, respectively.

The concept of donor number (DN) was proposed by Gutmann to describe the Lewis basicity of solvents (1d, 23). The empirical DN parameter has been defined as the negative $\Delta H$ value in kilocalories per mole for the interaction of a basic solvent with antimony pentachloride in 1,2-dichloroethane solution at room temperature, according to

$$B:(soln) + SbCl_5 (soln) \rightleftarrows B:SbCl_5 (soln) \tag{7}$$

Problems related to the calorimetric method and to the nature of the reference acid (24) diminish the confidence previously placed in the DN scale.

We have proposed the use of boron trifluoride instead of antimony pentachloride as well as a new calorimetric titration method (25). A careful control of the experimental conditions leads to highly reproducible and accurate data. Following the DN concept, we have defined $-\Delta H^{\circ}_{BF_3}$ as the enthalpy change at 25°C, under 1 atm pressure and in dichloromethane

## TABLE 1
Selected Enthalpies of Complexation with Boron Trifluoride (Reaction 8), in kJ mole$^{-1}$

| B | $-\Delta H^{\circ}_{BF_3}$ |
|---|---|
| Dichloromethane | 10.0 $\pm$ 3.0 |
| *Nitro Compounds* | |
| Nitrobenzene | 35.79 $\pm$ 1.40 |
| Nitromethane | 37.63 $\pm$ 0.56 |
| *Sulfide* | |
| Tetrahydrothiophene | 51.62 $\pm$ 0.20 |
| *Nitriles* | |
| Chloroacetonitrile | 44 $\pm$ 2 |
| Benzonitrile | 55.44 $\pm$ 0.28 |
| Acetonitrile | 60.39 $\pm$ 0.46 |
| Dimethylcyanamide | 77.23 $\pm$ 0.61 |
| *Esters and Carbonates* | |
| Methyl benzoate | 59.4 $\pm$ 1.1 |
| Dimethyl carbonate | 67.63 $\pm$ 0.38 |
| Methyl fomate | 69.76 $\pm$ 0.11 |
| Methyl acetate | 72.79 $\pm$ 0.33 |
| *Ketones* | |
| Di-*tert*-butyl ketone | 31.32 $\pm$ 0.41 |
| *tert*-Butyl methyl ketone | 72.83 $\pm$ 0.37 |
| Acetone | 76.03 $\pm$ 0.21 |
| 4'-Nitroacetophenone | 67.07 $\pm$ 0.50 |
| Acetophenone | 74.52 $\pm$ 0.15 |
| 4'-(Dimethylamino) acetophenone | 98.84 $\pm$ 0.23 |
| 3-Cyano-5,5-dimethyl-2-cyclohexen-1-one | 64.46 $\pm$ 0.53 |
| 5,5-Dimethyl-2-cyclohexen-1-one | 83.58 $\pm$ 0.34 |
| 3-(Dimethylamino)-5,5-dimethyl-2-cyclohexen-1-one | 132.43 $\pm$ 0.47 |
| *Aldehydes* | |
| Acetaldehyde | 69.57 $\pm$ 1.23 |
| 4-Nitrobenzaldehyde | 62.32 $\pm$ 0.18 |
| Benzaldehyde | 74.88 $\pm$ 1.00 |
| 4-(Dimethylamino)benzaldehyde | 103.21 $\pm$ 0.38 |
| *Ethers* | |
| Diisopropyl ether | 76.61 $\pm$ 0.39 |
| Diethyl ether | 78.77 $\pm$ 0.38 |
| Dimethyl ether | 83.55 $\pm$ 0.20 |
| 1,3-Dioxolane | 68.63 $\pm$ 0.43 |
| 1,4-Dioxane | 74.09 $\pm$ 0.27 |
| Tetrahydrofuran | 90.40 $\pm$ 0.28 |

TABLE 1 *(Continued)*

| B | $-\Delta H^{\circ}_{BF_3}$ |
|---|---|
| *Phosphine* | |
| Trimethylphosphine | $97.43 \pm 0.30$ |
| *Sulfoxides* | |
| Diphenyl sulfoxide | $90.34 \pm 0.45$ |
| Methyl phenyl sulfoxide | $97.37 \pm 0.24$ |
| Dimethyl sulfoxide | $105.34 \pm 0.36$ |
| *Amides, Carbamates, and Ureas* | |
| N,N-Dimethylformamide | $110.49 \pm 0.18$ |
| N,N-Dimethyltrichloroacetamide | $55.74 \pm 0.25$ |
| N,N-Dimethylacetamide | $112.14 \pm 0.41$ |
| 4'-Nitro-N,N-dimethylbenzamide | $94.20 \pm 0.57$ |
| N,N-Dimethylbenzamide | $101.75 \pm 0.24$ |
| 4'-(Dimethylamino)- N,N-dimethylbenzamide | $108.76 \pm 0.34$ |
| N,N-Dimethyl methyl carbamate | $81.36 \pm 0.46$ |
| Tetramethylurea | $108.62 \pm 0.22$ |
| 1,3-Dimethyl-3,4,5,6-tetrahydro-2(1*H*)-pyrimidinone (DMPU) | $112.13 \pm 0.29$ |
| *Phosphine Oxides* | |
| Triphenyl phosphate | $66.41 \pm 0.34$ |
| Trimethyl phosphate | $84.75 \pm 0.22$ |
| Hexamethylphosphoramide | $117.53 \pm 0.45$ |
| Trimethylphosphine oxide | $119.68 \pm 0.45$ |
| Tripyrrolidinophosphine oxide | $122.52 \pm 0.14$ |
| *Pyridines* | |
| 2-*tert*-Butylpyridine | $80.10 \pm 0.36$ |
| 2-Cyanopyridine | $96.20 \pm 0.29$ |
| 4-Cyanopyridine | $113.27 \pm 0.31$ |
| Pyridine | $128.08 \pm 0.50$ |
| 4-(dimethylamino)pyridine | $151.55 \pm 0.76$ |
| *Amines* | |
| N,N-Dimethylaniline | $109.16 \pm 0.76$ |
| Trimethylamine | $139.53 \pm 1.79$ |
| Quinuclidine | $150.01 \pm 3.48$ |
| *Amidine* | |
| 1,8-Diazabicyclo[5.4.0.] undec-7-ene (DBU) | $159.36 \pm 0.86$ |

solution, for:

$$B: (soln) + BF_3(g) \rightleftharpoons B:BF_3 (soln) \qquad (8)$$
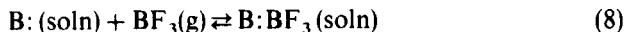
About $350 - \Delta H^{\circ}_{BF_3}$ are now available (26), including many functional families. Some selected values are presented in Table 1.

This scale covers a wide range of reactivity from $10 \, kJ \, mole^{-1}$ for the dissolution of $BF_3$ in the reference solvent to about $160 \, kJ \, mole^{-1}$ for the DBU complexation. The confidence limits at the 95% level on individual values are much less than $1 \, kJ \, mole^{-1}$ in most cases. The wide range associated with the good precision of the measurements confer to this scale a high discriminating power. Within series $-\Delta H^{\circ}_{BF_3}$ values exhibit a high sensitivity to substituent effects. The high steric requirements of $BF_3$ (27) is well exemplified by the dialkylketones and the *ortho*-substituted pyridines behavior and, to a lesser extent, in the case of ethers. When the steric hindrance of the basic center is kept constant within a series, pure electronic effects govern the basicity.

Among the selected values in Table 1, this is the case for nitriles, acetophenones, cyclohexenones, benzaldehydes, and *para*-substituted pyridines. Quantitative treatments of steric and electronic effects may be found in papers of our group cited in reference 25. A relationship between $-\Delta H^{\circ}_{BF_3}$ and gas-phase basicities in the nitrile series has been shown recently (28) and will be discussed hereafter. Both $SbCl_5$ and $BF_3$ may be considered as hard acids in the hard and soft acids and bases theory (1b). "Soft basicity" scales involving soft reference acids such as $I_2$ and $I-X$ compounds (X = electron-withdrawing substituent) (29) or $HgBr_2$ (30) bring complementary informations.

## C.  Hydrogen Bonding

The ubiquitous nature of hydrogen bonding has prompted a vast amount of conceptual and experimental works. The subject has been reviewed in classical books (31). In the domain of solvent effects, a recent survey may be found in the Reichardt's book (21).

The hydrogen bond is weak and consequently is difficult to characterize directly. Fortunately, this interaction induces structural modifications both in the HBA and the HBD partners, which are reflected in particular in their electronic, vibrational, and nuclear magnetic resonance spectra. The measure of the hydrogen bond strength may be based on these spectroscopic parameters. In addition, the concentration changes of the free and associated species can be monitored spectroscopically as a function of the experimental conditions, leading to the equilibrium constant $K$ and the derived thermodynamic quantities $\Delta G$ and $\Delta H$. The enthalpy may also be obtained directly by calorimetry, and in favorable cases $K$ may simultaneously be determined.

Infrared spectroscopy has been frequently used for the establishment of basicity scales. In most cases the reference acid was an alcohol or a phenol. For these hydroxylic HBD the association with a HBA induces a lowering of the O—H (or O—D) infrared stretching wavenumber. This shift, $\Delta\nu(OH)$ or $\Delta\nu(OD)$, is considered to mirror the HBA strength. The most extensive scales have been established by the use of the following reference acid–medium systems:

- MeOD/bulk—the deuterated methanol is diluted in the pure liquid base (32–34).
- PhOH/CCl$_4$—the phenol and the base are diluted in the inert solvent (35, 36).
- MeOH/bulk or MeOH/CCl$_4$—the methanol is diluted in the pure liquid base (37a) or the methanol and the base are diluted in the inert solvent, respectively (37).

The absorption maxima in the ultraviolet–visible range of many compounds are shifted when the medium is changed.

Among the various processes affecting the electronic transitions the hydrogen-bond contribution may be unraveled if some assumptions are made. One such approach, the so-called solvatochromic comparison method (38), consists in a comparison of the absorptions of two indicators of very different HBD or HBA properties in a series of solvents.

A basicity parameter $\beta$ (38a) was defined by Kamlet and Taft from the enhanced shift of a HBD-type indicator as compared to the reference shift of a homomorph non-HBD-type indicator. The two original homomorph pairs were 4-nitroaniline/$N$, $N$-diethyl-4-nitroaniline and 4-nitrophenol/4-nitroanisole. For weakly self-associated solvents, the two corresponding $\beta$ sets were correlated with the 4-fluorophenol $^{19}$F NMR chemical shift and with phenol and 4-fluorophenol association constants. New $\beta$ sets were back-calculated using the obtained equations, and the five sets were averaged. The $\beta$ scale was later expanded by the use of additional spectroscopic, thermodynamic, and kinetic results (39).

Kamlet and Taft used a similar method toward the formulation of the $\alpha$ scale of solvent HBD acidities (38b). This parameter was calculated from the enhanced solvatochromic shift of HBA-type dyes (Dimroth–Reichardt's betaine and Brooker's merocyanine) (21) relative to the non-HBA 4-nitroanisole. Further correlations were used to extend the database (39). A large number of solvent-dependent properties and physicochemical or biochemical properties of solutes in a given medium has been interpreted entirely or partially in terms of hydrogen-bond acidity ($\alpha$) and/or hydrogen-bond basicity ($\beta$) (40).

The correlation of basicity-dependent properties (BDPs) with $\beta$ showed in many cases a family-dependent behavior leading to crudely parallel regression lines (39b). To accommodate the various families into one general correlation, a new coordinate covalency parameter, $\xi$, was formulated to be used in conjunction with $\beta$ (41). The corresponding $\beta-\xi$ treatment formally and conceptually resembles the Drago E–C approach (22). The wide variety of properties used in the definition of $\beta$ leads to a large and useful database at the price of some loss of fine information contained in the original experimental data. To speak in terms of analytical instrument specifications, $\beta$ has gained a larger dynamic range at the expense of the resolution.

These considerations, along with improvements of instrumentation, have prompted Laurence and coworkers to refine the spectroscopic method (42a) and to establish purely solvatochromic hydrogen-bonding basicity scales (42b).

Although numerous thermodynamic data ($K$ and/or $\Delta H^\circ$) have been reported for various types of acid base hydrogen-bond complexing (31c), there have been but few attempts to set up general scales of hydrogen-bond acidity or basicity. One of the earliest wide-range basicity scale was proposed by Taft and coworkers (43).

The so-called $pK_{HB}$ was defined as the logarithm of the equilibrium constant for complex formation with 4-fluorophenol in tetrachloromethane at 25°C. Secondary values were obtained from correlations of the primary set of data with equilibrium constants for other hydroxylic reference acids. The entire $pK_{HB}$ scale thus obtained derives from equilibria and is a pure Gibbs free-energy parameter. As a component of the Kamlet–Taft $\beta$ scale (39) $pK_{HB}$ gives it a Gibbs free-energy character.

Concurrently, Sherry and Purcell showed that hydrogen-bonding enthalpies can be expressed simply by the product of two terms (44) according to:

$$\Delta H = \alpha_A \beta_B \qquad (9)$$

In this equation the subscripts A and B refer to the acid and the base, respectively. The $\alpha_A$ and $\beta_B$ parameters derive from enthalpies. A priori, similarities with the Kamlet–Taft $\alpha$ (45) and $\beta$ are not likely to be expected. Much more recently many efforts have been devoted to the construction of general HBA and HBD scales based on thermodynamic measurements (46–48).

The current research lines were reviewed in a workshop on scales of hydrogen bonding held in London in 1987 (49a). General recommendations were put forth for the establishment of new extended scales. It appears that great progress will be made in the definition of general solute or solvent scales (49), mainly on thermodynamic grounds, in the next few years.

## III. ACIDITY–BASICITY SCALES IN THE GAS PHASE

### A. Scales Relative to the Proton

#### 1. General Principles

The acidity of a substance AH in the gas phase is measured by the standard enthalpy change (50), $\Delta H^{\circ}_{acid}$, for the heterolytic bond dissociation:

$$AH \rightarrow A^- + H^+ \tag{10}$$

Since this process is very endothermic ($\Delta H \gg 0$) and endoergic ($\Delta G \gg 0$), it cannot be studied directly.

The same applies to the proton affinity $PA$ of a substance B, which is defined as the standard enthalpy change (50) for the formal reaction:

$$BH^+ \rightarrow B + H^+ \tag{11}$$

Absolute $\Delta H^{\circ}_{acid}$ values can be calculated from a thermochemical cycle (51) such as

$$AH \rightarrow A^{\cdot} + H^{\cdot} \qquad D(A\ H) \tag{12}$$

$$A^{\cdot} + e^- \rightarrow A^{\cdot\cdot} \qquad - EA(A^{\cdot}) \tag{13}$$

$$H^{\cdot} \rightarrow H^+ + e^- \qquad IE(H^{\cdot}) \tag{14}$$

<hr>

$$AH \rightarrow A^{\cdot\cdot} + H^+ \tag{10}$$
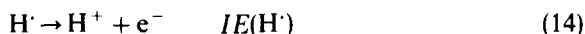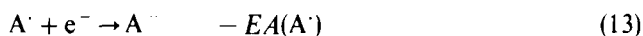
leading to

$$\Delta H^{\circ}_{acid} = D(A-H) - EA(A^{\cdot}) + IE(H^{\cdot}) \tag{15}$$

where $D$, $EA$, and $IE$ stand for the homolytic bond dissociation energy (or enthalpy) of AH, the electron affinity of $A^{\cdot}$, and the ionization energy of $H^{\cdot}$, respectively. Equation 15 is exact only if the spectroscopic observables corresponding to 0 K are corrected to 298.15 K. If $D$ is taken as a standard enthalpy, Equation 15 remains a good approximation (51). This method leads to highly accurate $\Delta H^{\circ}_{acid}$ (uncertainty less than $2 \, kJ \, mole^{-1}$) for small molecules, mainly di- and triatomic, but is rapidly limited for larger molecules.

Considering Equation 11, absolute $PA$ values may be obtained from the standard enthalpies of formation, $\Delta_f H^{\circ}$, of the three species (52); $\Delta_f H^{\circ}(H^+)$ is accurately known. Many $\Delta_f H^{\circ}(B)$ are available in the literature. Unfortunately, $\Delta_f H^{\circ}(BH^+)$ obtained through determinations of appearence energies

are much more difficult to establish reliably. Consequently, only a few *PA* values can be derived by this thermochemical method (53). There are few cases when *PA* values are known to better than $\pm 10\,\mathrm{kJ\,mole^{-1}}$.

Given Equations 10 and 11, one can note that $\Delta H^\circ_{\mathrm{acid}}$ of the neutral species AH is equal to the *PA* of the anion $A^-$ and that *PA* of the neutral species B is equal to the $\Delta H^\circ_{\mathrm{acid}}$ of the cation $BH^+$. Although these definitions are interchangeable, we have followed the scientific community practice of separating the acidity scale of protogenic neutrals from the basicity scale of protophilic neutrals and to use different symbolism for each quantity.

The same dichotomy applies to Gibbs free-energy scales. The terms "gas–phase acidity" ($\Delta G^\circ_{\mathrm{acid}}$) and "gas basicity" (*GB*) will be used hereafter. The Gibbs free energies for Equations 10 and 11, $\Delta G^\circ_{\mathrm{acid}}$ and *GB*, respectively, may be obtained from the corresponding enthalpies by using the fundamental equation

$$\Delta G^\circ = \Delta H^\circ - T\,\Delta S^\circ \qquad (16)$$

Since $S^\circ(H^+)$ is well known, the estimation of $\Delta S^\circ$ reduces to the calculation of the difference between the entropies of the anion $A^-$ (or the neutral base B) and the neutral acid AH (or the cation $BH^+$).

The absolute entropies of gaseous ions can be approximated in a simple way by using the value of the isoelectronic neutral, for example, $S^\circ(Cl^-)$ taken equal to $S^\circ(Ar)$ (51). Another approach consists of calculating the entropy change from the rotational symmetry numbers of the neutral and the ion (51, 53). Sometimes more exact calculations from the complete partition function are warranted.

Because of the approximations made on entropies, the resulting absolute $\Delta G^\circ_{\mathrm{acid}}$ and *GB* values are less accurate than the corresponding enthalpies.

Fortunately, *relative* $\Delta\Delta G^\circ_{\mathrm{acid}}$ and $\Delta GB$ values can be determined by the measurement of the equilibrium constants, $K_{\mathrm{acid}}$ and $K_{\mathrm{base}}$ for the proton-exchange reactions (Equations 17 and 18, respectively)

$$A_1H + A_2^- \rightleftarrows A_1^- + A_2H \qquad (17)$$

$$B_1H^+ + B_2 \rightleftarrows B_1 + B_2H^+ \qquad (18)$$
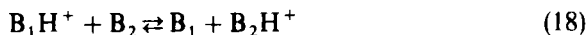
$$\Delta\Delta G^\circ_{\mathrm{acid}} = -RT\ln K_{\mathrm{acid}} \qquad (19)$$

$$\Delta GB = -RT\ln K_{\mathrm{base}} \qquad (20)$$

These relative values can be obtained with a precision better than $\pm 1\,\mathrm{kJ\,mole^{-1}}$ for a very large number of compounds.

The large gaps existing between the few well-defined absolute values used as anchor points can be filled, step by step, by relative equilibrium data leading to extended and precise scales. These Gibbs free-energy scales can, in turn, be converted into enthalpy scales with some loss of accuracy due to the approximate entropy term.

## 2.   Survey of the Experimental Methods

In the context of correlations between solution and gas-phase scales for various organic series, it is more important to dispose of internally consistent gas phase proton-transfer data rather than accurate absolute value. The present section is devoted to a discussion of the methods currently available for the establishment of precise acidity or basicity ladders.

The equilibrium constants $K$ for the proton-transfer reactions (Equations 17 and 18) in the preceding sections can be obtained by measurement of ion densities (ion signal intensities or ion currents) and neutrals partial pressures. An alternative approach is to determine the equilibrium constant as the ratio of the forward and reverse rate constants for Equations 17 and 18. Ion-density ratios can be monitored as a function of time, until equilibrium conditions are reached, using techniques such as pulsed electron beam high-pressure mass spectrometry (HPMS), ion cyclotron resonance (ICR), and flow reactor (FR) methods. In addition, the FR methods, flowing afterglow (FA), or selected ion flow tube (SIFT), allow easy measurements of the rate constants.

Short reviews dealing with the methodology of gas-phase ion thermo-chemistry also describe the classical techniques cited above (54, 185) and a detailed description of the FR techniques appeared recently (55).

To allow the establishment of equilibrium conditions the ions should be trapped for a sufficient time.

In flow reactors the trapping is accomplished by drawing the reactant ion, produced in a separate source, into a fast stream of carrier gas at about 50 Pa that minimalizes the ions diffusion toward the tube wall. The reactant neutral gases are introduced at fixed points downstream, allowing reaction with ions for a time that can be varied by changing the velocity of the carrier gas or the distance separating the neutral gas inlet from the mass spectrometer where the product ions are analyzed. The neutrals partial pressures are obtained from flow measurements.

The HPMS method can be considered the static counterpart of the flow reactor in the sense that the ions are generated, trapped and allowed to react with neutrals in the same housing. A bath gas at a pressure of about 500 Pa slows down the ions quenching on the walls. The ion–molecule reaction takes place after a short ionization pulse, and the resulting ions, diffusing out of the source through an exit slit, enter the mass spectrometer. The intensity of each

ion of interest is monitored as a function of its residence time in the ionization reaction chamber. The reactant gases partial pressures are measured when they are premixed before introduction in the chamber.

To avoid extensive cluster formation, HPMS measurements are usually done at rather high temperatures ($\leqslant 600$ K) and should be corrected to the usual standard state.

One of the advantages of the FR and HPMS techniques is the possibility of variable-temperature studies allowing the simultaneous determination of proton-transfer enthalpies and entropies from van't Hoff plots.

A potential problem associated with HPMS and FR techniques is that the collection and detection efficiency of the different ion types may not be identical and the measured ion current ratio requires correction for mass discrimination. This drawback may be circumvented when using flow reactors, FA and SIFT, if $K$ is calculated from the forward and reverse rate constants instead from ion currents (56).

The ICR spectrometry (57) relies on an entirely different trapping technique based on the use of a strong magnetic field, which constrains the ions on circular orbits in a plane perpendicular to the field direction. In addition, a weak electric field prevents ion drift along the magnetic field direction. By application of a radiofrequency corresponding to the ion cyclotron frequency, ions are accelerated (they resonate) to a coherent motion. An image current of this motion is used for the detection. Therefore, all the events—ionization, trapping and reaction, and detection—occur within the same cell.

Contrary to FR and HPMS, ICR is a low-pressure technique, typically less than $10^{-3}$ Pa. The resulting slow reaction rates are compensated for by the longer trapping times. An other unique feature of ICR is the possibility to eject selectively an ion (the so-called double-resonance experiments) with the aim to assess a reaction sequence such as Equation 17 to 18.

Many advantages have been gained by the application of Fourier transform (FT) techniques to the ICR spectrometry (58).

In the domain of ion–molecule reactions we can mention high resolutions, higher sensitivity due to the possibility of signal accumulation, and rapidity due to the simultaneous detection of all ions. Examples of FT–ICR applications to the determination of gas-phase basicity and acidity are given in references 59 and 60, and 186. For all the above techniques the roles played by the neutrals densities and by the ions densities are of equivalent status for the determination of $K$. Nevertheless, the problems linked to the pressure measurements have been frequently overlooked. In the case of ICR techniques, the low operating pressures are currently measured, directly in the vacuum chamber housing the cell, with Bayard–Alpert gauges. These ionization gauges have different responses for each gas and therefore need to be calibrated against absolute manometers (60, 61).

By far, the bulk of the gas-phase acidity and basicity data has been obtained by the HPMS or ICR methods. The former offers the widest range of reaction temperatures and pressures. The later appears to be more versatile in several respects such as sample introduction and ionization techniques.

### 3.   Typical Results and Structural Effects

Data from various sources have been critically compiled under the auspices of the Ion Kinetics and Energetics Data Center of the National Bureau of Standards (62). This document, which represents the state of knowledge on gas-phase acidities and basicities, was not yet available to the authors at the time of writing. Consequently, we have used, as data sources, the 1984 NBS table for basicities (53) and the unpublished 1987 gas-phase acidity scale (65) where the HPMS and ICR data have been reanchored to the best current absolute acidities.

As a result of the absence of electron repulsion (64) between $H^+$ and any other basic partner, bearing electron(s) by definition, the bare proton is the strongest acid known. As a consequence, every molecule (or atom) is a potential base in the gas phase. A quick perusal of Table 2, where a selection of gas-phase basicity parameters is presented, shows that archetypes of unreactive species (rare or inert gases, He, $N_2$, ..., and paraffines, $CH_4$) and Brønsted acids (HCl) react exothermically with the bare proton, although relatively weakly (low $PA$ values). At the other end of the scale, the strongest bases are the metal oxides and hydroxides. It is to be noted that all these species act as proton acceptors; for example, HCl and NaOH give $H_2Cl^+$ and $NaOH_2^+$, respectively.

The known basicities span a very wide range of about $1300\,kJ\,mole^{-1}$ from He to $Cs_2O$. Between these extreme cases, the more classical bases lay in a relatively restricted range, say, between about 700 and $1000\,kJ\,mole^{-1}$. The basicity of the vast majority of organic compounds fall within these bounds. It is the reason why the corresponding domain was covered by precise ladders that permit the analysis of structural effects and the comparison with condensed-phase results. Comparatively, the acidity scale, the backbone of which is presented in Table 3, covers only $450\,kJ\,mole^{-1}$ from HI to $C_2H_6$. Because of the necessity of separating opposite charges, the reaction in Equation 10 is highly endothermic and endoergic. The acidity *decreases* with the increase in $\Delta H^{\circ}_{acid}$ or $\Delta G^{\circ}_{acid}$, and the general trend fits better the chemist's "feeling" about acidity than in the case of basicity.

Before discussing the structural effects it is worth mentioning that, except in a few cases, the term $T\Delta S^c$ is almost constant at approximately $32\,kJ\,mole^{-1}$ for Equations 10 and 11. The lower $T\Delta S^c$ values are observed when the deprotonation process induces an increase in symmetry (less external

TABLE 2
Some Gas-Phase Basicities, Thermodynamic Data[a] in kJ mole$^{-1}$ for Reaction 11: $BH^+ \rightarrow B + H^+$

| B | PA | GB | $T \Delta S°$ |
|---|---|---|---|
| He | 178 | — | — |
| Ne | 201 | — | — |
| H· | 259.5[b] | — | — |
| $H_2$ | 424 | 396 | 28 |
| HF | 489 | 458 | 31 |
| $N_2$ | 494.5 | 464 | 30.5 |
| Xe | 496 | 474 | 22 |
| $CH_4$ | 551 | 527 | 24 |
| HCl | 563 | 538 | 25 |
| HI | 628 | 598 | 30 |
| $H_2C=CH_2$ | 680 | 651 | 29 |
| $H_2O$ | 697 | 665 | 32 |
| $H_2S$ | 712 | 681 | 31 |
| $H_2Se$ | 717 | 685 | 32 |
| $H_2C=O$ | 718 | 687 | 31 |
| $H_2Te$ | 736 | 703 | 33 |
| $AsH_3$ | 750 | 715 | 35 |
| $CH_3NO_2$ | 750 | 718 | 32 |
| $C_6H_6$ | 758.5 | 730.5 | 28 |
| $CH_3OH$ | 761 | 728 | 33 |
| $CH_3-C\equiv N$ | 787 | 755 | 32 |
| $PH_3$ | 789 | 753 | 36 |
| $(CH_3)_2O$ | 804 | 771 | 33 |
| $(CH_3)_2C=O$ | 823 | 790 | 33 |
| $(CH_3)_2S$ | 839 | 807 | 32 |
| $NH_3$ | 853.5 | 818 | 35.5 |
| $(CH_3)_2NCHO$ | 884 | 852 | 32 |
| $(CH_3)_2SO$ | 884 | 851 | 33 |
| $CH_3NH_2$ | 896 | 861 | 35 |
| $C_5H_5N$ | 924 | 892 | 32 |
| $(CH_3)_3N$ | 942 | 909 | 33 |
| $(CH_3)_3P$ | 950 | 917.5 | 32.5 |
| $(CH_3)_2N-(CH_2)_3-N(CH_3)_2$ | 1021 | 969 | 52 |
| NaOH | 1036 | — | — |
| CsOH | 1122 | ... | — |
| I$^{-c}$ | 1315 | 1294 | 21 |
| $Na_2O$ | 1375 | — | — |
| $Cs_2O$ | 1442 | — | — |

[a]From reference 53 unless stated otherwise. Standard state: see reference 50.

[b]Calculated from $\Delta_f H°$ values D. J. Wagman, W. H. Evans, V. B. Parker, R. H. Schumm, I. Halow, S. M. Bailey, K. L. Churney, and R. L. Nuttall, The NBS Table of Chemical Thermodynamic Properties, *J. Phys. Chem. Ref. Data, Vol. 11*, Suppl. 2 (1982).

[c]The conjugate acid HI is the most acidic compound in Table 3.

## TABLE 3

Some Gas-Phase Acidities; Thermodynamic Data[a] in kJ mole$^{-1}$ for Reaction 10: $AH \rightarrow A^- + H^+$

| AH | $\Delta H^\circ_{acid}$ | $\Delta G^\circ_{acid}$ | $T \Delta S^\circ_{acid}$ |
|---|---|---|---|
| HI | 1315 | 1294 | 21 |
| CCl$_3$COOH | 1338 | 1309 | 29 |
| CF$_3$COOH | 1351 | 1324 | 27 |
| HBr | 1354 | 1331 | 23 |
| HNO$_3$ | 1358 | 1330 | 28 |
| H$_2$Te[b] | 1386 | 1360 | 26 |
| HCl | 1395 | 1372 | 23 |
| CH$_2$(CN)$_2$ | 1405 | 1373 | 32 |
| H$_2$Se[c] | 1434 | 1408 | 26 |
| HCOO$H$ | 1445 | 1416 | 29 |
| CH$_3$COO$H$ | 1457 | 1427 | 30 |
| PhO$H$ | 1461 | 1432 | 29 |
| HCN | 1469 | 1438 | 31 |
| H$_2$S | 1470 | 1443 | 27 |
| CH$_3$NO$_2$ | 1491 | 1463 | 28 |
| LiH | 1492 | 1470 | 22 |
| CH$_3$S$H$ | 1493 | 1467 | 26 |
| AsH$_3$[d] | 1497 | 1465 | 32 |
| HCON$H_2$ | 1506 | 1476 | 30 |
| CH$_3$COCH$_3$ | 1544 | 1514 | 30 |
| PH$_3$ | 1552 | 1520 | 32 |
| HF | 1554 | 1530 | 24 |
| CH$_3$CN | 1560 | 1528 | 32 |
| CH$_3$SOCH$_3$ | 1563 | 1533 | 30 |
| *tert*-BuO$H$ | 1572 | 1544 | 28 |
| HC≡CH | 1576 | 1542 | 34 |
| PhC$H_3$ | 1593 | 1564 | 29 |
| CH$_3$O$H$ | 1597 | 1570 | 27 |
| H$_2$O | 1635 | 1607 | 28 |
| CH$_2$=CH—C$H_3$ | 1640 | 1612 | 28 |
| (CH$_3$)$_2$N$H$ | 1658 | 1628 | 30 |
| H$_2$ | 1675 | 1649 | 26 |
| CH$_3$N$H_2$ | 1687 | 1656 | 31 |
| NH$_3$ | 1689 | 1657 | 32 |
| CH$_4$ | 1743 | 1709 | 34 |
| CH$_3$—CH$_3$ | 1761 | 1725 | 36 |

[a] From reference 63 unless stated otherwise. Standard state: see reference 50. Selected values correspond to the best thermochemical values or the best reanchored equilibrium data.

[b] From reference 60.

[c] $\Delta H^\circ_{acid}$ in reference 60; $\Delta S^\circ$ evaluated using the isoelectronic approximation (see text).

[d] From ICR measurements, J.-F. Gal and P.-C. Maria, unpublished results.

rotational degrees of freedom) as for the acidity of hydrogen halides and the basicity of rare gases. To a lesser extent, this is also the case for benzene. On the other hand a loss of symmetry on deprotonation induces a larger $T \Delta S°$ value; see, for example the acidity of methane and ethane and the basicity of phosphine and ammonia. A much larger entropy term arises when the deprotonation corresponds to a striking gain in internal rotational degrees of freedom. The following reaction is a typical example:

$$\underset{\substack{\text{CH}_2 \quad \text{CH}_2 \\ \text{CH}_2}}{\text{Me}_2\text{N}}\overset{\text{H}}{\diagup}\text{NMe}_2 \longrightarrow \text{Me}_2\text{N}\underset{\text{CH}_2}{\diagup}\overset{\text{CH}_2 \quad \text{CH}_2}{\diagdown}\text{NMe}_2 + \text{H}^+ \qquad (21)$$
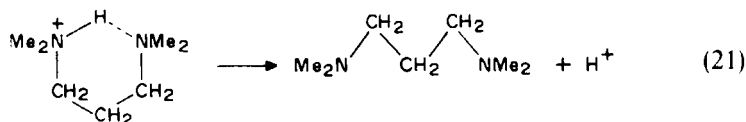
For the vast majority of organic compounds, the above-mentioned entropy variations are unimportant, and Equations 10 and 11 can be considered as isoentropic reactions. This approximation will hold even better within families.

In this context, enthalpies and Gibbs free energies become of equivalent status for the discussion of protonic acidities and basicities.

In the gas phase, where no external stabilization of neutrals or charged species may occur, the deprotonation processes (Equations 10 and 11) are governed only by intrinsic structural effects.

Following an order of increasing complexity of the molecule, the elements of structure at the origin of these effects are:

• The nature of the atom bound to the proton.
• The hybridization of this atom and its extension, the functionality.
• The nature of the substituent(s) in conjunction with the nature of the transmitting framework.

The simple hydrides have been choosen as model compounds for a thorough discussion of the first point (1 g) and the main conclusion was that no one factor is predominent in their acid–base behavior. The electronegativity stabilizes electron pairs both in anions and neutrals.

One might expect that an increase in electronegativity would induce an increase in acidity and a decrease in basicity. This is observed within *periods*: the acidity increases from $CH_4$ to HF and the basicity decreases from $NH_3$ to Ne. In contrast, within a *group* this explanation fails for all the acidities.

Electron repulsion, which destabilizes small anions ($^-CH_3$, $^-NH_2$, $^-OH$, and $^-F$ in particular, as indicated by their relatively small ionization potentials) was invoked as an effect counteracting electronegativity. Moreover, a smaller size of the atom bound to the proton favorizes a better orbital overlap with the

proton. These two effects, orbital overlap and electron repulsion, prevail over electronegativity within a given group and explain why acidity increases with each increase in period number.

In the case of basicities, the electronegativity appears to be the major effect even within groups, except for the group 15 hydrides ($NH_3$, $PH_3$, $AsH_3$). Taft has proposed an explanation based on the number and the relative importance of resonance structures stabilizing the conjugate acids (11 g). The reader will note that the favored orbital overlap with the smaller atoms runs in the same direction.

The next intrinsic structural effect after the nature of the atom is its hybridization, which induces changes in electronegativity, thus affecting acidities and basicities. In molecules, the elements C, N, and O present three types of hybridization: $sp^3$, $sp^2$, and $sp$. Their electronegativities increase with the $s$ character of the hybride $\sigma$-orbitals (65). Therefore, an increase in $s$ character is expected to increase acidity and to decrease basicity. The data of Tables 4 and 5, for series of homologous compounds, confirm this expectation.

In the hydrocarbon series (Table 4) there is a 62 kJ mole$^{-1}$ increase in acidity on going from $C_2H_6$ to $C_2H_4$ and 123 kJ mole$^{-1}$ from $C_2H_4$ to $C_2H_2$. These variations parallel almost exactly the variations in percent $s$ character (8% from $sp^3$ to $sp^2$ and 17% from $sp^2$ to $sp$) or in the Mulliken electronegativities (65b).

A similar relationship does not hold quantitatively for basicities (Table 5). In particular, the $sp^2$ hybridized nitrogen and oxygen bases are too close in $PA$ from the corresponding $sp^3$ bases. This may be accounted for by the extrastabilizing effect of the resonance structures represented in the following scheme:
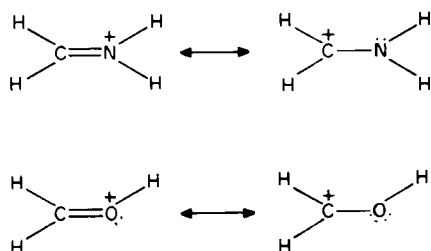


The extra stabilization of the conjugate acid reinforces the basicity. Evidently, resonance structures involving $\pi$-electrons cannot be drawn for protonated methylamine and methanol. In the case of $sp$ hybridization the linearity of the conjugate acids renders the contributing structures **1b** and **2b** (following scheme), where $sp^2$ hybridization is expected for nitrogen and

TABLE 4

Effect of Hybridization on $\Delta H^{\circ}_{acid}$ in kJ mole$^{-1}$

| AH | $\Delta H^{\circ}_{acid}{}^{a}$ |
|---|---|
| $H_3C-CH_3$ | 1761 |
| $H_2C{=}CH_2$ | 1699 |
| $HC{\equiv}CH$ | 1576 |

$^a$Experimental values from reference 63.

TABLE 5

Effect of Hybridization on $PA$ in kJ mole$^{-1}$

| B | $PA_{exptl}{}^{a}$ | $PA_{calc}{}^{b}$ |
|---|---|---|
| $H_3C-NH_2$ | 896 | 900 |
| $H_2C{=}NH$ | 845 | 869 |
| $HC{\equiv}N$ | 717 | 706 |
| $H_3C-OH$ | 761 | 755 |
| $H_2C{=}O$ | 718 | 710 |
| $:C{\equiv}O:{}^{c}$ | $456^d$ | $430^e$ |
|  | $427^f$ | 425 |

$^a$From reference 53, unless stated otherwise.
$^b$Large basis set ab initio calculations, including electron correlation and zero-point energy corrections, from reference 66a unless stated otherwise.
$^c$Oxygen protonation.
$^d$Estimated from a correlation between $O_{1s}$ binding energies and experimental $PA$ values; reference 66b.
$^e$From reference 66c.
$^f$From reference 66d.

oxygen, of less importance:

$$H-C{\equiv}\overset{+}{N}-H \leftrightarrow H-\overset{+}{C}{=}\overset{\cdot\cdot}{N}-H$$

$$\text{1a} \qquad\qquad\qquad \text{1b}$$

$$:C{\equiv}\overset{+}{O}-H \leftrightarrow :\overset{+}{C}{=}\overset{\cdot\cdot}{O}-H$$

$$\text{2a} \qquad\qquad \text{2b}$$
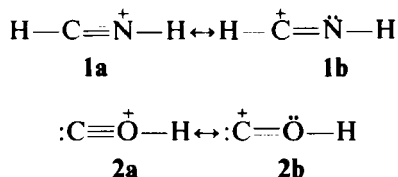
Should a general theory of substituent effects be available, this would permit the prediction, from the behavior of simple molecules discussed above, of the behavior of more complex structures (particular organic functions and their corresponding families). Such a theory for the treatment of gas-phase

acidities and basicities has been proposed by Taft and Topsom (1h). In their model substituent effects are of four primary kinds:

1.  The electronegativity effect $\chi$, earlier referred to as the "sigma-inductive through bond effect," originates from the difference in electronegativity between the substituent and the atom to which it is attached. Any effect of this kind, beyond this atom, is probably negligible.
2.  The field effect $F$ corresponds to an electrostatic (through space) interaction between the substituent dipole and the dipolar or charged reaction center.
3.  The resonance effect $R$ arises from charge transfer through $\pi$ systems of unsaturated molecular frameworks.
4.  The polarizability effect $P$ is also an electrostatic effect of the dipole-induced dipole or charge-induced dipole type arising from the interaction between the reaction center and the polarizable substituent.

These four primary effects have been parameterized by the $\sigma$ type ($\sigma_\chi, \sigma_F, \sigma_R$, and $\sigma_\alpha$, respectively) substituent constants to be used in multilinear regression treatments. In the systems studied so far, no statistically significant dependencies on *substituent* electronegativity parameters, $\sigma_\chi$, were found.

The field and resonance parameters $\sigma_F$ and $\sigma_R$ are based respectively on the $\sigma_I$ and $\sigma_R^\circ$ parameters derived from measurements in apolar solvents. Because of its long-range action, the field effect is always present except for series restricted to alkyl substitutions. The resonance effect will act only when an unsaturation is present between the substituent and the reaction center and is inherently dependent on the electron demand of the reaction center (67). The general $\sigma_R$ scale applies when a $\pi$-donor substituent stabilizes an electron-deficient cationic center (basicity enhancement) or when a $\pi$-acceptor substituent stabilizes an electron-rich anionic center (acidity enhancement). If a $\pi$-acceptor substituent is associated with an electron-deficient center (a "no blood from a turnip" situation), then $R \sim 0$. If a $\pi$-donor substituent is associated with an electron-rich center, $R$ is dramatically reduced. In series where this situation occurs, a special treatment is warranted.

As regard to the comparison between gas phase and solution properties undertaken in this chapter, it is worth noting that intrinsic $\sigma_F$ and $\sigma_R$ may need to be modified for solution studies as the result of specific substituent solvation.

Contrary to the $F$ and $R$ effects, the polarizability effect $P$ depends only on the distance between the substituent and the reaction center without any restriction tied to their nature.

The idea that effects of alkyl substituents in the gas phase arise from their polarizability was put forth by Brauman and Blair (68). In the early 1970s more data became available and quantitative interpretations of the polarizability effect were arrived at by using empirical approach (69), simple electrostatics (70), or ab initio calculations (71).

In fact, the comprehensive $\sigma_\alpha$ scale of directional substituent polarizability parameters was also obtained from ab initio calculations (1h, 72). On the other hand, an empirical substituent parameter, the so-called effective polarizability, $\alpha_d$, taking into account the attenuation of polarizability with distance, was devised by Gasteiger and Hutchings to be used, in conjunction with the residual electronegativity, to describe acidities and basicities in the gas phase (73). It is interesting to note that the concept of polarizability as described here did not emerged from solution studies. When an ion is embedded in a medium of high solvating power and of high relative permittivity, the charge is diluted in the attached solvent molecules and the resulting weakened charge-induced dipole stabilization is further damped.

Without the light shed by the gas-phase studies on this matter it was difficult to unravel the various effects of electrostatic origin affecting the proton transfer processes in solution.

As discussed later in this chapter, the polarizability effect prove to be an essential term for the interpretation of the differences between substituent effects in the gas phase and in solution.

## B. Metal Cation Binding

### 1. Methodology

By analogy with the basicity toward proton (Equation 11), the basicity toward monocharged metal ions, $M^+$, is defined through the thermodynamics of the reaction:

$$BM^+ \rightarrow B + M^+ \qquad (22)$$
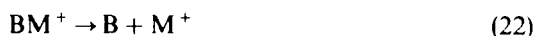
The enthalpy change for this reaction has been sometimes symbolized by $D(B\text{---}M^+)$, but the corresponding Gibbs free-energy change was never given a particular symbol. For the sake of homogeneity we will use hereafter $M^+(A)$ (metal-ion affinity) and $M^+(GB)$ (metal–ion gas basicity) for $\Delta H^\circ$ and $\Delta G^\circ$, respectively.

The estimation of entropy contributions needs more assumptions (74) than in the case of protonation and the calculation of $M^+(GB)$ from $M^+(A)$ or vice versa is less reliable than in the case of $GB$ and $PA$. This drawback along

with the paucity of absolute anchor points render the construction of absolute scales of metal–ion affinities more risky.

In the present state of knowledge, it is advisable to use experimental relative $M^+(GB)$ ladders (except when relative or absolute $M^+(A)$ are experimentally available) (75) obtained from metal–ion transfers:

$$B_1M^+ + B_2 \rightleftarrows B_1 + B_2M^+ \tag{23}$$
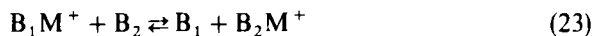
The basic principles and techniques of equilibrium constants determination are similar to those used for proton transfer studies. It will be noted that in a few favorable cases van't Hoff plots from variable-temperature HPMS measurements allow absolute $M^+(A)$ to be directly established.

The metal cations involved in Reactions 22 and 23 have been generated by

- Electron ionization of volatile metal complexes (76, 77) in ICR studies.
- Thermoionization. This method was successfully applied for the generation of alkali metal cations in both HPMS (78) and ICR (79) or FT–ICR (80).
- Laser volatilization–ionization (81) in ICR (82, 83), and FT-ICR (186a) studies.

## 2. Scales

Among the various alkali metal cations studies the basicity scale toward $K^+$ completed in 1984 by Kebarle and coworkers (78) is interesting for at least two reasons: (1) although measurements were done for only 18 compounds, the structural variations are representative of most of the common organic functionalities; and (2) the HPMS technique utilized for this study allowed a thorough thermodynamic analysis of the $K^+$–base interaction to be obtained. Moreover, the basicity parameters $K^+(A)$ and $K^+(GB)$ were put on absolute scales. Some values are given in Table 6.

The potassium ion affinities are always much smaller than the corresponding $PA$ values, as shown by a rapid inspection of data in Table 6 and in Table 2.

The $K^+(A)$ range spans $75\,kJ\,mole^{-1}$ (with an estimated uncertainty on each value of about $\pm 4\,kJ\,mole^{-1}$) from $H_2O$ to $(CH_3)_2SO$. This is only 40% of the $PA$ difference between the same compounds. More impressive is the comparison of differences in $K^+(A)$ and $PA$ from $H_2O$ to $(CH_3)_3N$ (13 and $245\,kJ\,mole^{-1}$, respectively). It appears clearly that the basicity orders toward $H^+$ and $K^+$ are very different.

The entropy term corresponding to the $K^+$–base interaction brings a

TABLE 6

Some Gas-Phase Basicities toward $K^+$; Thermodynamic Data[a]
in kJ mole$^{-1}$ for the Reaction $BK^+ \rightarrow B + K^+$

| B | $K^+(A)$ | $K^+(GB)$ | $T \Delta S^\circ$ |
|---|---|---|---|
| $H_2O$ | 71 | 46 | 25 |
| $NH_3$ | 75 | 50 | 25 |
| $C_6H_6$ | 79 | 50 | 29 |
| $(CH_3)_3N$ | 84 | 54 | 30 |
| $(CH_3)_2O$ | 88 | 54 | 34 |
| $C_5H_5N$ | 88 | 63 | 25 |
| $(C_2H_5)_2O$ | 92 | 63 | 29 |
| $CH_3CN$ | 100 | 75 | 25 |
| $(CH_3)_2CO$ | 109 | 79 | 30 |
| $HCON(CH_3)_2$ | 130 | 96 | 34 |
| $(CH_3)_2SO$ | 146 | 105 | 41 |

[a]From reference 78d. Standard state: see reference 50.

much larger relative contribution to the Gibbs free energy of Equation 22 as compared to the proton attachment. In addition the $T \Delta S^\circ$ term of $K^+$ attachment shows larger variations which seem to depend roughly on the strength of the interaction. As a consequence, the Gibbs free-energy scale appears to be shrunken as compared to the enthalpy scale.

More precise *relative* Gibbs free-energy scales were established for various metal ions (76, 79, 80, 82, 83, 185) via Equation 23 from ICR measurements. For three metal ions, $Li^+$, $Al^+$, and $Mn^+$, large data sets are available. A compendium of the corresponding $M^+(GB)$ scales is given in Table 7, where the bases are arranged in order of increasing $Li^+(GB)$.

As expected, this order follows roughly the $K^+(GB)$ order, but the $Li^+$ ladder is more discriminant because of the greater precision of its data (uncertainty $< 1$ kJ mole$^{-1}$) for a similar range. Metal ions $Li^+$, $Al^+$, and $Mn^+$ have different electronic structures and therefore behave differently toward the various functionalities.

The basicity order toward $Al^+$ and $Mn^+$ differs from the $Li^+$ order. One of the most striking example is $CH_3CN$, which, compared to the nitrogen bases, can be either a stronger or a weaker base depending on the metal ion. Analogous comparisons may be done for oxygen bases.

## C. Organometallic and Organic Cation Binding

Gas-phase interactions between some cations involving elements of the group 14 (C, Si, Ge, and Sn) and electron-donor molecules have been

TABLE 7

Gas Basicities toward Li$^+$, Al$^+$, Mn$^+$ for Representative Organic Molecules (Relative to H$_2$C=O)

$$BM^+ + H_2C=O \rightleftharpoons B + H_2C=OM^+$$

| | M$^+$(GB) in kJ mole$^{-1}$ | | |
|---|---|---|---|
| B | Li$^{+a}$ | Al$^{+b}$ | Mn$^{+c}$ |
| CH$_3$SH | $-20.9$ | — | $-3.7$ |
| (CH$_3$)$_2$S | $-8.8$ | — | 10.9 |
| H$_2$O | $-2.9$ | — | — |
| H$_2$CO$^d$ | 0.0 | 0.0 | 0.0 |
| HCN | 2.1$^e$ | — | 1.0 |
| C$_6$H$_6$ | 6.3$^e$ | — | 19.0 |
| CH$_3$OH | 13.0 | 26.8 | 10.2 |
| NH$_3$ | 16.3$^e$ | — | 20.1 |
| (CH$_3$)$_2$O | 16.7 | 45.6 | 17.6 |
| (CH$_3$)$_3$N | 23.0$^e$ | — | 38.7 |
| CH$_3$CHO | 26.8 | 36.4 | 18.2 |
| HCO$_2$CH$_3$ | 29.3 | 46.9 | 23.4 |
| (C$_2$H$_5$)$_2$O | 33.1 | 61.5 | 34.6 |
| CH$_3$CN | 36.0 | 38.5 | 30.6 |
| C$_5$H$_5$N | 40.2 | 73 $\pm$ 8 | — |
| CH$_3$CO$_2$CH$_3$ | 41.0 | 70.7 | 38.2 |
| (CH$_3$)$_2$CO | 41.4 | 64.0 | 37.6 |
| (CH$_3$)$_2$NCN | 56.9 | 90.4 | — |
| (CH$_3$)$_2$SO | 60.2 | — | — |
| HCON(CH$_3$)$_2$ | 64.4 | 115.9 | — |
| (CH$_3$O)$_3$PO | 67.8 | — | — |

$^a$From reference 80 unless stated otherwise.

$^b$From reference 83.

$^c$From reference 82b.

$^d$Reference compound. Absolute basicities in kJ mole$^{-1}$ (standard state: reference 50) Li$^+$(GB) = 118, Li$^+$(A) = 151(74); Mn$^+$(A) = 126(77). An ab initio calculation of the formaldehyde Al$^+$ complexation, including zero-point energy, gives 113 kJ mole$^{-1}$ (84).

sufficiently investigated to permit the construction of various basicity scales. The prime importance of the reactivity at carbon has prompted a number of studies devoted to the gas-phase reactions of bases with carbenium ions. The thermochemistry of these reactions leads to the evaluation of alkyl cation affinities. In particular, absolute methyl cation affinities (MCAs) (85) corresponding to the enthalpies of

$$ACH_3 \rightarrow A^- + CH_3^+ \tag{24}$$

$$BCH_3^+ \rightarrow B + CH_3^+ \qquad\qquad (25)$$

can be calculated by using $\Delta H^\circ$ or $PA$ values (86, 87).

Recently, relative MCAs have been derived from equilibrium measurements (HPMS and ICR) and used to complement the absolute MCA scale (87b). The known MCAs for neutral bases, B, span more than $300 \, kJ \, mole^{-1}$ from the inert gases to the alkylamines (roughly the same lower and upper limits as for the PA scale). Similarly to the $\Delta H^\circ_{acid}$ scale, the anion MCAs extend from $I^-$ to $CH_3^-$.

The thermochemical calculations lead to uncertainties regarding absolute MCAs of magnitudes similar to those of absolute $PA$ or $\Delta H^\circ_{acid}$ values. Even the relative MCAs may be in error by as much as $4 \, kJ \, mole^{-1}$ because of experimental difficulties (87).

Substituted methyl cation affinities may be established when thermochemical data are available. We think that a case being worth a more detailed study would be the trifluoromethyl cation $CF_3^+$ for which a very limited set of affinities is available (87a). This cation is isoelectronic with the classical Lewis acid $BF_3$, thoroughly studied in the condensed phase, and it would be interesting to search for relationships between the corresponding basicity scales.

Gas-phase bonding toward other cations of group 14 elements has been approached through studies of trimethyl derivatives. Quantitative scales have been established for $(CH_3)_3Si^+$ (88) and $(CH_3)_3Sn^+$ (89). The former scale includes only oxygen and aromatic hydrocarbon bases. The latter is slightly more extended and of broader applicability, including nitrogen and sulfur bases in addition to oxygen and carbon bases. Finally, a qualitative basicity order have been established for oxygen bases toward $(CH_3)_3Ge^+$ (90).

To our knowledge, $CH_3Hg^+$ is the only alkylmetal cation not involving group 14 elements for which a relative affinity ladder was established (91).

## D.   Anion Binding and Electron Affinities

Anions, $A^-$, can interact with electron deficient centers belonging to compounds that may be recognized as hydrogen bond donors (HBD) or Lewis acids [electron pair acceptors (EPA)], including compounds for which the electron-deficient center is a carbon atom. Both ICR and HPMS have been used to determine the thermochemical data pertaining to

$$(A \cdot HBD)^- \rightarrow A^- + HBD \qquad\qquad (26)$$

$$(A \cdot EPA)^- \rightarrow A^- + EPA \qquad\qquad (27)$$

TABLE 8

Literature References for Gas-Phase Acidity Scales of Neutral Molecules Relative to Anions

| Acid Type | F⁻ | Cl⁻ | Br⁻ | I⁻ | CN | RO⁻, RCOO | NO₂⁻ |
|---|---|---|---|---|---|---|---|
| HBD[a] | | | | | | | |
|   HX[b] | 94b | 94b | 94b | 94b | 94b | — | — |
|   ROH, RCOOH | 92b | 92 | — | 92b | 94d | 93 | . . |
| | 94a | 94c | | | | 95 | |
| | | 98b | | | | | |
|   Others[c] | 94a | 92b | — | — | 94d | — | — |
| | 98a | 94c | | | | | |
| | | 98 | | | | | |
| Lewis acids | 96b | 97a | — | — | 97c | — | 96a |
| | 97a,b | 98 | | | | | |
| | 98a | | | | | | |

[a]Hydrogen bond donors.
[b]X stands for halogens.
[c]Various NH, CH, and SH compounds.

The halogenides, cyanide, alkoxydes and carboxylates were the most thoroughly studied anions. The acidic partners involved in Reaction 26 are mainly hydrogen halides, alcohols, carboxylic acids and a few CH, NH, and SH compounds. The EPA acids in Reaction 27 are principally oxides, fluorides, and oxofluorides, as well as alkyl derivatives of the main group elements. The literature references (94–98) for the corresponding gas-phase acidity scales are sorted in Table 8, according to the nature of the interacting partners.

The electron affinity $EA$ is a fundamental molecular property directly related to the energy of the lowest unoccupied molecular orbital (99), which conditions the chemical reactivity toward nucleophiles or bases.

A molecule, M, bearing electron-withdrawing substituent(s) will have vacant orbitals of energy sufficiently low to accommodate an electron and give a stable M⁻ anion. Here, $EA(M)$ is taken as the enthalpy at 0 K for (51)

$$M^- \rightarrow e^- + M \qquad (28)$$

The detachment of the elementary negative charge from an anion is analogous in some respect to Reaction 27. In the "stationary electron" convention (52) and owing to the structural similarity of M and M⁻, $EA$ is usually equated to the enthalpy at 298 K for Process 28 (100). Most of the absolute entropies associated with Process 28 are relatively small (100), leading to another approximate equality between $EA$ and the Gibbs free energy. The subject has been reviewed in detail (99, 100). Recently, electron

transfer equilibria were measured by using HPMS or ICR and anchored to absolute $EA$ values (100). Electron transfer is directly or indirectly implied in several condensed-phase processes such as chemical or electrochemical redox reactions and the so-called charge-transfer complexations. Thus, comparisons between gas-phase $EA$s and quantities related to electron transfer in the condensed phase (half-wave potentials or electronic transition energies of charge-transfer complexes) may be enlightening.

The definitions of acidity and basicity when extended to single-electron acceptance and donation, respectively, as in the Usanovich theory (1f) reach such a degree of generality that almost every reaction is of the acid-base type (65b).

### E.   Cationic Hydrogen Bonds

As seen above, anions can interact with neutral HBD molecules via hydrogen bond formation (Reaction 26). The cationic counterpart of Reaction 26 corresponds to the interaction of a protonated $BH^+$ (a strong HBD) with a neutral HBA according to

$$BH^+ \cdots HBA \rightarrow BH^+ + HBA \qquad (29)$$

This equation implies that the proton affinity of B is larger than, or equal to, that of the HBA molecule.

If the HBA is the same compound as base B in $BH^+$, $BH^+ \cdots HBA$ is a symmetric proton-bound dimer. The experimental methods used to establish the thermochemistry of Reaction 29 rely again on ICR and HPMS. The vast majority of the studied proton-bound dimers, symmetric or unsymmetric, corresponds to nitrogen or oxygen basic sites in both B and the HBA partners. Other systems include also $\pi$ bases and sulfur compounds as HBA or compounds bearing polarized $CH^{\delta+}$ bonds as HBD sites (101). The corresponding thermochemical data for these systems can be found in the Keesee and Castleman compilation on clustering reactions (102). By keeping either $BH^+$ or the HBA constant, one can expect to build a hydrogen bond basicity or acidity scale, respectively.

The water molecule acting as an HBA toward $BH^+$ (103, 104) is an interesting case as it may be compared with the bulk hydration of $BH^+$.

Another scale uses acetonitrile as the reference HBA, where the cations are protonated ethers and carbonyls (105). An important finding of this study is that such a "solvation" by a single molecule of acetonitrile in the gas phase reproduces the diverse effects of molecular structure on oxonium ion solvation by bulk water. Limited basicity scales relative to $NH^+$ and $CH^{\delta+}$ acids concerning $\pi$ (carbon), oxygen, and nitrogen bases have been established (102, 103a, 107) and may be considered as useful starting points for correlation analysis studies of various BDPs.

Anionic and cationic hydrogen bonding has been often studied as the first step of the formation of clusters constituted by an ion surrounded by more than one "solvent" molecule. These experiments were designed to mimic the first solvation shell present in solution.

## IV.  CORRELATION ANALYSIS

"Acid–base concepts help *correlate* empirical observations."
—James E. Huheey

### A.  Routes to Relate Solution and Gas-Phase Behaviors

Any process in the gas phase relevant to this study may be related to the same process in solution by a thermodynamic cycle:

$$
\begin{array}{ccc}
A(g) & \xrightarrow{\Delta X^\circ (g)} & B(g) \\
\Big\downarrow {\scriptstyle \Delta_{solv} X_A^\circ} & & \Big\downarrow {\scriptstyle \Delta_{solv} X_B^\circ} \\
A(soln) & \xrightarrow{\Delta X^\circ (soln)} & B(soln)
\end{array}
$$
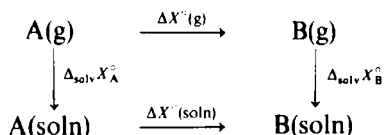
where A and B correspond to neutral or ionic reactants and products involved in the process used for the definitions of absolute or relative scales; $\Delta X^\circ$ stands for the change in either $H^\circ$, $G^\circ$, or $S^\circ$ thermodynamic functions; the subscript "solv" (solvation) corresponds to the transfer from the gas phase to the solution; and $\Delta X^\circ(soln)$ can be decomposed in an intrinsic gas-phase component and a differential solvation term:

$$\Delta X^\circ(\text{soln}) = \Delta X^\circ(g) + [\Delta_{solv} X_B^\circ - \Delta_{solv} X_A^\circ] \tag{30}$$

The differential solvation term quantitatively accounts for the variations of acidity or basicity order between the two phases. So far Equation 30 has been applied mostly to proton exchange in water or dipolar solvents such as DMSO.

This kind of reaction involves neutral molecules AH or B, ions $A^-$ or $BH^+$, and the proton. When Reactions 10 and 11 are involved in the above thermodynamic cycle, the $\Delta X^\circ$ values correspond to absolute quantities.

In this case the proton solvation being constant the variable differential solvation, between the neutral and the ion, accounts alone for the different acidity or basicity orders.

If the two members A and B of the cycle are referred to as "equilibrium partners," like those in Reactions 17 and 18, one obtains *relative* differential solvation quantities. Usually, the relative differential solvation quantities are referenced to a particular couple of neutral–conjugate ion of well-defined solvation behavior. To determine the contributions of the neutral and ionic

species to the differential solvation term one needs to know at least the solvation of one species.

For neutral molecules, $\Delta_{solv}X°$ can be calculated from experimental thermodynamic quantities of vaporization (or sublimation) and dissolution (6b, 15c, 108); various techniques involving vapor pressure, solubility, or calorimetric measurements are used for these determinations. In the case of water, group additivity schemes (109, 110) may be used to useful approximation for the estimation of such $\Delta_{solv}X°$ when experimental data are not available. Nevertheless, this approach gives accurate estimate only in the case of relatively simple monofunctional molecules. Then, $\Delta_{solv}X°$ for the ion may be calculated by difference. When compared to selected reference neutral conjugate ion couples, these solvation data can be discussed in the framework of particular structural effects on the nonspecific and specific interactions.

The effect of hydration on the basicity of the principal classes of organic compounds, mostly oxygen and nitrogen bases, has been studied in this way (1g). Pyridines represent the most thoroughly studied family for which the attenuation of electronic substituent effects by water (111a) and inhibition of solvation by steric effect (111b, 112) have been examined. The unique behavior of a family of enamino ketones was approached by using this method (113). The same kind of studies concerning the acidity — aliphatic alcohols in DMSO (114) and haloacetic acids in $H_2O$ (115) — demonstrates the prime importance of anion solvation in determining the acidity order in solution. Thermodynamic cycles have been constructed for the evaluation of the enthalpies of transfer of the protonated and deprotonated forms of $\alpha$-amino acids from the gas phase to aqueous solution (116).

Although the methodology leads at once to an *empirical* value for the $\Delta_{solv}X°$ factor for ions, the need to combine a variety of sophisticated techniques generally not available in the same laboratory has limited its scope to a few cases.

It was understandable that other approaches have been proposed to evaluate ion solvation. Several theoretical models have been used in this area, principally for ion hydration:

- The continuum methods based on dielectric solvation (117).
- The Monte Carlo and molecular dynamic simulations, performed on fairly large numbers of solvent molecules interacting with an ion according to a given intermolecular potential (118).
- The "supermolecule" approach (119), in which quantum calculations, in general high-level ab initio, are used to evaluate the interaction energy between an ion and a few surrounding molecules. With the present computer technology, this approach is time-consuming and limited to small clusters.

Although these calculations do not lead to the exact bulk solvation energies, they provide key insights into the origin of solvent effects on proton transfer equilibria (1g, 120).

The results of the supermolecule approach can be compared to the experimental stepwise gas-phase solvation. Thermodynamic investigations of step-by-step attachment of solvent molecules to ions were pioneered by Kebarle and coworkers (121). Using analogous HPMS methods, Castleman (102,122), Hiraoka (123), Meot-Ner (101,124), and their coworkers are accumulating data on various positive or negative ion–solvent systems.

In the context of the comparison with the condensed phase, it is worth mentioning the gas-phase solvation by water, $CH_3CN$, DMSO, and alcohols of metal cations and halide anions (121–123). Evidently, a large part of these works has also been devoted to protonated organic bases as well as $H_3O^+$ and $NH_4^+$ (102, 124). The results of these studies indicate that only a small number of solvent molecules is responsible for most of the behavior of ions in solution (1g, 6d).

Even the attachment of only one molecule of "solvent" to a bare cation has the significant effect to reduce the differences between gas-phase and solution behaviors (1g, 105).

## B.  Empirical Relationships

The approaches discussed above treat the problem of ion (or molecule) solvation, either bulk or discrete, case by case. So far these exhaustive analysis have been reserved to compounds of typical behavior.

A complementary approach applicable to larger sets of compounds is the search of quantitative relationships between gas phase and solution phase acidity or basicity parameters. In fact, the chemist expects to observe some regularities when comparing similar systems, and the principles of correlation analysis (125) will be applied here for this purpose.

The simple two-dimensional plot of an acidity or basicity dependent property against an other is a powerful visual aid for the analysis of their analogies and differencies. When interpreted, such a plot is also useful from a pedagogical point of view. Most of the discussions that follow are based on the analysis of plots relating various solution and gas phase acidity or basicity dependent properties to gas-phase proton transfer quantities.

### 1.  Solution versus Gas Phase

**a.  Proton Transfer and Electron Transfer.** The early attempt to relate basicities in aqueous solution, $\Delta G°(aq)$ with $GB$, shows a cloud-shaped plot, Fig. 2 in reference 6a. The elongated cloud shows however some tendency

of the two BDPs to correlate. For example, amines are stronger bases than oxygen bases, ketones, and ethers in the two media. The leveling effect of water is also observed for the strong bases. Even when restricted to oxygen bases, a large scatter is observed, indicating that aqueous medium effects on oxonium ion formation are relatively large and highly specific (105).

Further, Taft has shown that there is very little resemblance between $GB$ and the Gibbs free energy of hydrogen bond formation $\Delta G°_{HB}$ with $p$-fluorophenol in tetrachloromethane; see Fig. 3 in reference 6a.

The same kind of scatter is also observed for acidities when plotting $\Delta G°(aq)$ or $\Delta G°(DMSO)$ versus $\Delta G°_{acid}(1g, h)$, although restricted subclasses such as the $XCH_2OH$ family in water (126) can exhibit a linear trend.

Analogous results are observed when the enthalpy of ionization of AH acids in water (15a, 115, 127–130), $\Delta H°(aq)$ is plotted against $\Delta H°_{acid}$ (63). Within the cloud of points some degree of correlation can be distinguished for the *meta*- and *para*-substituted phenols as well as for some aliphatic acids, in particular acetic and halogenoacetic. The benzoic acids give a nearly horizontal line due to their almost constant $\Delta H°(aq)$.

For the approximate linear relationships, mentioned above for the solution versus gas-phase thermodynamic quantities, the slopes are invariably much less than one. Large attenuation of the substituent effect on the basicity in water for alkylamines (131) and pyridines (6a) have also been observed. In general, the structural effects are attenuated by a factor of 3–10 on going from the gas phase to the solvating media.

Nevertheless, Taft and coworkers showed that the basicities of large aromatic hydrocarbons $\Delta G°(aq)$ versus $GB$ are linearly related with a slope close to one (132). The unsaturated hydrocarbons (containing no heteroatom) are nonspecifically solvated. These hydrocarbons give highly charge-delocalized cations that are also nonspecifically solvated because of the absence of exposed atomic sites with appreciable positive charge. Negligible specific interactions, such as hydrogen bonding to C—H, are expected for such cation class. It was concluded that the variable $P$ and $R$ effects are nearly the same in the gas phase and in water, as the differential solvation between B and BH$^+$ (see Equation 30) is almost constant. For this hydrocarbon family the *relative* differential solvation is nil. In turn, any deviation from the reference hydrocarbon line is a measure of the relative differential solvation (6c).

These results have led to the search for a similar reference line concerning the acidity. There are several limitations to measurement of weak acidities in water. On the other hand, the use of DMSO allows the coverage of a wide range of representative structures (17a). Comprehensive sets of $\Delta G°(DMSO)$ (17) and $\Delta H°(DMSO)$ values (18) have been reported.

As shown on Fig. 1, $\Delta G°(DMSO)$ of large unsaturated hydrocarbons exhibits a good linear ralationship of unit slope with the gas phase $\Delta G°_{acid}$. On
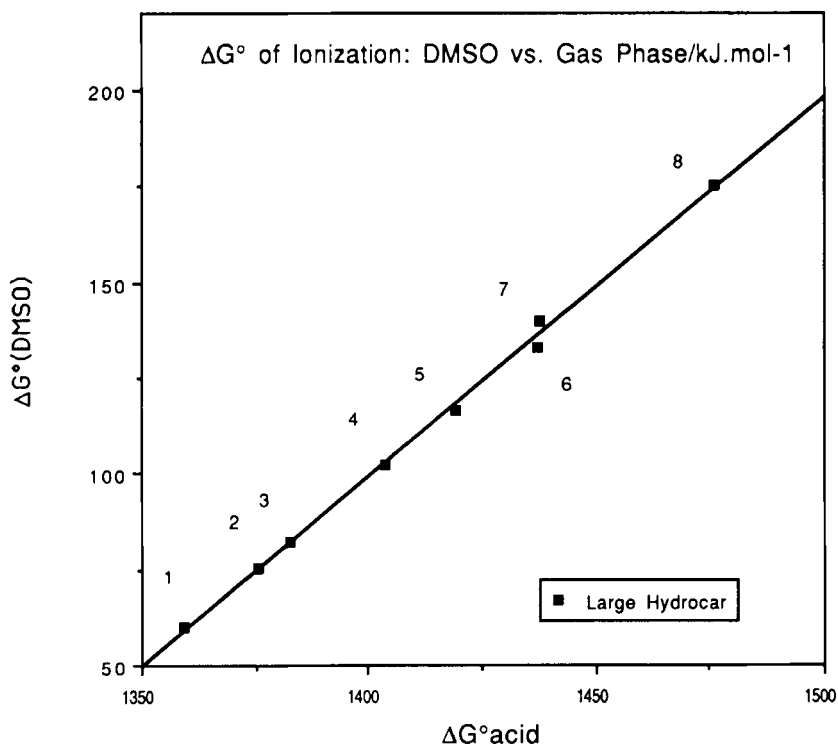
**Figure 1** Plot of DMSO versus gas-phase Gibbs free energies of ionization at 298 K in kJ mole$^{-1}$ for conjugated hydrocarbons giving highly charge dispersed carbanions; increasing $\Delta G°$'s correspond to decreasing acidities [$\Delta G°(DMSO) = (0.989 \pm 0.020) \Delta G°_{acid} - 1284.6; n = 8$, $r = .999$, sd = 2.1 kJ mole$^{-1}$; numbering: 1—fluoradene, 2—1,3-diphenylindene, 3—2,5-diphenylcyclopentadiene 4—9-phenylfluorene, 5—9-neopentylfluorene, 6—9-isopropylfluorene, 7—9-tertiobutylfluorene, 8—triphenylmethane]. The unit slope shows that there is a constant differential solvation between the anion and the corresponding neutral. Data sources: R. W. Taft and F. G. Bordwell, personal communication; see reference 17.

deprotonation, these compounds generate charge-delocalized anions. The absence of heteroatomic sites does not allow specific solvation. Similar to the case of basicity, a constant differential solvation between the ion and the corresponding neutral lead to very close structural effects on acidity in the gas phase and in solution.

Specific differential solvation leads to deviations from the reference line (Fig. 2). On deprotonation, hydrides of the second-row elements (CH$_4$, NH$_3$, H$_2$O, and HF) give small, highly charge-localized anions. Ion–dipole interactions with DMSO (17) are predicted to produce large solvation
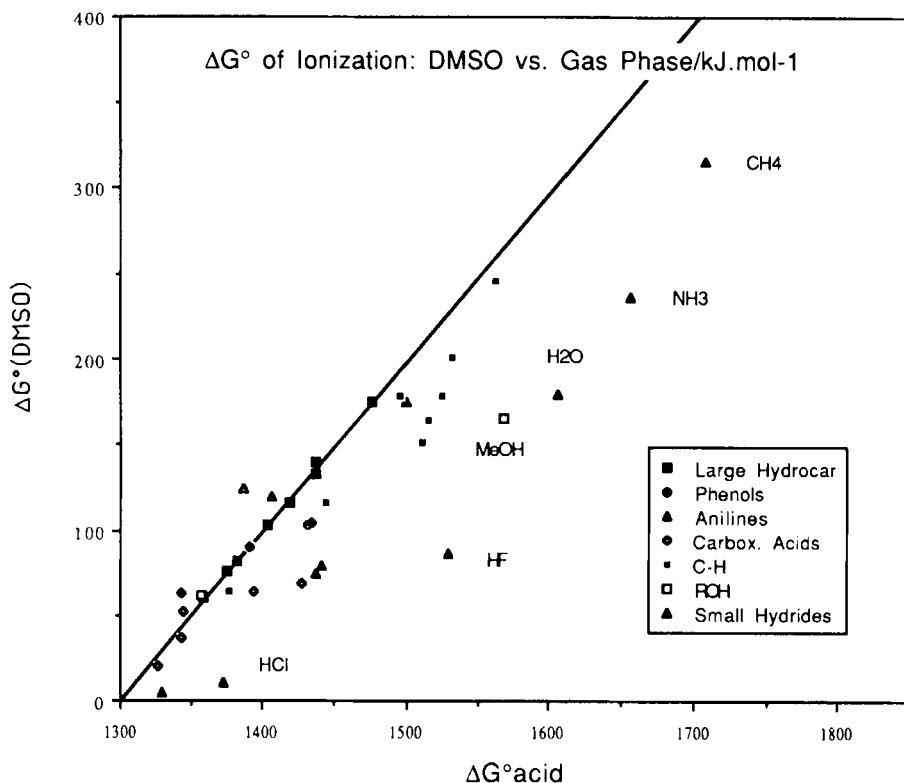
**Figure 2** DMSO versus gas-phase Gibbs free energies of ionization at 298 K in kJ mole$^{-1}$. The reference line is defined in Figure 1. Downward deviations correspond to enhanced acidity in DMSO. Data sources: R. W. Taft and F. G. Bordwell, personal communication; see reference 17.

energies. As the neutral solvation is relatively constant, the deviations toward enhanced acidities in DMSO (downward from the reference line) are largely attributable to the anion solvation alone. The acidity enhancement by DMSO follows the order of increased anion solvation:

$$F^- > OH^- > NH_2^- > CH_3^-$$
$$F^- > Cl^- > Br^-$$
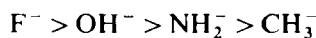
Larger acidic organic molecules are generally strong HBDs and give more or less delocalized anions. Therefore, some compensation occurs

between the neutral solvation and the anion solvation, leading to smaller deviations. This is the case for phenols, anilines, and carboxylic acids. In a few cases we observe deviations in the direction of a decreasing acidity in DMSO (upward from the reference line). The corresponding compounds are anilines or phenols bearing electron-withdrawing substituents. This kind of substitution leads to larger HBD strengths (larger neutral solvation) and to an extension of the charge delocalization in the anions (weaker ion solvation) to a point where there is a crossing of the reference line, that is, a sign change for the relative differential solvation term. This remarkable departure from the usual behavior has been also reported for the water versus gas-phase basicities of some enamino ketones (113).

The availability of enthalpies of acid ionization in DMSO (18), $\Delta H^\circ$(DMSO) values allows also the comparison with the corresponding gas-phase enthalpies, $\Delta H^\circ_{acid}$ values. Although there are less data than for the Gibbs free energies, qualitatively similar conclusions can be drawn from a plot of $\Delta H^\circ$(DMSO) against $\Delta H^\circ_{acid}$ (Fig. 3).

For four large hydrocarbons a line of nearly unit slope (0.9) is also found, and the same trend in the deviations is observed. This is not unexpected since there is a tendency for $\Delta H^\circ$(DMSO) and $\Delta G^\circ$(DMSO) to correlate. Nevertheless, entropic effects due to specific solvation (18) attributed in part to solvent electrostriction around charge-localized ions preclude the establishment of a unique family independent isokinetic relationship. Aliphatic alcohols represent an interesting case of acidity-order reversal when going from the gas phase to the solution.

From the enthalpies of ionization, Arnett et al. have analyzed the origins of this reversal by constructing a thermodynamic cycle as shown at the beginning of this section. They showed that the *solvation* of aliphatic alkoxide ions *increases* ($\Delta_{solv}H^\circ_{RO^-}$ more negative) as the size of the alkyl portion is made smaller (114), down to OH$^-$.

A visual inspection of Fig. 3 shows that the downward deviations from the reference line (relative differential solvations) for the aliphatic alcohols and water follow the same order. The small range of the $\Delta_{solv}H^\circ_{ROH}$ values in DMSO (114) explains the parallel variations between the $\Delta_{solv}H^\circ_{RO^-}$ values and the corresponding relative differential solvation enthalpies. In the gas phase, large polarizable alkyl groups intrinsically stabilize anions (and cations) by charge-induced dipole interactions and increase acidity.

The decreased acidity of large aliphatic alcohols in solution does not result from an electron-releasing "alkyl inductive" effect, but from a decreased anion solvation. The decrease is large enough to dominate the small $P$ effects that are present in solution.

On the contrary, changing $CH_3$ for electron withdrawing groups such as $CF_3$ leads to the same acidity order in both phases. In this subclass of alcohols,
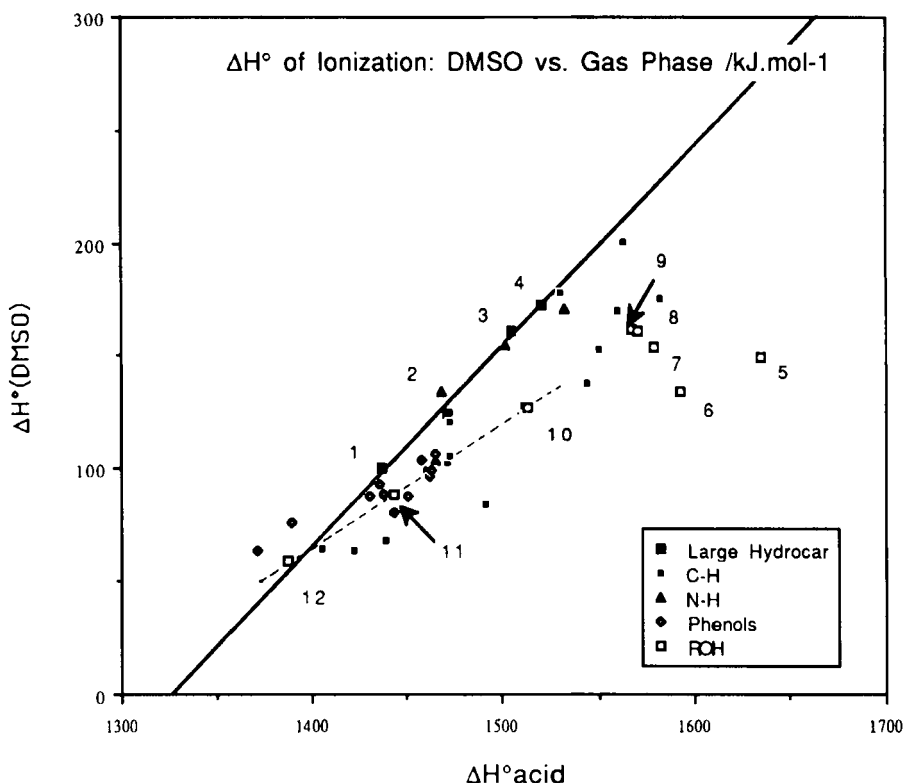
**Figure 3**   DMSO versus gas-phase enthalpies of ionization at 298 K in kJ mole$^{-1}$. Increasing $\Delta H^{\circ}$ values correspond to decreasing acidities; the solid line is defined for large hydrocarbons [$\Delta H^{\circ}$(DMSO) = (0.890 ± 0.062) $\Delta H^{\circ}_{acid}$ − 1180.1; $n = 4$, $r = .995$, sd = 4.1 kJ mole$^{-1}$]. The reversal in the acidity order appears for the aliphatic alcohols 6, 7, 8, and 9. The broken line shows up the parallelism of acidities for the CF$_3$-substituted alcohols 10, 11, and 12. (Numbering: 1—9-phenylfluorene, 2 - fluorene, 3—triphenylmethane, 4—diphenylmethane, 5—water, 6—methanol, 7—ethanol, 8—isopropanol, 9—tert-butanol, 10—2,2,2-trifluoroethanol, 11   hexafluoroisopropyl alcohol, 12—perfluoro-tert-butyl alcohol.) Data sources: $\Delta H^{\circ}$(DMSO), reference 18; $\Delta H^{\circ}_{acid}$, reference 63.

$F$ (field) is the main substituent effect acting in the same direction in the gas phase and (although somewhat attenuated) in solution. A part of this attenuation is attributed to the dielectric permittivity of the solvent. Another part of the attenuation of the CF$_3$ effect arises from the increased stabilization of neutrals by hydrogen bonding and from the correlatively weaker stabilization of anions. Similarly, the $F$ contribution to substituent effect on the basicity of dimethylamines is attenuated in water by a factor of 2 (133a). The corresponding $P$ effect is much more attenuated by the solvent (DMSO

$> CH_3CN > H_2O$) (133b). Some degree of correlation is seen on Fig. 3 for the enthalpies of ionization of phenols. This was already mentioned for the Gibbs free energies of ionization.

The substituent effects on the acidities of *meta-* and *para-*substituted phenols have been scrutinized by Taft and coworkers (134). The plots of relative Gibbs free energies of ionization—gas phase versus DMSO and aqueous solutions—are shown on Figs. 4 and 5, respectively.
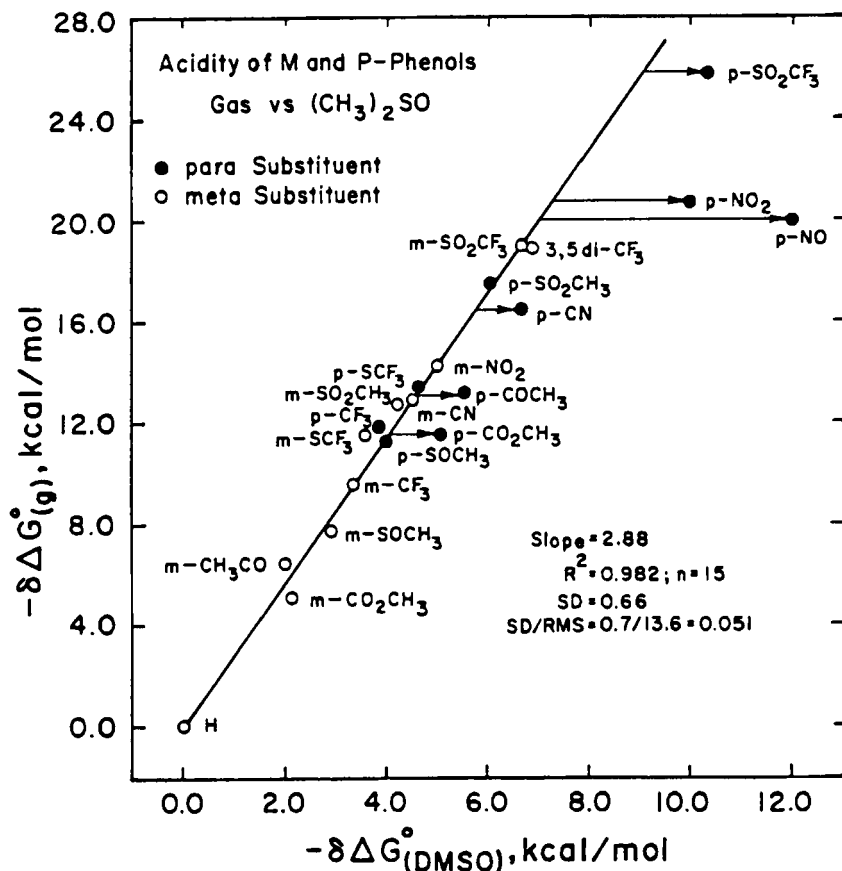


**Figure 4**  Relative acidities of *meta-* and *para-*substituted phenols; gas phase versus DMSO, in kcal mole$^{-1}$. Correlation statistics are as given. The deviating compounds (indicated by arrows, excluded from the correlation) show enhanced acidity in DMSO attributable to charge localization on the substituent. Reprinted with permission from M. Mishima, R. T. McIver, Jr., R. W. Taft, F. G. Bordwell, and W. N. Olmstead, *J. Am. Chem. Soc.*, *106*, 2717–2718 (1984). Copyright 1984 American Chemical Society.
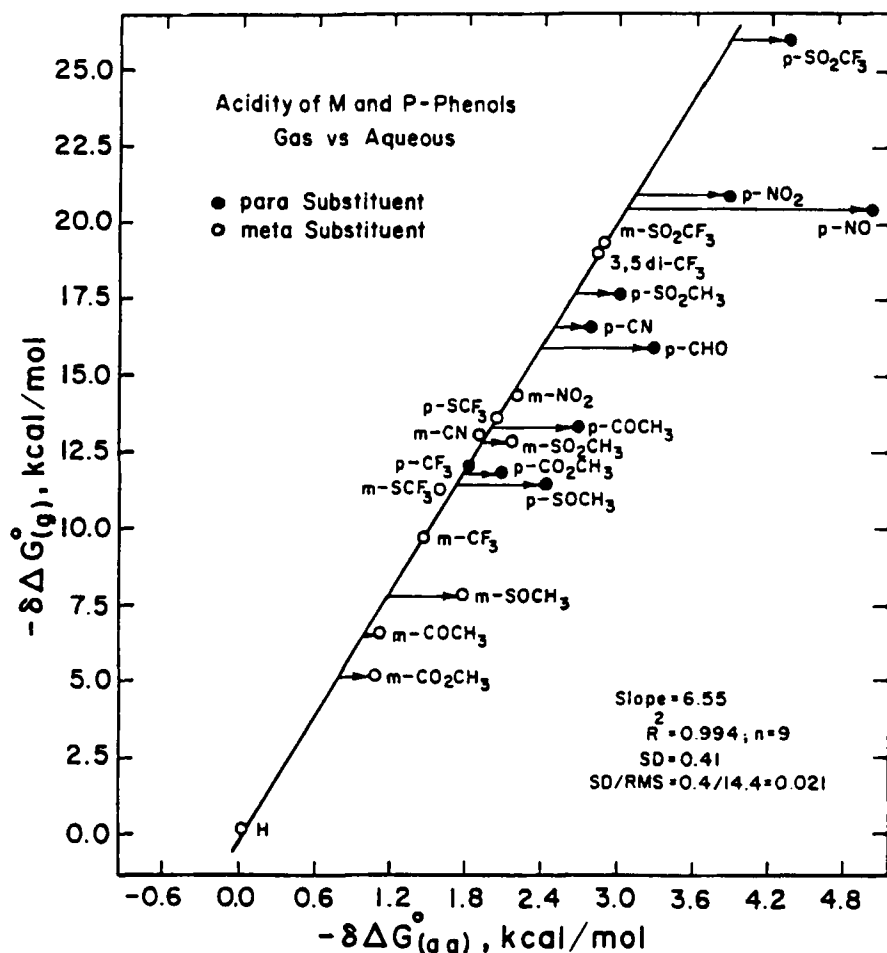
**Figure 5** Relative acidities of *meta*-and *para*-substituted phenols; gas phase versus $H_2O$, in kcal mole$^{-1}$. Correlation statistics are as given. The deviating compounds (indicated by arrows, excluded from the correlation) are the same as in Figure 4 as well as those compounds for which substituent is a strong HBA site. Reprinted with permission from M. Mishima, R. T. McIver, Jr., R. W. Taft, F. G. Bordwell, and W. N. Olmstead, *J. Am. Chem. Soc.*, *106*, 2717–2718 (1984). Copyright 1984 American Chemical Society.

In Fig. 4, a line of good statistics is drawn through the data points corresponding to phenols bearing electron-withdrawing substituents, provided the substituent is neither π-electron acceptor nor directly conjugated to the phenoxide oxygen. The last condition is fulfilled when the substituent is in the *meta* position. Deviations in the direction of enhanced acidity in DMSO

are observed only for those $\pi$-electron-accepting *para* substituents that become sufficiently charge localized by their $R$ effect as to cause electrostatic or electron pair acceptor solvation by DMSO, the so-called substituent solvation-assisted resonance (SSAR) effect. Figure 5 shows that deviating points encompass also *meta* substituents that are strong HBA sites. This is explained by an increased $F$ effect by hydrogen bonding in water, which is referred to as the specific substituent solvation-assisted field (SSSAF) effect.

The comparison of the slopes of lines in Figs. 4 and 5 reveals about a half attenuation of gas-phase substituent effects in DMSO (0.35) than in $H_2O$ (0.15). The absence of hydrogen bond solvation of phenoxide ions in DMSO and the relatively weak electrostatic or electron pair acceptor solvation explain the smaller attenuation of substituent effects in this solvent.

Like proton transfer, the thermodynamics of electron transfer can be studied in the gas phase (HPMS and ICR; see section III.D) and in various solvents (polarography and spectroscopy of charge-transfer complexes).

A plot of electron affinities ($EA$s), solution-derived (134) versus gas-phase, is shown in Fig. 6.

A fair correlation is observed. A part of the scatter in Fig. 6 is attributable to the uncertainties in solution-derived $EA$ values reflected in the different values obtained from polarographic half-wave reduction potentials $E_{1/2}$ and charge-transfer spectra (CTS). The regression line has a slope less than unity. Like for the phenoxide ions, charge delocalization leads to less favorable solvation and decreases the corresponding solution-derived $EA$ values. Higher $EA$ values are associated with substitution by electron-withdrawing groups, resulting, in turn, in an increased charge delocalization (100,135). The less-than-unity slope reflects the decrease in anion stabilization (smaller solution-derived $EA$ values) when $EA$ increases. Figure 6 corresponds to dipolar non-HBD solvents. There is indication that the slope is further lowered by HBD solvents (136).

Interestingly half-wave *oxidation* potentials $E_{1/2}$ and gas-phase ionization energies $IE$ both implying positive ions, are linearly correlated for a series of 2-phenyl indoles and indolizines (137). These nitrogen compounds have two phenyl rings to delocalize the positive charge. A slope of about 0.8 is obtained for the plot of $IE$ versus $E_{1/2}$, a value close to that observed in Fig. 6.

The substituent effects on gas-phase proton transfer reactions may be approached by using Hammett-type $\sigma$ constants. For instance, in the above example of phenols, $\sigma^-$ (or $\sigma^n$ for the *meta* position) are equivalent to solution $\Delta G^\circ$ values and have alternatively been used in the interpretation of phenol acidities. Deviations similar to those in Figs. 4 and 5 are observed. In this case these deviations can be attributed to the solvent–substituent interactions. In general, all the solute–solvent interactions that are included in solution-
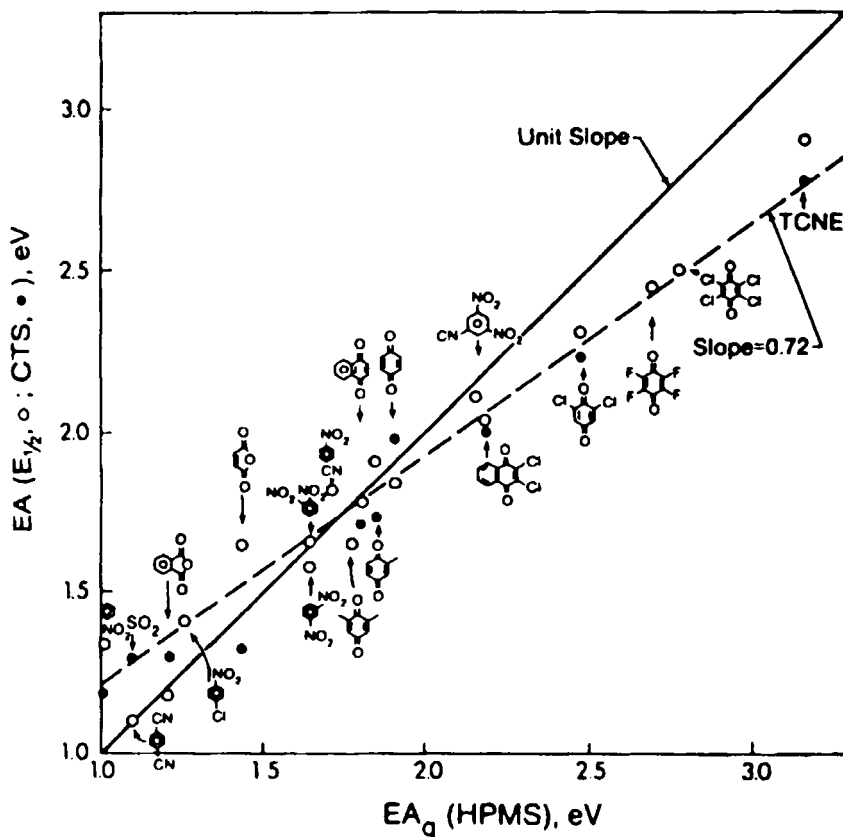
**Figure 6** Plot of electron affinities derived from half-wave reduction potentials and charge-transfer spectra in solution versus gas-phase electron affinities. The slope of the broken line is a measure of the dipolar non-HBD solvent attenuation. Electron affinity values are given in electron volts ($1 eV = 96.48456 kJ mole^{-1}$). Reprinted with permission from P. Kebarle and S. Chowdhury, *Chem. Rev.*, **87**, 513–534 (1987). Copyright 1987 American Chemical Society.

derived $\sigma$ constants limit their usefulness when applied to gas-phase acidities and basicities.

In 1975 Koppel and Karelson attempted to give a general account of structural effects on acidities and basicities in both gas phase and solution using various kinds of $\sigma$, together with a polarizability parameter (69).

More recently, correlations between gas-phase basicities of *meta-* and *para*-substituted styrenes, $\alpha$-methyl styrenes (138), and phenylacetylenes (139) with $\sigma^+$ have been reported. The substituents ($CF_3$, halogens, $CH_3$ and $CH_3O$) are expected to be weakly solvated, so a good linearity is obtained, as shown on Fig. 7.
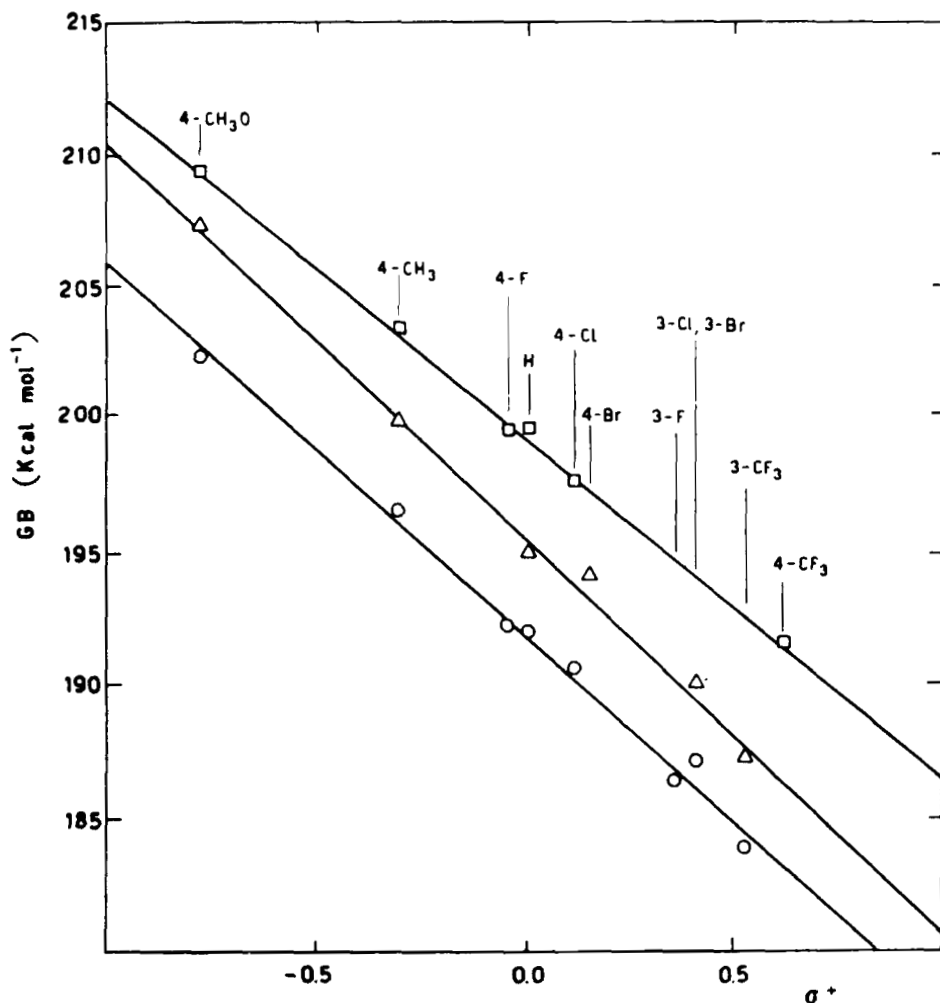
**Figure 7** Correlations of *GB* values in kcal mole$^{-1}$ for $\alpha$-methylstyrenes ($\square$), styrenes ($\Delta$), and phenylacetylenes ($\bigcirc$) with $\sigma^+$. Reprinted with permission from F. Marcuzzi, G. Modena, C. Paradisi, C. Giancaspro, and M. Speranza, *J. Org. Chem.*, 50, 4973–4975 (1985). Copyright 1985 American Chemical Society.

An electron-deficient benzene ring is created by the addition of a proton to the neutral base. In this case solvation may enhance basicities by electron enrichment of an electron-releasing substituent. This occurs when a hydrogen bond is formed between a HBA (electron pair donor) solvent and a HBD substituent. Mishima, Fujio, and Tsuno have reported a correlation of

excellent precision between *GB* and $\sigma^+$ for *meta-* and *para-*substituted benzaldehydes provided amino and hydroxyl HBD substituents are exluded (140b). They further excluded large alkyl groups on the basis of their enhanced polarizability effect on basicities in the gas-phase. The $\sigma^+$ plot for the very similar acetophenones series reveals another source of deviation, that is, the diminished resonance effect due to charge dispersal in the methyl group attached to the carbonyl, as compared to benzaldehydes (140a, c). The use of the Yukawa–Tsuno dual-substituent parameter equation (141) accounting for the variable *R* effect is warranted. This treatment has also been successfully applied to methyl benzoates and *N, N*-dimethylbenzamides *GB* values (140d), as well as to chloride transfer equilibria between benzyl cations (140e).

The solvent dependence of the classical Hammett-type $\sigma$ values has been well established (142), and this effect is clearly evidenced when correlating gas-phase versus solution properties, as shown above. This has led to the search of intrinsic substituent electronic parameters (see Section III.A.3 and reference 1h).

One of the most thoroughly studied series in regard to the various aspects of its basicity is that of the substituted pyridines. Therefore, this series is a good candidate for correlation of gas-phase proton transfer data not only with the corresponding data in solution but also with various other basicity-dependent properties (BDPs).

Very recently, Abboud et al. have analyzed the substituent effects on both *GB* and $\Delta G^{\circ}$(aq) in the pyridine series (143). We have plotted their data, first selecting the *para-*substituted compounds (Fig. 8*a*), and then adding the remaining available data (Fig. 8*b*).

The first plot shows a rather good proportionality covering large substituent effects (from $NO_2$ to $NMe_2$) with a few significant deviations. Carbonyl-containing substituents are expected to decrease the aqueous basicity, downward from the line, due to their HBA property. This effect is observed for $CO_2Me$, but not clearly for COMe. The HBD $NH_2$ substitutent, which is electron-enriched by hydrogen bonding, induces an upward deviation. As pointed out by Charton (144), $\sigma_I$ and $\sigma_R$ for substituents containing the OH or NH moiety are not generally applicable to nondipolar media, including the gas phase. Polarizability effect induces a relative increase in *GB* for compounds bearing alkyl substituents (e.g., *tert-*butyl). Such an effect is not detected on $\Delta G^{\circ}$(aq) (143). In the pyridinium cation a part of the charge is delocalized within the ring, thus rendering the polarizability-induced stabilization effective even in a position remote from the protonation site.

When data points for the *meta* and *ortho* substituents are displayed on the plot (Fig. 8*b*), additional systematic deviations appear. The special behavior of the amino group is confirmed and is similar for the three ring positions. On the other hand, most of the *ortho-*substituted pyridines deviate toward larger
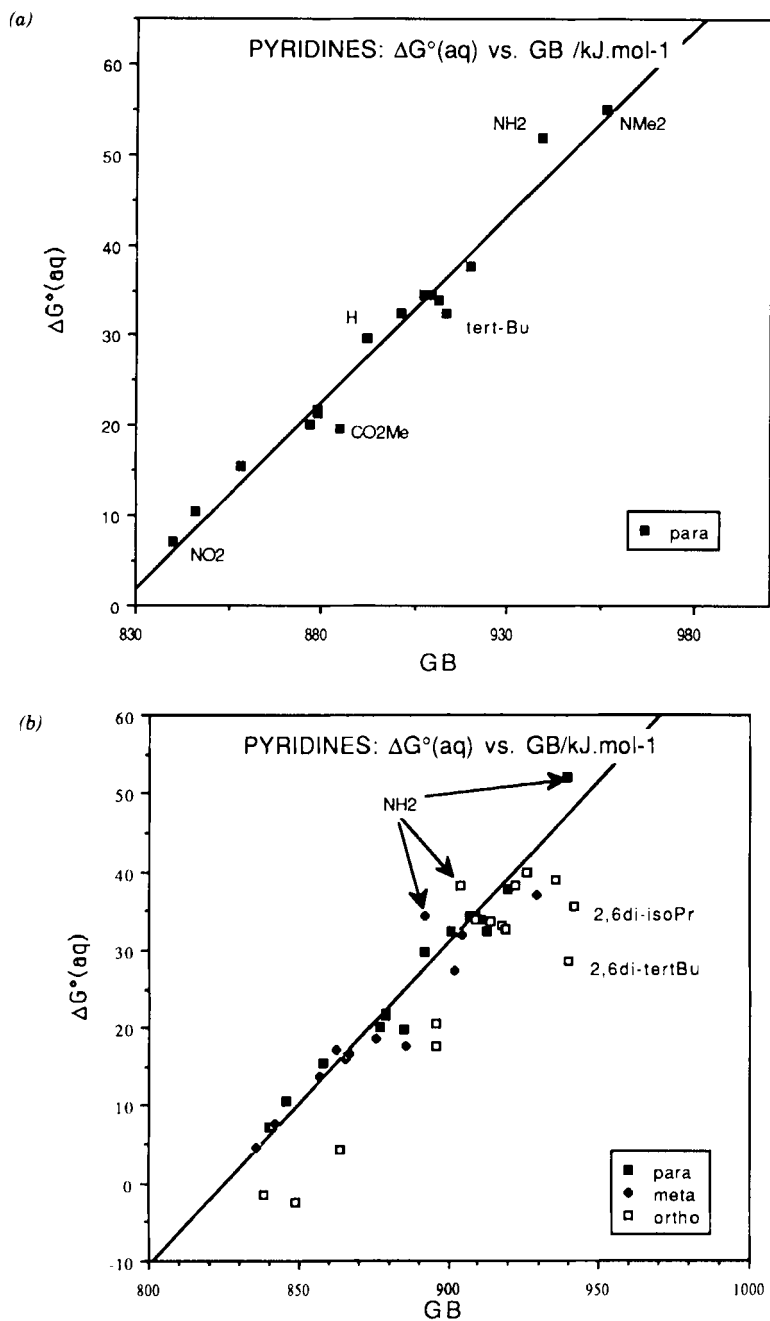
**Figure 8** Substituted pyridines: aqueous versus gas-phase Gibbs free energies of ionization (298 K, kJ mole$^{-1}$). The $\Delta G^{\circ}$(aq) values are taken from reference 143.

gas-phase basicities. These deviations may be attributed in part to a stronger $P$ effect (nil in water) than in the *meta* or *para* position because of the closeness of the substituent and the pyridine nitrogen. In an early quantitative comparison of substituted-pyridines basicities, Aue et al. suggested that the smaller attenuation of the basicity on going from the gas phase to water for the *ortho* compared to the *meta* and *para* positions could be explained, within the framework of the field-effect theory, by a decrease of the effectiveness of solvent (145). The smaller $F$ attenuation factor in the *ortho* position has also been noted by Abboud et al. (143). The large gas-phase $P$ effect associated with this position and the smaller $F$ attenuation by water lead to more scatter on both sides of a line of different slope than for the *meta* and *para* positions.

It is worth mentioning the case of two highly hindered bases, 2,6-di-*tert*-butylpyridine (2,6-DTBP)and 2,6-diisopropylpyridine (2,6-DIPP), for which large downward deviations are observed on the $\Delta G°$ plot (Fig. 8*b*). Their relatively high $GB$ is easily explained by the large $P$ effect of the two *ortho*-alkyl groups. On the other hand, the abnormally low basicity of 2,6-DTBP in water has long been recognized, but the exact origin was clarified quite recently (112). An analysis of the complete thermodynamic cycles of protonation of several mono- and di-*tert*-butylpyridines by Hopkins et al. (112) demonstrates that the enthalpy of hydration $\Delta_{solv}H°$ of 2,6-DTBPH$^+$ is normal, but not $\Delta_{solv}G°$. The corresponding abnormal entropy of hydration $\Delta_{solv}S°$ is attributed to the restriction of the rotation of the *tert*-butyl groups. This is in agreement with the thermodynamics of "gas-phase solvation" of 2,6-DTBPH$^+$ by one water molecule (146). So the 2,6-DTBPH$^+$ cation is hydrogen-bonded to a water molecule via N$^+$-H as reflected by the normal $\Delta_{solv}H°$ but the incoming water hinders the free rotation of the *tert*-butyl groups, causing a loss of entropy, an effect not seen for the other pyridinium ions in solution. In general, the consideration of ionization enthalpies, $PA$ and $\Delta H°$(aq) provides information complementary to that brought by Gibbs free energies.

Fortunately, $\Delta H°$(aq) values have been determined for a sufficient number of pyridines (111, 112, 145, 147, 148) as to obtain significant comparison with their proton affinities. The corresponding plot is given in Fig. 9.

As mentionned by Aue et al. (145), there is less scatter in the enthalpy plot than in the Gibbs free-energy plot, with the exception of a large deviation for the 4-dimethylaminopyridine. With the data set presently available, this may be visualized by drawing two separate lines, one for electron-withdrawing and one for electron-releasing (by resonance) substituents. We noted earlier (Section III.A.3) that $GB$ and $PA$ are almost equivalent within a series. Therefore, the separation into two subfamilies appears to be entirely due to solvation.
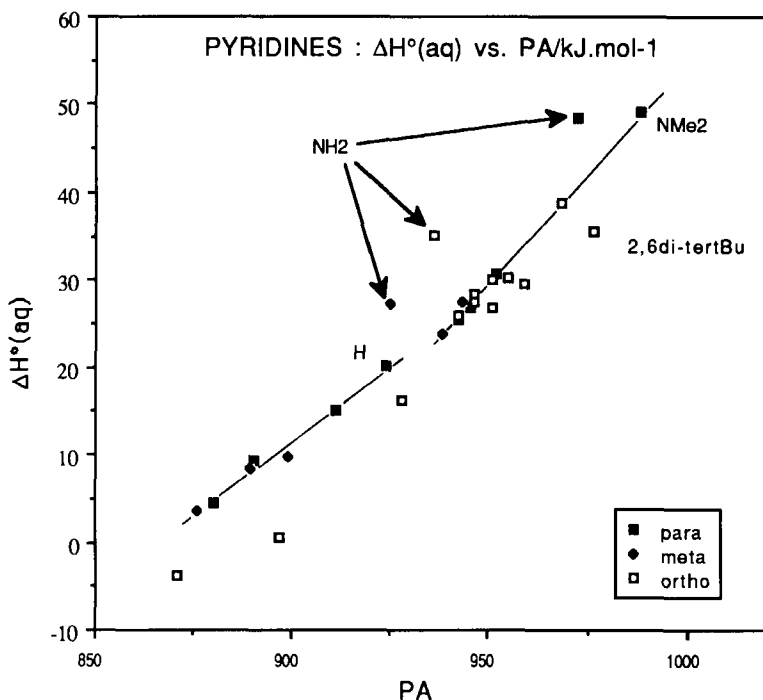
**Figure 9**  Substituted pyridines: aqueous versus gas-phase enthalpies of ionization (298 K, kJ mole$^{-1}$). The $\Delta H^\circ$(aq) values are taken from references 111, 112, 145, 147, and 148.

To obtain a unique correlation $\Delta G^\circ$(aq) versus $GB$, the breakdown in two lines seen in Fig. 9 for $\Delta H^\circ$(aq) versus $PA$ should be compensated for by two different enthalpy–entropy relationships corresponding respectively to electron-withdrawing and electron-releasing substituents. The different variations in $\Delta S^\circ$(aq) for the two kinds of substitution have been mentioned by Arnett et al. (111a). The deviations for the $NH_2$-substituted pyridines in Fig. 9 are in the same direction as that in Fig. 8b, but larger. The specific substituent solvation invoked above is therefore enthalpic in origin but is compensated in part in the $\Delta G^\circ$(aq) scale by the solvent organizing effect due to hydrogen bonding. Hindered rotation of the $NH_2$ group has been suggested as a cause of entropy loss in solution (148, 149), but this phenomenon operates also in the gas phase (150). We have argued that the entropy of hydration of the 2,6-DTBPH$^+$ cation was at the origin of a part of the large deviation seen in Fig. 8b. This is confirmed by the lesser deviation, compared to other *ortho* compounds, observed in Fig. 9.

**b.   Hydrogen Bonding and Lewis Acid–Base Interactions.** In all the examples of gas-phase  solution correlations of proton transfer data, the deviations have been analyzed in term of strong solvation effect affecting the reactive center and/or the substituent. Solvents of low solvating power do not allow protonated or deprotonated species to be free from counterion effects. On the other hand, other BDPs have been studied in such media, mainly spectroscopic and thermodynamic parameters associated with hydrogen bonding or Lewis acid–base interactions. These properties may be usefully compared to *PA* or *GB*.

In an extensive compilation of the phenol hydrogen bonding infrared (IR) shift in $CCl_4$, $\Delta v$ (PhOH, $CCl_4$), Koppel and Paju (35) alluded to the possibility of an approximate linear relationship between this basicity parameter and *PA*. Later a number of correlations between $\Delta v$ (PhOH, $CCl_4$) and *IE* for various families were reported (151). As *IE* and *PA* are closely proportional in some
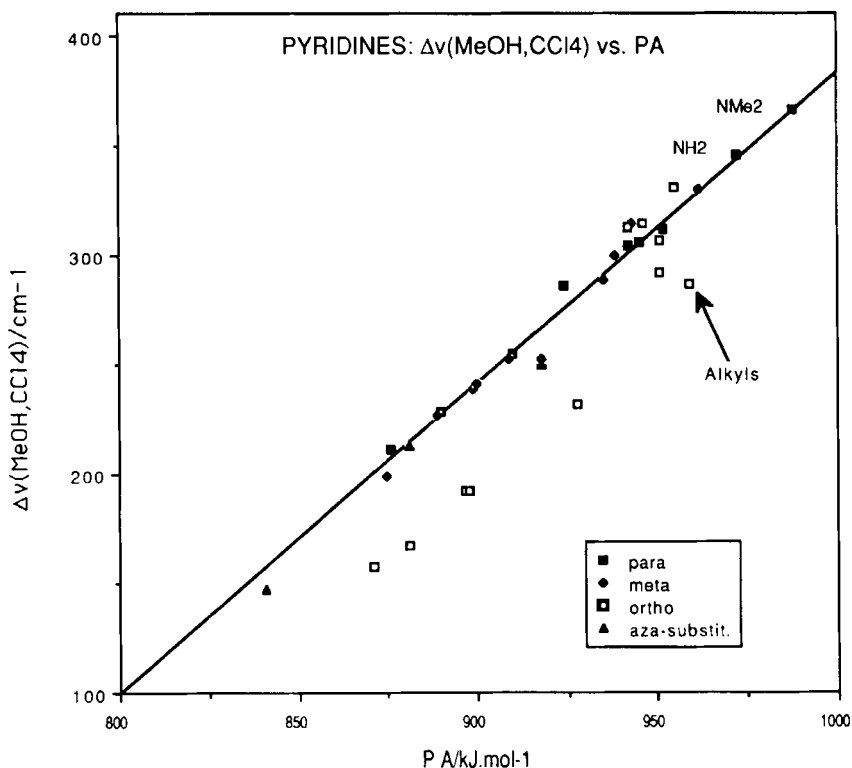


**Figure 10**   Substituted pyridines: methanol IR shifts in $CCl_4$ in $cm^{-1}$ versus proton affinities in kJ mole$^{-1}$. The $\Delta v$(MeOH, $CCl_4$) values are taken from reference 37b.

cases, it follows that $\Delta v$ (PhOH, $CCl_4$) and $PA$ should correlate as well. Such a correlation was observed in the pyridine family (152). More recently Laurence and coworkers have measured a wealth of methanol IR shifts in $CCl_4$, $\Delta v$ (MeOH, $CCl_4$) (37). The *meta*- and *para*-substituted pyridines, including pyrimidine and *s*-triazine, give a good linear relationship (see Fig. 10).

It is worth mentioning that in $CCl_4$ the 4-aminopyridine falls on the general line (along with the 4-dimethylaminopyridine), confirming that specific solvation by water was the origin of its deviation (see Figs. 8 and 9). The nonalkyl *ortho* substituents induce downward deviations that may be attributed to steric hindrance for the MeOH approach or to a relatively larger polarizability effect on $PA$. The steric effect is probably very weak if we consider that alkyl substitutions in the *ortho* position *increase* $\Delta v$ (MeOH, $CCl_4$) (37b). Nevertheless, the *ortho*-, *meta*-, and *para*-alkyl pyridines form a small cluster of points distributed on both sides of the line. Only the *ortho*-isopropyl and *tert*-butyl induce deviations in the direction of enhanced $PA$ values, but less than expected on the basis of their large polarizability. It seems
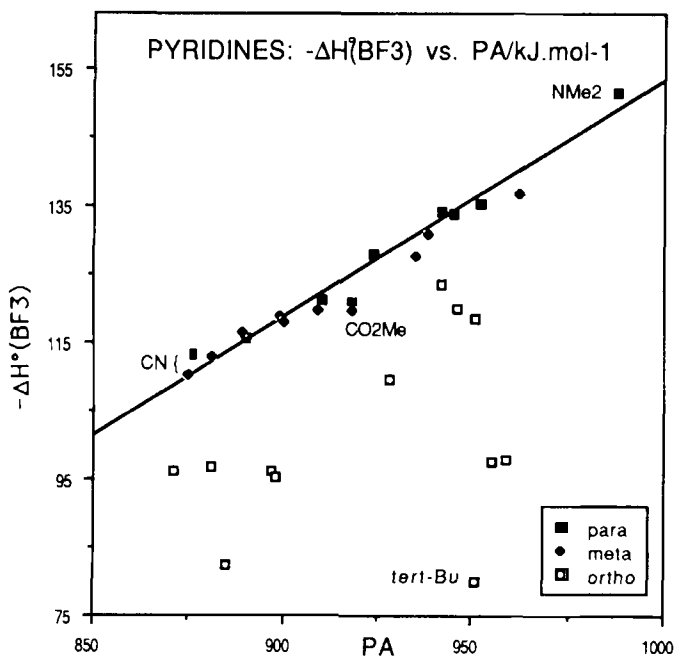


**Figure 11**  Substituted pyridines: enthalpies of complex formation with $BF_3$ in dichloromethane solution versus proton affinities. All values in kJ mole$^{-1}$, at 298 K. The $-\Delta H^\circ_{BF_3}$ values are taken from reference 37b.

that an effect specific to alkyls enhances $\Delta v$ (MeOH, $CCl_4$), for a reason that we have not yet identified.

As mentioned in Section II.B, we have measured a great number of enthalpies of complex formation with $BF_3$, with an aim to participate at the unraveling of EPD–EPA solute–solvent interactions and also to study intrinsic structural effects on the basicity. In particular, we have shown that very similar blends of electrostatic and covalent effects contribute to $-\Delta H^\circ_{BF_3}$ and $PA$ (153). In Fig. 11 we have plotted our $\Delta H^\circ_{BF_3}$ values for substituted pyridines (37b) against the corresponding $PA$ values.

A reasonably good linear relationship exists for *meta-* and *para-*substituted compounds. The *ortho* substituents give rise to dramatic downward deviations. The larger part of these deviations is attributable to the high steric requirement of $BF_3$. By analogy with the previous conclusions, it is possible that the enhanced polarizability effect in *ortho*, acting mainly on $PA$, contributes also to these deviations.

The polarizability and steric effects are short-range interactions and are not easily separated. Nevertheless, bases having structures with negligible steric effect, or presenting a constant steric environment around the basic center, can be found.

We have shown that substituted nitriles $X—C≡N$ fulfill this condition (28) for the $X—C≡N$ framework is linear in the boron trifluoride complex (154).

In the absence of steric effects on the $BF_3$ complexation, the scatter in a direct relationship $\Delta H^\circ_{BF_3}$ versus $PA$ will be due to the enhanced $P$ effect in the gas phase if the other electronic effects act proportionally on the two basicity parameters. In fact, the direct plot gives an elongated cloud of points (open squares in Fig. 12), but the points fall on a line of good statistics when $PA$ values are corrected for polarizability (full squares). The corrective term was obtained from the multiple linear regression (28):

$$PA = A_0 + A_1(-\Delta H^\circ_{BF_3}) + A_2\alpha_d \tag{31}$$

(This form corresponds to the smallest correlation coefficient between the independent variables.)

The group polarizability parameter $\alpha_d$ was calculated using a slightly modified version of the Gasteiger–Hutchings method (73). The use of $\sigma_\alpha$ (1h, 72) leads to equally good correlations. In Fig. 12 where

$$PA_{corr} = PA_{expll} - A_2\alpha_d \tag{32}$$

the only significant deviation corresponds to the phenyl substituent for which the polarizability seems to be underestimated. A tentative explanation
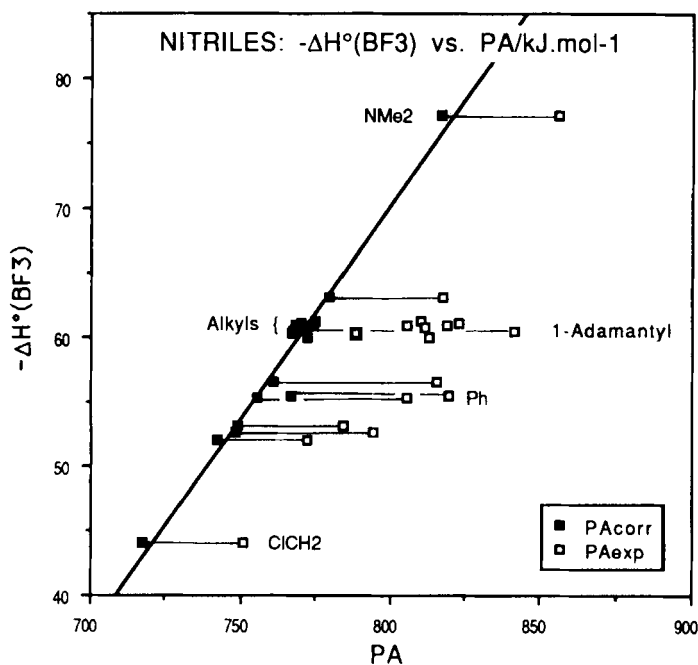
**Figure 12** Enthalpies of complex formation with $BF_3$ in dichloromethane solution versus proton affinities for nitriles. All values in kJ mole$^{-1}$, at 298 K. Horizontal lines correspond to enhanced polarizability effect on proton affinities. Data from reference 28.

based on charge delocalization at remote sites was proposed in reference 28. The large polarizability correction is typical of systems with a short substituent–charge distance, and moreover indicates that the $P$ effect is much less on $-\Delta H^{\circ}_{BF_3}$ (155). The slope of the line (0.33) indicates that $PA_{corr}$ is three times more sensitive to the remaining structural effects than $-\Delta H^{\circ}_{BF_3}$.

Although the $C\!=\!\!O\!-\!B$ angle differs from $180^{\circ}$ in carbonyl-$BF_3$ complexes (156), we anticipate a nearly constant steric environment in the series of 3-substituted-5,5-dimethyl-2-cyclohexen-1-ones:
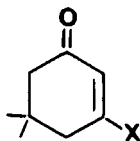
A treatment similar to that used for the $X\!-\!C\!\equiv\!N$ series was applied, except that the $P$ correction was taken as the product $\rho_{\alpha}\sigma_{\alpha}$ in which $\rho_{\alpha}$ was

calculated from the relative $GB$ values of these cyclohexenones (1h). Correcting $PA$ in this way means that we neglect any $P$ effect in $-\Delta H^{\circ}_{BF_3}$. This approximation appears to be justified from the study of nitriles (155). A plot of $-\Delta H^{\circ}_{BF_3}$ against $PA_{exptl}$ and $PA_{corr}$ is shown in Fig. 13.

The fact that there are few substituents with a large polarizability and that the substituent–basic site distance is larger than for nitriles leads to a reduction of the polarizability correction. However, we obtain a better fit with $PA_{corr}$ than with $PA_{exptl}$. The slope of the line shown in Fig. 13 (0.47) is somewhat larger than those obtained for nitriles (0.33) and pyridines (0.34). In general, we expect direct relationships between $-\Delta H^{\circ}_{BF_3}$ and $PA$ when the former is free from variable steric effects and when the latter is corrected for polarizability. The same conditions are required in order to obtain linear relationships with the hydrogen-bonding parameter $\beta$, although this parameter seems less sensitive to steric effects than $-\Delta H^{\circ}_{BF_3}$. Kamlet et al. have
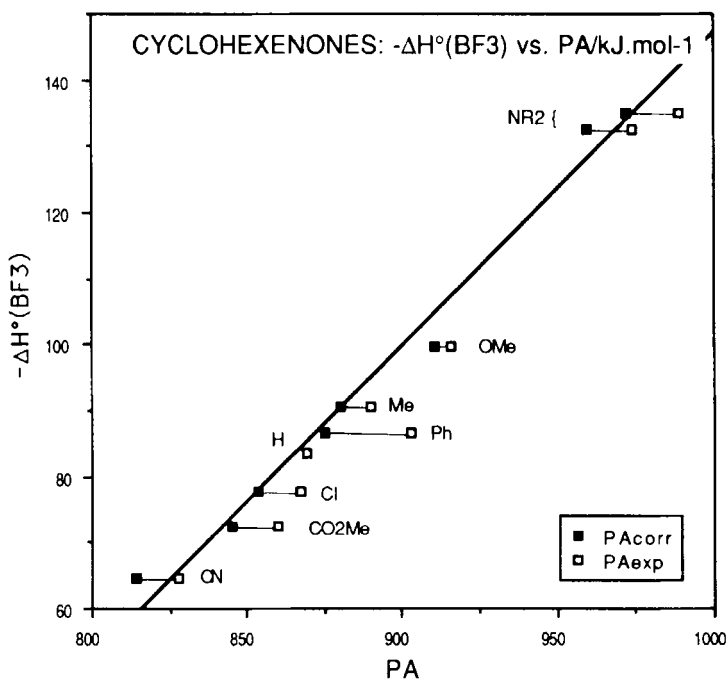


**Figure 13**   3-Substituted 5,5-dimethyl-2-cyclohexen-1-ones. Enthalpies of complex formation with $BF_3$ in dichloromethane solution versus proton affinities. Values in kJ mole$^{-1}$, at 298 K. Data sources: $-\Delta H^{\circ}_{BF_3}$, reference 157; $PA$, reference 158. Horizontal lines correspond to enhanced polarizability effect on proton affinities [$\sigma_{\alpha}$ values from reference 1h, except for $C_6H_5$, $-0.93$ (28) and $NEt_2$, $-0.56$ estimated].

reported linear relationships between $\beta$ and $PA_{corr}$ for five series of bases with O $sp^2$ and $sp^3$ and N $sp$, $sp^2$, and $sp^3$ coordinating atoms, respectively (40c). The proton affinities were corrected using $\sigma_\alpha$ for the variable substituent polarizability and a constant term depending on the nature of the basic functions (159). A somewhat scattered $PA_{expll}$ versus $\beta$ plot reduces to five nicely parallel lines when $PA_{corr}$ is substituted for $PA_{expll}$ (Fig. 14).

The $\beta$ parameter has a stronger electrostatic character than $PA_{corr}$ (153). Therefore, $\beta$ will be relatively increased for highly dipolar functions, that is, when the coordinating atom has a high electronegativity (160). Conversely, a
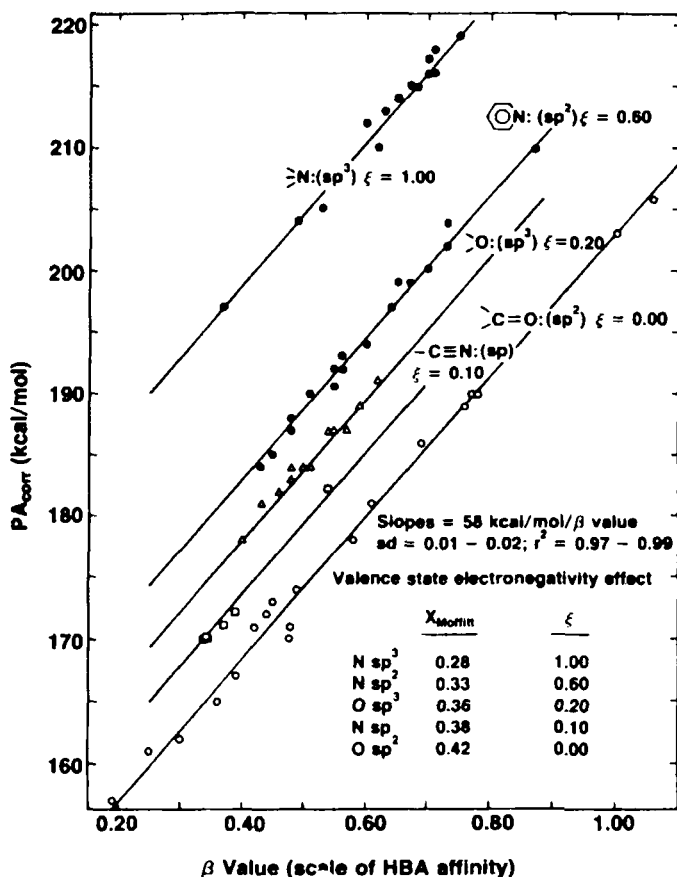


**Figure 14** Family relationship between gas-phase proton affinities corrected for polarizability ($PA_{corr}$) and corresponding HBA $\beta$ values. Reprinted from M. J. Kamlet, R. M. Doherty, J.-L. M. Abboud, M. H. Abraham, and R. W. Taft, *Chemtech*, 566–576 (1986) with permission of the authors.

low electronegativity favors the more covalent protonation. In fact, the intercept displacements closely follow the coordinate covalency parameter $\zeta$ (41). A family dependent correlation was also observed for $\beta$ versus $-\Delta H^\circ_{BF_3}$ (24).

Almost simultaneously to the publication of the paper by Kamlet et al. (40c), Zeegers-Huyskens published a similar type of family-dependent correlation between solution hydrogen bonding and gas-phase proton transfer parameters (161a), respectively:

- The Gibbs free energy of hydrogen bonding between various OH HBD and O or N HBA, $-\Delta G^\circ_{HB}$.
- The difference between the gas-phase acidity of the HBD and the gas phase basicity of the HBA, called $GA-GB$ in the original paper.

Although the absence of polarizability correction leads to more scatter, the separation into families is unquestionable. A plot for three classes of nitrogen bases is shown in Fig. 15.

The similarity with the previous $\beta$ plot originates in the Gibbs free-energy character of $\beta$ (153). In another paper (161b) Zeegers-Huyskens discussed the
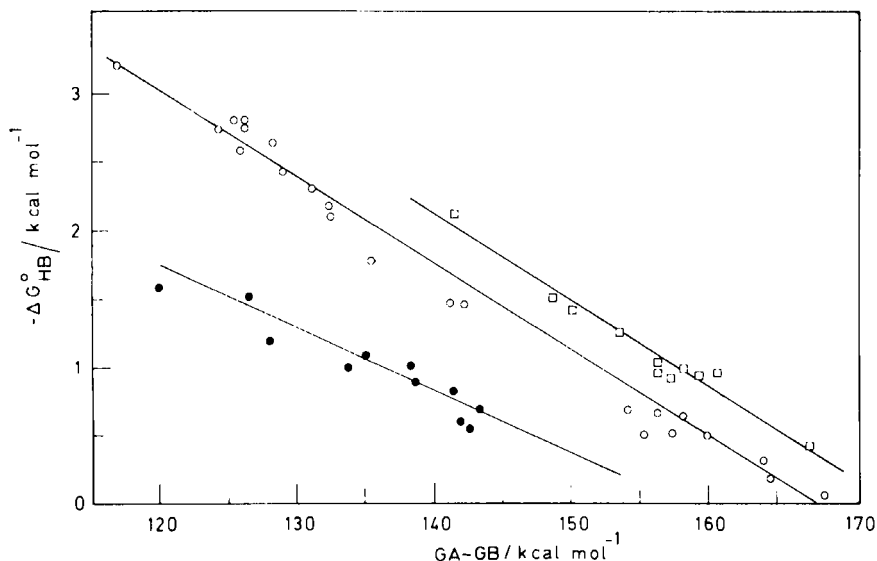


**Figure 15** Gibbs free energy of hydrogen bonding, in tetrachloromethane, between OH HBD and N HBA plotted against the difference between the gas-phase acidity of the HBD and the gas-phase basicity of the HBA ($\square$ nitriles, $\bigcirc$ pyridines, $\bullet$ anilines). Reprinted with permission from T. Zeegers-Huyskens, *J. Mol. Liq.*, *32*, 191–207 (1986). Copyright 1986 Elsevier.

same problem of hydrogen bonding in solution versus gas-phase proton transfer by using enthalpies (instead of Gibbs free energies); it is interesting to note that there is less distance between the different lines. This is due to the more covalent character of the enthalpy than the corresponding Gibbs free energy for a given interaction of intermediate strength (153) (As emphasized in Section III.3, $PA$ and $GB$ or $\Delta H^{\circ}_{acid}$ and $\Delta G^{\circ}_{acid}$ can be used interchangeably.)

### 2. Relationships between Gas-Phase Basicity Scales: Cations versus Proton

The first comparison between a cation affinity scale and $PA$ was proposed by Staley and Beauchamp (79a) in a study of the energies of $Li^+$ binding to a sample of organic functionalities. The plot of $Li^+(A)$ versus $PA$ showed little correlation in general, although a trend was seen for carbonyl compounds and nitriles. The disparity was attributed to the largely ionic character of bonding to $Li^+$, while bonding to $H^+$ may also reflect strong covalent interaction. This explanation is supported by ab initio calculations and Morokuma's (64) energy decomposition analysis (162, 163). When basicity scales (solution or gas) containing different electrostatic–covalent blends are compared, very often a family-dependent relationship is observed (41). The establishment of an extensive set of relative $Li^+(GB)$ values of various organic families is in progress (80) (see Table 7). A preliminary plot of unpublished results is given in Fig. 16.

The slopes ranging from 0.36 to 0.57 define crudely parallel lines. The vertical ordering does reflect the enhancement of the electrostatic character of the interaction with $Li^+$. It is noteworthy that the carbonyl family is not ranked as in a $\beta/PA$ plot. The $C{=}O \cdots Li^+$ geometry is linear, but other acids such as $H^+$ and HBDs, in most cases (37c), tend to form angular complexes. This may explain the relatively weakened interaction between $Li^+$ and carbonyl compounds.

Figure 16 shows different lines for alcohols and ethers and for thiols and sulfides, respectively. The differenciations between ROH and $R_2O$ and between RSH and $R_2S$ having $sp^3$ O and S basic centers may be explained by the effect of successive alkyl substitutions (163). Protonation induces a much larger charge transfer than lithiation because of the electropositive nature of the metal. Hence the gain in stabilization on going from ROH to $R_2O$ and from RSH to $R_2S$ is less for lithiated than for protonated species.

Some departures from the family lines deserve comment. Theoretical calculations indicate that hydrazine forms a single N—H sigma bond with $H^+$ (164a), but with $Li^+$ a symmetric three-membered ring is formed with enhanced stability (164b). This consideration provides an explanation for the greater $Li^+$ affinity of pyridazine than that expected from the pyridines line
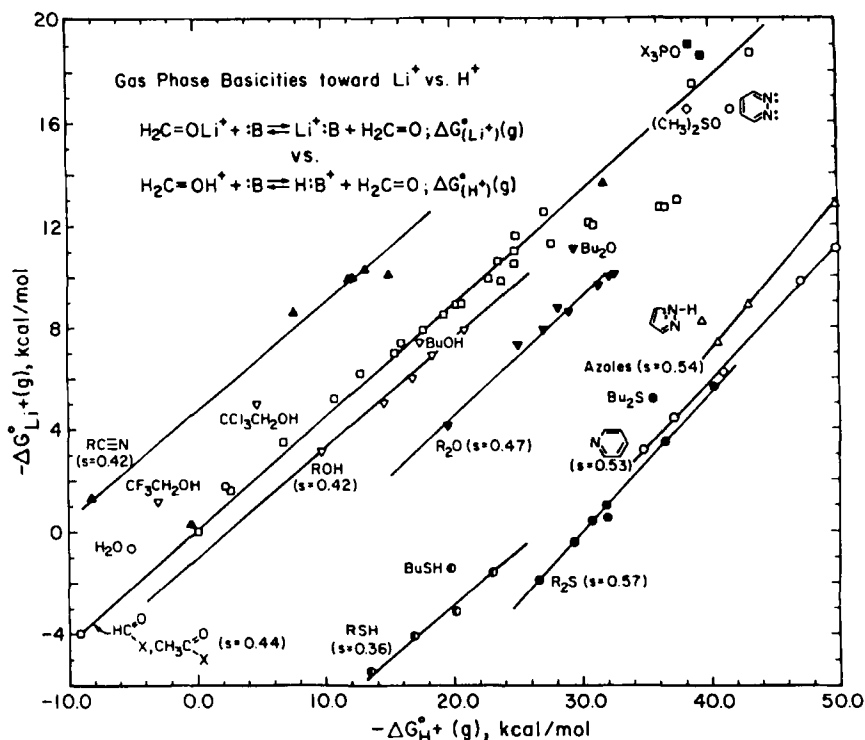
**Figure 16**  Relative Gibbs free energy of $Li^+$ binding versus relative Gibbs free energy of proton transfer in the gas phase. For each family, the slope is given between parenthesis (80).

(open circles in Fig. 16). Both $CF_3CH_2OH$ and $CCl_3CH_2OH$ deviate from the ROH line. A tentative explanation is an ion–dipole interaction between $Li^+$ and the $CX_3$ substituent.
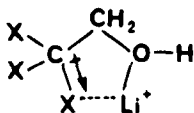


As a result of the small charge transfer in the $Li^+$ complexes, the metal retains most of its initial unit charge (84, 165, 166). This charge localization facilitates the charge–dipole stabilization as shown in the above scheme.

The $Li^+$ affinities of *n*-butyl alcohol, thiol, ether, and sulfide are systematically greater than expected from the lines defined by the points for methyl, ethyl, isopropyl, *tert*-butyl, and cyclic derivatives. A tentative explanation is that there is a significant ion-induced dipole stabilizing

interaction between the metal and the alkyl chain as shown in the following scheme:

$$\begin{array}{c} {}_{/}CH_2^-CH_2 \\ CH_2 \qquad O{-}H \\ {}_{\backslash}CH_3\cdots Li^+{}^{/} \end{array}$$
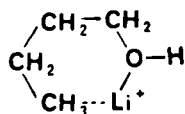
This kind of interaction is of interest in connection with the activation step of C—C and C—H bonds remote from the coordinating center during the gas-phase reaction of nitriles with transition-metal ions (167).

The other alkali metal cations have been less studied. On theoretical grounds $Li^+$ and $Na^+$ are supposed to behave remarkably alike (163). The small amount of charge transfer (covalency) in $Li^+$ complexes is predicted to decrease when changing the metal ion for $Na^+$ and $K^+$ (166). Further experimental studies are needed to establish whether this effect is large enough to differentiate the families of bases when two alkali metal-cation affinity scales are plotted, one against the other.

Ab initio calculations show that, as compared to alkali–metal-cations, $Al^+$ accepts more charge on complex formation (84,168), indicating a tendency to form more covalent bonds. An $Al^+(GB)$ scale was established for several $sp^2$ and $sp^3$ oxygen families and nitriles (83) (see Table 7). When plotted against $GB$, much less separation into families was observed than for the $Li^+$ plot.

Restricted to the carbonyl family the plot of $Al^+$ and $Li^+$ basicities against $GB$ give straight lines of slopes 0.74 and 0.41, respectively (Fig. 17).

Although $Al^+$ appears to be a stronger $\sigma$-electron pair acceptor than $Li^+$, it appears to be weaker than the bare proton. The slopes in Fig. 17 reflect the response of the substituted carbonyl to the electron demand, which is in the order $H^+$(unit slope) $> Al^+ > Li^+$. Uppal and Staley have also compared $Mn^+$ to $H^+$ (82b). The corresponding plot reveals a larger separation between nitriles, carbonyls, and ethers than for $Al^+$ and a smaller than for $Li^+$. This is an indication of the decrease of the electrostatic/covalent ratio in the $M^+$-base bonding, in the order $Li^+ > Mn^+ > Al^+$. Interestingly, the $Mn^+$ versus $H^+$ slope is 0.48 for carbonyls, a value intermediate between those obtained for $Al^+$ and $Li^+$. Therefore, this parameter may be considered as a good indicator of the electrostatic–covalent character of the bonding to the metal ion. The small value of 0.30 obtained for $CpNi^+$ (82b) indicates that the cyclopentadienyl ligand reduces the electron demand of $Ni^+$.

Basicity scales relative to the trimethyl cations of the group 14 elements (C, Si, Sn) have also been discussed in terms of electrostatic–covalent interaction (88). All these scales show family dependence when plotted against $PA$,
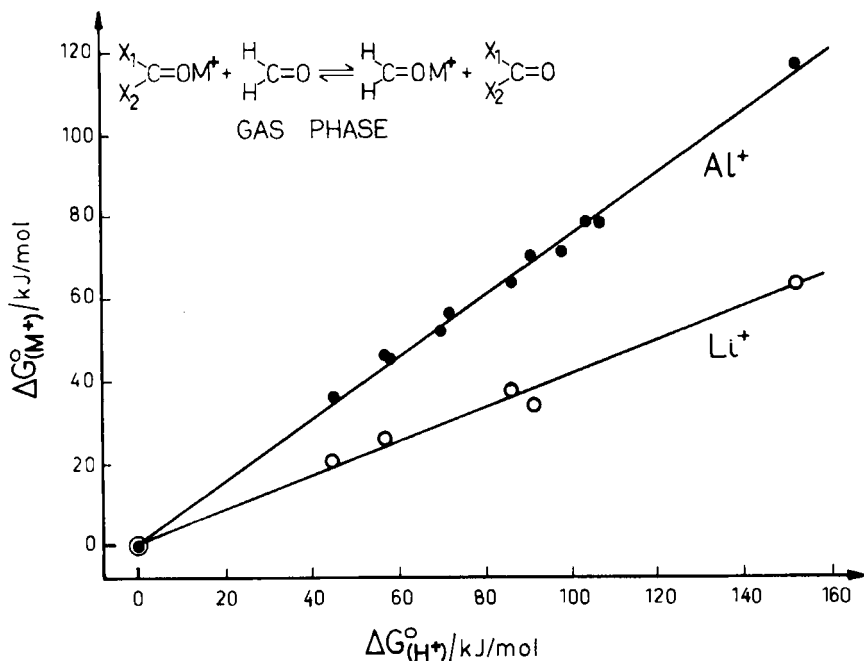
**Figure 17**   Relative Gibbs free energies: $Al^+$ and $Li^+$ binding versus protonation of carbonyl compounds. Reprinted with permission from J. F. Gal, R. W. Taft, and R. T. McIver, Jr., *Spectrosc. Int. J., 3*, 96–104 (1984). Copyright 1984 The J. R. J. Paré Establishment for Chemistry Limited.

but the restricted data sets preclude a detailed comparative analysis. Nevertheless, plots of $(CH_3)_3 M^+$ affinities versus $PA$ for the oxygen bases give the following slopes: 0.70, 0.64, and 0.43 for M = C, Si and Sn, respectively. This order corresponds to a decrease of covalent contribution to the interaction. It was also shown that for these bulky acids that steric effect play a role.

The bonding to carbon is of prime importance. This is the reason why the methyl cation affinity $(MCA)$ has been a matter of continuing interest (86, 87). The $MCA$ values have been determined experimentally for a series of weak bases (87b). The authors have also calculated $MCA$ values for stronger neutral bases (see Section III.C). When plotted against $PA$ values, these $MCA$ values define two rough correlations, one for the weak bases (slope $\sim 0.3$) and one of near unit slope for the stronger usual oxygen and nitrogen bases (sulfur bases are a little offset). There are not enough bases in each family to indicate or preclude the possibility of family dependence. It should be mentioned that $MCA$ values for various families of anions, when plotted against $\Delta H^\circ_{acid}(AH)$,

determine a line of slope close to one. From the available data, it is difficult to attribute the small deviations to a possible family dependence. Tentatively, $MCA$ and $PA$ may be considered of equivalent status in the framework of the electrostatic–covalent description of the donor-acceptor bonding.

### 3.   From the Gas-Phase Ionic Hydrogen Bond to the Bulk Solvation of Onium Ions

As seen in Section III.E, the first solvation shell of onium ions may be approached by gas-phase studies of solvent molecule attachment. The interaction results from a strong ionic hydrogen bond for which the dissociation enthalpy $\Delta H_D^\circ$ (see Equation 29) is typically $60–120 \, \text{kJ mole}^{-1}$. Similarly, gas-phase hydrogen bonding to anions (Section III.D, Equation 26) represents the first step of their bulk solvation. The ionic hydrogen bond results in partial proton transfer from $BH^+$ to the HBA, or from the HBD to $A^-$. The efficiency of the charing of the proton between the components of the proton-bound dimer is optimal when the $PA$ or $\Delta H_{acid}^\circ$ values of the two neutral partners (B and HBA or HBD and AH, respectively) are equal and decreases as

$$\Delta PA = PA(\text{B}) - PA(\text{HBA}) \tag{33}$$

or

$$\Delta \Delta H_{acid}^\circ = \Delta H_{acid}^\circ(\text{HBD}) - \Delta H_{acid}^\circ(\text{AH}) \tag{34}$$

increases (169) since the proton tends to be retained by the more basic (or the less acidic) species.

For example, when $BH^+$ is $H_3O^+$, $CH_3OH_2^+$, or $(CH_3)_2OH^+$ and the HBA is $H_2O$ as in Equation 29, the $\Delta H_D^\circ$ decreases from 132 to 101 and $95 \, \text{kJ mole}^{-1}$, respectively (103a), which is the order of increasing $PA(\text{B})$ (see Table 2).

The inverse relationship between $\Delta PA$ and $\Delta H_D^\circ$ has been extensively investigated by Meot-Ner and coworkers for a large number of dimers involving nitrogen, oxygen, and sulfur bases (see Table 9).

Linear relationships are observed over a wide range of $\Delta PA$ (from 0 to $200 \, \text{kJ mole}^{-1}$) and $\Delta H_D^\circ$ (from 120 to $60 \, \text{kJ mole}^{-1}$) when each type of ionic hydrogen bond is considered separately.

The slopes (always negative) and intercepts are highly structure dependent and have been discussed on the ground of electrostatic arguments (101, 103c). In brief, when series with a common ion and different HBAs are compared, the more dipolar HBA should exhibit higher intercept and steeper slope. Considering series with variable ions (different atoms bearing the

TABLE 9

Correlation between $\Delta H_D^\circ$ and $\Delta PA$ for $BH^+ \cdots HBA$ Bonds;
Intercepts and Slopes for the Least-Squares Lines:
$$\Delta H_D = A_0 + A_1 \Delta PA$$

| Type of Ionic Hydrogen Bond | $A_0$(kJ mole$^{-1}$) | $A_1$ | Reference |
|---|---|---|---|
| $SH^+ \cdots O$ | 78 | $-0.16$ | 103c |
| $NH^+ \cdots O$ | 118 | $-0.23$ | 103a |
| $NH^+ \cdots N$ | 97 | $-0.25$ | 103a |
| $OH^+ \cdots O$ | 127 | $-0.30$ | 103a |
| $C\equiv NH^+ \cdots O$ | 118 | $-0.31$ | 106 |
| $NH^+ \cdots N=C$ | 148 | $0.35$ | 106 |
| $C\equiv NH^+ \cdots N-C$ | 118 | $-0.37$ | 106 |
| $OH^+ \cdots N=C$ | 129 | $-0.43$ | 106 |

proton) and a common HBA, the ion with the larger positive charge on the attached proton should also exhibit a higher intercept and a steeper slope. A larger positive charge on the attached proton is assumed to result from a higher electronegativity of the protonated atom. The results in Table 9 agree roughly with this picture, taking into account that $\Delta H_D^\circ$ values are usually known to about $\pm 4$ kJ mole$^{-1}$ and that the reported correlations are not very precise in some cases.

Similar correlations have been reported for anionic hydrogen bonds (92 94a). In general, when a constant HBD is faced to various anions $A^-$ belonging to the same family, an approximate linear relationship of $\Delta H_D^\circ$ to $\Delta H_{acid}^\circ$ (AH) is found. The same kind of relationship is also observed when a constant anion is complexed with a family of HBDs. An example is shown in Fig. 18, where $\Delta H_D^\circ$ for the fluoride ion is plotted against $\Delta H_{acid}^\circ$ of the HBD.

The line of slope $-0.59$ corresponds to the alcohols and water family. Such a slope close to $-0.5$ indicates a nearly equal sharing of the proton. For HBDs more acidic than HF $(\Delta \Delta H_{acid}^\circ < 0)$, the proton-bound dimers may be expected to have the structure $(A^- \cdots HF)$ rather than $(AH \cdots F^-)$. In fact the *unique* linear correlation obtained for HBDs of higher and lower acidities than HF invalidates this hypothesis and provides support for the concept of a single potential well when the proton is moved between the oxygen and the fluorine atoms (94a). From the limited data available it appears that the order of $\Delta H_D^\circ$ for a series of acids AH of comparable gas-phase acidity should be in the order of the electronegativities or group electronegativities of A, specifically, $F > O > N \sim C > S$. Charge delocalization in the incipient anion of phenol and carboxylic acids reduces their hydrogen bonding ability as compared to alcohols.
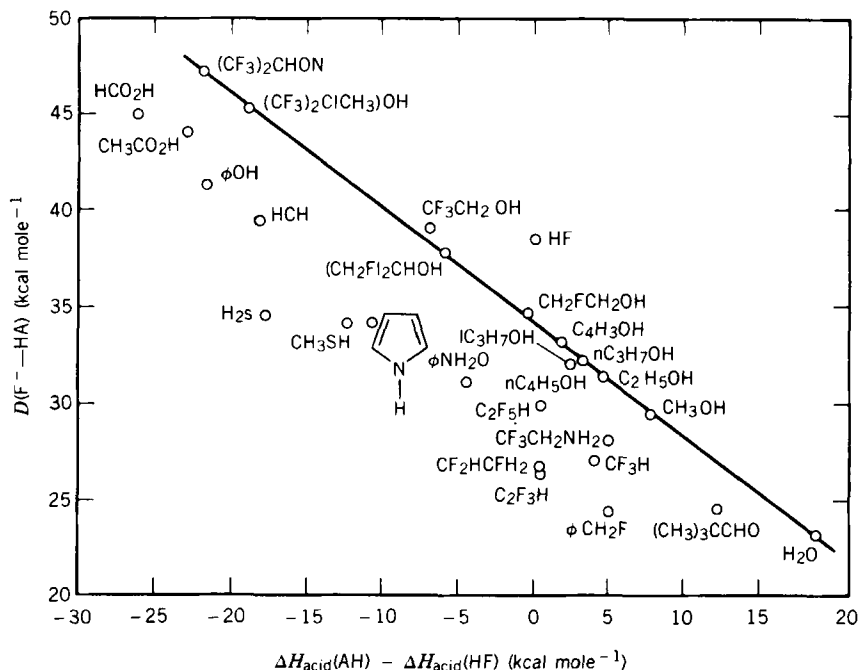
**Figure 18**   Correlation of dissociation enthalpies of the ionic hydrogen bonds with $F^-$ versus gas-phase acidities of the hydrogen bond donors (AH in the original paper). The line has a slope of $-0.59$. Reprinted with permission from J. W. Larson and T. B. McMahon, *J. Am. Chem. Soc., 104,* 5848 5849 (1982). Copyright 1983 American Chemical Society.

It seems that there is a connection between the magnitude of the slope of the relationship between hydrogen bonding versus gas-phase proton transfer and the strength of the created hydrogen bond. For example, the strong gas-phase hydrogen bonding with $F^-$ gives a $-0.59$ slope, whereas the slope is only about $-0.2$ for the weakly interacting $Cl^-$ (94c). A comparative study of $OH\cdots F^-$, $OH\cdots Cl^-$, and $OH\cdots I^-$ systems confirms this trend (170). For cationic hydrogen bonding the weak $SH^+\cdots O$ interaction leads to a slope of $-0.16$, to be compared with $-0.43$ for the strong $OH^+\cdots N\equiv C$ interaction (see Table 9, where intermediate cases are also given). This connection was shown to extend to neutral systems for which $\Delta H_D^{\circ}$ values measured in $CCl_4$ are relatively small, leading to a slope of about $0.1$ (161b). For the systems $OH^+\cdots O$, $NH^+\cdots O$, $OH\cdots O$, and $OH\cdots N$, one continuous curve of slope decreasing with $\Delta H_D^{\circ}$ can be drawn through all the data points bridging the gap between the gas phase and the solution.

The formation of clusters in the gas-phase consisting of one ion attached to more than one solvent molecule is a further step in the description of

solvation. Meot-Ner has analyzed the significance of the process

$$BH^+ + 4H_2O \rightarrow BH^+ \cdots (H_2O)_4 \tag{35}$$

with regard to the proton affinity of B, the monohydration, and the bulk hydration of $BH^+$ (124). We use here the Meot-Ner convention of *attachment* rather than our *dissociation* processes.

The variation of enthalpy for the attachment of four $H_2O$ molecules (Process 35), $\Delta H^\circ_{0,4}$ was shown to be proportional to the variation of enthalpy for the attachment of one $H_2O$ molecule for a variety of protonated organic bases. The proportionality factor, $\Delta H^\circ_{0,4}/-\Delta H^\circ_D$, is 2.8 for oxoniums and monoprotonic tertiary ammoniums and pyridiniums and 3.1 for polyprotonic primary and secondary ammoniums. Since $\Delta H^\circ_D$ is linear with $PA(B)$ (see Table 9), $\Delta H^\circ_{0,4}$ may be calculated from $PA(B)$. The standard deviation between the experimental and predicted values is 5.5 kJ mole$^{-1}$ and is smaller than the estimated experimental error. Since specific ion/solvent interactions are significant only in the first few solvation steps, the variations in $\Delta H^\circ_{0,4}$ should approach the variations of the bulk water solvation enthalpy. In other words, the difference between the two terms should be constant. For oxygen (alcohols, ethers, and carbonyls) and nitrogen (amines and pyridines) bases, mostly alkyl substituted, Meot-Ner showed that

$$\Delta_{solv}H^\circ(BH^+) - \Delta H^\circ_{0,4} = -112 \pm 8\,kJ\,mole^{-1} \tag{36}$$

This leads also to a constant value for the enthalpy of solvation of $BH^+ \cdots 4H_2O$. Taking into account the enthalpy of vaporization of four moles of water, one obtains

$$\Delta_{solv}H^\circ(BH^+ \cdots 4H_2O) - \Delta H^\circ_{0,4} = -288 \pm 8\,kJ\,mole^{-1} \tag{37}$$

regardless of the nature and size of the core ion.

For ions containing an aromatic ring 21 kJ mole$^{-1}$ should be added to $\Delta_{solv}H^\circ(BH^+ \cdots 4H_2O)$. This reflects the inefficient solvation associated specifically with the aromatic cations. On the other hand $\Delta_{solv}H^\circ(M^+ \cdots 4H_2O)$, with $M^+ = H^+$ or alkali metal cation, is better reproduced if the calculated value is made more negative. The rough constancy of $\Delta_{solv}H^\circ(BH^+ \cdots 4H_2O)$ indicates that compensating variations between the various physical contributions to solvation occur (101).

For a given family of bases B and a given solvating HBA, a linear relationship $\Delta H^\circ_D(BH^+ \cdots HBA)$ versus $PA(B)$ holds. Since $\Delta H^\circ_D$, $\Delta H^\circ_{0,4}$, and $\Delta_{solv}H^\circ(BH^+)$ are linearly related, a linear relationship follows:

$$\Delta_{solv}H^\circ(BH^+) = A_0 + A_1 PA(B) \tag{38}$$
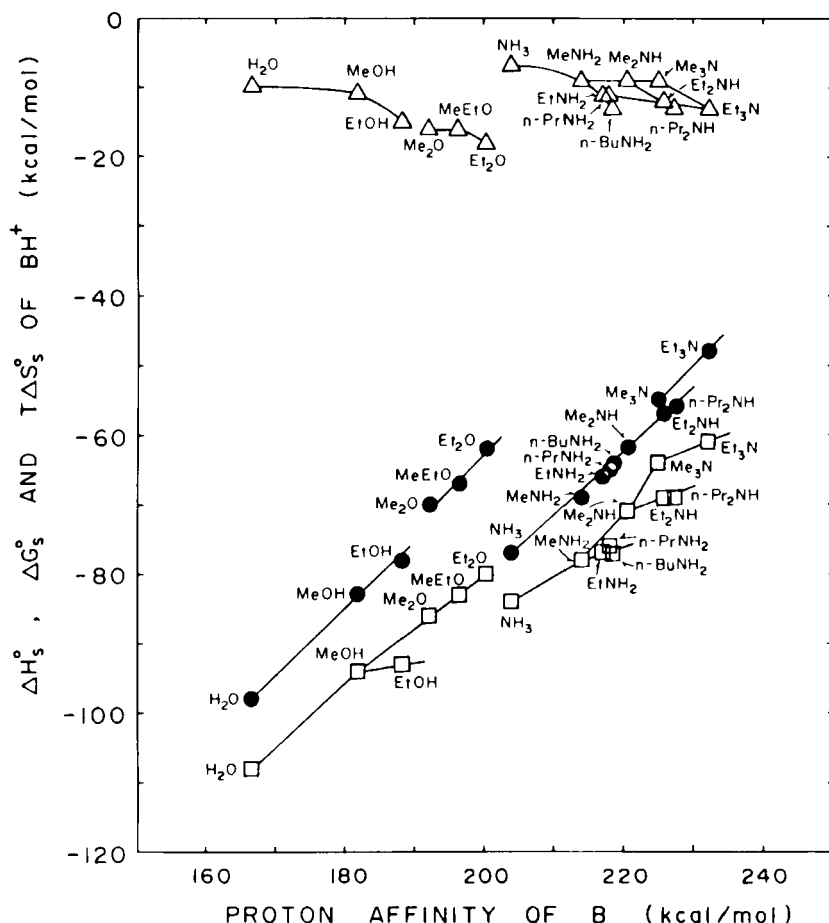
**Figure 19**    Relationship between the enthalpy (□), Gibbs free energy (●), entropy contribution (△) of bulk hydration of $BH^+$, and the proton affinity of B. Ordinate: In the original paper, the subscript "s" stands for solvation. Reprinted from K. Hiraoka, *Can. J. Chem.*, **65**, 1258–1261 (1987). Permission was granted by the National Research Council Canada.

Considering the complex nature of ion solvation phenomena, the predictive accuracy (sd = 6 kJ mole$^{-1}$) of the simple Equation 38 is unexpectedly good (124). Deviations may be also useful in identifying bulk solvation effects.

Simultaneously to Meot-Ner, Hiraoka published a paper (171) dealing with the relationships between $\Delta_{solv}G^\circ(BH^+)$ or $\Delta_{solv}H^\circ(BH^+)$ and $PA(B)$. The plot for a selection of alkyl-substituted O and N bases (Fig. 19) shows a family dependence more pronounced for $\Delta_{solv}G^\circ(BH^+)$ than for $\Delta_{solv}H^\circ(BH^+)$.

It was already noted (Section IV.B.1) that the more electrostatic character of the Gibbs free energy of hydrogen bonding in solution produced enhanced

separations between families when plotted against $PA$ or $GB$. The slopes of the lines corresponding to $\Delta_{solv}G°(BH^+)$ are close to unity. Therefore, the variations in $\Delta_{solv}G°(BH^+)$ almost cancel the variations in $PA(B)$ or $GB(B)$ (see Equation 30). Since the solvation of the neutral bases are roughly constant (1g), the basicities in water $(pK_a)$ of alkyl-substituted compounds are squeezed in a small range within a family. For $\Delta_{solv}H°(BH^+)$, Meot-Ner found slopes ranging from 0.84 to 0.64 (124), so a partial compensating effect occurs with $PA(B)$. The explanation for the small range of enthalpies of proton transfer in water in each series in Fig. 19 resides in the additional compensation occurring from the $\Delta_{solv}H°(B)$. The heteroatomic substituent effect appears to be less attenuated by the solvent than the alkyl substituent effect (133a). Taking the pyridine series as a model, it seems that, in general, for heteroatomic substitution there is less compensation of the intrinsic basicity by $BH^+$ hydration (the variable hydration of B also plays a role) (111a).

## V.   THE PRINCIPAL COMPONENT ANALYSIS APPROACH

The philosophies of the multilinear regression (MLR) and the principal component (PC) analysis have been frequently opposed (172). The MLR analysis needs parameters assumed to be exactly known and a priori relevant to the data set under examination. In this sense MLR analysis may be called a "hard model" (173). Conversely, in the PC analysis no assumption about the relevance of the variables is required, since this relevance is obtained from the statistical analysis. For this reason this treatment is given the epithet soft as for the soft independent modeling of class analogy (SIMCA) method (173). In fact, the softness of the PC analysis claimed by the chemometricians has some practical limits. The database is experimentally limited in both variables and objects and is intuitively selected (the "chemical feeling"). Furthermore, the PC analysis leads to a linear first-order model. Thus, both the database and the model impose a priori implicit constraints. Although the factors or components obtained from the PC analysis are pure mathematical constructs and do not necessarily embody a direct physical significance as in the MLR analysis, the advantage is that an otherwise hidden physical or chemical interpretation will emerge.

In their analysis of condensed-phase basicity, Drago and coworkers (22) and the Kamlet–Taft group (39a, 40a, 41) have shown that two parameters are necessary to correlate thermodynamic and spectroscopic BDPs.

We have contemplated a PC analysis of widely different basicity scales in order to check independently the dimensionality (174) of the various interactions relevant to the basicity concept (153).

## A. Condensed-Phase Basicity Scales

Because of the prominent role played by acidity and basicity in solute–solvent interactions, our study (153) focused on molecules commonly used as solvent. We believe, however, that the results summarized hereafter are of broader applicability.

After examining more than 50 BDPs related to hydrogen bonding, proton transfer, and interactions with hard and soft Lewis acids, a data matrix (less than 10% missing data) consisting of 10BDPs (columns or variables) and 22 bases (lines or objects) was selected. A preliminary step consisted in the analysis of a $10 \times 13$ *full* normalized-data matrix. The information theory, taking into account the experimental error, allowed the classification of the 10 BDPs according to a decreasing order of complementary information brought to the total information contained in the matrix. This classification is given in Table 10.

Seven basicity scales contain all the information of the initial matrix. The other scales bring only redundant informations. If we consent to a loss of 7% of

TABLE 10

Classification of the 10 Basicity Scales According to the Decreasing Order of Complementary Information Brought to the Total Information Contained in the $10 \times 13$ Matrix

| Number[a] | Basicity Scale | Percent Complementary Information | Percent Cumulated Complementary Information |
|---|---|---|---|
| 1 | $-\Delta H_{BF_3}^{\circ}$ | 29 | 29 |
| 2 | $pK_{HB}$ | 21 | 50 |
| 3 | $\Delta \nu_{PFP}$ | 18 | 68 |
| 4 | $-\Delta H_i$ | 16 | 84 |
| 5 | $\Delta \nu_{PhOH}$ | 9 | 93 |
| 6 | $\beta$ | 4 | 97 |
| 7 | $-\Delta H_{PFP}^{\circ}$ | 3 | 100 |
| 8 | $-\Delta H_{I_2}^{\circ}$ | 0 | 100 |
| 9 | $-\Delta H_{SbCl_5}^{\circ}$ | 0 | 100 |
| 10 | $\log K_{I_2}$ | 0 | 100 |

[a]Key: 1—heat of complexation with boron trifluoride; 2—cologarithm of the equilibrium constant of hydrogen bonding to *p*-fluorophenol (PFP); 3—IR frequency shift for the PFP OH group; 4—heat of transfer from $CCl_4$ to $HSO_3F$; 5—IR frequency shift for the phenol OH group; 6—the Kamlet–Taft hydrogen-bond acceptor parameter; 7—heat of hydrogen bonding to PFP; 8  heat of complexation with iodine; 9—heat of complexation with antimony pentachloride; 10—logarithm of the equilibrium constant of complexation with iodine.

TABLE 11

Contributions of the Five Independent Factors to the Total
Variance of the 5 × 22 Matrix

| | Dimensionality | | | | |
|---|---|---|---|---|---|
| Factor $F$ | 1 | 2 | 3 | 4 | 5 |
| % variance | 82.14 | 12.18 | 4.51 | 1.00 | 0.17 |
| Cumulated % variance | — | 94.32 | 98.83 | 99.83 | 100.00 |

complementary information brought by $\beta$ and $-\Delta H_{PFP}^{\circ}$, we can enlarge the set of bases to 22.

Results of the PC analysis on the 5 × 22 matrix, which contains new bases of widely different strength, are given in Table 11.

The first factor ($F_1$) explains 82% of the total variance, the second ($F_2$) 12%, and the third ($F_3$) 4.5%. The first two factors, $F_1$ and $F_2$, bring most of the chemical information (ca. 94% of the variance), but considering the general precision of the data, $F_3$ is certainly not only due to the experimental "noise".

## B. Physical Significance of the Principal Factors: Relationships with Intrinsic Gas-Phase Basicity Scales

A physical significance is clearly distinguishable for $F_1$ and $F_2$. The $-\Delta H_{BF_3}^{\circ}$ scale correlates with $F_1$ ($r = .92$) but is quasi-orthogonal with $F_2$ ($r = .02$). Therefore, $F_1$ contains chemical effects already evidenced for $-\Delta H_{BF_3}^{\circ}$, namely, a balanced blend of covalent and electrostatic characters (24). Factor $F_2$ takes its origins in the second most informative scale $pK_{HB}$ ($r = .72$), one of the first five basicity scales from which $\beta$ was averaged (38a). The largely electrostatic character of $\beta$ is apparent from the fact that a coordinate covalency parameter $\xi$ should be used in complement to describe a wide variety of basicity-dependent phenomena (41). It can be inferred that $F_2$ includes a large electrostatic contribution. Nevertheless, we did not find any reasonable combination of molecular properties—dipole moments (electrostatic effect), ionization or highest-occupied molecular orbital (HOMO) energies (covalency), and molar refractivities (polarizability)—that might explain $F_1$ or $F_2$. On the other hand, we obtained meaningful correlations with intrinsic basicity scales in the gas phase.

Proton affinity is explained by a linear combination of $F_1$ and the molecular polarizability $\alpha$(ahc) calculated according to the method of Miller and Savchick (175):

$$PA = (102.2 \pm 6.7)F_1 + (6.5 \pm 1.1)\alpha(\text{ahc}) + 815.3 \qquad (39)$$

where $F_1$ is dimensionless, $\alpha(\text{ahc})$ is in $(10^{-1} \text{ nm})^3$, $PA$ is in $\text{kJ mole}^{-1}$, $n = 18$, $r = .9828$, and $\text{sd} = 11.0$.

Proton affinity corrected for enhanced polarizability appears to be a good empirical descriptor of $F_1$. Morokuma (64) has shown that the largest components of $PA$, the covalent (charge transfer) and electrostatic interactions, are of similar magnitude. This confirms that $F_1$ embodies a blend of electrostatic and covalent contributions to the acid–base interaction. A logical step was to look for an empirical descriptor of electrostatic interaction. The bonding of organic bases to alkali-metal cations is governed largely by electrostatic interaction. Indeed, the potassium-ion affinity (78d) is collinear with $F_2$:

$$K^+(A) = (143.1 \pm 18.1)F_2 + 110.5 \tag{40}$$

where $F_2$ is dimensionless, $K^+(A)$ is in $\text{kJ mole}^{-1}$, $n = 8$, $r = .9553$, and $\text{sd} = 7.3$.

The addition of a polarizability term in Equation 40 does not improve the fit. The polarizability effect is predicted to be weaker for $K^+$ bonding than for protonation because of the larger distance between the charge and the induced dipole. Furthermore, the protonation induces more transfer of charge than metal cationization (84, 165, 166), thus rendering the polarizability stabilisation more effective.

Factors $F_1$ and $F_2$ appear to be practically free from steric strain, which seems to be accounted for by $F_3$ (153).

## C. A New Approach to Quantification of the Electrostatic–Covalent Contributions to the Acid–Base Interaction

For most solution $BDP$s for which polarizability is negligible, and provided severe steric strains are not present, we expect correlations of the form

$$BDP = BDP_0 + S_1F_1 + S_2F_2 \tag{41}$$

By examining a large number of $BDP$s we have found that $S_1$ and $S_2$ in Equation 41 (the sensitivities to $F_1$ and $F_2$, respectively) vary widely. Each $BDP$ may be represented by a point of coordinates $S_1$ and $S_2$ in the Cartesian plane. In polar coordinates, the corresponding vector has a module $\rho = (S_1^2 + S_2^2)^{1/2}$ and is at angle $\theta = \tan^{-1} S_2/S_1$ with the axis $S_1$.

If $\theta$ is close to $0°$, the $BDP$ presents a character similar to that of $F_1$ (electrostatic + covalent). An increase of $\theta$ corresponds to a larger dependence on $F_2$ and a more electrostatic character.

Negative values of $\theta$ arise from $S_2 < 0$ and correspond to substracting a part of electrostatic component to $F_1$. This originates from a more covalent character of the *BDP*.

Our analysis of reaction enthalpies with acids of a priori different behaviors gives the order of increasing electrostatic (decreasing covalent) character: $acid(\theta/^\circ)$; $I_2(-51)$; $SO_2(-45)$; $HSO_3F(-22)$; $BF_3(-4)$; $(CF_3)_2CHOH(29)$; $SbCl_5(40)$; 4-F phenol(42); $CHCl_3(60)$. This is in agreement with the classification obtained from the Drago's $E_A/C_A$ ratio (1e, 22) and the Kamlet–Taft $b/e$ ratio (41) ($b$ and $e$ are the sensitivities to $\beta$ and $\xi$, respectively).

For a given acid, the Gibbs free energy always lead to a greater $\theta$ value than does the enthalpy. The larger electrostatic character of $\Delta G^\circ$ as compared to $\Delta H^\circ$ implies a larger covalent character of $\Delta S^\circ$. The entropy of the acid–base interactions of intermediate strength can be viewed as the sum of two terms (19, 176):

- A large negative term $\Delta S_{tr+rot}$ due to the loss of translational and rotational degrees of freedom by the system that is almost constant.
- A smaller positive term $\Delta S_{vib+int\ rot}$ that was shown to arise essentially from vibrational and internal rotational degrees of freedom due to the formation of the donor–acceptor bond. This contribution is essentially variable for intermediate strength complexes due to the low variable frequencies involved and decreases when the donor–acceptor bond is stiffened.

A constant $\Delta S^\circ$ can be anticipated for extremely weak and extremely strong interactions (176). This leads to a same $\theta$ value for $\Delta G^\circ$ and $\Delta H^\circ$.

Hydrogen bonding is an especially instructive case to treat using Equation 41. Together with the thermodynamic parameters, spectroscopic data are also frequently available. We have chosen as examples three reference acids - p-fluorophenol, 2,2,2-trifluoroethanol, and cyclohexanol—for which comprehensive sets of $\Delta G^\circ$, $\Delta H^\circ$, $\Delta S^\circ$, and $\Delta v(OH)$ of hydrogen bonding are available. These properties are characterized by their $\theta$ angle, the variations of which can be visualized on a fan-shaped display (Fig. 20).

We observe that $\theta$ or the electrostatic character increases in the following order: $-\Delta S^\circ < \Delta v(OH) < -\Delta H^\circ < -\Delta G^\circ$.

The preceding remarks suggest that the high sensitivity of $\Delta S^\circ$ to covalency is related to variations of stiffness of the hydrogen bond. On the other hand, the electrostatic effect, which is a long-range interaction, is a minor contribution to $\Delta S^\circ$. So, $\Delta S^\circ$ depending on a short-range interaction (covalency) appears as a "probe" localized on the hydrogen bond.

The O—H bond, contiguous to the hydrogen bond, has a stretching frequency that is a little more sensitive to long-range interactions (increased
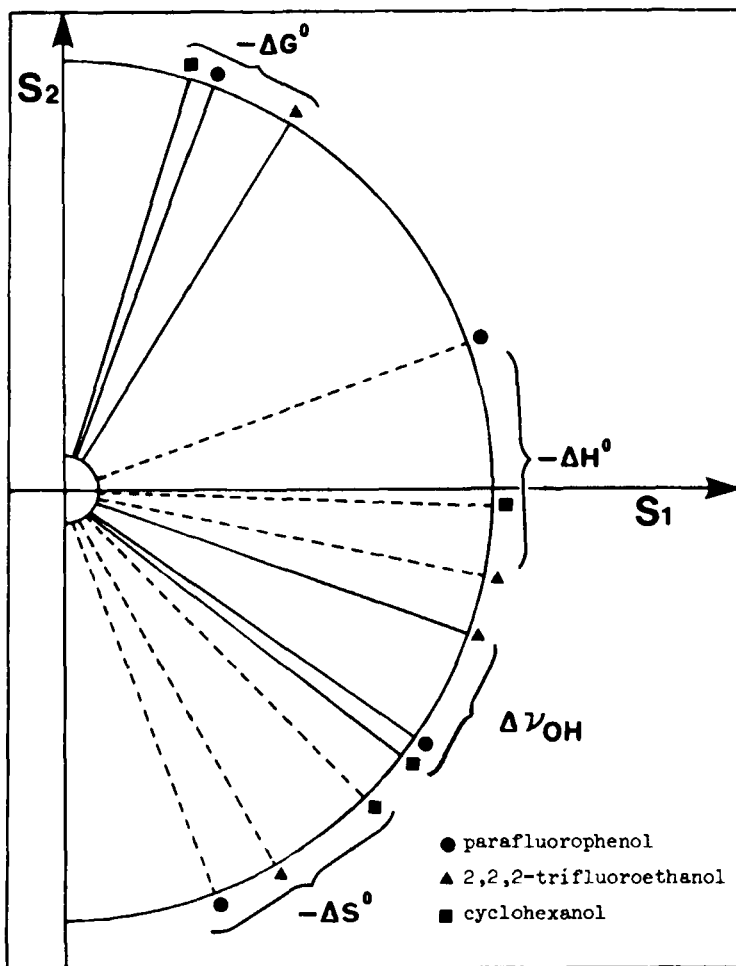
**Figure 20**   Fan-shaped display of the electrostatic–covalent character of hydrogen-bond basicity-dependent properties. The electrostatic contribution to a BDP increases with $\theta$. Reprinted with permission from P.-C. Maria, J.-F. Gal, J. de Franceschi, and E. Fargin, *J. Am. Chem. Soc.*, *109*, 483–492 (1987). Copyright 1987 American Chemical Society.

dependence on electrostatic effect) as compared to $\Delta S°$. Therefore, $\Delta v(OH)$ scales exhibit higher $\theta$ values than do $\Delta S°$ scales.

Enthalpies lie near the $S_1$ axis (small negative or positive $\theta$ values). As compared to $\Delta S°$ or $\Delta v(OH)$, $\Delta H°$ is a more global measure of both local and long-range components of the acid–base interaction. The dominant covalent contribution to $\Delta S°$ is substracted from the electrostatic + covalent contri-

butions to $\Delta H°$, giving a dominant electrostatic behavior to $\Delta G°$ (high $\theta$ values). From the examination of $\theta$ values, subtle structural and medium effects on methanol $\Delta v(OH)$ have also been pointed out (153).

An interesting application of $\theta$ is that two BDPs will be linear with each other only if their respective $\theta$ values are the same or nearly the same (same $S_2/S_1$ ratio). The applicability of the $\beta$ scale within the framework of a general linear solvation energy (LSE) equation have been developed in the field of chemical and biological applications, including the interpretation of partition coefficients and solubilities in water, organic, and biological media (40, 41,177). Gibbs free energies of hydrogen bonding contribute to most of these solvent or solute properties. For basic solvents or solutes, this contribution is assumed to be represented by the $\beta$ term in the LSE equation.

Indeed, the $\theta$ value obtained for $\beta$ falls in the middle of the range covered by those calculated from $\Delta G°$ of hydrogen bonding corresponding to various reference acid–solvent systems (Table 12).

In fact, most of the reference acids–solvent systems studies so far (48) exhibit a behavior very similar to $\beta$, as the corresponding range of $\theta$ values is $(68 \pm 5)°$. The NH and CH acids give systematically larger $\theta$ values in the range $(82 \pm 4)°$. This explains why plots of log $K$ (OH acid) show family-dependent behavior with respect to log $K$(NH acid) or log $K$(CH acid) (178). On the other hand, 4-fluorophenol studied in 1,2-dichloroethane or dichloromethane exhibits rather low $\theta$ values: 57 and 53°, respectively. This has been ascribed to the reduced electrostatic contribution due to the increased solvent dipolarity.

TABLE 12

Comparison of $\theta$ Values Based on $\Delta G°$ for Some Hydrogen-Bonding Processes with that obtained for $\beta$

| Reference Acid | Solvent | $\theta(°)$ | sd $(°)^a$ |
|---|---|---|---|
| Diphenylamine | $CCl_4$ | 86 | 2 |
| Indole | $CCl_4$ | 82 | 1 |
| 4-Fluorophenol[b] | $CCl_4$ | 70 | 1 |
| Water | $CCl_4$ | 69 | 5 |
| 4-Nitrophenol | $CCl_4$ | 67 | 2 |
| $\beta$ | — | 67 | 2 |
| Ethanol | $CCl_4$ | 67 | 3 |
| 1,1,1,3,3,3-Hexafluoro-2-propanol | $CCl_4$ | 64 | 2 |
| 4-Fluorophenol | $CH_2Cl_2$ | 53 | 3 |

$^a$Calculated from: $sd(\theta) = sd(S_2/S_1)\,180/[1 + (S_2/S_1)^2]\pi$

with: $sd(S_2/S_1) = (|S_2|/|S_1|)([sd(S_1)]^2/S_1^2 + [sd(S_2)]^2/S_2^2)^{1/2}$

$^b$The p$K_{HB}$ scale.

In the case of $CH_2Cl_2$, a weak CH acid ($\alpha = 0.30$) (39), hydrogen bonding to the solvent, may also play a role.

The $\theta$ angle has been utilized as a tool for selecting data in order to construct a scale of solute hydrogen bond basicity for over 500 compounds based on $\log K$ values for the hydrogen bonding of solutes against reference acids in $CCl_4$(46c).

## VI. CONCLUSION

One major motivation for the gas-phase acidity and basicity studies was to disentangle the intrinsic structural effects that govern the acid–base interactions in the condensed phase. The aim of this review was to show some ways that connect gas-phase proton and other ion affinity scales to solution scales (proton transfer, hydrogen bonding, and Lewis basicity). We have used both the direct correlation and PC analysis.

Considering series similar to those used to define Hammett-type substituent constants, the direct correlations of proton transfer scales, solution against gas phase, are in general fairly linear, showing that the classical substituent effect (field, induction and resonance) are closely proportional although attenuated on going from the gas phase to the solution. Within the Hammett series the reaction site is constant and the observed correlations result from the regular trend in the ion–neutral differential solvation. Deviations are observed when the substituents interact strongly with the solvent.

The greatest discrepancies arise when substitution, particularly by alkyl groups, is close to the reaction center. This is explained in terms of enhanced polarizability effect in the gas phase.

For the large aromatic hydrocarbons leading to highly charge delocalized ions the constant differential solvation produce a line of unit slope in a solution–gas-phase plot. The apparent scatter for compounds bearing different acidic or basic functions may be rationalized in terms of specific solvation.

Proton affinities have been frequently used as a standard basicity scale to correlate various basicity dependent properties. We have shown that precise linear relationships are obtained with solution data, provided $PA$ values are corrected for enhanced polarizability.

The correlation of $PA_{corr}$ with $\beta$ is particularly impressive. The observed family-dependent plot has been interpreted in terms of different electrostatic covalent contributions to proton transfer and hydrogen bonding. Such family dependent relationships were also observed for plots of gas-phase metal-

cation affinities versus $PA$ values and interpreted on grounds of the high electrostatic behavior of the bonding with metal ions as compared to the balanced electrostatic–covalent character of the bonding with the proton.

The absence of a significant family dependence when methyl cation affinities are plotted against $PA$ values leads us to consider that these two quantities have a similar electrostatic–covalent character.

The PC analysis, a complementary approach of the correlation analysis, allowed us to establish the dimensionality of the various properties relevant to the basicity concept. The first two factors, accounting for 94% of the total variance in the data, were shown to correlate respectively with $PA_{corr}$ and the potassium ion affinity. These factors were used as explicative variables in regressions of widely different BDPs, the sensitivities to $F_1$ and $F_2$ characterizing the electrostatic–covalent nature of the BDP. The electrostatic–covalent nature of any BDP depends on the reference acid, the observable physical effects, and the medium. To obtain extended solution basicity scales, one has to combine several of the numerous available scales provided they are adequately similar. The $F_1, F_2$ analysis may be used as a tool for testing the similarity between BDPs.

The direct comparison of gas-phase and condensed-phase properties allows to extract what is due to bulk solvation. Gas-phase studies of small clusters formed between ions and one or several solvating molecules have been fruitful in describing the step-by-step ion solvation. The relative solvation enthalpies by four water molecules reproduce closely the relative bulk solvation enthalpies of alkylated onium ions. These enthalpies exhibit family-dependent relationships with $PA$. The attenuation of the substituent effects on proton transfer, in water as compared to the gas phase, results to a great extent from a compensation of the variations in $PA$ by the opposite variations in solvation enthalpies of the protonated species.

There is little doubt that the use of specialized instruments, dedicated to gas-phase studies, not only of ion–molecule reactions but also of the interaction between neutrals, will continue to supply data very useful for the understanding of interactions in solution.

It is worth mentioning studies of hydrogen bonded systems between two or more neutral molecules in the gas phase for they provide structural (179) and spectroscopic (179, 180) parameters of isolated adducts.

A step toward a better understanding of the transition between hydrogen bonding and proton transfer has been made recently by a stepwise clustering of $NH_3$ molecules onto hydrogen halides (181). The relationships between IR shifts in the gas phase, in $CCl_4$, and in a low-temperature noble gas–solid matrix (182) showed that the structural effects on hydrogen bonding are very similar in these three media. Although relatively simple systems concerning Lewis acid–base (183a) and hydrogen bonding (183b, 184) interactions have

been studied so far using only the noble gas matrix technique, we believe these studies will contribute to a better description of the acid base interaction between neutrals in inert media.

In writing this chapter we hope to have convinced the reader that gas-phase experiments are not simply exotic techniques with little link with the real world but that they bring useful data and concepts for the bench chemist.

## ACKNOWLEDGEMENTS

## REFERENCES AND NOTES

1. (a) L. P. Hammett, *Physical Organic Chemistry*, 2nd ed., McGraw-Hill, New York, 1970; (b) R. G. Pearson, *Hard and Soft Acids and Bases*, Dowden Hutchinson and Ross, Strousburg, PA., 1973; *J. Chem. Educ.*, *64*, 561–567 (1987); (c) J. Hine, *Structural Effects on Equilibria in Organic Chemistry*, Wiley, New York, 1975; (d) V. Gutmann, *The Donor–Acceptor Approach to Molecular Interactions*, Plenum, New York, 1978; (e) R. S. Drago, *Coord. Chem. Rev.*, *33*, 251 277 (1980); (f) W. B. Jensen, *The Lewis Acid Base Concepts. An Overview*, Wiley, New York, 1980; (g) R. W. Taft, *Progr. Phys. Org. Chem.*, *14*, 247 350 (1983); (h) R. W. Taft and R. D. Topsom, ibid., *16*, 1–83 (1987).

2. (a) L. P. Hammett, *J. Am. Chem. Soc.*, *59*, 96–103 (1937); (b) L. P. Hammett, *Physical Organic Chemistry*, McGraw-Hill, New York, 1940.

3. O. Exner, in *Correlation Analysis in Chemistry. Recent Advances*, N. B. Chapman and J. Shorter, Eds., Plenum, New York, 1978, Chap. 10.

4. L. G. Hepler and E. M. Wooley, in *Water. A Comprehensive Treatise*, Vol. 3, F. Franks, Ed., Plenum, New York, 1973.

5. (a) T. Matsui and L. G. Hepler, *Can. J. Chem.*, *54*, 1296–1299 (1976); (b) see also the chapter by O. Exner in this volume (*Progr. Phys. Org. Chem.*, *17*) for a discussion of Hepler's theory.

6. (a) R. W. Taft, in *Proton-Transfer Reactions*, E. F. Caldin and V. Gold, Eds., Chapman and Hall, London, 1975, Chap. 2.; (b) E. M. Arnett, ibid., Chap. 3.; (c) R. W. Taft, in *Kinetics of Ion–Molecule Reactions*, P. Ausloos, Ed., Plenum, New York, 1979, pp. 271–293.; (d) C. R. Moylan and J. I. Brauman, *Ann. Rev. Phys. Chem.*, *34*, 187–215 (1983); (e) R. S. Mason, in *Thermochemistry and its Applications to Chemical and Biochemical Systems*, M. A. V. Ribeiro da Silva, Ed., Reidel, Dordrecht, 1984, pp. 627 651.

7. (a) G. G. Smith and D. A. K. Jones, *J. Org. Chem.*, *28*, 3496–3499 (1963); (b) G. G. Smith and D. V. White, ibid., *29*, 3533–3535 (1964); (c) G. G. Smith, K. K. Lum, and J. Posposil, ibid., *34*, 2090–2095 (1969).

8. G. Chuchani, I. Martin, A. Rotinov, J. A. Hernández, and N. Reikonnen, *J. Phys. Chem.*, *88*, 1563–1566 (1984) and references cited therein, see also G. Chuchani and R. M. Dominguez, ibid., *93*, 203–205 (1989).

9. (a) H. B. Amin and R. Taylor, *J. Chem. Soc., Perkin II*, 1802–1803 (1975); (b) R. Taylor, *J.

*Chem. Res. (S)*, 318–319 (1985); (c) R. August, I. McEwen, and R. Taylor, *J. Chem. Soc. Perkin II*, 1683–1689 (1987).

10. M. M. Bursey, in *Advances in Linear Free Energy Relationships*, N. B. Chapman and J. Shorter, Eds., Plenum, London, 1972.

11. P. Love, R. B. Cohen, and R. W. Taft, *J. Am. Chem. Soc.*, **90**, 2455–2462 (1968).

12. (a) D. D. Perrin, *Dissociation Constants of Organic Bases in Aqueous Solution*, Butterworth, London, 1965; (b) E. P. Serjeant and B. Dempsey, *Ionisation Constants of Organic Acids in Aqueous Solution*, Pergamon, Oxford, 1979.

13. A. Albert and E. P. Serjeant, *The Determination of Ionisation Constants. A Laboratory Manual*, 3rd ed., Chapman and Hall, London, 1984.

14. (a) R. A. Cox and K. Yates, *Can. J. Chem.*, **61**, 2225–2243 (1983); (b) A. Bagno, G. Scorrano, and R. A. More O'Ferrall, *Rev. Chem. Intermed.*, **7**, 313–352 (1987).

15. (a) J. W. Larson and L. G. Hepler, in *Solute–Solvent Interactions*, J. F. Coetzee and C. D. Ritchie, Eds., Marcel Dekker, New York, 1969, Chap. 1; (b) J. J. Christensen, R. M. Izatt, D. P. Wrathall, and L. D. Hansen, *J. Chem. Soc. (A)*, 1212–1223 (1969); (c) F. M. Jones and E. M. Arnett, *Progr. Phys. Org. Chem.*, **11**, 263–322 (1974).

16. (a) O. Exner, *Progr. Phys. Org. Chem.*, **10**, 411–482 (1973); (b) O. Exner, *Collect. Czech. Chem. Commun.*, **40**, 2762–2780 (1975).

17. (a) F. G. Bordwell, *Acc. Chem. Res.*, **21**, 456–463 (1988); (b) R. W. Taft and F. G. Bordwell, ibid., 463–469.

18. E. M. Arnett and K. G. Venkatasubramaniam, *J. Org. Chem.*, **48**, 1569–1578 (1983).

19. E. N. Gur'yanova, I. P. Gol'dshtein, and I. P. Romm, *Donor–Acceptor Bond*, Wiley, New York, 1975.

20. W. B. Jensen, *The Lewis Acid–Base Concepts. An Overview*. Wiley, New York, 1980.

21. C. Reichardt, *Solvents and Solvent Effects in Organic Chemistry*, VCH, Weinheim, 1988 (2nd revised and enlarged edition).

22. R. S. Drago, *Struct. Bonding*, **15**, 73–139 (1973).

23. (a) V. Gutmann, *Coordination Chemistry in Non-Aqueous Solutions*, Springer-Verlag, Vienna, 1968; (b) V. Gutmann, *Coord. Chem. Rev.*, **15**, 207–237 (1975).

24. P.-C. Maria and J.-F. Gal, *J. Phys. Chem.*, **89**, 1296–1304 (1985).

25. P.-C. Maria, J.-F. Gal, L. Elégant, and M. Azzaro, *Thermochim. Acta*, **115**, 67–81 (1987).

26. The $-\Delta H_{BF_3}$ values for 75 nonprotogenic solvents are gathered in reference 24. Data on other families of compounds can be found in papers cited under section "Application" in reference 25. A complete list including unpublished results is available from the authors.

27. H. C. Brown, *J. Chem. Soc.*, 1248–1268 (1956).

28. P.-C. Maria, J.-F. Gal, and R. W. Taft, *New J. Chem.*, **11**, 617–621 (1987).

29. C. Laurence, M. Queignec-Cabanetos, T. Dziembowska, R. Queignec, and B. Wojtkowiak, *J. Am. Chem. Soc.*, **103**, 2567–2573 (1981).

30. (a) I. Persson, *Pure Appl. Chem.*, **58**, 1153–1161 (1986); (b) I. Persson, M. Sandström, and P. L. Goggin, *Inorg. Chim. Acta*, **129**, 183–197 (1987).

31. (a) G. C. Pimentel and A. L. McClellan, *The Hydrogen Bond*, Freeman, San Francisco, 1960; (b) S. N. Vinogradov and R. H. Linnell, *Hydrogen Bonding*, Van Nostrand Reinhold, New York, 1971; (c) M. D. Joesten and L. J. Schaad, *Hydrogen Bonding*, Marcel Dekker, New York, 1974; (d) P. Schuster, G. Zundel, and C. Sandorfy Eds., *The Hydrogen Bond. Recent Developments in Theory and Experiments*, North-Holland, Amsterdam, 1976.

32. (a) A. Buckley, N. B. Chapman, M. R. J. Dack, J. Shorter, and H. M. Wall, *J. Chem. Soc. (B)*, 631–638 (1968). (b) N. B. Chapman, J. R. Lee, and J. Shorter, ibid., 769–778 (1969).

33. I. A. Koppel and V. A. Palm, in *Advances in Linear Free Energy Relationships*, N. B. Chapman and J. Shorter, Eds., Plenum, London, 1972, Chap. 5.

34. A. G. Burden, G. Collier, and J. Shorter, *J. Chem. Soc., Perkin II*, 1627–1632 (1976).

35. I. A. Koppel and A. I. Paju, *Org. React. (Tartu)*, *11*, 121–136 (1974).

36. M. H. Aslam, G. Collier, and J. Shorter, *J. Chem. Soc., Perkin II*, 1572–1576 (1981).

37. (a) M. Berthelot, G. Grabowski, and C. Laurence, *Spectrochim. Acta, Ser. A*, *41*, 657–660 (1985); (b) M. Berthelot, J.-F. Gal, C. Laurence, and P.-C. Maria, *J. Chim. Phys. Phys. Chim. Biol.*, *81*, 327–331 (1984); (c) M. Berthelot, J.-F. Gal, M. Helbert, C. Laurence, and P.-C. Maria, ibid., *82*, 427–432 (1985).

38. (a) M. J. Kamlet and R. W. Taft, *J. Am. Chem. Soc.*, *98*, 377–383 (1976); (b) R. W. Taft and M. J. Kamlet, ibid., *98*, 2886–2894 (1976).

39. (a) M. J. Kamlet, J.-L. M. Abboud, and R. W. Taft, *Progr. Phys. Org. Chem.*, *13*, 485–630 (1981); (b) M. J. Kamlet, J.-L. M. Abboud, M. H. Abraham, and R. W. Taft, *J. Org. Chem.*, *48*, 2877–2887 (1983).

40. (a) R. W. Taft, J.-L. M. Abboud, M. J. Kamlet, and M. H. Abraham, *J. Solution Chem.*, *14*, 153–186 (1985); (b) M. H. Abraham, R. M. Doherty, M. J. Kamlet, and R. W. Taft, *Chem. Br.*, *22*, 551–554 (1986); (c) M. J. Kamlet, R. M. Doherty, J.-L. M. Abboud, M. H. Abraham, and R. W. Taft, *Chemtech*, 566–576 (1986); (d) M. J. Kamlet and R. W. Taft, *Acta Chem. Scand., Ser. B*, *39*, 611–626 (1985).

41. M. J. Kamlet, J.-F. Gal, P.-C. Maria, and R. W. Taft, *J. Chem. Soc., Perkin II*, 1583–1589 (1985).

42. (a) P. Nicolet and C. Laurence, *J. Chem. Soc., Perkin II*, 1071–1079 (1986); (b) C. Laurence, P. Nicolet, and M. Helbert, ibid., 1081–1090 (1986).

43. (a) D. Gurka and R. W. Taft, *J. Am. Chem. Soc.*, *91*, 4794–4801 (1969); (b) R. W. Taft, D. Gurka, L. Joris, P. von R. Schleyer, and J. W. Rakshys, ibid., *91*, 4801–4808 (1969).

44. (a) A. D. Sherry and K. F. Purcell, *J. Phys. Chem.*, *74*, 3535–3543 (1970); (b) ibid., *J. Am. Chem. Soc.*, *94*, 1853–1857 (1972).

45. The Kamlet-Taft $\alpha$ scale has two Gibbs free-energy components: $\Delta G°$ of transfer of the $Et_4N^+I^-$ ion pair between solvents and $\log k$ for the *tert*-butylchloride solvolysis.

46. (a) M. H. Abraham, P. P. Duce, J. J. Morris, and P. J. Taylor, *J. Chem. Soc., Faraday Trans. 1*, *83*, 2867–2881 (1987); (b) M. H. Abraham, P. P. Duce, P. L. Grellier, D. V. Prior, J. J. Morris, and P. J. Taylor, *Tetrahedron Lett.*, *29*, 1587–1590 (1988); M. H. Abraham, P. L. Grellier, D. V. Prior, P. P. Duce, J. J. Morris, and P. J. Taylor, *J. Chem. Soc., Perkin II*, 699–711 (1989); (c) M. H. Abraham, P. L. Grellier, D. V. Prior, R. W. Taft, J. J. Morris, P. J. Taylor, C. Laurence, M. Berthelot, R. M. Doherty, M. J. Kamlet, J.-L. M. Abboud, K. Sraidi, and G. Guihéneuf, *J. Am. Chem. Soc.*, *110*, 8534–8536 (1988); M. H. Abraham, P. L. Grellier, D. V. Prior, J. J. Morris, P. J. Taylor, C. Laurence, and M. Berthelot, *Tetrahedrons Lett.*, *30*, 2571–2574 (1989).

47. J.-L. M. Abboud, C. Roussel, E, Gentric, K. Sraidi, J. Lauransan, G. Guihéneuf, M. J. Kamlet, and R. W. Taft, *J. Org. Chem.*, *53*, 1545–1550 (1988) and preceding papers in the series.

48. M. H. Abraham, P. L. Grellier, D. V. Prior, J. J. Morris, P. Taylor, P.-C. Maria, and J.-F. Gal, *J. Phys. Org. Chem.*, *2*, 243–254 (1989).

49. (a) M. H. Abraham, *Final Report, Scales of Hydrogen-Bonding Workshop*, London, July 1–3, 1987; (b) M. H. Abraham, G. J. Buist, P. L. Grellier, R. A. McGill, D. V. Prior, S. Olliver, E. Turner, J. J. Morris, P. J. Taylor, P. Nicolet, P.-C. Maria, J.-F. Gal, J.-L. M. Abboud, R. M. Doherty, M. J. Kamlet, W. J. Shuely, and R. W. Taft, *J. Phys. Org. Chem.*, *2*, 540–552 (1989).

50. For the gas-phase reactions the usual standard state is ideal gas, 1 atm, 298.15 K. The change to the recommended new standard-state pressure, 0.1 MPa, is much less than the inaccuracy in the literature values. See R. D. Freeman, *Bull. Chem. Thermodyn.*, *25*, 523–530 (1982).

51. J. E. Bartmess and R. T. McIver, Jr., in *Gas-Phase Ion Chemistry*, Vol. 2, M. T. Bowers, Ed., Academic Press, New York, 1979, Chap. 11.

52. Values for the enthalpies of formation of gaseous ions are almost invariably calculated from ionization or appearance potentials that are applicable at (or have been corrected to) 0 K. In using tabulated $\Delta_f H^\circ$ values, care should be taken for the consistency of data in regard to the convention used, that is, electrons in thermal motion or the so-called "stationary electron" convention.

53  (a) S. G. Lias, J. F. Liebman, and R. D. Levin, *J. Phys. Chem. Ref. Data*, *13*, 695–808 (1984); (b) S. G. Lias, *Gas Phase Basicities and Proton Affinities. Additions and Corrections, 1987*, personal communication.

54. (a) R. S. Mason, in *Thermochemistry and Its Applications to Chemical and Biochemical Systems*, M. A. V. Ribeiro da Silva, Ed., Reidel, Dordrecht, 1984, pp. 601–620; (b) N. G. Adams and D. Smith, *Sci. Prog. Oxford*, *71*, 91–116 (1987).

55. S. T. Graul and R. R. Squires, *Mass Spectrom. Rev.*, *7*, 263–358 (1988).

56. B. J. McIntosh, N. G. Adams, and D. Smith, *Chem. Phys. Lett.*, *148*, 142- 148 (1988).

57. K. P. Wanczek, *in Dynamic Mass Spectrometry*, Vol. 6, D. Price and J. F. Todd, Eds., Heyden, London, 1981, Chap. 2.

58. (a) A. G. Marshall, *Acc. Chem. Res.*, *18*, 316–322 (1985); (b) M. V. Buchanan and M. B. Comisarow, in *Fourier Transform Mass Spectrometry, Evolution, Innovation and Applications*, M. V. Buchanan, Ed., ACS Symposium Series 359, ACS, Washington, D.C., 1987, Chap. 1.

59. I. Santos, D. W. Balogh, C. W. Doecke, A. G. Marshall, and L. A. Paquette, *J. Am. Chem. Soc.*, *108*, 8183- 8185 (1986).

60. J.-F. Gal, P.-C. Maria, and M. Decouzon, *Int. J. Mass Spectrom. Ion Processes*, in press.

61. (a) J. E. Bartmess and R. M. Georgiadis, *Vacuum*, *33*, 149- 153 (1983); (b) M. Decouzon, J.-F. Gal, S. Geribaldi, P.-C. Maria, M. Rouillard, and A. Vinciguerra, *Analusis*, *14*, 471–479 (1986).

62. S. G. Lias, J. E. Bartmess, J. L. Holmes, R. D. Levin, J. F. Liebman, and W. G. Mallard, *J. Phys. Chem. Ref. Data*, Suppl. No. 1 to Vol. 17, 1988.

63. J. E. Bartmess, *The 1987 Gas-Phase Acidity Scale*, personal communication. This document was a prefiguration of the absolute acidity scale in reference 62.

64. K. Morokuma, *Acc. Chem. Res.*, *10*, 294–300 (1977).

65. (a) W. Moffitt, *Proc. Roy. Soc. London, Ser. A*, *202*, 548–564 (1950); (b) J. E. Huheey, *Inorganic Chemistry. Principles of Structure and Reactivity*, 2nd ed., Harper and Row, New York, 1978.

66. (a) J. E. Del Bene, *J. Comput. Chem.*, *6*, 296–301 (1985); (b) T. B. McMahon and P. Kebarle, *J. Chem. Phys.*, *83*, 3919 -3923 (1985); (c) D. J. De Frees and A. D. McLean, *J. Comput. Chem.*, *7*, 321- 333 (1986); (d) C. G. Freeman, J. S. Knight, J. G. Love, and M. J. McEwan, *Int. J. Mass Spectrom. Ion Processes*, *80*, 255–271 (1987).

67. R. W. Taft, J.-L. M. Abboud, F. Anvia, M. Berthelot, M. Fujio, J.-F. Gal, A. D. Headley, W. G. Henderson, I. Koppel, J. H. Qian, M. Mishima, M. Taagepera, and S. Ueji, *J. Am. Chem. Soc.*, *110*, 1797-1800 (1988).

68. (a) J. I. Brauman and L. K. Blair, *J. Am. Chem. Soc.*, *90*, 6561–6562 (1968); (b) ibid., *91*, 2126–2127 (1969); (c) ibid., *92*, 5986 5992 (1970).

69. I. A. Koppel and M. M. Karelson, *Org. React. (Tartu)*, *11*, 985 1010 (1975).

70. D. H. Aue, H. M. Webb, and M. T. Bowers, *J. Am. Chem. Soc.*, *98*, 311–317 (1976).

71. L. Radom, *Aust. J. Chem.*, *28*, 1–6 (1975).

72. W. J. Hehre, C.-F. Pau, A. D. Headley, and R. W. Taft, *J. Am. Chem. Soc.*, *108*, 1711–1712 (1986).

73. J. Gasteiger and M. G. Hutchings, *J. Am., Chem. Soc.*, *106*, 6489–6495 (1984).

74. R. L. Woodin and J. L. Beauchamp, *J. Am. Chem. Soc.*, *100*, 501–508 (1978).

75. Direct measurements of metal-cation affinities are scarce. Actually, most of the claimed $D(B-M^+)$ enthalpic scales are merely Gibbs free-energy ladders.

76. R. R. Corderman and J. L. Beauchamp, *J. Am. Chem. Soc.*, *98*, 3998–4000 (1976): cyclopentadienyl nickel cation, $CpNi^+$.

77. B. S. Larsen, R. B. Freas, III, and D. P. Ridge, *J. Phys. Chem.*, *88*, 6014 6018 (1984); $Mn^+$.

78. (a) W. R. Davidson and P. Kebarle, *J. Am. Chem. Soc.*, *98*, 6125–6133 (1976): $Na^+$, $K^+$, $Rb^+$, $Cs^+$; (b) ibid., 6133 6138: $K^+$; (c) J. Sunner, K. Nishizawa, and P. Kebarle, *J. Phys. Chem.*, *85*, 1814–1820 (1981): $K^+$; (d) J. Sunner and P. Kebarle, *J. Am. Chem. Soc.*, *106*, 6135–6139 (1984): $K^+$.

79. (a) R. H. Staley and J. L. Beauchamp, *J. Am. Chem. Soc.*, *97*, 5920 5921 (1975): $Li^+$; (b) see reference 74: $Li^+$; (c) R. L. Woodin and J. L. Beauchamp, *Chem. Phys.*, *41*, 1–9 (1979): $Li^+$.

80. R. W. Taft, F. Anvia, S. Walsh, and J.-F. Gal, unpublished results: $Li^+$, $K^+$.

81. B. S. Freiser, *Talanta*, *32*, 697–708 (1985). This paper gives an account of the various analytical aspects of metal-ion gas-phase chemistry monitored by laser ionization FT–ICR.

82. (a) J. S. Uppal and R. H. Staley, *J. Am. Chem. Soc.*, *104*, 1235 1238 (1982): $Al^+$; (b) ibid., 1238–1243: $Mn^+$; (c) M. M. Kappes and R. H. Staley, *J. Am. Chem. Soc.*, *104*, 1813–1819 (1982): $Ni^+$; (d) ibid., 1819 1823: $BrFe^+$; (e) R. W. Jones and R. H. Staley, *J. Phys. Chem.*, *86*, 1387 1392 (1982): $Co^+$; (f) R. W. Jones and R. H. Staley, *J. Am. Chem. Soc.*, *104*, 2296–2300 (1982): $Cu^+$.

83. J.-F. Gal, R. W. Taft, and R. T. McIver, Jr., *Spectros. Int. J.*, *3*, 96–104 (1984): $Al^+$.

84. S. F. Smith, J. Chandrasekhar, and W. L. Jorgensen, *J. Phys. Chem.*, *87*, 1898–1902 (1983).

85. (a) D. Holtz, J. L. Beauchamp, and S. D. Woodgate, *J. Am. Chem. Soc.*, *92*, 7484–7486 (1970); (b) D. Holtz and J. L. Beauchamp, *Nature*, *231*, 204–205 (1971).

86. (a) J. I. Brauman, J. A. Dodd, and C.-C. Han, in *Nucleophilicity*, J.-M. Harris and S. P. McManus, Eds., Advances in Chemistry Series, No. 215, ACS, Washington, D.C. 1987, Chap. 2; (b) J. I. Brauman and C.-C. Han, *J. Am. Chem. Soc.*, *110*, 5611–5613 (1988): $CH_3^-$, anion MCAs.

87. (a) T. B. McMahon and P. Kebarle, *Can. J. Chem.*, *63*, 3160–3167 (1985); (b) T. B. McMahon, T. Heinis, G. Nicol, J. K. Hovey, and P. Kebarle, *J. Am. Chem. Soc.*, *110*, 7591–7598 (1988): $CH_3^-$, neutral base MCAs, and references cited therein.

88. A. C. M. Wojtyniak and J. A. Stone, *Int. J. Mass Spectrom. Ion Processes*, *74*, 59–79 (1986): $(CH_3)_3Si^+$.

89. J. A. Stone and D. E. Splinter, *Int. J. Mass Spectrom. Ion Processes*, *59*, 169–183 (1984): $(CH_3)_3Sn^+$.

90. V. Craige Trenerry, G. Klass, J. H. Bowie, and I. A. Blair, *J. Chem. Res. (S)*, 386–387 (1980): $(CH_3)_3Ge^+$.

91. J. A. Stone and D. E. Splinter, *Can. J. Chem.*, 59, 1779–1786 (1981): $CH_3Hg^+$.

92. (a) R. Yamdagni and P. Kebarle, *J. Am. Chem. Soc.*, 93, 7139–7143 (1971).; (b) M. A. French, S. Ikuta, and P. Kebarle, *Can. J. Chem.*, 60, 1907–1918 (1982); (c) G. Caldwell and P. Kebarle, *J. Am. Chem. Soc.*, 106, 967–969 (1984).

93. G. Caldwell, M. D. Rozeboom, J. P. Kiplinger, and J. E. Bartmess, *J. Am. Chem. Soc.*, 106, 4660–4667 (1984).

94. (a) J. W. Larson and T. B. McMahon, *J. Am. Chem. Soc.*, 104, 5848–5849 (1982); ibid., 105, 2944–2950 (1983); (b) ibid., *Inorg. Chem.*, 23, 2029–2033 (1984); (c) ibid., *J. Am. Chem. Soc.*, 106, 517–521 (1984); (d) ibid., *J. Am. Chem. Soc.*, 109, 6230–6236 (1987).

95. M. Meot-Ner (Mautner) and L. W. Sieck, *J. Am. Chem. Soc.*, 108, 7525–7529 (1986).

96. (a) E. P. Grimsrud, S. Chowdhury, and P. Kebarle, *Int. J. Mass Spectrom. Ion Processes*, 68, 57–70 (1986); (b) G. W. Dillow and P. Kebarle, *J. Am. Chem. Soc.*, 110, 4877–4882 (1988).

97. (a) J. W. Larson and T. B. McMahon, *J. Am. Chem. Soc.*, 107, 766–773 (1985); (b) ibid., *Inorg. Chem.*, 26, 4018–4023 (1987); (c) J. W. Larson, J. E. Szulejko, and T. B. McMahon, *J. Am. Chem. Soc.*, 110, 7604–7609 (1988).

98. (a) J. W. Larson and T. B. McMahon, *J. Phys. Chem.*, 88, 1083–1086 (1984); (b) ibid., *Can. J. Chem.*, 62, 675–679 (1984).

99. B. K. Janousek and J. I. Brauman, in *Gas-Phase Ion Chemistry, Vol. 2*, M. T. Bowers, Ed., Academic, New York, 1979, Chap. 10.

100. P. Kebarle and S. Chowdhury, *Chem. Rev.*, 87, 513–534 (1987).

101. M. Meot-Ner (Mautner), in *Molecular Structure and Energetics, Vol. 4, Biophysical Aspects*, J. F. Liebman and A. Greenberg, Eds., VCH, New York, 1987, Chap. 3.

102. R. G. Keesee and A. W. Castleman, Jr., *J. Phys. Chem. Ref. Data*, 15, 1011–1071 (1986).

103. (a) M. Meot-Ner (Mautner), *J. Am. Chem. Soc.*, 106, 1257–1264 (1984); (b) ibid., 1265–1272; (c) M. Meot-Ner (Mautner) and L. W. Sieck, *J. Phys. Chem.*, 89, 5222–5225 (1985).

104. G. Nicol, J. Sunner, and P. Kebarle, *Int. J. Mass Spectrom. Ion Processes*, 84, 135–155 (1988).

105. J. Bromilow, J.-L. M. Abboud, C. Lebrilla, R. W. Taft, G. Scorrano, and V. Lucchini, *J. Am. Chem. Soc.*, 103, 5448–5453 (1981). Additional data concerning nitriles and ammonium and nitrilium ions can be found in reference 106.

106. C. V. Speller and M. Meot-Ner (Mautner), *J. Phys. Chem.*, 89, 5217–5222 (1985).

107. (a) M. Meot-Ner (Mautner), *J. Am. Chem. Soc.*, 105, 4912–4915 (1983); (b) M. Meot-Ner (Mautner) and C. A. Deakyne, ibid., 107, 469–474 (1985); (c) C. A. Deakyne and M. Meot-Ner (Mautner), ibid., 107, 474–479 (1985).

108. E. M. Arnett, *Acc. Chem. Res.*, 6, 404–409 (1973).

109. J. Hine and P. K. Mookerjee, *J. Org. Chem.*, 40, 292–298 (1975).

110. (a) S. Cabani, P. Gianni, V. Mollica, and L. Lepori, *J. Solution Chem.*, 10, 563–595 (1981); (b) P. Gianni, V. Mollica, and L. Lepori, *Z. Phys. Chem. Neue Folge*, 131, 1–15 (1982).

111. (a) E. M. Arnett, B. Chawla, L. Bell, M. Taagepera, W. J. Hehre and R. W. Taft, *J. Am. Chem. Soc.*, 99, 5729–5738 (1977); (b) E. M. Arnett and B. Chawla, ibid., 101, 7141–7146 (1979).

112. H. P. Hopkins, Jr., D. V. Jahagirdar, P. S. Moulik, D. H. Aue, H. M. Webb, W. R. Davidson, and M. D. Pedley, *J. Am. Chem. Soc.*, 106, 4341–4348 (1984).

113. R. W. Taft, J.-F. Gal, S. Géribaldi, and P.-C. Maria, *J. Am. Chem. Soc.*, 108, 861–863 (1986).

114. E. M. Arnett, L. E. Small, R. T. McIver, Jr., and J. S. Miller, *J. Am. Chem. Soc.*, 96, 5638–5640 (1974).

115. P. Haberfield and A. K. Rakshit, *J. Am. Chem. Soc.*, 98, 4393–4394 (1976).

116. M. J. Locke and R. T. McIver, Jr., *J. Am. Chem. Soc.*, *105*, 4226–4232 (1983).

117. (a) M. H. Abraham, J. Liszi, and E. Kristóf, *Aust. J. Chem.*, *35*, 1273–1279 (1982): *Calculations on Ionic Solvation, VII*, and previous papers in this series. (b) M. H. Abraham, E. Matteoli, and J. Liszi, *J. Chem. Soc., Faraday Trans. 1*, *79*, 2781–2800 (1983).

118. J. Chandrasekhar, D. C. Spellmeyer, and W. L. Jorgensen, *J. Am. Chem. Soc.*, *106*, 903–910 (1984).

119. (a) A. Pullman, in *The World of Quantum Chemistry*, B. Pullman and R. Parr, Eds., Reidel, Dordrecht, 1976, pp. 149–187; (b) A. Pullman, in *Quantum Theory of Chemical Reactions*, Vol. 2, R. Daudel, A. Pullman, L. Salem, and A. Veillard, Eds., Reidel, Dordrecht, 1980, pp. 1–24; (c) A. Pullman, *Study Weak on Chemical Events in the Atmosphere and Their Impact on the Environment*, November 7–11, 1983, G. B. Marino-Bettolo, Ed., *Pontif. Acad. Sci. Scripta Varia*, *56*, 25–50 (1985).

120. I. A. Koppel, *Org. React. (Tartu)*, *24*, 263–313 (1987).

121. (a) P. Kebarle, *Ann. Rev. Phys. Chem.*, *28*, 445–476 (1977); (b) P. Kebarle, W. R. Davidson, J. Sunner, and S. Meza-Höjer, *Pure Appl. Chem.*, *51*, 63–72 (1979); (c) T. F. Magnera, G. Caldwell, J. Sunner, S. Ikuta, and P. Kebarle, *J. Am. Chem. Soc.*, *106*, 6140–6146 (1984).

122. (a) P. M. Holland and A. W. Castleman, Jr., *J. Phys. Chem.*, *86*, 4181–4188 (1982); (b) A. W. Castleman, Jr. and R. G. Keesee, *Acc. Chem. Res.*, *19*, 413–419 (1986); (c) ibid., *Chem. Rev.*, *86*, 589–618 (1986).

123. (a) K. Hiraoka, *Bull. Chem. Soc. Jpn.*, *60*, 2555–2560 (1987); (b) K. Hiraoka and S. Mizuse, *Chem. Phys.*, *118*, 457–466 (1987); (c) K. Hiraoka, S. Mizuse, and S. Yamabe, *J. Phys. Chem.*, *91*, 5294–5297 (1987); (d) ibid., *92*, 3943–3952 (1988).

124. M. Meot-Ner (Mautner), *J. Phys. Chem.*, *91*, 417–426 (1987).

125. O. Exner, *Correlation Analysis of Chemical Data*, Plenum, New York, 1988.

126. J. E. Bartmess, J. A. Scott, and R. T. McIver, Jr, *J. Am. Chem. Soc.*, *101*, 6056–6063 (1979).

127. (a) T. Matsui and L. G. Hepler, *Can. J. Chem.*, *51*, 1941–1944 (1973); (b) T. Matsui, H. C. Ko, and L.-G. Hepler, *Can. J. Chem.*, *52*, 2906–2911 (1974); ibid., 2912–2918.

128. P. D. Bolton, K. A. Fleming, and F. M. Hall, *J. Am. Chem. Soc.*, *94*, 1033–1034 (1972).

129. G. H. Parsons and C. H. Rochester, *J. Chem. Soc. Perkin II*, 1313–1318 (1974).

130. J. R. Jones and S. P. Patel, *J. Chem. Soc. Perkin II*, 1231–1234 (1975).

131. (a) D. H. Aue, H. M. Webb, and M. T. Bowers, *J. Am. Chem. Soc.*, *94*, 4726–4728 (1972); (b) ibid., *98*, 318–329 (1976).

132. (a) J. F. Wolf, P. G. Harch, and R. W. Taft, *J. Am. Chem. Soc.*, *97*, 2904–2906 (1975); (b) J. F. Wolf, J.-L. M. Abboud, and R. W. Taft, *J. Org. Chem.*, *42*, 3316–3317 (1977).

133. (a) A. D. Headley, *J. Am. Chem. Soc.*, *109*, 2347–2348 (1987); (b) A. D. Headley, *J. Org. Chem.*, *53*, 312–314 (1988).

134. (a) M. Fujio, R. T. McIver, Jr., and R. W. Taft, *J. Am. Chem. Soc.*, *103*, 4017–4029 (1981); (b) M. Mishima, R. T. McIver, Jr., R. W. Taft, F. G. Bordwell, and W. N. Olmstead, *J. Am. Chem. Soc.*, *106*, 2717–2718 (1984).

135. The literature solution-derived *EA* values from half-wave reduction potentials or charge-transfer spectra are put on a common scale to account for the various experimental conditions. See E. C. M. Chen and W. E. Wentworth, *J. Chem. Phys.*, *63*, 3184–3191 (1975).

136. T. Heinis, S. Chowdhury, S. L. Scott, and P. Kebarle, *J. Am. Chem. Soc.*, *110*, 400–407 (1988).

137. M. Colonna, L. Greci, M. Poloni, G. Marrosu, A. Trazza, F. P. Colonna, and G. Distefano, *J. Chem. Soc. Perkin II*, 1229–1231 (1986).

138. A. G. Harrison, R. Houriet, and T. T. Tidwell, *J. Org. Chem.*, *49*, 1302–1304 (1984).

139. F. Marcuzzi, G. Modena, C. Paradisi, C. Giancaspro, and M. Speranza, *J. Org. Chem.*, *50*, 4973–4975 (1985).

140. (a) M. Mishima, M. Fujio, and Y. Tsuno, *Mem. Fac. Sci. Kyushu Univ.*, *Ser. C*, *14*, 365–374 (1984); (b) ibid., *15*, 111–118 (1984); (c) M. Mishima, M. Fujio, and Y. Tsuno, *Tetrahedron Lett.*, *27*, 939–942 (1986); (d) ibid., 951–954; (e) M. Mishima, K. Arima, S. Usui, M. Fujio, and Y. Tsuno, *Mem. Fac. Sci. Kyushu Univ.*, *Ser. C*, *15*, 277–286 (1986).

141. J. Shorter, in *Correlation Analysis in Chemistry. Recent Advances*, N. B. Chapman and J. Shorter, Eds, Plenum, New York, 1978, Chap. 4.

142. C. Laurence, M. Berthelot, M. Luçon, M. Helbert, D. G. Morris, and J.-F. Gal, *J. Chem. Soc. Perkin II*, 705–710 (1984).

143. J.-L. M. Abboud, J. Catalán, J. Elguero, and R. W. Taft, *J. Org. Chem.*, *53*, 1137–1140 (1988).

144. M. Charton, *Progr. Phys. Org. Chem.*, *13*, 119–251 (1981).

145. D. H. Aue, H. M. Webb, M. T. Bowers, C. L. Liotta, C. J. Alexander, and H. P. Hopkins, Jr., *J. Am. Chem. Soc.*, *98*, 854–856 (1976).

146. M. Meot-Ner (Mautner) and L. W. Sieck, *J. Am. Chem. Soc.*, *105*, 2956–2961 (1983).

147. G. Berthon, O. Enea, and E. M'Foundou, *Bull. Soc. Chim. Fr.*, 2967–2969 (1973).

148. C. L. Liotta, E. M. Perdue, and H. P. Hopkins, Jr., *J. Am. Chem. Soc.*, *96*, 7308–7311 (1974).

149. C. U. Pittman, Jr., O. M. Attallah, and L. D. Kispert, *J. Chem. Soc., Perkin II*, 1776–1778 (1975).

150. Tabulated $PA$ values for $NR_2$ substituted pyridines, obtained from relative $GB$ values (53) do not seem to be corrected for possible restricted rotation induced by protonation.

151. U. H. Mölder, I. A. Koppel, R. J. Pikver, and J. J. Topfer, *Org. React. (Tartu)*, *24*, 314–331 (1987) and previous papers in the series.

152. U. H. Mölder and I. A. Koppel, *Org. React. (Tartu)*, *21*, 27–39 (1984).

153. P.-C. Maria, J.-F. Gal, J. de Franceschi, and E. Fargin, *J. Am. Chem. Soc.*, *109*, 483–492 (1987).

154. (a) B. Swanson, D. F. Shriver, and J. A. Ibers, *Inorg. Chem.*, *8*, 2182–2189 (1969); (b) K. R. Leopold, G. T. Fraser, and W. Klemperer, *J. Am. Chem. Soc.*, *106*, 897–899 (1984).

155. A Taft–Topsom treatment (see reference 1h) of $-\Delta H^\circ_{BF_3}$ values in kJ mole$^{-1}$ for the $XCH_2CN$ series (28) shows that the $P$ effect is not significant: $-\Delta H^\circ_{BF_3} = (-36.04 \pm 1.32)\sigma_F + (-0.32 \pm 0.86)\sigma_\alpha + 60.73$, $n = 9$, $r = .9961$, sd $= 0.60$ kJ mole$^{-1}$.

156. In general, the $C=O \cdots B$ angle in carbonyl-$BF_3$ complexes is close to 120°. See, for example, in the case of $\alpha, \beta$-unsaturated carbonyl compounds: (a) J. Torri and M. Azzaro, *Bull. Soc. Chim. Fr.*, *II*, 283–291 (1978); (b) M. T. Retz, M. Hüllmann, W. Massa, S. Berger, P. Rademacher, and P. Heymanns, *J. Am. Chem. Soc.*, *108*, 2405–2408 (1986); (c) F. D. Lewis, J. D. Oxman, L. L. Gibson, H. L. Hampsch, and S. L. Quillen, *J. Am. Chem. Soc.*, *108*, 3005–3015 (1986); (d) O. F. Guner, R. M. Ottenbrite, D. D. Shillady, and P. V. Alston, *J. Org. Chem.*, *52*, 391–394 (1987).

157. (a) M. Azzaro, J.-F. Gal, and S. Géribaldi, *J. Org. Chem.*, *47*, 4981–4984 (1982); (b) M. Azzaro, J.-F. Gal, S. Géribaldi, B. Videau, and A. Loupy, *J. Chem. Soc. Perkin II*, 57–65 (1983).

158. J.-F. Gal and R. W. Taft, *unpublished results*; X, $PA$/kJ mole$^{-1}$: H, 869; OMe, 916; Cl, 867; $CO_2Me$, 860; $NH_2$, 940; $NMe_2$, 974; $NEt_2$, 989. (All the preceding values have been scaled by Lias and coworkers and are compiled in reference 53b) Me, 890; CN, 828; Ph, 903. We have anchored these three values to the scale in reference 53.

159. R. W. Taft, personal communication, a preliminary report appears in reference 40c.

160. W. Moffitt, *Proc. Roy. Soc. London, Ser. A, 202,* 548 564 (1950).

161. (a) T. Zeegers-Huyskens, *J. Mol. Liq., 32,* 191 207 (1986); (b) ibid. *J. Mol. Struct. (Theochem) 135,* 93–103 (1986); linearity is only observed for a limited $\Delta PA$ range: ibid., *J. Mol. Struct., 177,* 125 141 (1988).

162. P. Kollman and S. Rothenberg, *J. Am. Chem. Soc., 99,* 1333 1342 (1977).

163. S. F. Smith, J. Chandrasekhar, and W. L. Jorgensen, *J. Phys. Chem., 86,* 3308 3318 (1982).

164. (a) J. E. Del Bene, M. J. Frisch, K. Raghavachari, and J. A. Pople, *J. Phys. Chem., 86,* 1529 1535 (1982); (b) J. E. Del Bene, M. J. Frisch, K. Raghavachari, J. A. Pople, and P. von R. Schleyer, *J. Phys. Chem., 87,* 73 78 (1983).

165. K. Hirao, S. Yamabe, and M. Sano, *J. Phys. Chem., 86,* 2626 2632 (1982).

166. S. Ikuta, *Chem. Phys., 95,* 235–242 (1985).

167. T. Prüsse, C. B. Lebrilla, T. Drewello, and H. Schwarz, *J. Am. Chem. Soc., 110,* 5986–5993 (1988) and references cited therein.

168. I. A. Koppel, *Org. React. (Tartu), 24,* 115 127 (1987).

169. In Equation 29, B is conventionally taken as more basic than its partner. In Equation 26, A⁻ is conventionally taken as less basic (AH more acidic) than its partner. This results in positive values for the differences 33 and 34.

170. T. Zeegers-Huyskens, *Chem. Phys. Lett. 129,* 172 175 (1986).

171. K. Hiraoka, *Can. J. Chem., 65,* 1258–1261 (1987).

172. S. Alunni, S. Clementi, U. Edlund, D. Johnels, S. Hellberg, M. Sjöström, and S. Wold, *Acta Chem. Scand., Ser. B, 37,* 47–53 (1983).

173. M. L. Bisani, S. Clementi, and S. Wold, *Chim. Ind. (Milan), 64,* 655–665 (1982); ibid., *64,* 727–741 (1982).

174. The minimum number *n* of orthogonal factors required to reproduce (within experimental errors or with a tolerable loss of information) the original parameters submitted to the PC analysis represents the "dimensionality" of the *n*-dimensional factor space in which the original parameters may be represented.

175. K. J. Miller and J. A. Savchik, *J. Am. Chem. Soc., 101,* 7206–7213 (1979).

176. W. B. Person, *J. Am. Chem. Soc., 84,* 536–540 (1962).

177. (a) R. W. Taft, M. H. Abraham, R. M. Doherty, and M. J. Kamlet, *Nature, 313,* 384–386 (1985); (b) M. J. Kamlet, R. M. Doherty, R. W. Taft, M. H. Abraham, G. D. Veith, and D. J. Abraham, *Environ. Sci. Technol., 21,* 149–155 (1987) and the preceding papers in the series entitled "Solubility Properties in Polymers and Biological Media"; (c) M. J. Kamlet, R. M. Doherty, G. R. Famini, and R. W. Taft, *Acta Chem. Scand., Ser. B, 41,* 589 598 (1987); (d) M. J. Kamlet, R. M. Doherty, M. H. Abraham, Y. Marcus, and R. W. Taft, *J. Phys. Chem., 92,* 5244–5255 (1988).

178. B. Panchenko, N. Oleinik, Yu. Sadovsky, V. Dadali, and L. Litvinenko, *Org. React. (Tartu), 7,* 65–87 (1980).

179. A. C. Legon and D. J. Millen, Chem. Rev., *86,* 635–657 (1986); ibid., *Acc. Chem. Res., 20,* 39–46 (1987).

180. For gas-phase electronic spectra of hydrogen-bonded clusters, see, for example: (a) E. M. Gibson, A. C. Jones, A. G. Taylor, W. G. Bouwman, D. Phillips, and J. Sandell, *J. Phys. Chem., 92,* 5449–5455 (1988); (b) M. R. Nimlos, D. F. Kelley, and E. R. Bernstein, *J. Phys. Chem., 93,* 643–651 (1989).

181. J. T. Cheung, D. A. Dixon, and D. R. Herschbach, *J. Phys. Chem., 92,* 2536 2541 (1988).

182. O. Schrems, H. M. Oberhoffer, and W. A. P. Luck, *J. Phys. Chem.*, *88*, 4335–4342 (1984).

183. (a) N. P. Machara and B. S. Ault, *J. Phys. Chem.*, *92*, 2439–2442 (1988); (b) B. S. Ault, *J. Phys. Chem.*, *93*, 279–282 (1989) and references cited therein.

184. L. Andrews and R. D. Hunt, *J. Phys. Chem.*, *92*, 81–85 (1988) and references cited therein.

185. See also the recent reviews: (a) HPMS—P. Kebarle, in *Techniques for the Study of Ion/Molecule Reactions*, J. M. Farrar and W. Saunders, Jr., Eds., Wiley, New York, 1988, Chap. 5; (b) FT-ICR—B. Freiser, ibid., Chap. 2.

186. After completion of this manuscript we have become aware of recent works by Freiser and co-workers and Taft and co-workers using the FT-ICR technique concerning the establishment of a basicity scale relative to $Mg^+$ and the protonic basicity and acidity of azoles: (a) L. Operti, E. C. Tews, and B. S. Freiser, *J. Am. Chem. Soc.*, *110*, 3847–3853 (1988); (b) J. Catalàn, R. M. Claramunt, J. Elguero, J. Laynez, M. Menéndez, F. Anvia, J. H. Quian, M. Taagepera, and R. W. Taft, *J. Am. Chem. Soc.*, *110*, 4105–4111 (1988).

# Correlation Analysis in Organic Crystal Chemistry

BY TADEUSZ MAREK KRYGOWSKI
*Department of Chemistry*
*University of Warsaw*
*Warsaw, Poland*

## CONTENTS

# I.  INTRODUCTION

### A.  History and Scope of Correlation Analysis in Organic Chemistry

About 50 years after the discovery of methods permitting the measurement of rate and equilibrium constants for chemical processes (1, 2), there was a sufficient accumulation of numerical data to allow the first attempts to relate them to the nature of structure or medium of the reaction. In 1924 Brønsted and Pedersen (3) related the rate constant for the decomposition of nitramide.

$$H_2N_2O_2 \xrightarrow{k_c} H_2O + NO_2 \tag{1}$$
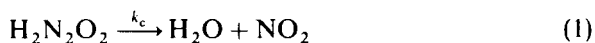
to the basicity constants $K_b$ of

$$RCOO^- + H_3O^+ \underset{}{\overset{k_b}{\rightleftharpoons}} RCOOH + H_2O \tag{2}$$

in which $RCOO^-$ and $RCOOH$ are the components of the buffer in which Reaction 1 is carried out. The shape of the dependence introduced by Brønsted and Pedersen (3) was of the form

$$\delta_R \cdot \log k_c = \beta \cdot \delta_R \cdot \log K_b \tag{3}$$

where $\delta_R$ is the Leffler  Grunwald (4) chemical operator describing structural effects on the reactivity of the chemical species (i.e., on rate and equilibrium constants) and $\beta$ is the linear regression coefficient (most often referred to as the slope). Equation 3 was the first presentation of a linear free-energy relationship (LFER) since it may be expressed in the form

$$\delta_R \cdot \Delta G^{\#} = \beta' \cdot \delta_R \cdot \Delta G^{\circ} \tag{4}$$

where $\Delta G^{\#}$ and $\Delta G^{\circ}$ are the change in free energy of activation for Reaction 1 and the free-energy change for Reaction 2, respectively.

Within 10 years, as a result of many observations (5–8) that the same substituent has a similar effect on the reactivity of benzene derivatives in two reaction series, the Hammett equation was established (9, 10):

$$\delta \cdot \log k = \rho \cdot \sigma \tag{5}$$

This equation may be considered as an example of a linear free-energy relationship (for details, see references 11 - 13). It may also be considered as a similarity model in which better known chemical reactions are used to explain or describe less known ones, provided the same variation in a controlled

variable is applied in both reactions. In the case of Hammett and Hammett-like equations, we have the same variation in substituents in the two series that are compared, and the parameter $\sigma$ in Equation 5 is called the *substituent constant*. The general equation of similarity models has the form of multiparameter regression:

$$\delta_R Q_i = \sum_{j=1}^{N} \alpha_j P_{ij} + \alpha_0 \qquad (6)$$

Here $i$ refers to a common variation in structure (usually of the substituent) and $j$, to a particular mechanism of interaction between the substituent and the reaction site (usually inductive, resonance or steric). The $\alpha_j$ values are regression coefficients (slopes) describing the sensitivity of the property measured to the mechanism $j$ while $P_{ij}$ is an explanatory parameter. (For further details, see references 11 and 14 16.) It may be concluded that to a great degree correlation analysis in organic chemistry (CAOC)* is a term equivalent to similarity models applied in organic chemistry. The scope of this latter field of research is the construction and application of similarity models in order to interpret the dependence of chemical reactivity and physicochemical properties on changes in structure (chiefly the substituent effect), the medium (chiefly) the solvent effect, and the nature of the reagent.

The main purposes of research in the field of CAOC as well as most important directions in studies are as follows:

1. Application of the known similarity models, that is, equations such as Equation 6 with various explanatory parameters (various $\sigma$ values, steric parameters, etc.) in order to better understand the experimental data in question; analysis of regression coefficients ("sensitivity" parameters) in order to study such matters as the transmission of substituent effects through various "bridges"; effects of solvents (or even more general media) on the reactivity of systems; the analysis of effects of substituent in terms of various factors influencing the data in question; the estimation of inductive, resonance, or steric effects; and the analysis of solvent effects on these effects as well as on the overall reactivity parameters or physicochemical properties $\delta Q_i$.

2. The prediction of the unknown or uncertain data.

3. The construction of new similarity models as well as seeking either a better understanding of already known parameters or new explanatory

---

*Every 3 years since 1979 CAOC meetings have been held in Europe: Assisi (1979, Italy), Hull (1982, Great Britain), Louvain la Neuve (1985, Belgium), and Poznań (1988, Poland).

parameters. Known parameters may also be improved as experimental techniques are developed, allowing higher precision (and even accuracy).

4. One important direction of the CAOC is associated with the application of statistics and statistical tools. There has been much misunderstanding regarding this field, and some problems have arisen that are still not practically solved. For example, it is not clear whether to use single or multiple regression and how to take into account covariance in explanatory parameters in the case of multiple regression. Another problem is how to test the goodness of fit of a given regression. Most methods of doing this in CAOC involve the arbitrary use of the correlation coefficient $r$ or its function (Otto Exner's $\psi$) (17), but they are not based on statistical testing of appropriate hypotheses.

Similarity models in CAOC are at present applied very widely in various branches of chemistry: applied chemistry, biochemistry, and related fields. The aim of this contribution is to show how this kind of approach works in the field of organic crystal chemistry.

## B.  Relation of Organic Crystal Chemistry to CAOC

Some 50 years after the discovery of X-ray diffraction in crystals by Bragg and Bragg (18) as well as by Knipping and von Laue (19), the application of X-ray and then neutron and electron diffraction techniques has proved to be very successful in the determination of the structure of molecules in crystals (X-ray and neutron) and in the gas phase (electron diffraction).

Additionally, determination of geometry by microwave techniques and nuclear magnetic resonance (NMR) measurements in nemetic phase appeared to be very useful. Nevertheless, X-ray measurements are most often used to determine molecular geometry since other methods are either very expensive or must meet special requirements and limitations.

Crystal chemistry can yield most useful results concerning the structure of molecules. Crystallographic studies using X-ray and neutron diffraction techniques yield positions for atoms (and ions) in elementary crystal cells and hence the geometry of chemical species building up the crystal. Thus, as a result of careful determinations of crystal and molecular structure, one may obtain:

1. Structural (geometric) parameters of chemical species such as bond lengths, bond, torsion, and dihedral angles; and any other geometric parameters needed to describe the molecular structure.

2. Interatomic distances and related angles between atoms belonging to

different chemical species in the crystal lattice, or to the same one but not directly bonded.

These two structural parameters may then be applied to further analysis to yield:

- Relationships between various structural parameters within the molecule or some fragment of it.
- Relationships between structural parameters and reactivity parameters and/or physicochemical properties.
- Reinterpretation and new findings in the field of substituent effects based on analysis of structural parameters of various systems in question.
- Relationships arising from intramolecular responses to intermolecular interactions.

Before discussing the application of CAOC-type approaches to the geometrical parameters of molecules, it is necessary to make a few remarks regarding the precision and factors influencing the observed geometries of chemical species in the crystalline state obtained by X-ray diffraction techniques.

## C.  Precision of Determination of Molecular Geometry by Use of X-ray Diffraction

Most information about the geometry of chemical species comes from X-ray diffraction measurements and hence comments on this techniques are given here. (For other techniques, see reference 20.)

It should be taken into account that bond lengths estimated by X-ray measurements do not exactly measure the distance between the two nuclei forming the bond but rather the distance between the centroids of the electron clouds of the atoms. For the sake of convenience, however, they will be called "bond lengths" throughout this chapter. The difference between the real bond length and that measured by X-ray is for C—C bonds about 1 pm or less except for some special cases (for ethene, it is close to 2 pm).

The thermal motions of species in the crystal lattice may also lead to changes in geometry. As a result of benzene ring libration, the estimated bond length by X-ray is shorter by 1.4 pm than that after using corrections for thermal motion (21)—139.2 pm in comparison to 139.7 pm for microwave determination (22). This additional shortening seems to arise because the X-ray technique measures the distance between the centroids electron population rather then between the nuclei.

In many cases the geometry of chemical species in crystals may be affected

by either static or dynamic disorder. Sometimes this may be resolved during the evaluation of the data, but in the case of small differences in geometry produced by various orientations, it is impossible to avoid imprecision in geometric parameters.

Another difficult problem arises when strong intermolecular interactions exist in the crystal. If the crystal lattice forces are of lower symmetry than the molecule itself, then the observed deformation may be quite considerable (23).

In conclusion, it should be mentioned that care should be exercised in comparing the geometric parameters of chemical species taken from different sources and obtained by the use of various techniques with differing precision and accuracy.

## D. Some Statistics

Finally it should be mentioned how precision is presented and taken into consideration in crystallographic studies. Every geometric parameter, say, bond length or any type of angle, is accompanied by the value of the estimated standard deviation ($\sigma$) in paranthesis, as, for example, 139.1 (3) pm or 119.1 (2)°.*

If two structural parameters are compared in order to ascertain whether the difference between them is significant, one must use the estimated standard deviations ($\sigma$ values) for geometric parameters, and following the rule of propagation of variance for independent variables, to calculate a common $\sigma$:

$$\sigma = (\sigma_1^2 + \sigma_2^2)^{1/2} \tag{7}$$

If the difference between two geometric parameters $P_1$ and $P_2$ is greater than $3\sigma$, then one may reject the null hypothesis

$$H_0 : P_1 = P_2 \tag{8}$$

and accept the alternative one that $P_1 \neq P_2$ with a probability of error $p = .0027$. This simply means, that accepting the alternative hypothesis, we may be in error in 27 cases out of 10,000. Only for such cases are differences in structural parameters meaningful and in need of interpretation.

This kind of procedure, often used in crystallography, is referred to as the "$3\sigma$ rule." Note that in many cases users do not distinguish between individual $\sigma_1$ or $\sigma_2$ and $\sigma$ (Equation 7); this leads to an unduly optimistic conclusion and in consequence may be a source of invalid interpretations.

---

*The estimated standard deviation is given in parentheses after the value of structural parameter as a digit of the last significant figure.
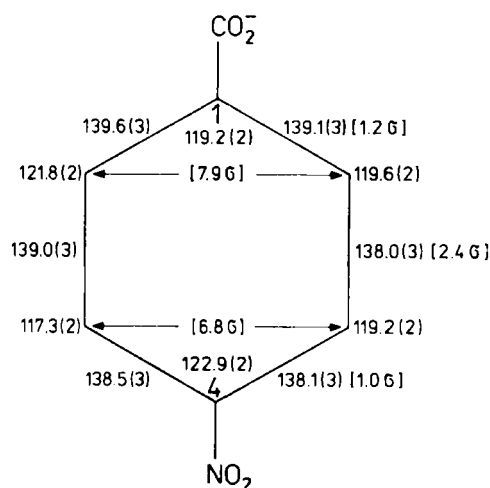
**Figure 1** Geometry of $p$-nitrobenzoate anion (24). Arrows join symmetrically equivalent bond angles; the values in brackets give the difference between them expressed in terms of $\sigma_{1,2} = (\sigma_1^2 + \sigma_2^2)^{1/2}$. Bond lengths are given in picometers; the values in brackets give the differences in lengths between equivalent bond expressed in units of estimated standard deviation for difference $(\sigma_{1,2})$.

As an example, Fig. 1 presents the angular geometry of the $p$-nitrobenzoate anion (24), which as an isolated species should posses $C_{2v}$ symmetry. However, one may observe differences between symmetrically equivalent angles, which expressed in terms of $\sigma = (0.2^2 + 0.2^2)^{1/2} = 0.28$, have the values $7.9\sigma$ and $6.8\sigma$ and obviously are highly significant. An analysis of the force field in the crystal lattice of sodium $p$-nitrobenzoate hydrate revealed that these differences are due to very strong intermolecular interactions (23).

For geometry analysis the proper tools are elementary statistics (as mentioned above) together with some knowledge about symmetry. The example in Fig. 2 illustrates the problem. This shows the angular geometry of the $N$-$n$-propylquinoxalinium cation (25). We want to know the extent to which the charged substituent at nitrogen affects the angular geometry of the whole aromatic system. The null hypothesis for this system yields

$$H_0: \hat{C}_2 \phi_i = \phi_i \tag{9}$$

That is, the angles $\phi_i$ should be equal to those that are symmetrically equivalent by $C_2$. Thus, for example, $\angle\,\text{N1C1C2} = \angle\,\text{C1C2N2}$. We observe, however, that these angles are $120.0(2)^\circ$ and $123.3(2)^\circ$ and the difference $\Delta = 3.3^\circ$. If we express this difference in terms of estimated standard deviation
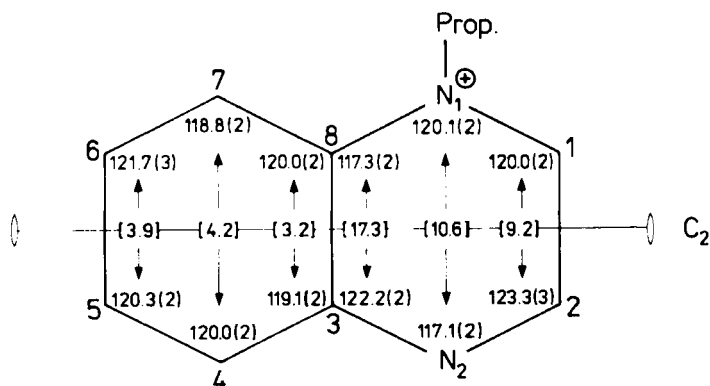
**Figure 2**  Geometry of $N$-propylquinoxalinium cation (25). Equivalent, by null hypothesis ($H_0$: $\phi_i = \hat{C}_2 \cdot \phi_i$), bond angles are joined by arrows with the values of differences expressed in units of estimated standard deviation $\sigma_{1,2} = (\sigma_1^2 + \sigma_2^2)^{1/2}$ written in brackets.

(esd) $\sigma = (0.2^2 + 0.2^2)^{1/2}$ we find the result as in Fig. 2, where equivalent angles are joined by arrows with the difference expressed in units of $\sigma$ in the bracket.

Since the difference, which is called the *deformation parameter* $DP = |\hat{C}_2 \phi_i - \phi_i|$, is always greater than $3\sigma$, the substituent effect on angles in $N$-$n$-propylquinoxalinium is strong and significant for all positions taken into account. To show how conclusions drawn from structural data depend on their precision, let us consider the situation if the precision were three times worse, that is, if $\sigma$ for angles were equal to 0.6 instead of 0.2. Figure 3 shows this situation; only in the substituted ring is the substituent effect greater than the noise of imprecision; in the other ring no significant effect
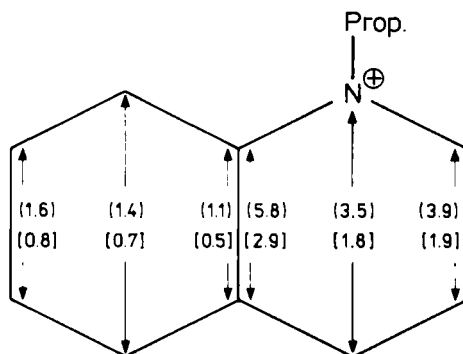


**Figure 3**  Differences between equivalent bond angles (see Fig. 2) for situation if the precision of the measurement is three times worse (esd = 0.6°) in square brackets and six times worse (esd = 1.2°) in round brackets.

is observed. If the precision falls to an individual $\sigma = 1.2$, then $\sigma_{total} = 1.7$ and none of the angles is observed as significantly deformed. This example illustrates the importance of precision in the geometrical parameters of chemical species. We summarize the reliable conclusions that may be drawn from structural data only if they are of very high quality (as low $\sigma$-values as possible). The more subtle the effect under study, the higher the precision that is required. Fulfillment of this requirement is particularly important when individual measurements are taken into consideration. The situation is slightly better if instead of individual measurements, sets of data are subject of study. Nevertheless, in many structural papers this condition of reliability is violated. Moreover, even if most precise data are retrieved from the Cambridge Structural Data Base, that is, those with AS-flag $= 1$, the geometries from this collection of data are within the range of precision $0.1-0.5$ pm; that is, esd values for bond length are in this range. For subtle problems this dispersion of precision (by a factor of 5) may be too large. This problem will be discussed later in further detail.

## II.  RELATIONSHIPS BETWEEN STRUCTURAL PARAMETERS OF MOLECULES

### A.  Electronic Structure and Geometry of Molecules (and Ionic Chemical Species)

The structure of a molecule may be understood in two ways. It is either an electronic structure and is described in terms of electron charges and bond orders (or equivalent terms) or is a geometric structure, described by structural (geometric) parameters such as bond lengths and bond, torsional, and dihedral angles. These two sets of descriptive parameters are related to the wavefunction describing the molecule and are obtainable from it if sufficiently reliable quantum-chemical calculations are carried out. These calculations, if carried out for individual molecules, may not, however, be a reliable source of information; this depends on the level of sophistication of the method used. In principle, the larger the molecule size and the lower level of sophistication of the quantum-chemical method used, the lower the reliability of the calculation carried out. Hence, most reliable quantum-chemical results refer to series of relatively similar systems and are then used in a comparative way. As far as molecular geometry is concerned, except for small molecules, which are of rather little interest for organic chemistry, quantum-chemical calculations (even by use of an initio techniques at various levels of basis sets applied in simulation of atomic orbitals) seldom give conclusive values of structural parameters. A recent study (26) of the basis-set dependence of the ab initio calculated geometries of a series of hydrocarbons

showed that these geometries need additional statistical treatment in order to yield precise and accurate reproduction of experimental bond lengths and angles.

In spite of these limitations, recent applications of ab initio calculations at various basis-set levels used have proved (27–38) their utility in clarification of classical notions of physical organic chemistry. The most important results seem to be:

1. The use of quantum chemical models to show in a very illustrative way the mechanisms of substituent effects (31–34).

2. The interpretation of $\sigma$ and $\pi$ charges at *meta-* and *para*-carbon atoms in monosubstituted derivatives of benzene (35) in terms of inductive and resonance substituent constants (DSP treatment) (36).

3. The interpretation of Hammett's $\sigma$ parameters for *meta* and *para*-positions in terms of $\sigma$ and $\pi$ charges at carbon atoms as well as $\sigma$ charges at hydrogen atoms joined to *meta-* and *para*-carbon atoms (37). Surprisingly, it was found that the most effective single parameter equation relating the dependence of $\sigma$ (*meta* or *para*) on charges is that in which the explanatory parameter is charge at hydrogen atoms *meta* or *para*-position.

4. The application of advanced valence-bond (VB) techniques of calculation revealed that in classical molecules exhibiting through resonance effects, *p*-nitro aniline and *p*-nitrophenol, the resonance form with full charge transfer from the electron-donating to electron-accepting substituent (structure **6** in Scheme 1) has the lowest weight of all those taken into account (structures **1–6**) (38).

These examples, as well as many others presented in numerous series and monographs and reviews (27–36), confirm the great utility of quantum-chemical methods in attempts to better understand the intramolecular interactions determining chemical and physicochemical properties of molecular and ionic species. However, quantum-chemical calculation carried out for large molecules do not serve as a source of molecular geometry, but rather, if the agreement with experimental geometry is acceptable, other structural (electronic) parameters are used in description of molecules. Undoubtedly, the main source of information for molecular geometry are experimental techniques, of which X-ray diffraction is the cheapest and most widely applicable. According to Hoffmann (39): "There is no more basic enterprise in chemistry than the determination of the geometric structure of a molecule. Such a determination, when it is well done, ends all speculation as to the structure and provides us with the starting point for understanding of every physical,
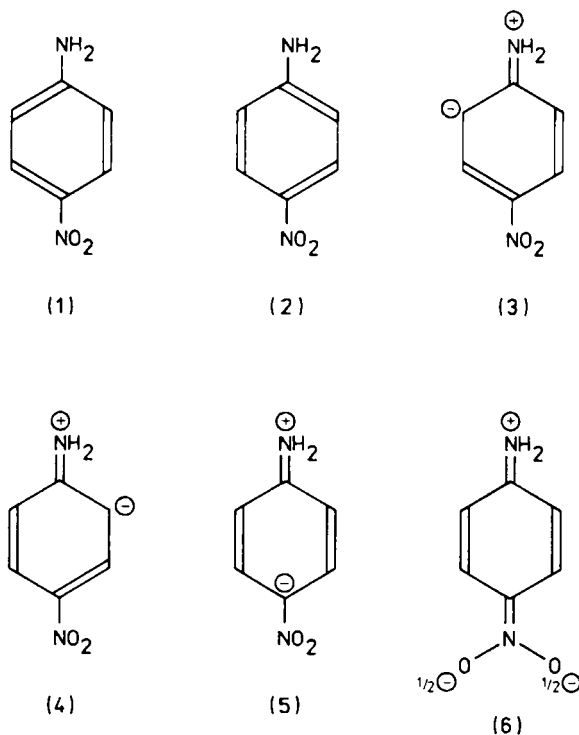
**Scheme 1**

chemical and biological property of the molecule." However, while having known geometry of molecules (or ionic chemical species), one fundamental problem is to translate this information into the language of chemical and physicochemical properties; another is how reliable the geometry of chemical species estimated in crystalline state is in comparison to the shapes in gaseous or liquid states of these species. The first issue here will be subject of this chapter; the second needs only brief mention, as follows.

## B. Hard and Soft Structural (Geometric) Parameters of Molecules

Full information about the geometry of chemical species is given in crystallographic papers by listing the final fractional coordinates of all atoms. These figures are given as fractions of the unit cell dimensions $a$, $b$, and $c$ and within the crystallographic system (characterized additionally by angles $\alpha$, $\beta$, and $\gamma$) of the crystal in question. By use of simple and easily available computer programs, these data are translated into terms understandable by chemist —

that is, into values of bond lengths and bond, torsional, and dihedral angles. These structural parameters are the subject of further analysis in this chapter. Before doing this, we should be aware that they do differ not only by definition but as well by their susceptibility to deformation. This property of structural parameters may be approximately described by listing the force constants to deform them. Table 1 consists of a few of the most illustrative force constants (taken from reference 40), as well as of the appropriate deformation energies (calculated by use of harmonic oscillator model) necessary to change structural parameters by 1% of their magnitude. It is immediately clear that, bond length deformation is about one order of magnitude more costly than bond angle deformation, whereas torsional or dihedral angle deformation is still one order of magnitude less costly. This situation has important consequences in the further treatment of structural parameters. Bond lengths and, to lesser extent, bond angles may be considered as hard parameters. According to older points of view (41), they are not deformed by crystal packing forces. Recent studies based on much more precise structural data do not support this point of view (23, 40), but as a rule these parameters are rather seldom affected by intermolecular interactions in crystals. Hence they may be used to study intramolecular interactions, and this is one of their main uses in structural chemistry.

A quite different situation arises in the case of torsional and dihedral angles, which may be called "soft" structural parameters. These are very sensitive to intermolecular interactions in crystals and hence are used to study such problems in chemistry.

TABLE 1

Typical Force Constants (in $10^5$ dyne cm$^{-1}$) for Various Kinds of Deformation and Energies of Deformation Due to 1% Change in Value of Structural Parameter (Calculated by use of Harmonic Oscillator $E_{def} = -\frac{1}{2}k(\Delta X)^2$

| Stretching of | $k^a$ | 1% $E_{def}^b$ (kJ mole$^{-1}$) |
|---|---|---|
| C—C (ethane) | 4.5 | 0.3 |
| C=C (ethene) | 9.6 | 0.6 |
| C≡C (ethyne) | 15.7 | 1.1 |
| C—C (benzene) | 7.6 | |
| Deformation of CCC bond angle in benzene (in plane) | 0.7 | 0.04 |
| Torsional out-of-plane deformation in benzene | 0.06 | 0.004 |

$^a$Taken from reference 39.
$^b$Taken from reference 40.

Because of this difference between hard and soft structural parameters, they will be discussed separately.

## C.   Bond Angles as Indicators of Substituent Effects on the Geometry of Molecules

Bond angles determined by X-ray diffraction are estimated much more precisely than bond length (42) because X-ray shortening of bond length does not greatly affect the precision of the bond angle estimation. The same is true for thermal motion effects that affect bond angles insignificantly. As early as the mid-1970s, therefore, bond angles were studied as structural parameters in descriptions of substituent effect. In a series of papers Domenicano et al. (43) demonstrated that bond angles, $\alpha$, at *ipso* carbon in monosubstituted benzene derivatives as well as in *para*-disubstituted derivatives with weak intra-molecular interactions, are a convenient descriptor of substituent effect on ring geometry. It was demonstrated (45) that the $\alpha$ angle depends linearly on the corresponding inductive substituent constant or on the group electronegativ-ity $\chi$ of the substituent [Huheey's electronegativity (46)] with correlation coefficients $R$ equal to 0.90 and 0.89 for 10 and 13 data sets, respectively. These results undoubtely express the general trend of dependence of $\alpha$ values on $\sigma_I$ and $\chi$, but the predictive power of these correlations is very low, accounting for 81 and 79% of the explanation of the total variance (calculated as $100\,R^2$).

Changes of geometry in the close neighborhood of the substituent may well be rationalized in terms of the Walsh rule (47, 48). Thus, in summary, if a group X attached to carbon atom is replaced by more electronegative group X', then the carbon atom valency toward X' yields more $p$ character than it had toward X. This is illustrated by Fig. 4: the $sp^2$ hybrid orbital at ipso carbon changes toward CX direction into $sp^{2+2\delta}$, whereas two remaining orbitals realizing $a$-bonds in the benzene ring (Scheme 2) change into $sp^{2-\delta}$. As a result of decrease of $p$ character of hybrid orbitals building up $a$-bonds, the $\alpha$ angle increases and $a$-bond lengths are decreased. The $\pi$-conjugative effect of the substituent may be taken into account in the following way. If the C—X bond has some double-bond character (i.e., if X is somewhat conjugated to the ring), the C‑‑X bond length decreases. Since the covalent radius of carbon atoms decreases as the $s$ character of the hybrid orbital increases, it may be accepted that shortening of C‑‑‑X bond length is associated with an increase in the $s$ character of the orbital of carbon used to realize this bond ($sp^{2-2\delta}$). As a result, one may expect an increase in the $p$ character of the other two orbitals involved in the $a$-bonds in the ring. In consequence, the $a$-bonds become longer and the angle $\alpha$ becomes decreased.

A more detailed analyses of factors contributing to variation of $\alpha$ values in monosubstituted benzenes yielded a slightly more complex view. If the $\alpha$
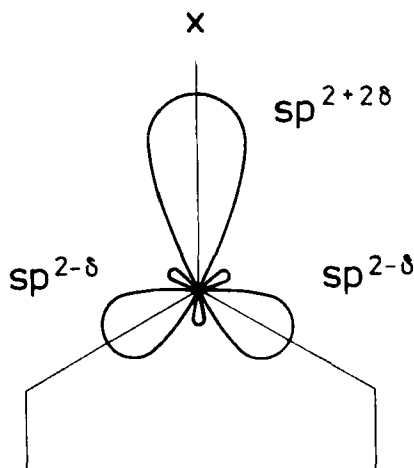
**Figure 4** Illustration of the Walsh rule by showing changes in hybridization of the $\sigma$-electron core of the substituted benzene ring fragment (56).
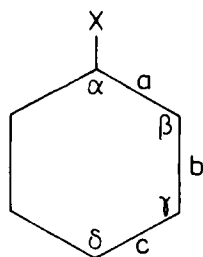


**Scheme 2**

values are plotted against electronegativity $(\sigma_\chi)$ and resonance $(\sigma_R)$ constants (28), the planar regression for 11 data points gives the blend of these two factors equal to $\rho_\chi/\rho_R = 1.39$ or 58% of $\sigma_\chi$ contribution. Explanation of the total variance by this model is 95%. This result is in line with the other one in which $\alpha$ values were plotted against Mulliken $\sigma$- and $\pi$-electron charge densities at the *ipso* carbon for 12 monosubstituted benzene derivatives (49) calculated by use of an ab initio STO-3G model with optimization of geometry. The linear model $\alpha$ versus $\Delta q_\sigma$ explained 70% of the total variance, whereas addition of the explanatory parameter $\Delta q_\pi$ provides explanation of the total variance to 91.4%. The same kind of treatment revealed that $\gamma$ angle (at the *meta* position) depends almost solely on $\pi$-electron effects (92.3% of variance explained) and $\delta$ values depending on both $\sigma$- and $\pi$-electron densities with the blend $q(\sigma)/q(\pi) = 1.2$ and 84% of the variance explained by the planar model.

Undoubtedly, one may conclude that $\alpha$ values in monosubstituted derivatives of benzene are governed chiefly by the electronegativity $\chi$ of the substituent and to less extent by resonance (or $\pi$-electron) factors. These results seem to support the view that angles at the *ipso* carbon of the substituted molecules may serve as structural (geometric) parameters for substituent effects of geometry. The idea of using endocyclic angles in substituted benzene derivatives as structural parameters developed some 10 years ago. Norrestam and Schepper (50, 51) and Domenicano and Murray-Rust (52) published lists of angular substituent parameters (ASP) defined as differences between the values $\varphi_i$ (X) perturbed by substituent X in position $i$ and the unperturbed value (i.e., 120°)

$$\Delta\varphi_i(X) = \varphi_i(X) - 120° \tag{10}$$

where $i = ipso$, *ortho, meta,* or *para* positions and the angles are denoted $\alpha$, $\beta$, $\gamma$, and $\delta$, respectively, as shown in Scheme 2. Table 2 presents a collection of ASP

TABLE 2

Angular Substituent Parameters, $\Delta\varphi$ (after Reference 52 Unless Stated Otherwise)

| X\($\Delta\varphi$) | $\Delta\alpha$ | $\Delta\beta$ | $\Delta\gamma$ | $\Delta\delta$ |
|---|---|---|---|---|
| COO [a] | − 2.8(2) | 1.8(2) | 0.4(3) | − 1.2(1) |
| NMe$_2$ | − 2.4(3) | 0.6(2) | 1.4(2) | − 1.7(3) |
| Ph | − 2.3(2) | 1.0(1) | 0.6(1) | − 0.9(2) |
| Me | − 1.9(2) | 1.0(1) | 0.4(1) | − 0.8(2) |
| CH—CHR | − 1.8(2) | 0.8(1) | 0.3(1) | − 0.4(2) |
| 9 Antr.[b] | − 1.5(2) | 0.4(1) | 0.4(1) | − 0.2(2) |
| NH$_2$ | − 1.2(2) | 0.2(1) | 1.0(1) | − 1.3(2) |
| CH − NR | − 1.2(3) | 0.4(2) | 0.4(2) | − 0.5(3) |
| N=CHR | − 1.0(3) | 0.2(2) | 0.5(2) | − 0.5(3) |
| COMe | − 1.0(2) | 0.4(2) | 0.2(2) | − 0.3(2) |
| COOR | − 0.6(2) | 0.2(1) | 0.3(1) | − 0.3(2) |
| N=NR | − 0.1(2) | − 0.3(1) | 0.5(1) | − 0.4(2) |
| NHCOMe | − 0.1(3) | − 0.3(2) | 0.7(2) | − 0.6(3) |
| COOH | 0.1(2) | − 0.2(1) | 0.1(1) | 0.2(2) |
| OH | 0.2(2) | − 0.4(1) | 0.6(1) | − 0.6(2) |
| OMe | 0.2(2) | − 0.6(1) | 1.1(1) | − 1.1(2) |
| CN | 1.1(2) | − 0.8(1) | 0.3(1) | − 0.1(2) |
| SO$_3$ | 1.2(2) | − 1.1(1) | 0.5(1) | 0.0(2) |
| OAc[b] | 1.5(1) | − 1.2(1) | 0.4(1) | 0.1(1) |
| SO$_2$Me | 1.6(2) | − 1.3(1) | 0.2(1) | 0.6(2) |
| NH$_3^+$ | 1.8(2) | − 1.2(1) | 0.4(1) | − 0.1(2) |
| Cl | 1.9(2) | − 1.4(1) | 0.6(1) | − 0.2(2) |
| NO$_2$ | 2.9(2) | − 1.9(1) | 0.3(1) | 0.4(2) |
| F | 3.4(2) | − 2.0(1) | − 0.5(1) | − 0.4(2) |

[a]Reference 24.
[b]Reference 44.
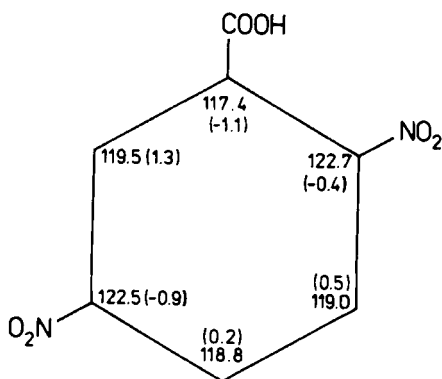
**Figure 5** Angular geometry of 2,5-dinitrobenzoic acid (53). Esd for angles 0.2°; in brackets $\Delta\phi_i = \phi_i(\text{obs}) - \phi_i$ (additive rule).

values. The values published by Norrestam and Schepper were estimated from a collection of 48 polysubstituted benzene and even pyridine derivatives. Thus, their ASP values contain much more complex contributions than do those originating from a single substituent, as tentatively may be said about ASP values reported by Domenicano and Murray-Rust (52), who extracted their ASP values from the geometries of 71 different mono- and para-disubstituted* benzene derivatives. Table 2 also contains a few other ASP values estimated in line with these requirements. These values may be used to study polysubstituted benzene derivatives in order to estimate additivity of substituent effect on angular geometry of the substituted ring in benzene derivatives. A nonadditivity parameter *NAP* (24) may be defined as

$$NAP = \sum_{i=1}^{\sigma} |\phi_{i,\text{exp}} - \phi_{i,\text{calc}}| \qquad (11)$$

where $\phi_{i,\text{calc}}$ are calculated by use of ASP values, whereas $\phi_{i,\text{exp}}$ are those determined experimentally. If the *NAP* value is greater than $3\sigma$ for a given system, then a strong nonadditivity effect is operating as a result of interaction between substituents. The same is true for individual *NAP* values (i.e., $\phi_{i,\text{exp}} - \phi_{i,\text{calc}}$).

Let us consider an example to illustrate the problem. Figure 5 presents the angular geometry of 2, 5-dinitrobenzoic acid (53) with $\varphi_{i,\text{exp}} - \varphi_{i,\text{calc}} = \Delta\varphi_i$ values in parentheses. The calculated *NAP* value is 4.4°, whereas individual $\sigma = 0.2°$. For six angles involved in the calculation of *NAP*, $\sigma = [(0.2)^2.6]^{1/2} = 0.49°$ and $3\sigma = 1.47° < 4.4°$. Thus the observed deformation is highly signi-

---

*It is assumed that geometries used were not affected too much by other than $\sigma$-electron effects.
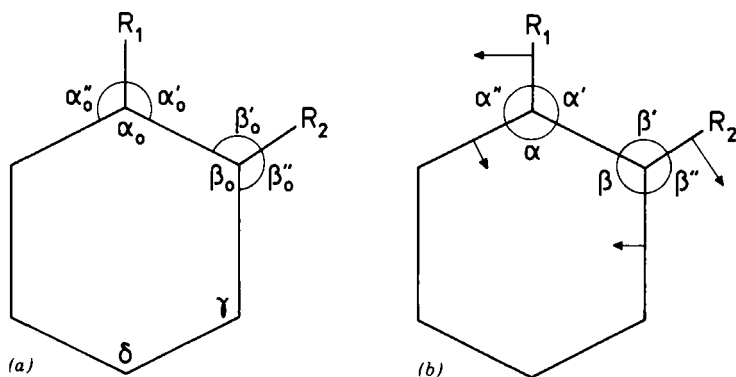
**Figure 6** (a) Assignment of angles in *ortho*-disubstituted benzene derivative; (b) steric interactions between $R_1$ and $R_2$ indicated by repulsive forces (as arrows).

ficant and needs interpretation, which may be done as follows (54). If there are no steric interactions between substituents $R_1$ and $R_2$ (Fig. 6a), $\alpha'_0 = \alpha''_0$, and $\beta'_0 = \beta''_0$, however $\alpha_0$ and $\beta_0$ depend on the nature of substituents $R_1$ and $R_2$. For the situation where no mutual interactions occur, one may follow the additivity scheme and apply ASP values from Table 2 to calculate $\alpha_0$ and $\beta_0$. Knowing these values for the unperturbed situation, one can calculate $\alpha'_0$ and $\alpha''_0$ by using the formula

$$\alpha'_0 = \frac{360° - \alpha_0}{2} \tag{12}$$

The same can be done for $\beta'_0$, and $\beta''_0$.

If there are any repulsive interactions between $R_1$ and $R_2$, then forces acting are as presented in Fig. 6b by arrows. In consequence, one may expect an increase of $\alpha'_0 \rightarrow \alpha'$ and $\beta'_0 \rightarrow \beta'$ (53, 55). The sum of the differences $(\alpha' - \alpha'_0)$ and $(\beta' - \beta'_0)$ may be used as a parameter numerically describing the repulsive deformation due to steric interaction between $R_1$ and $R_2$. We define a repulsive deformation parameter as

$$RDP = (\alpha' - \alpha'_0) + (\beta' - \beta'_0) \tag{13}$$

Let us apply this way of description to the angular geometry of 2,5-dinitrobenzoic acid (Fig. 5). Thus, in this case $R_1 = COOH$ and $R_2 = NO_2$, and using ASP values and additive scheme, one finds $\alpha_0 = 120.1°$ and $\beta_0 = 122.9°$ (assignements as in Fig. 5). Hence:

$$RDP = (123.5° - 120.0°) + (121.1° - 118.5°) = (3.5° + 2.6°) = 6.1°$$

and by this value $(\alpha' + \beta')$ in 2,5-dinitrobenzoic acid is greater than it could be expected if (1) no steric effects operate between COOH and $NO_2$ and (2) no $\pi$-electronic effects deform $\alpha$ and $\beta$. The latter may be neglected since the substituents in question are of the same nature and such interactions are not expected.

The increase in $(\alpha' + \beta')$ means that as a result of repulsion between COOH and $NO_2$, the other two angles ($\alpha''$ and $\alpha$ in Fig. 6a,b) must be decreased, $\alpha''$ to a greater and $\alpha$ to a lesser degree. The same is true for $\beta$ angles. Thus, the observed $\alpha$ and $\beta$ must be less than expected from additivity rules. Indeed, figures for angles in 2,5-dinitrobenzoic acid are in line with this conclusion: $\alpha = 117.4°$ instead of $118.5°$ and $\beta = 122.7°$ instead of $123.1°$.

If, however, ASP values are for some kind of systems not available, or the system in question is not a benzene derivative, an approximate procedure may be applied. Instead of (12) we may use

$$\alpha' = \frac{360° - \alpha}{2} \tag{14}$$

in which case we assume that deformation expressed in Fig. 6b by the shorter arrow is negligible in comparison to the direct one illustrated by the longer arrow. If we compare the first-order effect expressed by the $RDP$ value for $\alpha'$ and $\beta'$ and the second-order effect given by nonadditivity parameter for $\alpha$- and $\beta$-angles, then

$$NAP(\alpha,\beta) = |\alpha - \alpha_0| + |\beta - \beta_0| \tag{15}$$

We find for our example (Fig. 5) that $RDP = 6.1°$ and $NAP(\alpha, \beta) = 1.5°$ with a $3\sigma$ value for these cases of $1.2°$ and $0.85°$, respectively (difference in $3\sigma$ results from the number of variables in both cases — 4 and 2, respectively — individual $\sigma = 0.2°$). It is immediately apparent that the effect in $RDP$ is much larger and more significant. (But both are highly significant!) Thus, assuming $\alpha \approx \alpha_0$ (and $\beta \approx \beta_0$), we are in error, which, however, should not obscure the main effect. For qualitative aspects, it seems to be quite acceptable. In many papers on polysubstituted benzene derivatives, this kind of analysis has been found to be fruitful (24, 53–56).

The other interaction that may affect angular geometry of benzene derivatives is that due to strong resonance effects. This was indicated earlier by Domenicano and Murray-Rust (52). Analysis of p-nitroaniline (57) as well as N,N-diethylparanitroaniline (58) and series of para-substituted benzoic acid (59) revealed good examples for this kind of interaction.

Of these systems, the $NAP$ value for p-nitroaniline is 2.9°; for N,N-diethylparanitroaniline, 5.4° and 4.3° (two independent molecules in the
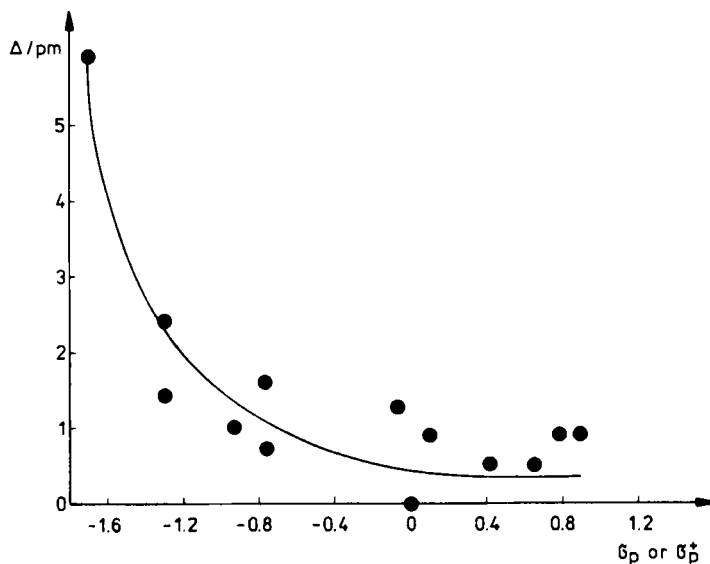
**Figure 7**   Dependence of $NAP$ value as $\sum_{i=1}^{6} NAP_i$ on $\sigma_p$ or $\sigma_p^+$ values for 13 *para*-substituted derivatives of benzoic acid.

crystal cell); and for $N,N$-dimethyl-p-benzoic acid, 5.9°. All these deformations are highly significant and indicate the importance of the $\pi$ effect in contributing to the angular geometry of *para*-disubtituted derivatives of benzene. This may additionally be illustrated by Fig. 7, which presents the plot of $NAP$ value against $\sigma_p^+$-values of countersubstituents for a series of *para*-substituted benzoic acids. Obviously, $NAP$ values reach significantly high levels only for strongly donating substituents ($NH_2$, $NMe_2$).

It is important to mention, however, that most contributions to the nonadditivity of bond angles ($NAP$ values) come from bond angles at *ipso* carbon atoms: $|\Delta\alpha = \alpha_{obs} - \alpha_{add}| > 1.0°$ (for $N,N$-diethylparanitroaniline (58), $\Delta\alpha(NO_2) = -1.25°, \Delta\alpha(NEt_2) = -1.2°$, whereas for $N,N$-dimethyl$-$p-aminobenzoic acid (59), $\Delta\alpha(NMe_2) = -1.2°$ and $\Delta\alpha(COOH) = -1.2°$. These strong deviations from additivity require rationalization. This may be done on the basis of the Walsh rule. At the carbon atom bonded to $NAlk_2$ group, one observes a C—N bond significantly shorter than that observed in $N,N,N',N'$-tetramethyl-p-phenylenediamine. This should be associated with an increase of $s$ character in C $-$ N bond (due to its shortening cf. p. 251) and consequently a decrease of $s$ character for orbitals realizing $a$-bonds. But this implies a decrease of the bond angle $\alpha$ — in agreement with the above-mentioned finding $\Delta\alpha(NO_2) < 0$. Comparison of $CN(NO_2)$ bond length in $N,N$-diethyl- $p$-nitroaniline and $p$-dinitrobenzene again reveals significant shortening, and hence this effect may contribute to the observed negative value of $\Delta\alpha(NO_2)$.

Additionally, at the carbon atom joined to the $NO_2$ group the net calculated $\pi$-electron population is large—1.155 (38)—and hence its electronegativity is decreased.

In the analysis of bond angles in benzene derivatives one should be aware that, apart from the empirical mutual dependence between $\alpha$ and $\beta$ angles, which has an approximate form that $\Delta\beta \approx - 1/2\Delta\alpha$ (Table 2), of the six bond angles only four are independent variables as a result of two geometric constraints (49, 52):

$$\alpha + 2\beta + 2\gamma - \delta = 4\pi \tag{16}$$

and

$$a\cdot\sin\alpha/2 - b\cdot\sin\frac{\beta - \alpha}{2} - c\cdot\sin\frac{\delta}{2} = 0 \tag{17}$$

For analysis of geometric constraints, see references 60 and 61.

### D.   Bond Lengths as Indicators of Substituent Effect on Geometry of Molecules

In contrast to bond angles, bond lengths are less accurately measured by X-ray diffraction for two reasons:

1. They are much more sensitive to thermal motion effects.
2. The measured distance is not between the two nuclei of the atoms that form the bond, but between centroids of the electron clouds.

Thermal motion effects can, however, be diminished by use of the standard THMB-computer program (*t*hermal *m*otion analysis *b*ased chiefly on papers by Huber-*B*use) (62), by which the appropriate corrections for bond lengths are calculated. In general, the corrections for libration for bond lengths are less than 1.0 pm; that is, the real bond may be longer in magnitude than that determined by X-ray diffraction in the crystalline state. The other way to decrease thermal motion effects is to carry out measurements at low temperature.

Inaccuracies due to nonsphericity of electron clouds (by which the X-ray are diffracted) are less dangerous if all the data analyzed result from X-ray measurements, since part of the inaccuracy cancels out. If attempts are undertaken to compare X-ray bond lengths with neutron or electron diffraction measurements (or measurements otherwise determined), then a great advantage is to standardize these data internally, that is, instead of bond lengths to use their appropriate differences. This will be exemplified later.

A great advantage of using bond lengths as structural parameters to estimate intramolecular interactions is that they are 10 times more difficult to deform than bond angles (see Table 1). Thus repulsion forces must be 10 times greater to deform significantly bond lengths than bond angles. A very good example is the geometry of sodium *p*-nitrobenzonate (Fig. 1), which as a result of short interatomic contacts exhibits very significant deformation of angles, but not of bond lengths (24).

It should be pointed out that for a long time bond lengths served as sui generis indicator of chemical reactivity. Thus the CC double bonds of length 1.34 pm were suspected to undergo addition reactions whereas atoms forming CC aromatic bonds, 1.40 pm, were susceptible to substitution. This, however, has now proved to be inadequate. Topsom (29) has presented much of the recent developments in this field. These results are not repeated here, except those needed for comparison and for discussion. The minor shortcoming of that review is that in many cases instead of using esd to show the precision of geometry, bond length values are rounded off to 0.01 Å (1 pm). In modern X-ray and other techniques of molecular geometry determination, precisions of 0.1–0.2 pm may be achieved. Convincing examples should be taken for those structural data for which application of the $3\sigma$ rule can eliminate any doubt.

### 1.   Dependence of Bond Lengths on the Nature of the Substituent

For monosubstituted benzene derivatives and *para*-disubtituted benzene derivatives, the Walsh rule should be obeyed. Thus one should expect dependence of $\alpha$ values on $a$-bond lengths with negative slope. An increase of $\alpha$ should be accompanied by an increase in electronegativity $\chi$ and a decrease of $a$-bond lengths. This, could not be achieved, however, until $a$ were replaced by $b - a = \Delta$. The subtraction leading to $\Delta$ cancels at the common error in measurement of $a$ and $b$. Hence $\Delta$ values appear to be a quite reliable structural parameter (63). The dependence of $\Delta$ versus $\alpha$ for monosubstituted and particularly for symmetrically *para*-disubtituted benzene derivatives proved to be more precise (64) than $\alpha$ versus $\chi$ (Huheey) or $\alpha$ versus $\alpha_1$ (45). Figure 8$a,b$ shows the dependence of $\Delta$ versus $\alpha$ for 11 monosubstituted benzene derivatives (correlation coefficient $r = .942$) for which geometry was determined other than in the crystalline state (microwave, or gas-phase electron diffraction. For a set of data from one experiment technique (gas-phase electron diffraction), the $R$ value increases to 0.994 for $n = 7$ (Fig. 8$b$). Detailed statistical analysis of a $\Delta$ versus $\alpha$ plot for a large crystallographic data set as well as the dependence of the quality of the model on the quality of the data applied is presented in reference 64. For symmetrically *para*-disubtituted benzene derivatives, the $\Delta$ versus $\alpha$ relationship is followed more precisely and
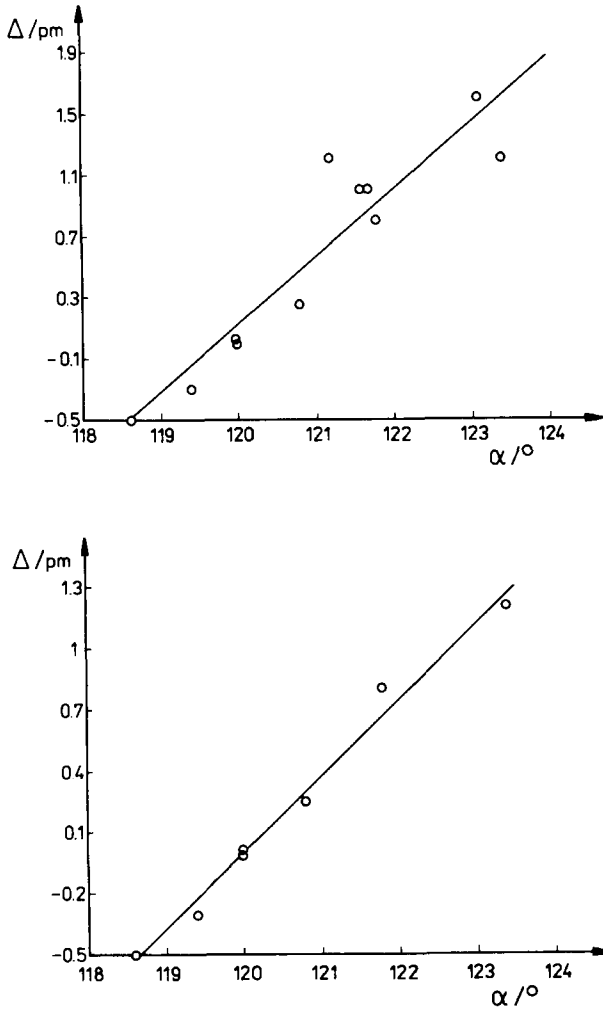
**Figure 8** Dependence of $\Delta$ versus $\alpha$ for ($a$) 11 monosubstituted benzene derivatives—noncrystalline phase for geometric determination (electrodifraction in the gas phase, microwave, and NMR in nematic phase); ($b$) seven data sets for only ED and MW.

is described by the equation (63)

$$\Delta = 0.38 \cdot \alpha - 45.64 \qquad (18)$$

with $R = .979$ for 10 precisely measured data points.

To summarize, it may be said that $\Delta$ versus $\alpha$ plots may serve as a

qualitative realization of the Walsh rule applied to mono- and *para*-symmetrically disubstituted derivatives of benzene.

Further evidence for the utility of using the Walsh rule to describe substituent effects on the geometry of the benzene ring in *para*-symmetrically substituted benzene derivatives is found in the observations by Hargittai et al. (65, 66). They found that the interatomic distance $d(C_1C_4)$ depends linearly on $\alpha$ values with a high correlation coefficient ($R = .97$) for 33 data points (65). This type of plot is presented in Fig. 9 for measurements made by electron diffraction and microwave techniques. This dependence was then described in terms of geometric considerations (66) leading to the formula

$$d(C_1C_4) = 2a\cdot\cos\frac{\alpha}{2} + b \approx a + b - a\Delta\alpha\cdot\frac{3\pi}{2.180} \qquad (19)$$

where $\Delta\alpha = \alpha - 120^\circ$. It was found (67) by analysis of variance of $a$, $b$, and $c$ bond lengths for a collection of 17 geometries of monosubstituted derivatives of benzene that only the $a$ values depend strongly on the nature of the substituent. We may assume that the term $b$ in (19) is approximately constant and that $d(C_1C_4)$ depends almost solely on $a$ and $\alpha$ values. After substituting $\Delta\alpha = \alpha - 120^\circ$ into equation 19 and calculating constant term, one obtains

$$d(C_1C_4) = b + a\cdot(2.81 - 0.015\cdot\alpha) \qquad (20)$$

Since, according to the Walsh rule, $a$ and $\alpha$ are inversely proportional (i.e., increase of $a$ is associated with decrease of $\alpha$), as $a$ increases, so does
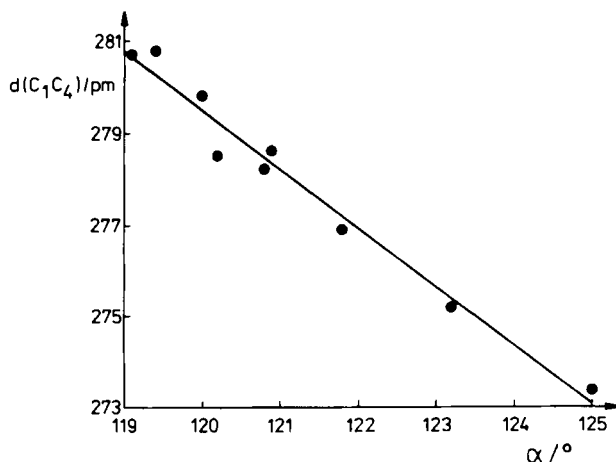


**Figure 9** Dependence of $d(C_1C_4)$ on $\alpha$ for nine data points taken from reference 30.

the term in parentheses. Thus, $a$ and $\alpha$ values act in Equation 19 in line. Accepting $b = 138.5$ [mean value taken for 17 geometries (67)] and using $\alpha$ and $a$ values for $p$-bis(trimethylsilyl)benzene (66) and $p$-dinitrobenzene (68), we estimate from these values $d(C_1 C_4) = 290.2$ pm and 269.5 pm, respectively. In comparison, experimental values are 289.8 pm (66) and 272.0 pm (68), respectively. Another support for the Walsh rule is the finding that the mean CC bond length in the ring, $\bar{r}(CC)$ in $para$-symmetrically substituted benzenes depends approximately on $\alpha$. Again, the most important contribution to the $\bar{r}$ value comes from $a$ values, as $b$ is almost constant. Thus, this kind of dependence is approximately equivalent to that of $a$ versus $\alpha$, and the negative slope is in line with expectation.

We may conclude in the following: ASP values may be used to determine whether the substituent effects on angular geometry are additive. If the $(\Delta, \alpha)$ point for a given $p$-XPhY system does obey Equation 18, then either X and Y do interact with the ring following the Walsh rule; that is, electronegativity of substituents is the main factor in interactions, or other factors are colinear with electronegativity, or, in broader terms with $\sigma$-electron effects.

## 2. Analysis of the Geometry in *para*-Disubstituted Benzene Derivatives

In *para*-disubstituted derivatives of benzene one may expect a strong deviation from the Walsh rule for cases if X and Y differ in $\pi$-electron properties, particularly if one of them is electron-accepting and the other is electron-donating. One problem is to determine the extents to which $\pi$-electron-accepting and $\pi$-electron-donating properties of substituents perturb geometry of the ring and $\sigma$-electron effects are still observable.

Let us discuss these problems by taking the geometry of $N,N$-diethyl-$p$-nitroaniline (DPNA)* as an example (58) (Fig. 10). This is a typical system
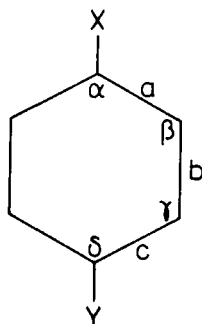


**Scheme 3**

*There are two independent molecules in the crystal cell of DNPA; hence the geometry parameters used are averaged over both molecules and assuming $C_{2v}$ symmetry.
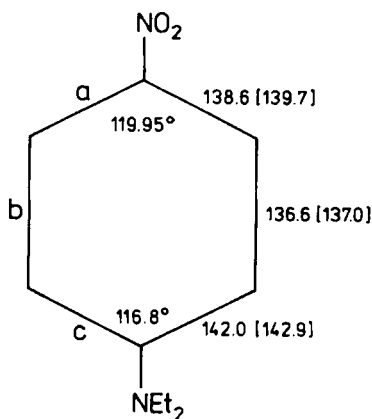
**Figure 10**   Bond lengths for *p-N,N*-diethylnitroaniline (58) as average structure from two independent molecules in the assymetric unit with $C_{2v}$ symmetry assumed. Values in brackets are corrected for libration.
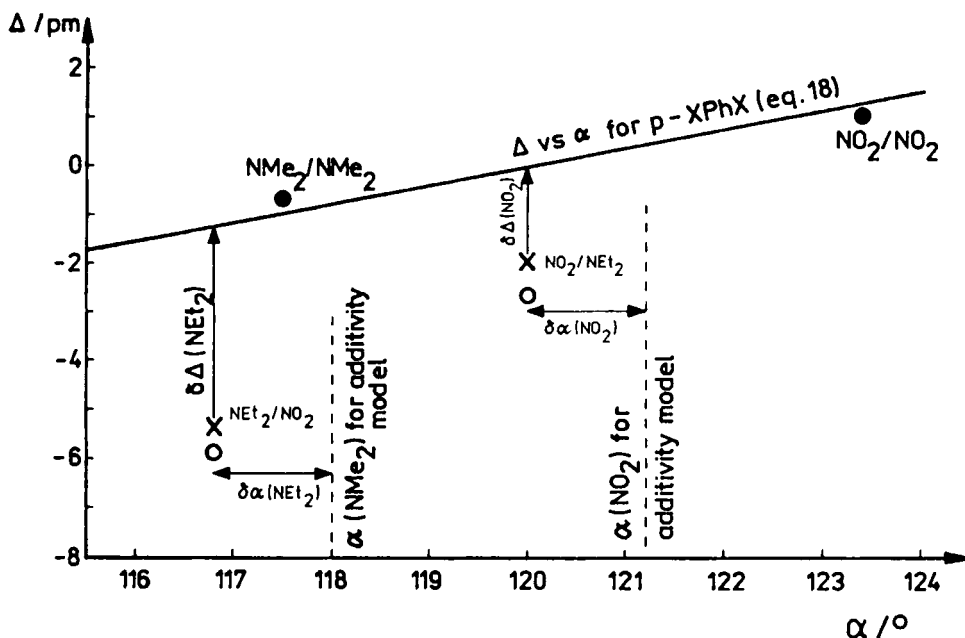


**Figure 11**   Plot of $\Delta$ versus $\alpha$ for *p-N,N*-diethylnitroaniline. The line describes the $\Delta$ versus $\alpha$ plot for symmetrically disubstituted benzene derivatives with two points, full circles, for *p*-dinitrobenzene ($NO_2/NO_2$) and $N,N,N'$, $N'$-tetramethyl-*p*-phenylenediamine ($NMe_2/NMe_2$). Crosses: $\Delta(NEt_2) = b - c$ and $\Delta(NO_2) = b - a$. Empty circles: values corrected for thermal motion; $\alpha$ value as measured. Perpendicular dotted lines: $\alpha$-values calculated by use of additive scheme and ASP- values from Table 2.

with a strongly $\pi$-electron cooperative substituent effect. In terms of $\Delta$ and $\alpha$ values, we have two $\Delta$ values for DPNA: $\Delta(NEt_2) = b - a = - 5.4$ pm and $\Delta(NO_2) = b - c = - 2.0$ pm. If corrections for thermal motion are taken into account, these figures change to $- 5.9$ pm and $-2.7$ pm, respectively. Plotting these values against $\alpha(NEt_2) = 116.8°$ and $\alpha(NO_2) = 119.95°$, we observe that both points deviate strongly from the line by values $\delta\Delta = \Delta(\text{real}) - \Delta(\text{the line})$ equal to $-4.2$ and $-2.0$ pm, respectively (Fig. 11). If we apply bond lengths corrected for thermal motion (data in brackets), we obtain $-4.7$ and $-2.7$ pm, respectively. The effect is even greater, and obviously for so strong interactions it seems that thermal motion does not affect the general picture observed in the ring geometry. If we analyze the substituent effects on angular geometry, applying ASP values, we can calculate $\alpha(NEt_2)$ and $\alpha(NO_2)$ resulting from an additive scheme of interactions that yield $118.0°$ and $121.2°$, respectively. The differences $\delta\alpha = \alpha\ (\text{real}) - \alpha(\text{additive scheme})$ are equal to $- 2.5°$ and $-2.4°$, respectively. All these data are presented in Fig. 11. It is apparent that $\delta\alpha$ are almost the same for both substituents (horizontal arrows), whereas $\delta\Delta$ is two times greater (as to absolute value) for $NEt_2$ than $NO_2$. This may be explained as on the scheme shown in Fig. 12. The $a$- and $c$-bonds are both lengthened as a result of $\pi$-electron effect (quinoid structures) whereas $b$-bond is shortened for the same reason. The $a$-bond is affected by the
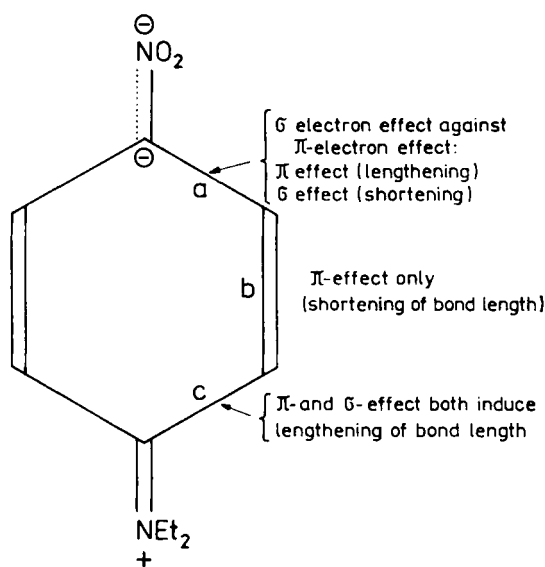


**Figure 12** Scheme of $\pi$- and $\sigma$-electron effects on geometry (bond lengths) in $p$-$N$, $N$-diethylnitroaniline.

strongly electronegative substituent ($NO_2$) and hence is shortened according to the Walsh rule. As a result of opposite $\sigma$ and $\pi$ effects, one observes $a$-bond lengths close to those of unsubstituted benzene derivative 139.2 pm [X-ray measurement corrected for libration (69)]. In contrast, $c$-bonds are subject to concerted $\sigma$ and $\pi$ effects since the $NEt_2$ group is of low electronegativity [$\chi(NEt_2) = 2.36$ in comparison to $\chi(NO_2) = 4.83$; both figures in Pauling's (70) scale of electronegativity (46)]. In consequence, $|\Delta(NO_2)| < |\Delta(NEt_2)|$.

This kind of effect may be expected in all $p$-XPhY systems in which X and Y are electron-accepting and electron-donating substituents, respectively. Another consequence of oppositely acting components for $\sigma$ and $\pi$ effect in the overall substituent effect of strongly electronegative substituents is the observation that if one defines a parameter built up of bond lengths but taking into account the whole ring, that is

$$\sum \delta\Delta = \Delta(X) + \Delta(Y) = 2b - a - c \tag{21}$$

then the plot of $\Sigma\,\delta\Delta$ depends only on the electron-donating power of substituents described by the $\sigma^+, \sigma^-$ effect being negligible (67). The dependence of 16 precise geometries (esd for bond length $\sigma \leqslant 0.5$ pm) of $p$-XPhY systems exhibiting various degrees of $\pi$-electron cooperative effect on $\sigma^+$ and $\sigma$ -values gave the reggression (67)

$$\sum \Delta = 1.3 \pm 1.3 - (1.6 \pm 1.2)\cdot\sigma^- + (3.5 \pm 0.2)\cdot\sigma^+ \tag{22}$$

with a correlation coefficient $R = .971$. The high value of esd for $\sigma^-$ implies that the $\rho^-\cdot\sigma^-$ term is of negligible importance. Indeed, a linear regression of $\Delta$ versus $\sigma^+$ alone yields $R = .970$ for the same data sets. The change in correlation coefficient on going from planar to linear regression is evidently insignificant. Figure 13 presents the plot of $\Sigma\,\Delta$ versus $\sigma^+$ for presently available data set.

### 3. Do the Bond Lengths in $p$-XPhY Systems Support the Classical View of a through Resonance effect?

Recent quantum-chemical studies (38), combined with gas-phase studies on the acidity or basicity of *para*-substituted derivatives of aniline, phenol, and related systems (28, 27–74), have revealed that the classical description of through resonance in terms of a considerable contribution of the quinoid structure **6** and less important other structures is not justified.

Nevertheless, even recent data (geometry) of such systems has usually been interpreted in terms of classical view (57, 75, 76). Some subtle aspects of differences in bond lengths have already been discussed. Now, in order to decide the answer to the title question, we consider the geometry of those
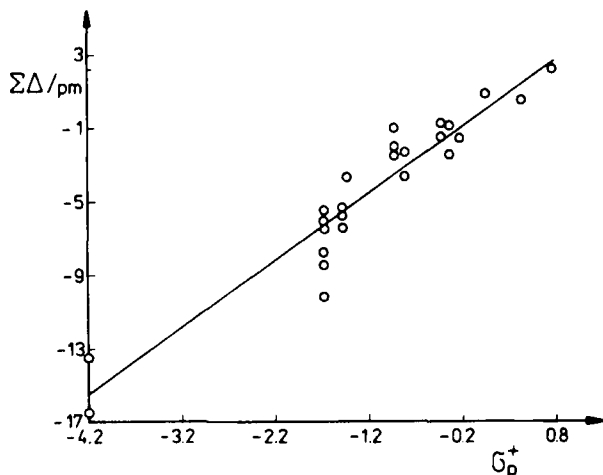
**Figure 13**   Plot of $\sum \Delta$ versus $\sigma_p^+$ for 25 recently available data sets; only crystal structures with esd of bond length $\leqslant 0.5$ pm taken into account.
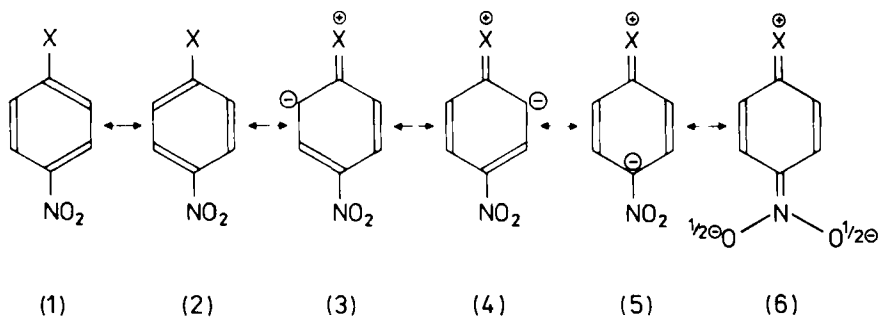


**Scheme 4**

systems in which $o,o'$-dimethyl substitution causes a significant twist of 1,4-substituents expected to exert a strong cooperative effect. Figure 14 presents the geometry of the following systems: $p$-$N,N$-dimethylnitroaniline (DPNA) (58), $N,N$-dimethyl- 4-nitro- 3,5-xylidine (3,5-DNXy), (77) and $N,N$-dimethyl-4-nitro- 2,6-xylidine (2,6-DNXy) (56).

It is apparent that the geometry of 3,5-DNXy does not differ from DPNA as 2,6-DNXy does, even though in both cases substituents able to conjugate ($NO_2$ and $NMe_2$, respectively) do twist significantly from coplanarity with the ring by 50.6° and 60.4°, respectively. If we want to analyze these differences more precisely, we have to define a structural parameter in order to calculate

differences between the appropriate bond lengths expressed in units of estimated standard deviation for the difference $[\sigma_{\text{diff}} = (\sigma_1^2 + \sigma_2^2)^{1/2}]$. These data are given in Table 3. It is immediately apparent that differences between appropriate bond lengths of 3,5-DNXy and DPNA are usually less than $3\sigma$, except C4-$N_{\text{nitro}}$, which is directly exposed on steric effect of $o,o'$-dimethyl substitution and the CN bond is an axis of the twist of $NO_2$ by $50.6°$). The situation is quite different if one compares geometry of 2,6-DNXy and DPNA. In this case all appropriate bonds differ by $3\sigma$ or more, and undoubtedly the steric hindrance of $o,o'$-methyl groups results in a twist of $NMe_2$ group by $60.4°$, which is a cause of dramatic change of bond lengths both in the ring as well as in both CN bonds.

It may be concluded that the resonance effect from $NAlk_2$ group to the ring is of high importance while the electron demanding property of $NO_2$ group is less important as far as the $\pi$-electron charge transfer to this group is concerned. This means that the classical picture of through resonance, which is the dominant contribution of structure **6**, is not justified. This conclusion is in line with the earlier findings by Exner (78, 79) that the assumed conjugation of the nitro group through the benzene ring is merely a conjugation of the donating substituent with the benzene $\pi$ system, while the accepting substituent acts directly by its inductive effect. The conclusion made above may even be strengthened if one applies the harmonic oscillator stabilization energy (*HOSE*) mode to the geometry of these three systems (80). This model permits the estimation of the weights of canonical structures participating in the
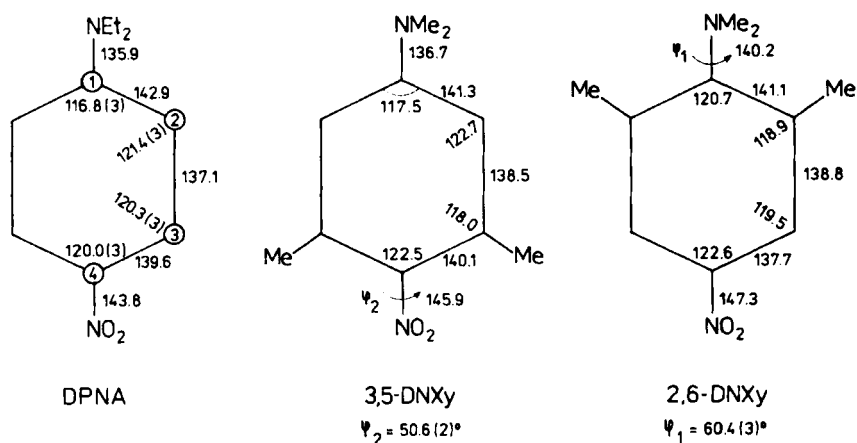


**Figure 14** Geometry of *N,N*-diethyl-*p*-nitroaniline, 3,5-dinitroxylidine, and 2,6-dinitroxylidine; $\phi_1$ and $\phi_2$ represent twist of $NMe_2$ and $NO_2$ as a result of $o,o'$-substitution by methyl groups.

TABLE 3

Analysis of Differences in Bond Lengths in DPNA and 2,6- and 3,5-DNXy (Data Corrected for Thermal Motion Applied)

| Molecules Compared | Differences[a] in Bond Lengths in pm (Units ESD[b] in Parentheses) | | | | |
|---|---|---|---|---|---|
| | C1–N(am) | C1–C2 | C2–C3 | C3–C4 | C4–N (nitro) |
| 2,6-DNXy–DPNA | 4.3 | −1.9 | +1.9 | −1.9 | 3.5 |
| | (9.6) | (−3.1) | (3.0) | (−3.3) | (7.0) |
| 3,5-DNXy–DPNA | 0.8 | −1.6 | 1.4 | 0.5 | 2.1 |
| | (1.6) | (−2.8) | (2.4) | (0.7) | (4.2) |

[a]Differences obtained by substraction of the bond lengths in 2,6- and 3,5-DNXy from those in DPNA.

[b]For difference equal to $(\sigma_1^2 + \sigma_2^2)^{1/2}$.

overall description of the molecule directly from the experimental geometry. First we summarize briefly the idea of the HOSE model. This is based on the calculation of the deformation energy of the molecule from its geometry based on assumed cannonical structures by use of the simple harmonic potential

$$E_{\text{def}} = -\frac{1}{2} \cdot \sum_{r=1}^{n} \Delta_r^2 \cdot k \tag{23}$$

where $k$ stands for a force constant assumed to be linearly related to bond length

$$k_r = a + b \cdot R_r \tag{24}$$

where $a$ and $b$ are calculated from bond lengths, $R$ and force constants $k$ for purely single and double bonds. For CC bonds, values for ethane and ethene were used. The $\Delta_r$ values in Equation 23 represent differences between the real bond length and the appropriate bond length in the canonical structure. For CC bonds the canonical structures are supposed to have single and double bonds such as in 1,3-butadiene measured in the gas phase by electron diffraction (81). This choice is in line with modern concepts of resonance energy (82,83) in which the reference structures have CC bond lengths as in acyclic polyenes. Thus the final formula for calculating $HOSE$ for a given $i$th resonance (canonical) structure is

$$HOSE_i = 301.15 \left[ \sum_{r=1}^{n_1} (R' - R_0^s)^2 \cdot (a + bR_r') + \sum_{r=1}^{n_2} (R'' - R_0^d)^2 \cdot (a + bR_r'') \right] \tag{25}$$

where $R'_r$ and $R''_r$ are the lengths of $\pi$ bonds in the real molecule and $n_1$ and $n_2$ are the numbers of single and double bonds in the $i$th canonical structure, respectively. In the process of deformation, $n_1$ bonds are lengthened and $n_2$ bonds are shortened to the bond lengths $R_0^s$ and $R_0^d$, respectively. [For CC bonds they are simply C—C and C=C bond lengths in 1,3-butadiene (81).] The factor 301.15 allows to use $R$ values expressed in Angstroms and to obtain $HOSE$ values in kJ mole$^{-1}$. Most molecules with $\pi$ systems have to be described by at least a few and in some cases many canonical structures. For each of these, $HOSE_i$ may be different in principle. Following the ideas of VB theory, as well as in agreement with chemical experience and tradition, two assumptions have been made:

1. All important structures must be taken into account in calculating the total $HOSE$ value for a given molecule:

$$HOSE = \sum_{i=1}^{N} C_i \cdot HOSE_i \qquad (26)$$

2. The contribution (weight) of the $i$th resonance structure $C_i$ in a description of the real molecule is reversely proportional to its $HOSE_i$ value:

$$C_i = \frac{HOSE_i^{-1}}{\sum_{j=1}^{N} (HOSE_j)^{-1}} \qquad (27)$$

In Equation 27 the denominator is the summation over all structures in question. Thus, $C_i$ is in the range $0 \div 1$, which multiplied by 100, gives the percent contribution of the $i$th canonical structure. The physical meaning of $HOSE_i$ values is that it is the energy by which the real molecule is more stable than its $i$th canonical structure. The less stable a canonical structure (i.e., the higher $HOSE_i$), the lower its contribution to the description of the real molecule. Consider as an example the geometry of benzene [X-ray diffraction data CC length 139.2 pm (21)]:

$$HOSE_i = 301.15 \cdot [3(1.392 - 1.349)^2 \cdot (44.39 - 26.02 \cdot 1.349)$$

$$+ 3 \cdot (1.392 - 1.467)^2 \cdot (44.39 - 26.06 \cdot 1.467)]$$

$$= 45.25 \text{ kJ mole}^{-1}$$

$$C_i = \frac{1/45.25}{2/45.25} = 0.5$$

Here the $HOSE$ values had been plotted against resonance energies calculated

within the scheme of Hess and Schaad (82) for both alternant and nonalternant hydrocarbons, giving very good fits (80) ($r = .991$, $n = 22$ and $r = 0.937$, $n = 12$, respectively). Additionally, weights of Kekule structures, $C_i$ calculated by use of the *HOSE* (80) and the Randic quantum-chemical approach (84) gave very good agreement ($r = 0.985$, $n = 63$). The *HOSE* model, which has been used in

TABLE 4

Weight (in %) of Canonical Structures 1–6 (Scheme 4) Calculated by Use of *HOSE* Model (80) for DPNA and 2,6- and 3,5-DNXy
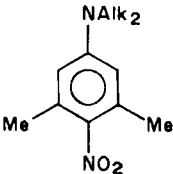
| Canonical Structure | (3,5-DNXy) | (2,6-DNXy) | (DPNA) |
|---|---|---|---|
| 1 and 2 | 31.5 | 41.1 | 25.2 / 28.0 |
| 3 and 4 (symmetrized) | 36.4 ⎫<br> ⎬ 57.2<br>20.8 ⎭ | 33.1 ⎫<br> ⎬ 49.6<br>16.5 ⎭ | 36.7 / 36.7 ⎫<br> ⎬ 60.7<br>25.4 / 22.7 ⎭ |
| 5 | | | |
| 6 | 11.4 | 9.3 | 12.7 / 12.6 |
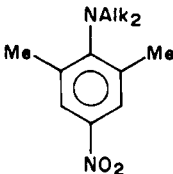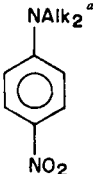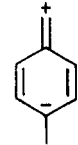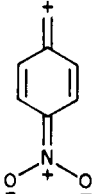
[a] Two independent molecules in asymmetric unit.

many other problems of organic chemistry, has proved to be a useful and reliable tool for the rationalization of various physicochemical and chemical properties (25, 55, 56, 58, 59, 63, 80, 85, 86).

Application of the *HOSE* model to the geometry of DPNA 2,6- and 3,5-DNXY leads to results in line with the conclusion based on comparison of appropriate bond length in these systems. Weights of canonical structures **1–6** of Scheme 4 are given for those systems in Table 4. Once again, it is immediately clear that DPNA and 3,5-DNXY show much more similarity than do DPNA and 2,6-DNXY. In other words, 60° twist of the $C_2N$ plane of the *N,N*-dimethylamine group causes a dramatic effect in geometry of the ring, lowering the *o,o′*- and *p*-quinoid structure (3–5) contribution to 10% less than in DPNA. Similarly, a twist of the $NO_2$ plane results in only a 3.5% decrease of weights for these canonical structures. Once again this seems to strongly support Exner's suggestion (78, 79) that the nitro group acts chiefly by means of an inductive effect. This is in line with STO-3G data on $\pi$-electron transfer from the planar amino group, which increases from $0.120e$ aniline to $0.139e$ in *p*-nitroaniline, while the $\pi$-electron transfer into the nitro group increases from $0.031e$ in nitrobenzene to only $0.044e$ for *p*-nitroaniline (30). The same conclusion was reached by Hiberty and Ohanessian in their VB study of *p*-nitroaniline and *p*-nitrophenol (38). It is immediately apparent that:

1. The least important contribution is that for full charge transfer from the
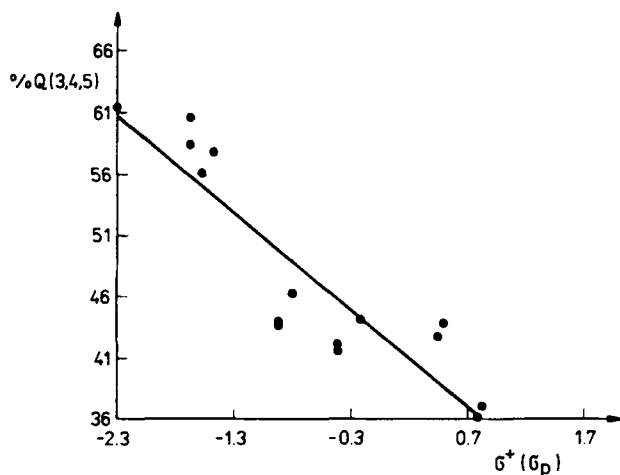


**Figure 15**   Plot of $\%Q(3,4,5)$ versus $\sigma^+(\sigma_p)$ for 15 *para*-disubstituted benzene derivatives.

TABLE 5

Weights of Contributions of Canonical Structures for $p$-Nitroderivatives of Benzene

| X | 1 | 2 | 3 | 4 | 5 | 6 |
|---|---|---|---|---|---|---|
| NH$_2$ | 14.7 | 14.4 | 17.5 | 18.1 | 22.1 | 13.2 |
| —NEt$_2$ | 13.8 | 12.6 | 17.1 | 20.0 | 23.4 | 13.1 |
| | 14.2 | 14.4 | 18.7 | 18.2 | 21.4 | 13.1 |
| -- NHCH$_3$ | 15.6 | 15.8 | 20.0 | 16.2 | 19.8 | 12.6 |
| OCH$_3$ | 23.2 | 19.3 | 13.2 | 16.2 | 16.9 | 11.2 |
| —COCH$_3$ | 19.2 | 27.3 | 15.3 | 12.9 | 15.6 | 9.7 |
| --Ph | 23.0 | 23.6 | 15.4 | 14.2 | 14.6 | 9.2 |
| —NH$_3^+$ | 26.9 | 27.4 | 12.5 | 12.4 | 12.2 | 8.6 |
| —NO$_2$ | 27.8 | 27.8 | 12.2 | 12.2 | 11.7 | 8.3 |
| --O | 11.9 | 11.7 | 18.7 | 18.7 | 24.0 | 15.0 |
| ·· OH | 22.6 | 22.9 | 14.8 | 14.2 | 15.0 | 10.5 |
| | 22.0 | 23.6 | 14.5 | 14.2 | 15.2 | 10.5 |
| - COO$^-$ | 24.3 | 24.6 | 14.3 | 13.9 | 13.9 | 9.0 |
| | 24.7 | 25.0 | 14.6 | 14.0 | 13.1 | 8.6 |
| ·· COOH | 25.2 | 23.5 | 14.3 | 14.7 | 13.7 | 8.6 |

electron donating to the electron-accepting substituent (structure 6) and that this is true for all systems studied.

2. All weights $C_i$ $(i = 1-6)$ depend considerably on the nature of the substituent.

Application of the *HOSE* model to 15 *para*-substituted derivatives of nitrobenzene supports these conclusion very clearly. Figure 15 presents this property as the dependence of $C_i$ versus $\sigma_p$ (or $\sigma_p^+$) $(i = 3, 4, 5)$, whereas Table 5 presents $C_i$ values $(i = 1, 2, \ldots, 6)$ for 15 *para*-substituted derivatives of nitrobenzene (86). These results are a good rationalization of the internal interaction between the substituents and their influence on the geometry of the ring in *para*-substituted benzene derivatives. The *HOSE* calculation leads to the VB-type picture and summarizes changes in geometry in line with modern points of view regarding the through resonance effect and, importantly, was deduced entirely from experimental geometry of $p$-XPhY systems. Thus, geometric parameters (bond lengths) of these systems are good descriptors of the through-resonance effect in molecules, provided the data applied are of sufficiently good quality (precision) and properly analyzed.

Additional information that may be extracted from geometry of molecules by use of the *HOSE* model is the approximate $\pi$-charge distribution and even the electric dipole moment (87). Taking from Table 5 the weights of the contribution of canonical structures 1-6, one can calculate $\pi$ charges at atoms as shown in Fig. 16 for $p$-nitroaniline. We assume for this calculation that unit charges are localized in positions as required by structures 3 6
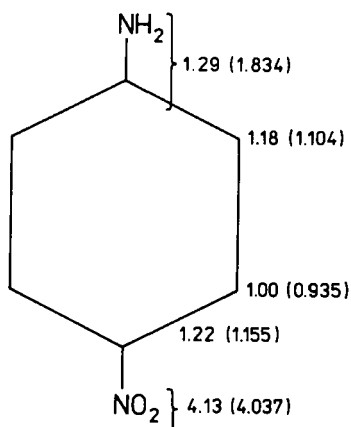
**Figure 16**  $\pi$-electron population for *p*-nitroaniline estimated by *HOSE* model (80); numbers in brackets are values calculated by VB method (38).

whereas in structures **1** and **2** all atoms are fully neutral. Comparison with the net $\pi$-electron population from a Mulliken population analysis for *p*-nitroaniline (38) shows reasonable agreement between theoretical and purely empirical $\pi$-electron charges. The dipole moment calculated from *HOSE* $\pi$ charges is $\mu = 9.11$D, in comparison to an experimental value $\mu = 6.33$D (88).

### 4.   Use of Geometry of $\pi$-Electron Systems to Estimate Charge Transfer in EDA Complexes and Salts

It has been shown (89, 90) that for EDA complexes of tetracyanoquino-dimethane (TCNQ), bond lengths may be used to estimate approximate values of the intermolecular charge transfer. Most popular is the method suggested by Flandrois and Chasseau (89). They assumed that in the radical anion of TCNQ, namely, TCNQ$^-$, the *a*-, *b*-, and *c*-bonds are of the same length. Thus for TCNQ$^-$ where $q = -1$, $b - c = c - d = 0$, whereas for a neutral molecule $(q = 0)$ $b - c = 6.9$ pm and $c - d = -6.2$ pm (91). From these data one can calculate $q$ for any TCNQ species provided precise $b$, $c$ and $d$ values are known. Application of the *HOSE* model (80) permits calculation of the weights of particular canonical structures $Q$, $B_1$, and $B_2$ (structures **1, 2**, and **3**, respectively in Scheme 6, taking into account only the two closest exocyclic CC bonds and those in the ring, that is, bonds *a*, *b*, and *c*. We may construct the model (99,100) taking as a ground %$Q$ for a neutral TCNQ and for the singly charged TCNQ species in (TCNQ$^-$, Na$^+$) salt (92), that is, the most precisely measured geometry of TCNQ salts with univalent
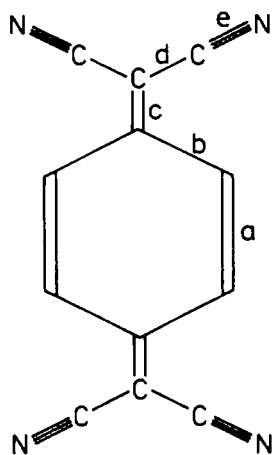
**Scheme 5**
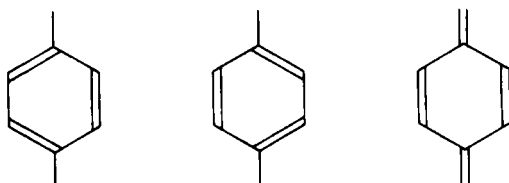
**1**     **2**     **3**

**Scheme 6**

metallic cation with 1:1 stoichiometry. These $\%Q$ values for $q = 0$ and $q = -1$ were found to be 91.28 and 50.59%, respectively. For these two points in coordinates $q$ versus $\%Q$ one obtains

$$q_k = -2.24 + 0.0246 \cdot Q_k \tag{28}$$

an equation that permits us to estimate the charge at the TCNQ species $q_k$ in any EDA complexes or salts for which the precise geometry allows us to estimate $Q_k$ via the *HOSE* model.

To test the accuracy of this model as well as for the model proposed by Flandrois and Chasseau (89), we apply them both to estimate the charges at TCNQ species for eight salts with inorganic cations. For these it may be assumed that the charge at cations must be either $+1$ or $+2$, and hence for the TCNQ-species associated with them it must be either $-1$ or $-2$. The differences between the charges at TCNQ estimated from electrical neutrality $q_{TCNQ}^{en}$ and those calculated by *HOSE* model and Equation 28

$$\Delta = q_{TCNQ}^{en} - q_{TCNQ}^{model} \tag{29}$$

may be used to estimate the standard deviation for the model. Calculations carried out on eight salts and one neutral system lead to the results collected in Table 6.

$$s = \left[ \sum_{i=1}^{8} \frac{\Delta_i^2}{7} \right]^{1/2} \tag{30}$$

TABLE 6

Percent Contributions and Charge for TCNQ Species Calculated by Use of *HOSE* Model ($q_{HOSE}$)
and Application of Flandrois–Chasseau Model ($q_{FC}$)

| | Ref. | R | ESD | % Q | $q_{HOSE}$ | $\Delta^b$ | $q_{FC}$ | $\Delta^b$ |
|---|---|---|---|---|---|---|---|---|
| 1. TCNQ | 0.039 | 0.005 | 91.28 | 0.00 | 0 | | | 91 |
| 2 NaTCNQ (357 K) | 0.033 | 0.003 | 50.59 | 1.00 | 0 | 0.94 | +0.06 | 92 |
| 3. NaTCNQ (296 K) | 0.046 | 0.008 | 45.73 | 1.12 | −0.01 | 0.98 | +0.19 | 93 |
| | | | 55.08 | 0.89 | | 0.83 | | |
| 4. KTCNQ (298 K) | 0.44 | 0.05 | 39.51 | 1.27 | −0.36 | 1.14 | −0.08 | 94 |
| | | | 47.12 | 1.09 | | 0.94 | | |
| 5. KTCNQ (413 K) | 0.052 | 0.013 | 56.07 | 0.86 | +0.14 | 0.73 | +0.27 | 94 |
| 6. RbTCNQ (113 K) | 0.066 | 0.004 | 51.22 | 0.98 | +0.02 | 1.01 | −0.01 | 95 |
| 7. RB$_2$TCNQ$_3$ (113 K) | 0.038 | 0.004 | 84.46 | 0.17 | −0.15 | 0.00 | +0.40 | 96 |
| | | | 51.06 | 0.99$^a$ | | 0.80$^a$ | | |
| 8. RB$_2$TCNQ$_3$ (294 K) | 0.063 | 0.009 | 90.96 | 0.01 | +0.15 | 0.01 | +0.47 | 97 |
| | | | 53.83 | 0.92$^a$ | | 0.76$^a$ | | |
| 9. Cs$_2$TCNQ$_3$ (294 K) | 0.039 | 0.004 | 91.03 | 0.01 | +0.27 | 0.00 | +0.36 | 98 |
| | | | 56.45 | 0.86$^a$ | | 0.82$^a$ | | |

$^a$Two molecules of this geometry and the third one electrically balance two cations.
$^b\Delta = q_{TCNQ}^{en} - q_{TCNQ}^{model}$.

The *s* value (Equation 30) found for the Chasseau–Flandrois method is 0.28*e*, whereas for the *HOSE* model *s* = 0.18*e*. A slightly better precision of the *HOSE*-model estimation than that determined by the Flandrois–Chasseau model seems to result from the following:

1. There is better chemical ground for the *HOSE* model since the assumption $b = c = d$ in TCNQ$^-$ geometry is not always correct. A deeper inspection into geometry of (TCNQ$^-$, Me$^+$) (Me$^+$- univalent cation) leads to the conclusion that this condition is not well fulfilled (99).

2. There is a slightly greater variance for *a*-, *b*-, and *c*-bonds (taken into calculation of *Q*, $B_1$, and $B_2$ canonical structures; for 39 geometries it is 46.5, in comparison to *b*, *c*, and *d* equal to 44.6).

3. During the computation of %*Q*, $B_1$, and $B_2$ some kind of averaging takes place, which is not the case with direct subtraction of $c - b$ and $c - d$.

Nevertheless, by use of structural parameters (bond lengths) one can, theoretically, obtain information about such an important process as charge transfer in EDA complexes. The only condition necessary is to have precise experimental data. Table 7 presents a small collection of data obtained by the above-mentioned methods.

Another application of molecular geometry in study of charge transfer in EDA complexes and salts is the use of a Δ versus α plot for *N*,*N*,*N'*,*N'*-

TABLE 7

The *HOSE* and Flandrois–Chasseau Estimated Charge at TCNQ Species in Selected EDA Complexes

| Donor | Stoichio-metry | ESD for Bond Lengths | $q_{HOSE}$ | $Q_{FC}$ | Ref. |
|---|---|---|---|---|---|
| 1. Terphenyl | 1:1 | 0.003 | −0.14 | −0.17 | 101 |
| 2. Morpholinum | 2:3 | 0.003 | −0.54 | −0.46 | 102 |
| | | | −1.03 | −0.98 | |
| 3. N, N, N′, N′-tetramethyl | | | −0.50 | −0.50 | 102 |
| p-phenylenodiamine | 1:2 | 0.003 | −0.50 | −0.50 | 103 |
| 4. Ethylene-1, 1′- | | | −0.93 | −0.87 | 104 |
| bipyridinium-2, 2′ | 1:2 | | −0.98 | −0.93 | |
| 5. Di-N-pyridinium | 1:4 | 0.003 | −0.91 | −0.79 | 105 |
| methyl-1, 4-benzene | | | −0.21 | −0.23 | |
| 6. Naphthalene | 1:1 | 0.003 | −0.19 | −0.13 | 106 |
| 7. Tetraphenylphosphonium | 1:2 | 0.003 | −0.51 | −0.43 | 107 |
| 8. Perylene | 1:1 | 0.004 | +0.02 | −0.10 | 108 |
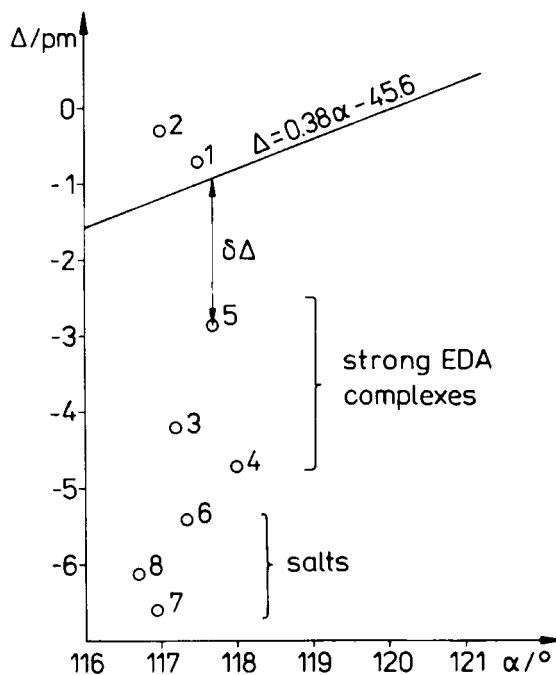


Figure 17   Plot of $\Delta$ versus $\alpha$ for $p$-$N,N,N,'N,'$-tetramethyl-$p$-phenylendiamine (1), its EDA complexes (2 5) and salts (6–8).
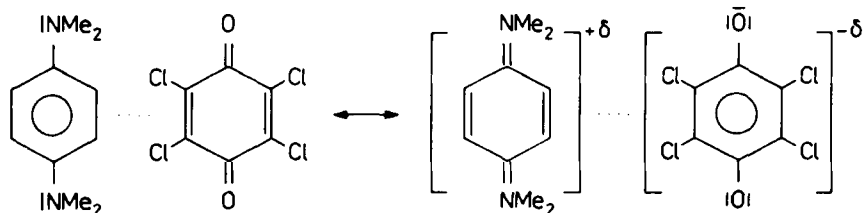
**Scheme 7**

tetramethyl-*p*-phenylenediamine (TMPD) in similar systems (67). One may expect that complexation between TMPD and electron acceptors is described by Scheme 7 where chloranil is taken as electron acceptor.

The greater the charge transfer from TMPD to the acceptor in the EDA complex, the greater the contribution of the quinoid form for TMPD molecule. This should be easily estimated by the simple $\Delta$ value. Indeed, in plotting $\Delta$ versus $\alpha$ for eight EDA complexes and salts of TMPD (Fig. 17), one observes deviation down from the Walsh line (Equation 18). The greatest downward shift is found for salts, being less for the EDA complexes and the value of $\delta\Delta$ depending on the strength of the complex. The application of $\Delta$ is highly equivalent to using $\%Q$ calculated by the *HOSE* model. For eight data points the correlation coefficient for the $\Delta$ versus $\%Q$ plot was found to be 0.98 (67). Apart from an obvious conclusion that the geometry of the ring depends strongly on the charge transfer, $\alpha$-angles do not change much in the process. This is in line with former finding that $\alpha$ values do depend chiefly on $\sigma$-electron effects (28, 49) and to a much less extent on $\pi$-electron effects.

### E.   How Does Quality of the Model Depend on Quality of the Structural Data

#### 1.   Some More Statistics

It was shown in Section I that the precision of an individual measurement is of major importance in the analysis of structural effects arising from inter- and intramolecular interactions observed via changes in geometry of molecular and/or ionic systems. The question arises as to how far the quality of experimental data, in our case the structural parameters, may obscure the expected picture of certain types of interaction.

As an example, let us consider the model $\Delta$ versus $\alpha$ (Equation 18). It was shown (63) that it works well for relatively small and homogenous sets of data for mono- and symmetrically *para*-disubstituted derivatives of benzene. From the Walsh rule one may, however, expect two relationships;

$$a = A' \cdot \alpha + B' \tag{31}$$

and (from Equation 18)

$$\Delta = A \cdot \alpha + B \tag{32}$$

Statistical analysis of both these models (64) is based on a large sample of 207 data points taken from a collection of very precise geometries (Cambridge Structural Data Base flag AS-1) (109). Detailed analysis of the quality of these databases on a search through the literature (not based on averaged geometries provided by CSDB with assumed $C_{2v}$ symmetry) permitted the definition of the following criteria to build up subsamples:

1. Those data with esd for bond length $\leqslant 0.5$ pm and $0.3°$ for bond angles (subsample a).

2. Symmetry $C_{2v}$ is assumed for structural parameters of the ring. If the difference between symmetrically equivalent bond lengths is greater than 1.0 pm, that is, $|a - a'|$ or $|b - b'|$ or $|c - c'| \geqslant 1.0$ pm, and for angles greater than $0.6°$, these data are not taken into further analysis. The assumption of $C_{2v}$ symmetry within the ring is quite justified since for monosubstituted benzene derivatives, ab initio 6–31 G calculations (110) indicated insignificant differences of substituent effect for nonaxially symmetric substituents such as OH, CHO, NO, and COOH on the $\beta$ and $a$ values, less than $0.3°$ and $0.5$ pm, respectively (subsample b).

3. Chemically equivalent rings in polyphenyl derivatives or in crystallographically independent molecules should not differ by more than 1.0 pm in bond lengths or by $0.6°$ in bond angles (subsample c).

4. Interatomic contacts no shorter than the sum of van der Waals radii are acceptable for geometries for further analysis (subsample d). (Equations 31 and 32).

The results of statistical models eqs. (Equations 31 and 32) for entries taken from various subsamples a through d as well as two more samples consisting of only noncrystalline state measurements (subsample e) and electron diffraction and microwave measurements (subsample f) are presented in Table 8.

In order to judge the correctness of a fit of regressions (Equations 31 and 32, subsamples $a–f$) the correlation coefficient $R$ should be compared with its limited value $R_L$ to test the null hypothesis:

$$H_0: R = 0$$

If $R > R_L$ (at significance level $= .01$), then we reject the null hypothesis with
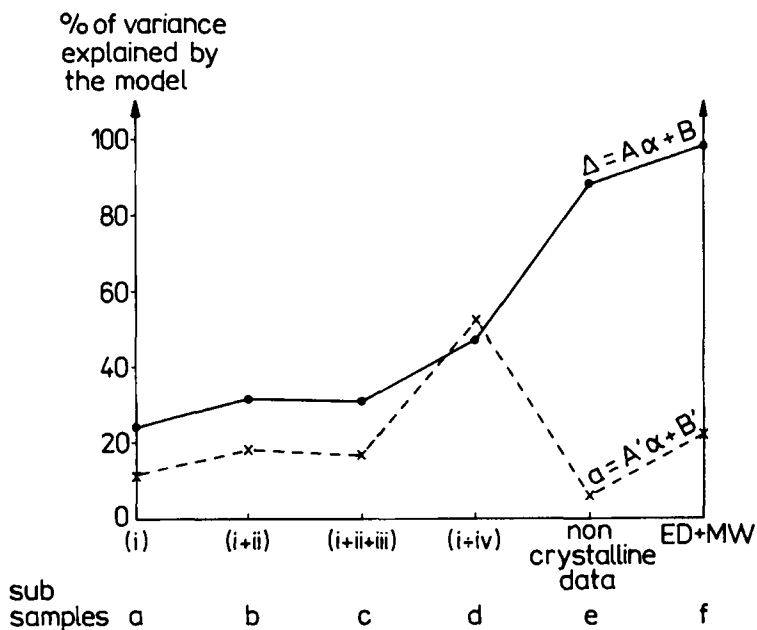
**Figure 18** Plot of the explained variance versus quality of subsamples based on criteria 1 and 5 (see text).

TABLE 8

Statistical Parameters for Equations 31 and 32 for and Data Sets of Variance Precision

| Criteria Fulfilled by the Sample | Equation No. (Subset No.) | A A′ | B B′ | $100R^2$ | R | n | $R_L = 0$ (at 0.01) |
|---|---|---|---|---|---|---|---|
| 1 | 32 (a) | 0·22 | −26.5 | 24.0 | 0.49 | 207 | 0.178 |
| | 31 (a) | $-1.5 \cdot 10^{-3}$ | 1.57 | 12.2 | 0.35 | | |
| | 32 (b) | 0·26 | −30.7 | 31.4 | 0.56 | 105 | 0.2506 |
| 1 + 2 | 31 (b) | $-2.0 \cdot 10^{-3}$ | 1.63 | 17.6 | 0.42 | | |
| 1 ÷ 3 | 32 (c) | 0.23 | −28.0 | 30.2 | 9.55 | 64 | 0.318 |
| | 31 (c) | $-1.8 \cdot 10^{-3}$ | 1.60 | 16.8 | 0.41 | | |
| 1 ÷ 4 | 32 (d) | 0.34 | −41.4 | 47.6 | 0.69 | 17 | 0.599 |
| | 31 (d) | $-2.1 \cdot 10^{-3}$ | 1.64 | 51.8 | 0.72 | | |
| Noncrystalline data only | 32 (e) | 0.44 | −52.2 | 88.4 | 0.94 | 11 | 0.719 |
| | 31 (e) | $-1.0 \cdot 10^{-3}$ | 1.51 | 6.2 | 0.25 | | |
| ED and MW data only | 32 (f) | 0.37 | −44.5 | 98.8 | 0.994 | 7 | 0.842 |
| | 31 (f) | $-1.4 \cdot 10^{-3}$ | 1.56 | 20.2 | 0.45 | | |

the risk of being in error in 1% of cases. In all cases (except subsamples e and f in Equation 31) we may accept the alternative hypothesis, which states that both $\Delta$ versus $\alpha$ and a versus $\alpha$ plots are statistically significant. Two points here require further comment. For all cases (except subsamples e and f in Equation 31) the correlation is significant, but its predictive power depends strongly on the data precision. Figure 18 presents the dependence of the explained variance on the precision of the data used. Practically only Equation 32, subsamples e and f, for noncrystalline geometries and for electron diffraction (ED) and microwave (MW) geometries, give acceptable predictive power (88.4 and 98.8%). For these data sets, however, Equation 31 is statistically insignificant (null hypothesis cannot be rejected) and its predictive power is extremely low as well (6.3 and 20.2%). Why do we observe these discrepancies? For large samples (a, b, and c), both models (Equations 31 and 32) are statistically significant and illustrate the trend described by the Walsh rule. Because of many random and systematic contributions to the error involved, however, the predictive power of these two equations is very low. For more precise data (d, e, and f) the predictive power becomes better, but with data sets e and f, Equation 31 fails completely. Why? The answer is very simple: in the case of the $\Delta$ versus $\alpha$ plot, in the subtraction $\Delta = b - a$ some part of the systematic errors may be canceled, whereas this is not the case in the model involving the a versus $\alpha$ plot. Thus, slight differences in the definition of bond lengths between determinations by use of MW, ED, and NMR in nematic phase are large enough to destroy the model in Equation 31, which describes relatively weak interactions.

## 2. Conclusions

We may conclude the following regarding dependence of model quality on structural data quality:

1. Statistical significance for the model in question may result even for less precise data provided a large data set is used. In this way we may support trends expressed by model equations, but their predictive power is of very low or even no value.

2. For precise data sets the statistical significance obtained may depend on such small effects as differences in the definition of interatomic distances for various measurement techniques. Hence subtraction in $\Delta$ provides us with the structural parameter that better describes the modeled property, that is, fulfillment of the Walsh rule, than would the direct use of bond lengths.

3. Undoubtedly the effect of interatomic interactions (packing forces), thermal motion effects, and errors in the refinement of the structure are responsible for the low precision of $\Delta$ versus $\alpha$ plots.

4. In general, if the model is to describe weak effects, the quality of the structural data must be much higher than in other cases. For instance, for a strong effect such as in the case of *para*-disubstituted benzene derivatives with substituents interacting with $\pi$-electron cooperative effects (through resonance), the $\Delta$ versus $\sigma^+$ plot is practically independent of the quality of data sets (67). However, variation in $\Delta$ in this case is some five times greater than in the case described in the case of Equations 31 and 32.

## III.  APPLICATION OF SOFT STRUCTURAL PARAMETERS IN THE FIELD OF CORRELATION ANALYSIS IN ORGANIC CRYSTAL CHEMISTRY

Soft structural parameters, that is, parameters that are easily deformable, may be formally divided into two groups:

1. Those in which the atoms forming these fragments of the molecular structure are bonded between themselves in a normal way, or where the bond lengths are not longer than the sum of the covalent (ionic) radii. Torsional angles, dihedral angles, and some valence angles, if not endocyclic in aromatic systems, belong to this group.
2. The other group in which the atoms involved in building up the fragment of the crystal structure are at distances longer than the sum of covalent and/or ionic radii. Hydrogen bonds as well as contacts in EDA complexes are good examples of these kinds of systems.

The most important applications of these structural parameters are derived from a series of papers by Bürgi, Dunitz, and their coworkers (111–117). They have used both kinds of parameters to construct models simulating the variation of geometry of the molecular and/or intermolecular fragment of the crystal structure along the reaction path. They have found that in many cases interatomic distances and angles describing the structure of a given fragment cover a range that is many times larger than the $3\sigma$ value. The changes of various structural parameters of a fragment in question are correlated with each other. Moreover, the observed mutual dependence may be described by use of Pauling's (119, 120) equation relating a given bond length $r(n)$ to the reference bond length (usually single bond) $r(1)$ and the bond number $n$. The $n$ value was originally

$$r(n) = r(1) - c \log n \qquad (33)$$

which is interpreted as a number (or a fraction) of electron pairs participating

in a bond $r(n)$. The quantity $c$ is an empirical constant and may easily be obtained when there are two known bond lengths of known bond number value. Thus, for the CC bond, we may take bond lengths for ethane ($n = 1$) and ethene ($n = 2$) to obtain, from Equation 33, $c = 0.664$. It should be pointed out that bond numbers may also be expressed in terms of bond angles (116) and used to interpret angular deformations.

In a series of ingenious papers, Bürgi, Dunitz, and their coworkers have found sufficient arguments to develop the concept known at present as the "principle of structural correlation" (120, 121). This idea, as well as its application in various branches of structural chemistry, has already been reviewed (120, 121) and does not need to be repeated here. However, to direct the reader's attention to such an important contribution in the field of application of structural parameters for a better understanding of chemical reactivity, one simple example (122) is described in more detail.

## A.  Principle of Structural Correlation: An Example

Consider a series of crystal structures of compounds in which one may expect interaction between a nitrogen atom and a carbonyl group. Two examples of such compounds, methadone (M) and cryptopine (C) will serve as an illustration of this series (Scheme 8).



Methadone                          Cryptopine
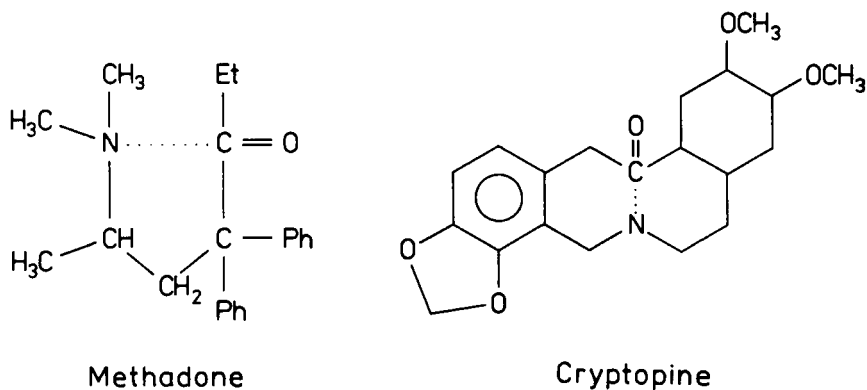
**Scheme 8**

Analysis of six crystal structures with a possible intramolecular interaction of $N \cdots C{=}O$ type, leads to the conclusion that the deviation of the carbon atoms $\Delta$ (see Fig. 19) from the plane consisting of the $R_1R_2$ and oxygen atoms depends in a regular way on the $d_1$ distance. It had been shown that dependence of $\Delta$ on $d_1$ may be expressed by a smooth line, as shown in Fig. 20:

$$d_1 = -1.701 \log \Delta + 0.867 \tag{34}$$
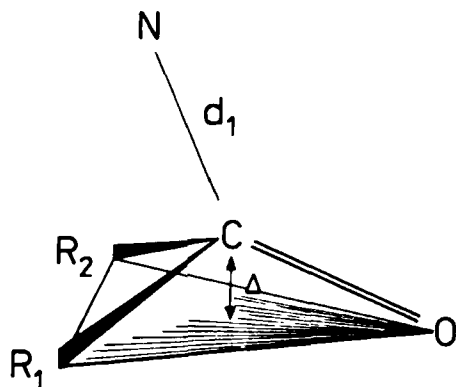
**Figure 19**  Definition of $\Delta$ and $d_1$ parameters for Equations 34 and 35.

where the constants were obtained by least squares calculations. Extrapolating $d_1$ to the standard C—N bond lengths leads to $\Delta_{max} = 0.437\,\text{Å}$ and Equation 34 may be rewritten to give

$$d_1 = -1.701 \log n + 1.479\,\text{Å} \tag{35}$$

where $n = \Delta/\Delta_{max}$. In a similar manner one can obtain Equation 36 describing the variation of the C—O bond length:

$$d_2 = -0.71 \log(R - n) + 1.426\,\text{Å} \tag{36}$$
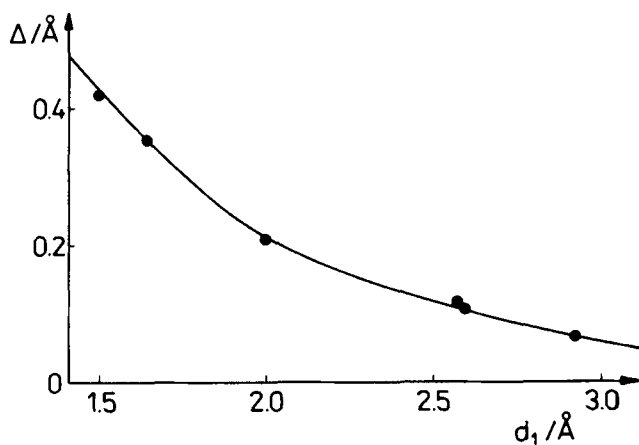


**Figure 20**  Plot of $\Delta$ versus $d_1$. The smooth line was obtained from Equation 34.

Both equations reproduce the observed interatomic distances $N \cdots C$ and $C-O$ with relatively high precision, and hence imply that the sum of the bond numbers for these two bonds is equal to 2.

Analysis of the angles at which the N atom approaches the C atom is in line with the orientation of nucleophilic attack postulated by an analysis of the kinetic data (123).

This example is a simple illustration of how soft structural parameters may be used to interpret chemical properties, in particular mechanisms and kinetics of chemical reactions. The principle of structural correlation may be described as follows (120): "If a correlation can be found between two or more independent parameters describing the structure of a given structural fragment in various environments, then the correlation function maps (approximately) a minimum energy path in the corresponding parameter space."

## B. Application of More Advanced Statistical Treatments to Study the Variation of Soft Structural parameters

There is no uniform opinion in the literature as to whether the distribution of energy of a molecule or molecular fragment in a large number of crystal environments should have a Boltzmann-like character. Some studies seem to support such character (124), but other authors have no doubt that this is not the case (125). Indirect evidence in favor of the Boltzmann-like distribution was given by Murray-Rust (126). He assumed that the exponential distribution does operate in crystals and that the energy of torsional distortion $E_{dis}$ applies for small distortions proportional to $\varphi^2$ (harmonic approximation), where $\varphi$ is the torsion angle in question. Hence he concluded that the torsion angle $\varphi$ should follow the normal distribution with variances proportional to $a/V$, where $V$ is a rotational barrier in question. He applied the Cambridge Structural Data Base to analyze the scatters of the torsion angles in a number of functional groups for which the rotation barriers were known to give experimental variances $\sigma^2(\varphi)$ for these torsion angles. The plot of $\sigma^2(\varphi)$ versus $1/V$ turned out to be roughly linear, in agreement with the prediction based on a Boltzmann-like distribution and gave $a$ as a value of $0.15 \, \text{kcal mole}^{-1}$ for the constant $a$ in Equation 27. The same problem, for the same set of data, was undertaken by Jaskólski (128). He also assumed that energy of distorsion $E$ has an exponential distribution, and the density of distribution was

$$\text{Probability of distribution} = \exp\left(-\frac{E_{dis}}{a}\right) \qquad (37)$$

$$Z(E) = a_1 \exp\left(-\frac{E}{a_2}\right) \qquad (38)$$

Application of standard statistical procedures gave

$$-\ln F(E) = \frac{1}{a_2 E} \tag{39}$$

where $F(E)$ is the probability of finding an energy in the range between $E$ and $\infty$. Testing this hypothesis by use of a procedure similar to the normal probability plot (128, 129) gave the final result at $a_2 = 0.32\,\text{kcal mole}^{-1}$. Both cases studied distorsions of differently substituted ethyl esters. The angle in question, $\tau$, is shown in Scheme 9, whereas the total number of entries analyzed was 101. The linear dependence between $-\ln_{F\text{obs}}(E_i)$ versus $E_i$ was fulfilled with correlation coefficient 0.963.
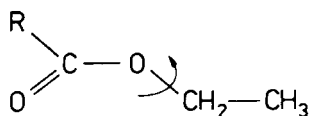
**Scheme 9**

It should be pointed out that very recently (131) the idea of Boltzmann-like distribution of molecular distortions in crystalline environments has been strongly criticized. Undoubtedly, this field of study is open to further and deeper studies.

## C.   How Intermolecular Interactions May Obscure Intramolecular Ones

In the last decade a large number of crystal and molecular structures of *para*-substituted benzoic acids have been solved. On the other hand, such systems had been used by Professor Hammett to describe the substituent effect by definition of the substituent constant $\sigma$. This constant is simply a measure of acidity of such acids. One should expect that in dimers of these acids in crystals, the H bonding should reflect the substituent effects. If one accepts as a rough measure of the energy of H bond in dimers the distance between oxygen atoms in the bridge, then plotting $R(O\cdots O)$ versus $\sigma_p$ values should lead to a rough linear dependence (see Scheme 10).
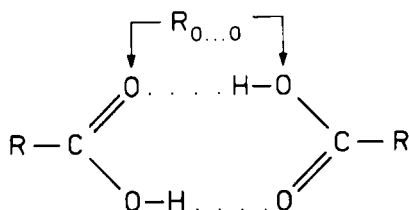
**Scheme 10**
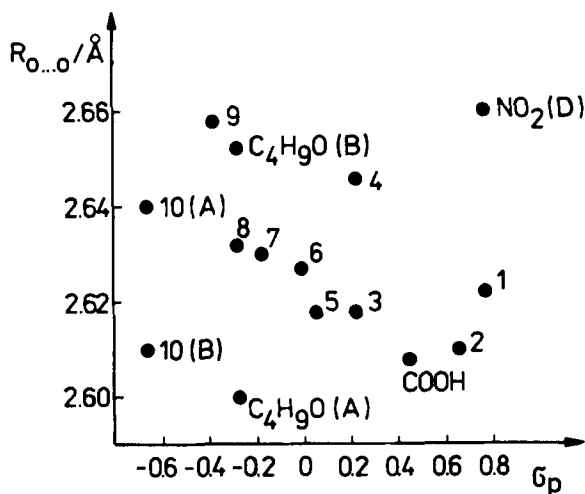
**Figure 21** Plot of $R(O \cdots O)$ versus $\sigma_p$ for 15 dimers of *para*-substituted benzoic acids. Numbering of points: 1—$NO_2$; 2—CN; 3—Cl; 4—Br; 5—F; 6—H; 7—$CH_3$; 8—$CH_3$; 9—OH; 10—$NH_2$. The other points are already assigned by the symbol of the group. Reproduced by permission from T. M. Krygowski, T. Więckowski, and A. Sokołowska, *Croat. Chim. Acta*, 57, 229 (1984).
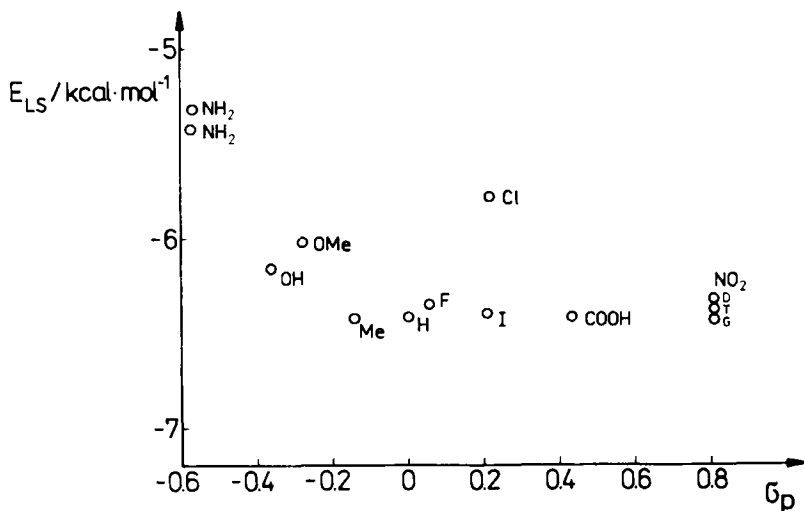


**Figure 22** Plot of Lippincott–Schroeder energy of the H bond versus $\sigma_p$ for *para*-substituted benzoic acids; D, T. and G assignments at $NO_2$ denote various refinements and different polimorphs. For details, see reference 133.

Examination of this hypothesis gave a strongly scattered plot (131, 132), as shown in Fig. 21. In order to escape from the crude assumption that $R(O \cdots O)$ is a measure of H-bonding energy, for well-solved crystal and molecular structures, of para-substituted benzoic acid H-bonding energy $E_{LS}$ was calculated by use of the Lippincott–Schroeder potential utilizing the experimental geometry of the bond (133). The plot of $E_{LS}$ versus $\sigma_p$ is shown in Fig. 22. Once again the observed picture is far from any regularity. The explanation of these findings may be as follows. The dispersion in the $\sigma_p$ values for the para-substituted benzoic acids in question is 1.4 $\sigma$ unit. If we multiply this value by $1.38 \, \text{kcal mole}^{-1} = RT$ for room temperature, we obtain a difference in energy in acid–base equilibria for these acids equal to $1.93 \, \text{kcal mole}^{-1}$. Taking into account the soft character of H bond as a structural parameter, we may conclude that the packing forces operating in the crystal lattice may easily overcome this value and hence that H-bond structure in these cases is governed by these forces rather than by internal substituent effects.


## IV.  GENERAL CONCLUSIONS

Structural (geometrical) parameters of chemical species (molecules and molecular ions) may successfully be applied to describe the effects of both intra- and intermolecular interactions on the geometry of chemical species.

Hard geometric parameters are the most suitable for detection of the effect of intramolecular interactions on geometry (e.g., substituent effect). Soft geometric parameters are well suited for study of intermolecular interactions in the crystals. Simulation of the reaction path may be obtained by proper use of these parameters.

The more subtle the effect under study, the more precise and homogenous structural the data to be used. The current state-of-the-art technique of X-ray and neutron diffraction determination of crystal and·molecular structure may be sufficiently precise to allow for many valuable conclusions to be drawn, provided careful selection of the data is made.


## ACKNOWLEDGEMENTS

# REFERENCES

1. K. J. Laidler, *Chemical Kinetics*, McGraw-Jill, New York, 1965, Chap. 1.
2. W. Ostwald, *Lehrbuch der Allgemeinen Chemie*, Akademische Verlagsgesellschaft, Leipzig, 1902.
3. J. N. Brønsted and K. Pedersen, *Z. Physik. Chem. 108*, 185 (1924).
4. J. E. Leffler and E. Grunwald, *Rates and Equilibria of Organic Reactions as Treated by Statistical, Thermodynamic, and Extrathermodynamic Methods*, Wiley, New York, 1963, p. 22.
5. K. Kindler, *Ann. Chem. 450*, 1 (1926).
6. L. P. Hammett and H. L. Pfluger, *J. Am. Chem. Soc., 55*, 4079 (1933).
7. G. N. Burkhardt, W. G. K. Ford, and E. Singleton, *J. Chem. Soc., 17*, (1936).
8. J. F. J. Dippy and H. B. Watson, *J. Chem. Soc.*, 436 (1936).
9. L. P. Hammett, *Chem. Rev., 17*, 125 (1935).
10. L. P. Hammett, *Physical Organic Chemistry*, McGraw-Hill, New York, 1940, p. 186.
11. R. W. Taft, Jr. in *Steric Effects in Organic Chemistry*, M. S. Newman, Ed., Wiley, New York, 1956, Chap. 13.
12. V. A. Palm, *Osnovy Kolitchestvennoy Teorii Organitcheskich Reaktsii (Principles of Quantitative Theory of Organic Reactions)*, Izdat. Khimiya, Leningradskoe Otdelenie, Leningrad, 1967.
13. N. B. Chapman and J. Shorter, Eds., *Advances in Linear Free Energy Relationships*, Plenum, New York, 1972.
14. S. Ehrenson, R. T. C. Brownlee, and R. W. Taft, *Progr. Phys. Org. Chem.*, **10**, (1973).
15. M. Charton, *Progr. Phys. Org. Chem., 16*, 267 (1987).
16. T. M. Krygowski and R. I. Zalewski, *Match Communication in Mathematical Chemistry, 22*, 119 (1989).
17. O. Exner, *Coll. Czech. Chem. Commun., 31*, 3222 (1966).
18. W. L. Bragg, *Proc. Cambridge Phil. Soc., 17*, 43 (1913).
19. W. Friedrich, P. Knipping, and M. von Laue, *Ann. Physik, 41*, 971 (1913).
20 I. Hargittai and M. Hargittai, *Molecular Structure and Energetics*, Vol. 2, J. F. Liebman and A. Greenberg, Eds., Verlag Chemie, 1986, Chap. 1.
21. D. W. J. Cruickshank, *Acta Cryst., 9*, 754, 757 (1956).
22. B. P. Stoicheff, *Can. J. Phys., 32*, 448 (1954).
23. T. M. Krygowski and I. Turowska-Tyrk, *Chem. Phys. Lett. 138*, 90 (1987).
24. I. Turowska-Tyrk, T. M. Krygowski, M. Gdaniec, G. Häfelinger, and G. Ritter, *J. Mol. Struct., 172*, 401 (1988).
25. K. Woźniak and T. M. Krygowski, *J. Mol. Struct., 193*, 81 (1989).
26. G. Häfelinger, G. Regelmann, T. M. Krygowski, and K. Woźniak, *J. Comput. Chem.*, in press.
27. W. J. Hehre, L. Radom, J. A. Pople, and P. von R. Schleyer, *Ab initio Molecular Orbital Theory*, Wiley, New York, 1986.
28. R. W. Taft and R. D. Topsom, *Progr. Phys. Org. Chem., 16*, 1 (1987).
29. R. D. Topsom, *Progr. Phys. Org. Chem., 16*, 85 (1987).
30. R. D. Topsom, *Progr. Phys. Org. Chem., 16*, 125 (1987).
31. R. D. Topsom, *Progr. Phys. Org. Chem., 16*, 193 (1987).

32. R. D. Topsom, *Molecular Structures and Energetics*, Vol. 4, Verlag Chemie, Deerfield Beach, Fla., 19.
33. W. F. Reynolds, R. W. Taft, S. Marriott, and R. D. Topsom., *Tetrahedron Lett.*, 1982, p. 1055.
34. R. D. Topsom, *Acc. Chem. Res.*, *16*, 292 (1983).
35. W. J. Hehre, R. W. Taft, and R. D. Topsom, *Progr. Phys. Org. Chem.*, *12*, 159 (1976).
36. R. T. C. Brownlee, S. Ehrenson, and R. W. Taft, *Progr. Phys. Org. Chem.*, *10*, 1 (1973).
37. T. M. Krygowski and G. Häfelinger, *J. Chem. Res.*, 348 (1986).
38. P. C. Hiberty and G. Ohansessian, *J. Am. Chem. Soc.*, *106*, 6963 (1984).
39. R. Hoffmann, foreword to the monograph by I. V. Vilkov, V. S. Mastryukov, and N. I. Sadova, *Determination of the Geometrical Structure of Free Molecules*, Mir Publishers, Moscow, 1983.
40. J. Bernstein, in *Effects of Crystal Environment on Molecular Structure*, lecture notes of Internatinal School of Crystallography held in Erice (Italy) May–June 1985, CNR Reparto Technografico, Rome, 1985, p. 267.
41. A. I. Kitajgorodski, *Molecular Crystals and Molecules*, Academic Press, New York, 1973 (Russian edition 1971).
42. A. Domenicano, *Geometrical Substituent Effects in Benzene Derivatives*, lecture notes of International School of Crystallography held in Erice (Italy), May June, 1985, p. 316.
43. A. Domenicano, A. Vaciago, and C. A. Coulson, *Acta Cryst.*, *B31*, 221, 1630 (1975).
44. A. Roszak, Ph.D. thesis, Poznań University, Poznań, Poland, 1986; A. Roszak and T. Borowiak, *Acta Cryst.*, *C42*, 343 (1986).
45. A. Domenicano, P. Mazzeo, and A. Vaciago, *Tetrahedron Lett.*, 1029, (1976).
46. J. E. Huheey, *J. Phys. Chem.*, *69*, 3284 (1965); *70*, 2086 (1966).
47. A. D. Walsh, *Discus. Faraday Soc.*, *2*, 18 (1947).
48. H. A. Bent, *Chem. Rev.*, *661*, 275 (1961).
49. T. M. Krygowski, G. Häfelinger, and Schüle, *Z. Naturforsch.*, *416*, 895 (1986).
50. R. Norrestam and L. Schepper, *Acta Chem. Scand.*, *A33*, 889 (1978).
51. R. Norrestam and L. Schepper, *Acta Chem. Scand.*, *A35*, 91 (1981).
52. A. Domenicano and P. Murray-Rust, *Tetrahedron Lett.*, 2283 (1979).
53. S. J. Grabowski and T. M. Krygowski, *Acta Cryst.*, *C41*, 1224 (1985).
54. T. M. Krygowski, R. Anulewicz, T. Daniluk, and T. Drapała, *Struct. Chem.*, in press.
55. T. Wieckowski and T. M. Krygowski, *Croat. Chim. Acta*, *58*, 5 (1985).
56. J. Maurin and T. M. Krygowski, *J. Mol. Struct.*, *158*, 359 (1987).
57. M. Colapietro, A. Domenicano, C. Marciante, and G. Portalone, *Z. Naturforsch.*, *37b*, 1309 (1982).
58. J. Maurin and T. M. Krygowski, *J. Mol. Struct.*, *72*, 413 (1988).
59. R. Anulewicz, G. Häfelinger, T. M. Krygowski, C. Regelmann, and G. Ritter, *Z. Naturforsch.*, *42b*, 917 (1987).
60. D. Britton, *Acta Cryst.*, *B33*, 3727 (1977).
61. D. Britton, *Acta Cryst.*, *B36*, 2304 (1980).
62. K. N. Trueblood, Program THMB-6, Department of Chemistry, University of California, Los Angeles, 1982.
63. T. M. Krygowski, *J. Chem. Res. (S)*, 234 (1984).

64. I. Turowska-Tyrk and T. M. Krygowski, *Pol. J. Chem.*, 63,000 (1989).

65. A. Domenicano, G. Schultz, and I. Hargittai, *J. Mol. Struct.*, 78, 97 (1982).

66. B. Rozsondai, B. Zelei, and I. Hargittai, *J. Mol. Struct.*, 95, 187 (1982).

67. T. M. Krygowski, *j. Chem. Res. (S)*, 120 (1987).

68. N. P. Penionzhkevich, N. I. Sadova, N. I. Popik, L. V. Vilkov, and Yu. A. Pankrushev, *Zh. Strukt. Khim.*, 20, 603 (1979).

69. E. G. Cox, D. W. J. Cruickshank, and J. A. S. Smith, *Nature*, 125, 766 (1955).

70. L. Pauling, *The Nature of the Chemical Bond*, 3rd ed., Cornell University Press, Ithaca, N. Y., 1960.

71. For review see A. Pross and L. Radom, *Progr. Phys. Org. Chem.*, 13, 1 (1981).

72. W. J. Hehre, R. W. Taft, and R. D. Topsom, *Progr. Phys. Org. Chem.*, 12, 159 (1976).

73. W. J. Hehre, L. Radom, and J. A. Pople, *J. Am. Chem. Soc.*, 94, 1496 (1972).

74. S. K. Pollach, J. L. Devlin, K. Summerhays, R. W. Taft, and W. J. Hezhre, *J. Am. Chem. Soc.*, 99, 4583 (1977).

75. H. J. Talberg, *Structural Aspects of Nitrosobenzene*, Ph.D. thesis, Department of Chemistry, University of Oslo, Oslo, Norway, 1979.

76. G. L. Butt, M. F. Mackay, and R. D. Topsom, *Acta Cryst.*, C43, 1092 (1987).

77. T. M. Krygowski and J. Maurin, *J. Chem. Soc. Perkin II*, 695 (1989).

78. O. Exner, *Collect. Czech. Chem. Commun.*, 31, 65 (1966).

79. O. Exner, U. Folli, S. Marcacciolli, and P. Vivarelli, *J. Chem. Soc. Perkin II*, 757 (1983).

80. T. M. Krygowski, R. Anulewicz, and J. Kruszewski, *Acta Cryst.*, B39, 732 (1983).

81. K. Kveseth, R. Seip, and D. A. Kohl, *Acta Chem. Scand.*, A34, 31 (1980).

82. B. A. Hess and L. J. Schaad, *J. Am. Chem. Soc.*, 93, 305 (1971).

83. B. A. Hess and L. J. Schaad, *J. Org. Chem.*, 36, 3418 (1971).

84. M. Randić, *Tetrahedron*, 33, 1905, (1977).

85. J. Karolak-Wojciechowska, *Acta Cryst.*, B43, 574 (1987).

86. T. M. Krygowski and I. Turowska-Tyrk, *Coll. Czech. Chem. Commun.*, in press.

87. T. M. Krygowski and M. Krawiec, manuscript in preparation.

88. C. P. Smyth, *Dielectric Behavior and Structure*, McGraw-Hill, New York, 1955, p. 326.

89. S. Flandrois and D. Chasseau, *Acta Cryst.*, B53, 2744 (1977).

90. P. Coppens and T. N. Guru, *Ann. N.Y. Acad. Sci.*, 313, 244 (1978).

91. R. E. Long, R. A. Sparks, and K. N. Trueblood, *Acta Cryst.*, 18, 932 (1965).

92. M. Konno, and Y. Saito, *Acta Cryst.*, B31, 2007 (1975).

93. M. Konno, and Y. Saito, *Acta Cryst.*, B30, 1294 (1974).

94. M. Konno, T. Ishii, and Y. Saito, *Acta Cryst.*, B33, 763 (1977).

95. A. Hoekstra, T. Spolder, and A. Vos, *Acta Cryst.*, B28, 14 (1972).

96. R. J. Wal and B. Bodegom, *Acta Cryst.*, B35, 2003 (1979).

97. R. J. Wal and B. Bodegom, *Acta Cryst.*, B34, 1700 (1978).

98. C. Frichtie and P. Arthur, *Acta Cryst.*, 21, 139 (1966).

99. T. M. Krygowski and R. Anulewicz, in *Proceedings of the 4th ERPOS Conference* (Electric and Related Properties of Organic Solids), Zamek Książ, Poland, 1984, p. 145.

100. T. M. Krygowski and K. Woźniak, *J. Mol. Struct.*, in press.

101. G. C. Lisenky, C. K. Johnston, and H. A. Levy, *Acta Cryst.* B32, 2188 (1976).

102. T. Sundaresan and S. C. Wallwork, *Acta Cryst.*, *B28*, 491 (1972).

103. A. W. Hanson, *Acta Cryst.*, *B24*, 768 (1968).

104. T. Sundmaresan and S. C. Wallwork, *Acta Cryst.*, *B28*, 3065 (1972).

105. G. J. Ashwell, S. C. Wallwork, S. R. Baker, and P. I. C. Berthier, *Acta Cryst.*, *B31*, 1174 (1975).

106. B. Shaanon, U. Shmueli, and D. Rabinowitch, *Acta Cryst.*, *B32*, 2574 (1976).

107. J. Jand, D. Chasseau, J. Guiltier, and C. Hauw, *C. R. Acad. Sci. Paris, Ser. C*, *278*, 769 (1974).

108. J. Tickle and K. Prout, *J. Chem. Soc. Perkin II*, 720 (1973).

109. A. Domenicano, P. Murray-Rust, and A. Vaciago, *Acta Cryst.*, *B39*, 457 (1983).

110. C. W. Bock, M. Trachtman, and P. George, *J. Mol. Struct.* (Theochem.), *122*, 155 (1985).

111. H. B. Bürgi, *Inorg. Chem.*, *12*, 233 (1973).

112. H. B. Bürgi, J. D. Dunitz, and E. Shefter, *Acta Cryst.*, *B30*, 1517 (1974).

113. H. B. Bürgi, J. M. Lehn, and G. Wipff, *J. Am. Chem. Soc.*, *96*, 1956 (1974).

114. P. Murray-Rust, H. B. Bürgi, and J. D. Dunitz, *J. Am. Chem. Soc.*, *97*, 921 (1975).

115. H. B. Bürgi, *Angew. Chem. Int. Edn.*, *14*, 460 (1975).

116. H. B. Bürgi, J. D. Dunitz, J. M. Lehn, and G. Wipff, *Tetrahedron*, *30*, 1563 (197).

117. H. B. Bürgi, E. Shefter, and J. D. Dunitz, *Tetrahedron*, *31*, 3089 (1975).

118. L. Pauling, *J. Am. Chem. Soc.*, *69*, 542 (1947).

119. L. Pauling, *The Nature of the Chemical Bond*, Cornell University Press, Ithaca, N. Y., pp. 239, 255.

120. J. D. Dunitz, *X-ray Analysis and the Structure of Organic Molecules*, Cornell University Press, Ithaca, N.Y., 1979, Chap. 7.

121. H. B. Bürgi and J. D. Dunitz, *Acc. Chem. Res.*, *16*, 153 (1983).

122. H. B. Bürgi, J. D. Dunitz, and E. Shefter, *J. Am. Chem. Soc.*, *95*, 5065 (1973).

123. D. R. Storm and D. E. Koshland, Jr., *J. Am. Chem. Soc.*, *94*, 5805, 5815 (1972).

124. H. P. M. de Leeuw, C. A. G. Haasuoot, and C. Altona, *Israel J. Chem.*, *20*, 108 (1986).

125. M. Levitt, and A. Warshel, *J. Am. Chem. Soc.*, *100*, 2607 (1978).

126. P. Murray-Rust, in *Molecular Structure and Biological Activity*, J. A. Griffin and W. L. Duax, Eds., New York, 1982, pp. 117–133.

127. M. Jaskólski, *Pol. J. Chem.*, *60*, 263 (1986).

128. M. B. Wilk and R. Granadesikan, *Biometrica*, *55*, 1 (1968).

129. S. C. Abrahams and E. T. Keve, *Acta Cryst.*, *A27*, 157 (1971).

130. H. B. Bürgi and J. D. Dunitz, *Acta Cryst.*, *B44*, 445 (1988).

131. T. M. Krygowski and T. Wieckowski, *Croat. Chim. Acta*, *54*, 193 (1981).

132. T. M. Krygowski, T. Wieckowski, and A. Sokołowska, *Croat. Chim. Acta*, *57*, 229 (1984).

133. S. J. Grabowski and T. M. Krygowski, unpublished communication, 1988.

# Author Index

Numbers in parentheses are reference numbers and indicate that an author's work is referred to although his name is not mentioned in the text. Numbers in *italics* indicate the pages on which the full reference appears.

# Subject Index

# Cumulative Index, Volumes 1–17